Final Report:

Feasibility Study of a Track-While-Scan Navigation Concept

Prepared for:
Langley Research Center
N A S A

B Y : R E S E A R C H D I V I S I O N
C O N T R O L D A T A C O R P O R A T I O N

Final Report:

FEASIBILITY STUDY OF A TRACK-WHILE-SCAN NAVIGATION CONCEPT

Contract No. NAS1-2902

Control No. L-3336

Control Data Project No. 9552

April 20, 1964

Prepared for:

National Aeronautics and Space Administration
Langley Research Center
Langley Station
Hampton, Virginia

(Prepared by Control Data Corporation, Research Division,
3101 East 80th Street, Minneapolis, Minnesota 55420.
Authors: J. E. Carroll, Project Engineer; R. L. Lillestrand,
B. D. Vannelli, D. C. Harrington, C. B. Grosch, B. A. Schmidt,
T. J. Lee, L. D. Kane.)

ABSTRACT

33335

This is the final report for Contract NAS1-2902: Feasibility Study of a Track-While-Scan Navigation Concept. It presents the results of studies performed under this contract and also during those relevant company-sponsored projects both before and during the contract existence. In general, the navigation concept consists of a scanning wide-angle camera with slits positioned on its focal surface, equations for rigid body rotation and planetary triangulation, and on-board computer processing of the camera data to obtain navigational information.

The efforts during the study were devoted to the areas of optical, electrical, and mechanical design; error analysis both by means of computer simulations and analytical studies; and the determination of computer requirements such as word length, memory size, execution time, etcetera needed to identify the scanned targets and extract navigational information

TABLE OF CONTENTS

Abstract		iii
Table of Contents		v
List of Figures		vii
List of Tables		xi
Forward		xiii
I.	GENERAL DESCRIPTION	1
	A. Navigation Concept	2
	B. Applications	24
	C. Target Identification	38
	D. Characteristics of Celestial Targets	49
II.	INSTRUMENTATION	61
	A. Optical Design	64
	B. Electronics	94
	C. Mechanical Design	104
III.	SYSTEM ANALYSIS	115
	A. System Equations	115
	B. Corrections	131
	C. Optical Transmissivity	151
	D. System Noise	163
	E. Simulation and Error Analysis	173
IV.	COMPUTER REQUIREMENTS	205
	A. Data Input	210
	B. Target Identification	220
	C. Solution of Navigation Equations	249
	D. Space Computer Characteristics	257
V.	CONCLUSIONS AND RECOMMENDATIONS	277

TABLE OF CONTENTS (Cont'd)

APPENDIX A: Torque-Free Motion of a Nearly Symmetric Rigid Body

APPENDIX B: Explicit Functions for Computation of Attitude

APPENDIX C: Explicit Functions for Computation of Position

APPENDIX D: Target Identification Program - BAKER

APPENDIX E: Camera-Computer Simulator Program - ABLE

APPENDIX F: Interrupt Program for Data Input

APPENDIX G: Analysis of a Torque-Free Body Containing a Swiftly Rotating Wheel

LIST OF FIGURES

Figure I-1.	Geometry of Mid-Course Navigation	2
Figure I-2.	Representative Wide-Angle Camera	5
Figure I-3.	Use of Slits at Focal Surface of Rotating Camera to Determine Target Position	5
Figure I-4.	Techniques for Viewing Sky with Wide-Angle Camera	9
Figure I-5.	Effect of Earth Obscuration	9
Figure I-6.	Example of Scan Field	13
Figure I-7.	Types of Optical Instruments for Mid-Course Navigation	16
Figure I-8.	Methods of Position Fixing	20
Figure I-9.	Methods of Satellite Navigation	27
Figure 1-10.	Minimum Operational Altitude for Triangulation	28
Figure I-11.	Transfer Trajectories to and from Mars	32
Figure I-12.	Distances to Planets During Earth-Mars-Earth Transfer	33
Figure I-13.	Angular Separations of Planets During Earth-Mars-Earth Transfer	33
Figure I-14.	Application of Scanning Camera to Surface Navigation	35
Figure I-15.	Sequence of Identification of Three Bright Stars	40
Figure I-16.	Distribution of Angular Separations Between Fifty Brightest Stars	43
Figure I-17.	Pair Ambiguities for Angular Separation Measurement Error	43
Figure I-18.	Differences in Magnitude Between Star Pairs Having Similar Angular Separations	44
Figure I-19.	Spectral Energy Distribution for Several Stars	51
Figure I-20.	Relative Response versus Wavelength for S-4 Photocathode Surface	52
Figure I-21.	Range of Planet Sizes as Function of Vehicle Distance from Sun	55
Figure I-22.	Minimum and Maximum Planetary Magnitudes as a Function of Vehicle Distance from the Sun	58
Figure II-1.	Components of Navigation Instrument	62
Figure II-2.	Fraction n/N of Sky Scanned vs. Field of View β and Half-Angle Between Slits Γ	71
Figure II-3.	Minimum Field of View β for N Brightest Stars Over Sky	73
Figure II-4.	Optical Designs Considered for Scanning Camera	74
Figure II-5.	Focal Surface and Support Details	79
Figure II-6.	Maximum Incident Angle of a Ray of Light Which Will Be Transmitted by Total Reflection Within a Fiber for Various Differential Indices of Refraction of Core and Coating Materials	88
Figure II-7	Operation of High Intensity Detector	90

LIST OF FIGURES (Cont'd)

Figure II-8.	Basic Design of Independent High Intensity Detector	91
Figure II-9.	Shutter and Fiber Arrangement at Photomultiplier	92
Figure II-10.	Representative Phototube Output Current and Multiplier Voltage as a Function of Target Magnitude Using Logarithmic Feedback	96
Figure II-11.	Schematic of Electronics in Capsule	96
Figure II-12.	Schematic Representation of Vehicle Electronics Prior to Data Formation Logic	98
Figure II-13.	Block Diagram for Transit Data Formation	100
Figure II-14.	Nutation Amplitude vs. ω_o/ν_s for a Rigid Body	107
Figure II-15.	Camera with Momentum Wheel	109
Figure II-16.	The Motion of the Camera (with Momentum Wheel)	111
Figure II-17.	Amplitude, γ	113
Figure II-18.	Amplitude, θ_o (Precession)	113
Figure II-19.	Amplitude, Nutation	113
Figure III-1.	Relations Between Various Coordinate Systems	117
Figure III-2.	Relationship of Camera Reference System to Angular Momentum Frame	120
Figure III-3.	Number of Stars Requiring Correction for Proper Motion	133
Figure III-4.	Number of Stars Requiring Correction for Parallax	133
Figure III-5.	Diagram Illustrating the Effect of Parallax (Due to parallax, star is shifted by $-\bar{R}$ to a new position on the celestial sphere.)	139
Figure III-6.	Diagram Illustrating the Effect of Aberration (x, y plane in Celestial Equator. Star is displaced towards the point on the celestial sphere towards which the observer is moving.)	141
Figure III-7.	Spherical Triangle Used in Aberration Calculations	144
Figure III-8.	Percent Reflection from a Polished Metal Surface versus Wavelength of Incident Light	153
Figure III-9.	Transmissivity in a Clean Glass Fiber	155
Figure III-10.	Light Absorption Characteristics of Two Typical Types of Optical Glass	157
Figure III-11.	Reflectance at a Glass-Air Interface	158
Figure III-12.	Transmissivity of Scanning Camera Optical System	162
Figure III-13.	Comparison of Signal Photon Noise and Photomultiplier Dark Current Noise	168
Figure III-14.	Comparison of Signal Photon Noise and Background Photon Noise	168
Figure III-15.	Angular Error in Location of Target Due to Signal Photon Noise	172

LIST OF FIGURES (Cont'd)

Figure III-16. Experimental Results of Gaussian Random Number Generator 179
Figure III-17. Flow Diagram for Simulation of Target Identification 180
Figure III-18. Number of Tests Required to Complete Identification 186
Figure III-19. General Flow Chart for Program ABLE 187
Figure III-20. Solar System on J.D. 2440600.5 (Jan. 15, 1970) 191
Figure III-21. Dependence of Spin Axis and Position Errors on Number of Targets Detected 192
Figure III-22. Dependence of ξ and t_o Errors on Angle τ Between Spin Axis and Angular Momentum Vector 194
Figure III-23. Dependence of Spin Axis and Position Errors on the Angle τ 195
Figure III-24. Position Errors as a Function of Time for Two Vehicle Positions 197
Figure III-25. Constant Error Contours in the Ecliptic Plane for J.D. 2440600.5 (σ = 10 seconds) 201
Figure III-26. Constant Error Contours in the Ecliptic Plane for J. D. 2440600.5 (σ = 10 seconds) 203

Figure IV-1. Flow Diagram for Data Interrupt Sequence 213
Figure IV-2. Data Lists Affected by Input Routine 215
Figure IV-3. General Identification Procedure 222
Figure IV-4. Diagram for Pre-Processing of Camera Data 223
Figure IV-5. Flow Diagram for Triplet Identification 229
Figure IV-6. Flow Diagram for Verification of Remaining Targets 240
Figure IV-7. Flow Diagram and Computer Requirements for Solution of the Navigation Equations 251
Figure IV-8. Expected Number of Targets Reviewed Before One lost 261
Figure IV-9. RMS of Error Matrix A 266
Figure IV-10. RMS of Error Matrix B 268
Figure IV-11. Memory Units 272

APPENDIXES

Figure 1. Schematic Flow Diagram of BAKER D-2
Figure 2. Schematic Flow Diagram of the Identification Subroutine (CHARLIE) D-5
Figure 3. Method of One-Dimensional Searching D-8
Figure 4. Example of Output from Program BAKER D-25

Figure 1. Schematic Flow Diagram for ABLE E-3

LIST OF FIGURES (Cont'd)

Figure 2.	Ordered Grid Points	E-2
Figure 3.	Example of Output from Program ABLE	E-22
Figure 1.	The Relationship Between the Inertial Frame $\hat{I}\hat{J}\hat{K}$ and the Body Frame i_4, j_4, k_4	G-2
Figure 2.	The Motion of the Camera (with Momentum Wheel)	G-3

LIST OF TABLES

Table I-1.	Stars Shown in Figure I-6	11
Table I-2.	Applications of Scanning Camera to Space Navigation	25
Table I-3.	Schedule for Interplanetary Trip	31
Table I-4.	Orbital and Physical Characteristics of Planets	54
Table I-5.	Magnitudes of the Planets	57
Table I-6.	Selected Minor Planets	50
Table II-1.	Characteristics of Several Possible Instruments for Scanning Camera	65
Table II-2.	Important Characteristics of Baker-Nunn Camera Optical Elements	76
Table II-3.	Characteristics of Scanning Camera Optical System	77
Table II-4.	Shapes of Apertures in Focal-Surface Mask	83
Table III-1.	Typical Photomultiplier Characteristics	169
Table III-2.	Typical Background Conditions	170
Table III-3.	100 Brightest Stars	174
Table III-4.	Planetary Characteristics Used in Simulation Programs	176
Table III-5.	Two Configurations for Which the Results of the Identification Simulation are Presented	182
Table III-6.	Percentage of Cases in Which Less than Three Slit-to-Slit Unique Intensity Matches Occurred	183
Table III-7.	False Identification Results	184
Table IV-1.	Summary of Computer Requirements for Processing Scanning Camera Navigation Data	208
Table IV-2.	Memory Requirements and Execution Speeds for Data Input Interrupt Routine	218
Table IV-3.	Storage Requirements for Pre-Processing Sequence	226
Table IV-4.	Computer Requirements Derived from Figure IV-7	254
Table IV-5.	Method for Computing Total Requirements	255
Table IV-6.	Total Number of Equivalent Additions for Solution of Navigation Equations	256

FOREWORD

This final report represents a complete technical documentation of all efforts performed under Contract NAS1-2902 and does not require any supplementation from the various interim technical reports. The study was performed between June 3, 1963 and April 20, 1964, for the Flight Mechanics Branch, Space Mechanics Division, NASA Langley Research Center, Langley Station, Hampton, Virginia. Mr. Harold A. Hamer was the project director at NASA and Mr. Leon W. Fitchett, the contracting officer.

The study was performed by the Aerospace Research Group, Research Division, Control Data Corporation, Minneapolis, Minnesota. The project engineer was Mr. Joseph E. Carroll. Other participants were R. L. Lillestrand, B. D. Vannelli, D. C. Harrington, C. B. Grosch, B. A. Schmidt, T. J. Lee, and L. D. Kane. Mrs. C. Nisula typed the manuscript and N. C. Fleischhacker and W. F. Kidder completed the illustrations.

I. GENERAL DESCRIPTION

The scanning camera navigation technique is a combination of optical sensor, rigid body dynamics, and computer executed data processing. Its application is in the area of interplanetary space navigation as far as the principle emphasis of this report is concerned. Satellite and surface navigation can also be implemented, however, with only minor alterations as discussed in Section I-B.

It is the purpose of this first section to generally describe the navigational concept, various applications, the identification of detected targets, and some of the characteristics of the targets themselves. The remainder of this report is devoted to a more detailed study of the three areas: camera design, system analysis, and computer requirements. Previous publications concerning this system are:

(1) R. L. Lillestrand and J. E. Carroll, "Self-Contained System for Interplanetary Navigation," presented at the AAS Annual West Coast Meeting, August 1961, Preprint 61-95.

(2) R. L. Lillestrand, et al., "Navigation in Cislunar Space - Final Report," ASD-TDR-62-960, Contract No. AF 33(657)-8215, December 1962.

(3) D. C. Harrington, "Noise Error Analysis of an Optical Star and Planet Scanner," 1963 National Conference Proceedings of NAECON, IEEE Dayton section, May 13-15, 1963, pp. 134-142.

(4) J. E. Carroll and R. L. Lillestrand, "Error Contours in Interplanetary Navigation," presented at National Space Meeting, Institute of Navigation, May 1, 1964, St. Petersburg.

A. Navigation Concept

The application of a scanning camera having permanently positioned slits in its focal plane to the problem of interplanetary (midcourse) navigation is conceptually very simple. As shown in Figure I-1, the

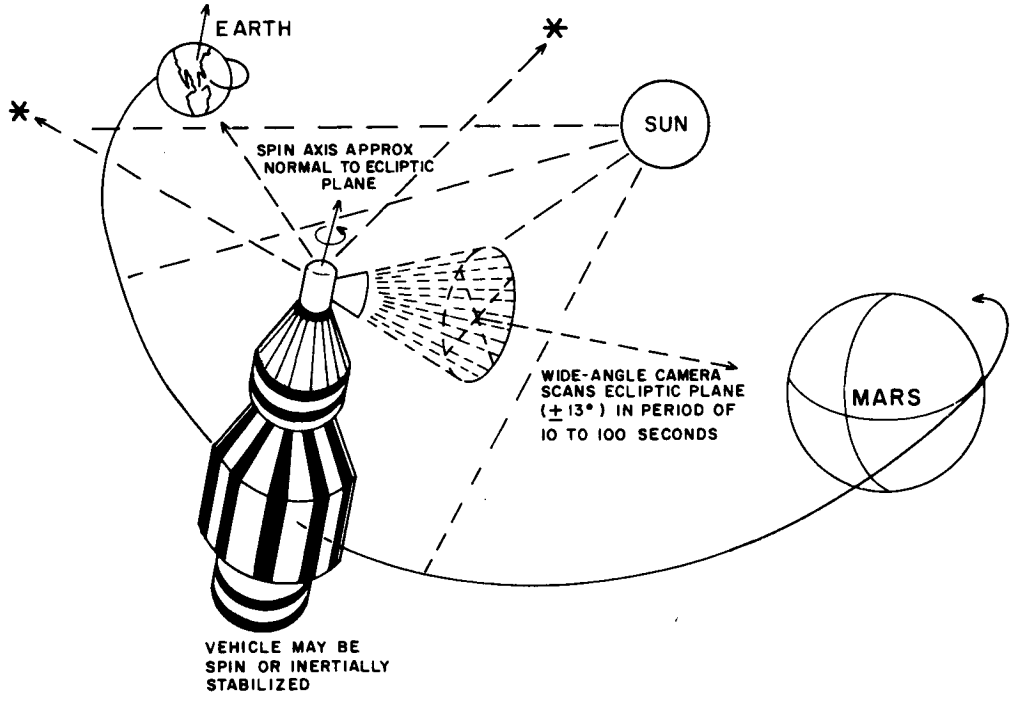

Figure I-1. Geometry of Mid-Course Navigation

camera scans the celestial sphere by rotating about an axis perpendicular to the optical axis and approximately normal to the plane of the ecliptic. Two quantities are measured:

(a) the times of the transits of targets across the slits, and

(b) the approximate magnitudes of the targets.

The magnitudes are measured only to about 0.1 (10% in intensity) and are

used to aid in identification. (See Section I-C below.) The transit times are entered into a set of navigational equations which, when solved, yield both the attitude and position of the space vehicle.

The camera can be mounted relative to the vehicle in three configurations depending mainly on the purpose of the mission. (a) For a vehicle whose only motion is torque-free rotation, the camera may be rigidly attached, the scanning motion being derived from the vehicle itself. (b) If the vehicle is inertially stabilized, the mount must provide one degree of rotational freedom. (c) A vehicle disturbed by random motions (such as caused by the movement of personnel) should have the camera completely detached from the main body and enclosed in its own capsule which then rotates as a rigid body similar to Case (a).

The basic postulate of this system which measures time rather than angle (except, possibly, Case (b)), is that, dynamically, the spinning vehicle behaves like a rigid body rotating in a field free of externally imposed torques. Typical spin periods are in the range 1 to 100 seconds per rotation, although this is not critical and need not be known beforehand. The direction of the spin axis need only be such as to bring at least two planets into the scan field of view. As a result, attitude control equipment can remain quiescent over prolonged periods and useful navigational information can be collected with no mechanisms for precision pointing of the camera or the spin axis. The fact that angle measurements are not made directly but only through the intermediary of time measurements is particularly advantageous since time measurements can be made to an

accuracy of one part in 10^6 relatively easily, while angle measurements to this accuracy are extremely difficult and often require complex instrumentation.

The accuracy with which the slits can be positioned in the camera is at least 10^{-4} inches, so that a 4 inch focal length leads to an angular accuracy of five seconds of arc. With a field of view of 30°, an equivalent resolution of 1/20,000 is obtained. In contrast, a camera equipped with an image orthicon or vidicon cannot be expected to achieve a resolution better than about 1/1,000.

1. Scanning Camera

The optical design which, from studies described in Section II, appears most promising is shown in Figure I-2. It consists of a wide-angle camera with permanently positioned slits in its focal plane. Immediately behind these slits are a series of glass fibers which carry light to photomultipliers mounted to the side of the camera.* If the camera is given a spinning motion in inertial space, a measurement of the time of appearance of stellar and planetary targets at the slits will supply sufficient information to determine the three axes of orientation of the vehicle as well as its position. If this detector is mounted on an inertially stabilized vehicle, one rotational degree of freedom must be supplied, otherwise the detector has no moving parts.

---

* Throughout this report one photomultiplier has been assumed for each slit to permit autonomous operation. There could just as well be four detectors, one for each half slit, or only one detector for both slits. The fewer photomultipliers, the more difficult becomes the data processing and target recognition problems.

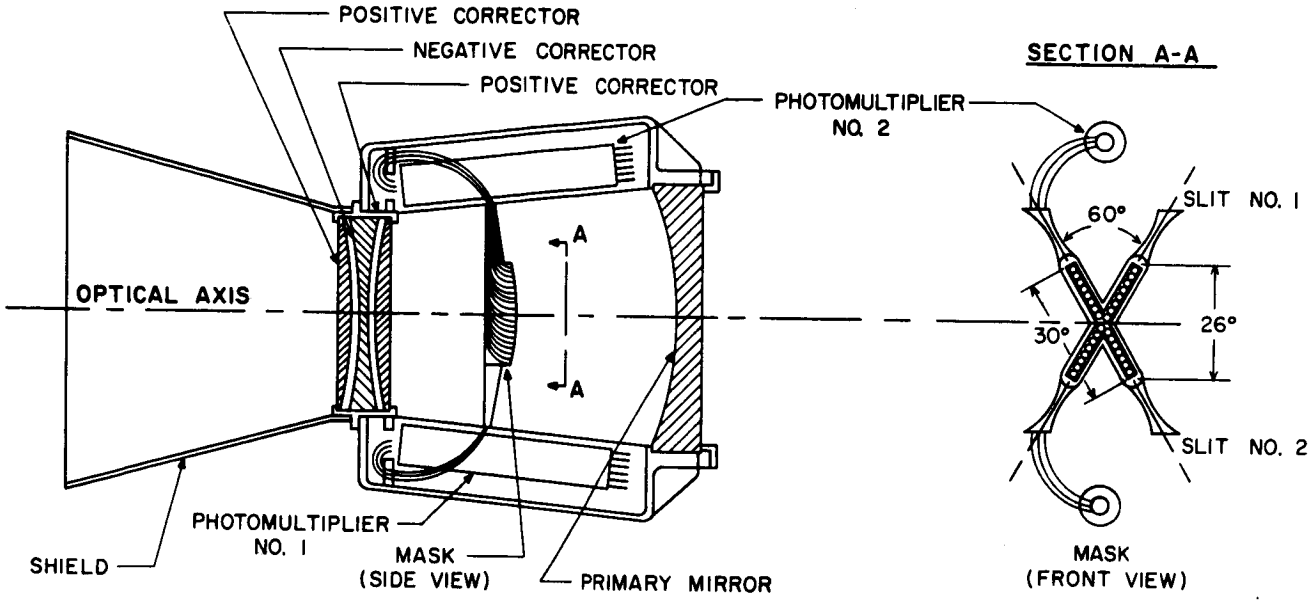

Figure I-2. Representative Wide-Angle Camera

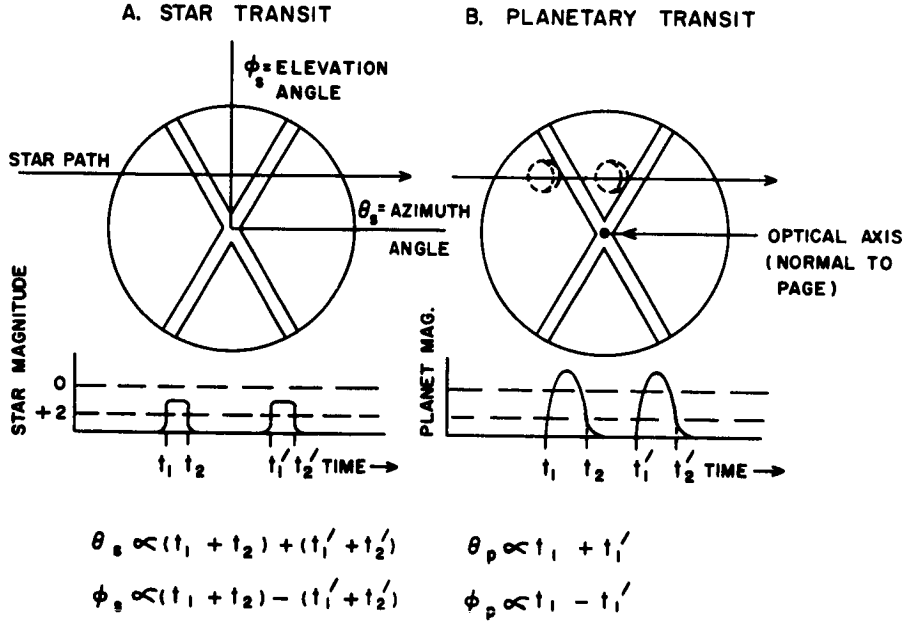

Figure I-3. Use of Slits at Focal Surface of Rotating Camera to Determine Target Position

A typical slit configuration is shown on the right in Figure I-2. Navigational information is derived as shown in Figure I-3. As the camera spins, the stellar or planetary images will move across the optical field of view. When the energy from such a target falls on one of the slits, it is conducted out of the optical system to a photomultiplier whose output pulse then appears as in Figure I-3A for a star and Figure I-3B for a planet. By measuring the rise and fall times of each pulse the average time of transit for that slit can be determined. From the transit times of the two slits, the direction to the target can be determined with respect to a coordinate system internal to the scanning camera. As depicted at the bottom of Figure I-3, the difference in the transit times is a measure of the elevation of the target above the scan plane. The average of the transit times is, in turn, a measure of the target azimuth relative to an arbitrary zero.

In the case of a partially illuminated planet, only the side of the pulse with the steepest slope is used and hence the direction to the planet is derived from a measurement of its illuminated limb. Since the approximate position of the space vehicle is known, a correction for the separation between the planetary limb and the center of the planet can easily be introduced.

Once the directions to various bodies are determined, they are identified as discussed in Section I-C below. The stars are used to associate the internal coordinate system with the celestial system. Knowing the direction to two or more planets in this latter system then

permits one to compute the position of the vehicle relative to the planets by simple triangulation or by least squares polyangulation.

2. Scan Field of View

It should be noted that the technique recommended here differs basically from several other schemes which have been proposed in the past. This can be seen from Figure I-4 which shows three techniques for viewing the sky with a wide-angle camera.

(a) Random Static Viewing

This is perhaps the simplest technique and it also leads to the most severe requirements in terms of the accuracy of the observing instrument, its field of view and in terms of the computer memory requirements. It is nothing more than a wide angle camera which points in a single random direction and which must find a sufficient number of stars within the camera FOV to achieve a unique identification. This system has the further disadvantage that, unless the camera FOV is very large, only two of the three attitude angles can be accurately measured. That is, the direction of pointing of the camera can be accurately determined but the orientation about this axis may be poorly determined. If this camera were rigidly mounted on an inertially stabilized platform, it might happen to look at the earth.

(b) Search with Static Terminal Field

This technique is superior to Number (a) in that the camera searches across the sky until it finds a field of view which contains a sufficient

number of bright stars to achieve a unique identification. However, it is similar to the first technique in that it only uses information contained in a single field of view.

(c) 360° Scan about Random Axis

This is the technique which is recommended in the present report and, of the three, leads to the least severe requirements in terms of camera field of view, number of stars required, and computer requirements. The camera scans across the sky and records the time of passage of all stars brighter than a predetermined intensity. If the rotational axis is orthogonal to the optical axis a 30° field of view (with 60° scanning slits) covers a region of the sky comparable with a camera of 85° field of view for Number (a). With the slits at the focal plane of the camera we are able to derive useful information from all stars which pass through the field of view without stopping the camera. Thus, only three stars are required in the entire scan region; under certain conditions only two stars are needed. This yields as much information, within the width of the scanned region, as would have been obtained from Number (b) if we had stopped to identify all the stars in each of the search regions through which it was necessary to pass in order to get to the static terminal field of view.

The result of the reduction in the required camera field of view is that a greater accuracy potential exists in the measurement of star angular separations, and that false target discrimination and background discrimination problems are relieved. By scanning through an extended region of the

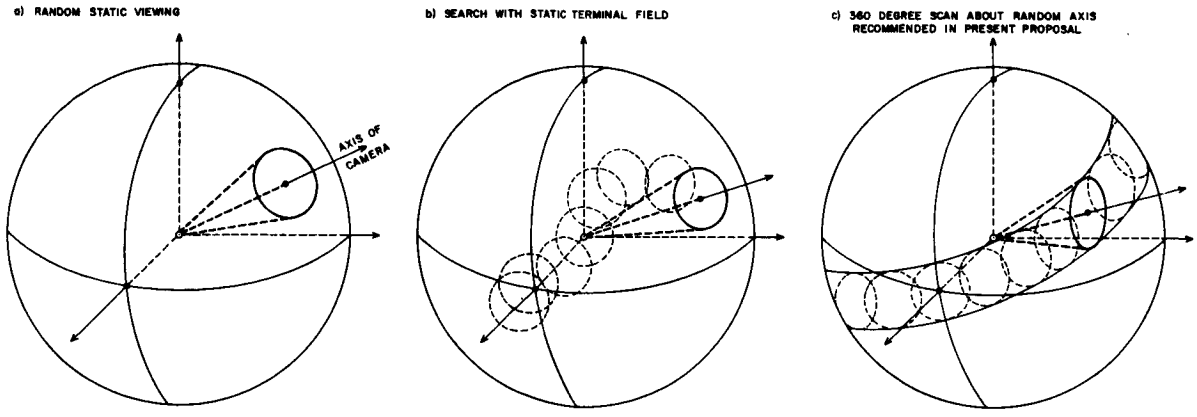

Figure I-4. Techniques for Viewing Sky with Wide-Angle Camera

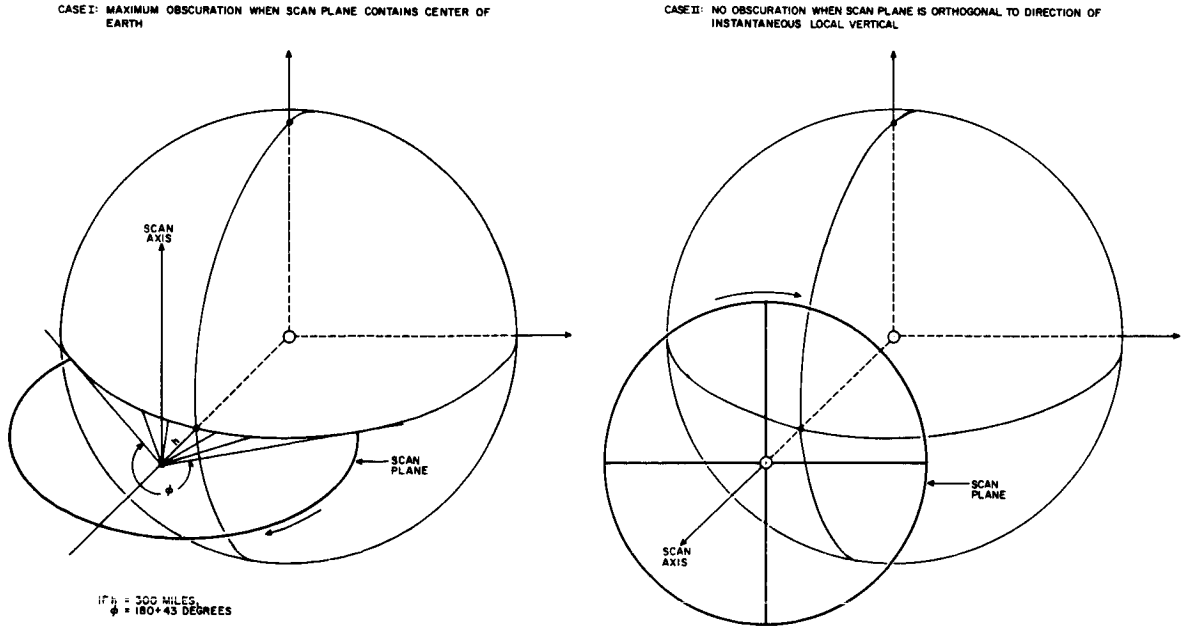

Figure I-5. Effect of Earth Obscuration

sky it becomes possible to use a relatively small camera field of view, about 30^{o}, and yet use two stars which are separated by 90^{o}--as is required to make the most accurate determination of space vehicle attitude.

Since the attitude detection system can be used on planetary satellites as well as interplanetary space vehicles, the effect of planetary obscuration must be considered. If the orientation of the vehicle is assumed to be completely random initially, the effect of, say, Earth obscuration is not possible to predict. The worst case for the system under consideration is that in which the scan plane passes through the center of the earth. In this case slightly less than half of the potentially observable region of the sky is obscured, with the amount of obscuration decreasing as the satellite altitude increases. This is shown in the first case of Figure I-5. In the second case, the scan axis is along the local vertical vector and there will be no Earth obscuration provided the altitude of the satellite is at least 100 miles. Since we have no way of predicting the orientation of the scan axis in the general case, we must design the system so that it always can detect at least three stars under the worst condition shown in Figure I-5.

Both of the other techniques shown in Figure I-4 will also be confronted with the earth obscuration problem. If the vehicle is suddenly stabilized in inertial space and if these cameras happen to be pointed in the direction of the earth, their pointing direction must be changed. In our system, no matter what the orientation of the vehicle at the time of inertial stabilization, the scan cycle will carry the camera through the open sky

region for at least half of its motion.

An advantage can be gained in terms of Earth obscuration if we provide a shutter between the end of the optical fibers and the photomultiplier which can cut out the upper and lower scanning slits independently. This can be easily instrumented and would provide a means of collecting data from half of the field of view while the other half is illuminated by solar energy reflected from the earth or its atmosphere.

As an example of a typical scan field of view, see Figure I-6 in which the associated photomultiplier outputs are also depicted. (No planets have been inserted.) Here we have assumed that the camera scans the specific region of the sky identified by the lines of right ascension and declination. The scan axis has an inclination of 25 degrees and a nodal longitude of 7 hours 20 minutes. To take account of possible planet obscuration, it was assumed that the search region is 223^{o} in length and not the full 360^{o}. With scanning slits positioned at 60^{o} angular separation, the width of the search region is 26^{o}. Table I-1 shows the General Catalog numbers and magnitudes of the stars in the scan field of Figure I-6.

TABLE I-1. STARS SHOWN IN FIGURE I-6

General Catalog Number	Magnitude
8833	-1.43
8302	-0.73
6410	0.37
1979	0.53
10438	1.16
9188	1.49
30942	1.75
9443	1.84
8223	1.97
31685	2.25

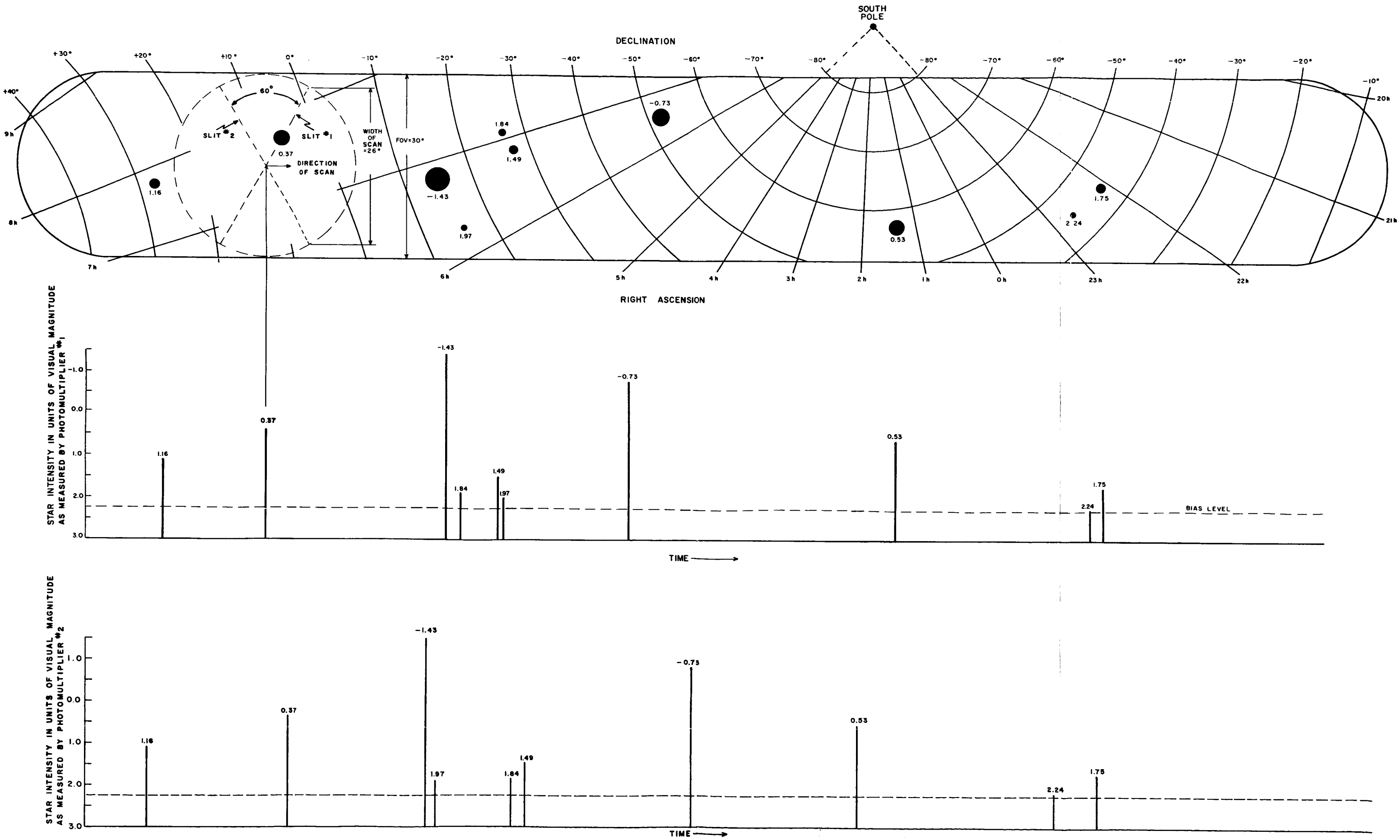

Figure I-6. Example of Scan Field

3. Comparison with Other Instruments

In the past, several types of optical instruments have been proposed for mid-course navigation. However, most of these instruments require the use of gimballed optical trackers or cameras for determining the positions of the various planets and they therefore lead to relatively complex instrumentation. Three optical devices which might be applied to the mid-course navigation problem and which are shown in Figure I-7 are:

1) Absolute measurement of angles between planets with gimballed star tracker mounted on inertially stabilized platform,
2) Relative measurement of position of planets and surrounding star field with wide-angle camera equipped with image tube, and
3) Measurement of transit time for stars and planets with rotating wide-angle camera equipped with slits in focal plane.

Larmore* has discussed a variety of techniques for the determination of the orientation and position of a space vehicle which rely on the measurement of angles between various planetary and stellar targets. In this case, a gimballed optical tracker is assumed to be available which is accurate to approximately 0.2 second of arc. Aside from the difficulty of constructing the tracker's angle encoder to this accuracy, this

* Larmore, L., "Celestial Observations for Space Navigation", Aero/Space Engineering, January 1959, pp. 37-42.

A. AUTOMATIC TRACKING THEODOLITE PROVIDING MEASUREMENT OF ABSOLUTE ANGLES BETWEEN WIDELY SEPARATED TARGETS

B. WIDE-ANGLE TELESCOPE FOR MEASUREMENT OF PLANETARY POSITION RELATIVE TO NEARBY STARS

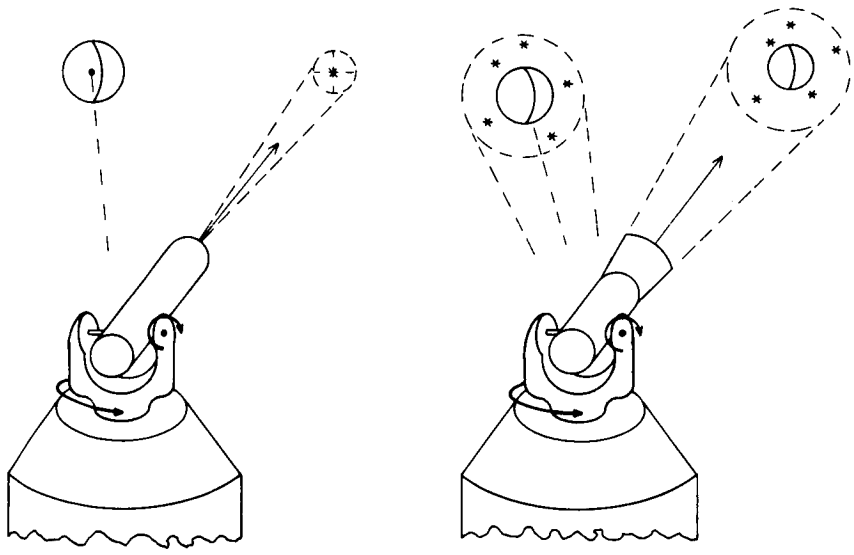

C. WIDE-ANGLE SCANNING CAMERA USING SLIT TRANSIT TIME MEASUREMENTS

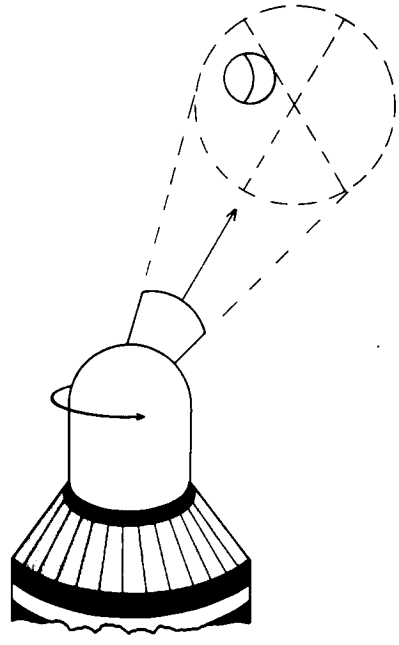

Figure I-7. Types of Optical Instruments for Mid-Course Navigation

instrument presents difficult design problems in terms of the target acquisition, in terms of locating the center of gravity of the planets, and in terms of the considerable weight and complexity of an automatic tracking theodolite. Similar difficulties would be encountered with the optical tracker mounted on an inertial platform as proposed by Bement.*

The second type of system mentioned above which measures the position of the planetary target relative to the field of stars which surround it, circumvents the problem of accurate large-angle measurement. In this case the position of the planet relative to stars lying within a radius of a few degrees is determined. This system has the added advantage that the orientation of the platform to which the wide-angle camera is attached need not be known, or held constant. However, with this system one must either employ two wide-angle cameras to concurrently track two objects within our solar system, or one must be prepared to point the camera back and forth from one target to the next. Thus this technique may require auxiliary equipment for target acquisition. In addition, this approach has the disadvantage of requiring the use of relatively faint stars--between 8^{th} and 10^{th} magnitude. Thus the star identification problem becomes difficult. If one attempts to minimize this problem by enlarging the field of view of the camera to find brighter stars, a loss of accuracy results. Typically the resolution of an image tube ranges from 300 to 1,000 lines and therefore to obtain an accuracy of five seconds of

* Bement, H. D., "Stellar-Inertial System Looks Best for Interplanetary Mid-Course Guidance", Space/Aeronautics, May 1961, pp. 128-132.

arc one cannot use a field of view greater than about two degrees. Examples of this type of system are those described by Bock,* Cardozo,** and de Kler.***

The instrument which employs a wide-angle camera with a system of slits in the focal plane and a photomultiplier as a detector (Number C) is the one described here. In terms of both mechanical and electrical complexity, it represents an improvement over the other two detection instruments. In terms of accuracy potential, it is at least comparable. Depending on the specific design and use of the detection instrument, an accuracy ranging from one second of arc to about one minute of arc may be expected.

Probably the most important advantages of the instrument described in the present report are: (1) that it involves few or no moving parts, (2) that it uses stars brighter than second magnitude, (3) that time is measured rather than angle, and (4) that the problem of finding the center of the planets is solved by measuring the position of the illuminated planetary limb. Certain additional advantages can be gained in terms of the reduction of the position error sensitivity coefficients because the

---

* Bock, C. D., "A High Precision Stellar Navigator for Interplanetary Guidance", IVth Symposium on Ballistic Missiles and Space Technology, August 24-27, 1959, UCLA, Los Angeles.

** Cardozo, A. N., "Automation for Interplanetary Navigation", IXth International Astronautical Congress, 1958, p. 652.

*** de Kler, J. J., "On the Degree of Accuracy to be Attained by Astro-Scanners as an Aid in Automatic Interplanetary Course-Computation", IXth International Astronautical Congress, 1959, p. 669.

positions of all of the solar system bodies brighter than some predetermined magnitude are measured during each 360° rotation of the camera.

An instrument similar to the scanning camera is described by Willmore* for tracking satellites from a ground-based station. This instrument achieved an accuracy ranging from 15 to 60 seconds of arc with a telescope of five inch aperture and fourteen inch focal length; however, it had a very much smaller field of view. A further description of Willmore's instrument was made by Groves and Davies** in their paper on methods of analyzing observations of satellite orbits.

4. Position Fixing

Regardless of the instrument used, two basic methods of position fixing are available and these are shown in Figure I-8. The first method is that of the measurement of the relative angles between three planets. This method does not require any star position measurements to determine the position of the space vehicle. It is commonly used in surveying and photogrammetric work. Papers by Carroll,*** Atkinson,**** and Stearns and

---

* Willmore, A. P., "A New Method of Tracking Artificial Earth Satellites," Nature, 182, 1009 (1958).

** Groves, G. V. and Davies, M. J., "Methods of Analyzing Observations on Satellites," Xth International Astronautical Congress - II, 1958, pp. 933-946.

*** Carroll, J., "Interplanetary Navigation by Optical Resection and Inertial Systems," Aero/Space Engineering, March 1959, p. 53.

**** Atkinson, R. d'E., "Some Problems of Interplanetary Navigation," Jour. Inst. of Navigation, Vol. 3, no. 4, 1950, pp. 365-377.

Frye* describe this technique. The Three-Planet Method is subject to large errors when the position of the space vehicle lies on the circle defined by the three known planets.** A study of various space vehicle viewing geometries indicates that one of the three planets is often at

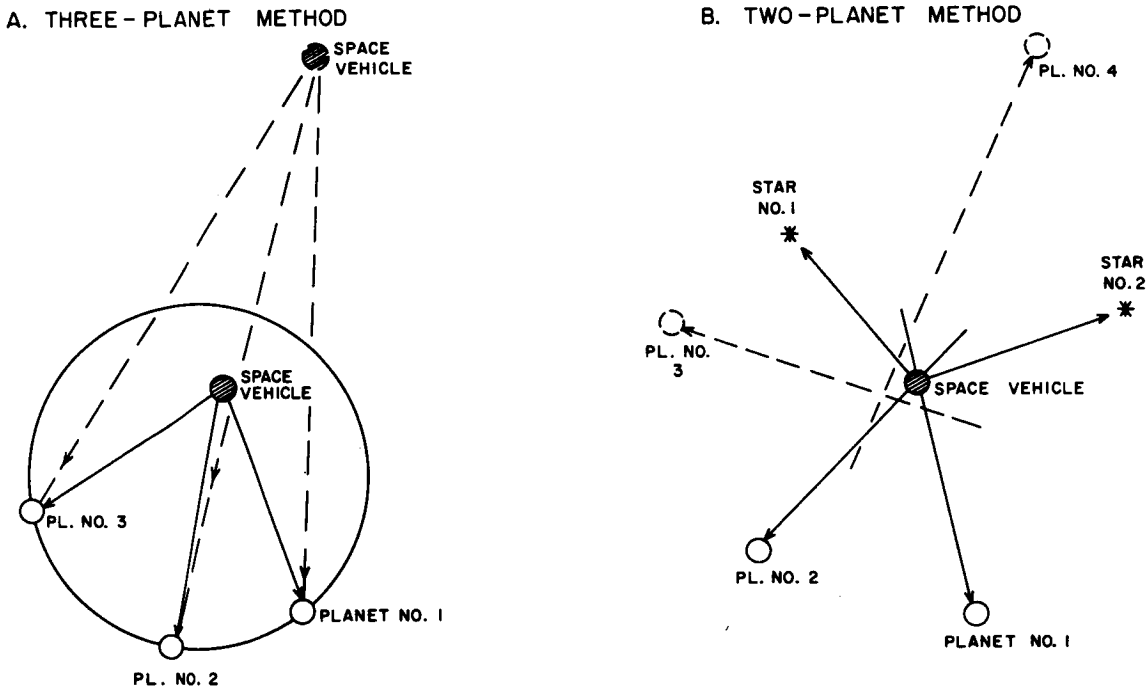

Figure I-8. Methods of Position Fixing

---

* Stearns, E. V., and Frye, W. E., "Interplanetary Navigation: An Extension of an Ancient Art," Jour. Inst. of Navigation, Vol. 6, no. 8 (Winter 1959-1960), pp. 526-535.

** Carroll, J., p. 53.

a considerably larger distance than the other two and thus it contributes disproportionately to the position error. Also when the three planets fall within an azimuth angle significantly less than 90^{o} (as shown by the case of the dotted lines in Figure I-8A), the error sensitivity coefficient for the position of the space vehicle normal to the ecliptic plane becomes large.

A method which appears to yield smaller error sensitivity coefficients over a wider range of interplanetary vehicular positions is shown in Figure I-8B. This method is that of simple triangulation using two known solar-system bodies, and as such it can be used for a lunar mission while the Three-Planet Method cannot. In this case information obtained from the star transits is used to provide a spatial attitude reference. A non-redundant position fix is obtained from the two angular coordinates of one planet (thus establishing the direction of a line in space) and one angular coordinate of the second planet. This coordinate will be the azimuth angle, i.e., the angular bearing of the planet measured in the ecliptic plane. The error sensitivity for the triangulation will be minimized by selecting the shortest sight lines which are most nearly orthogonal, thus it is evident that the earth and the terminal planet will not always be the best selection for triangulation during an interplanetary mission.

Since our detection instrument provides angular position data from up to six solar-system bodies, the question presents itself as to how one selects the best pair of bodies for the position fix. In fact, at any

one time certain space vehicle position errors might be minimized by one pair of bodies while other position coordinate errors are minimized with other planetary pairs. For the Earth-Mars flight described in the Applications section, it happens that these two planets form the best basis for position calculation over most of the transfer orbit. However, since conditions will vary widely for various transfer orbits, the Two-Planet Method requires a careful study of position error sensitivity coefficients if the greatest accuracy is to be achieved. In this respect, it is no better than the Three-Planet Method.

In order to resolve this problem and to take full advantage of all observational data on solar-system bodies, a statistical technique has been developed which is based on least squares polyangulation. This technique regards each body as defining a line in space whose positional uncertainty may be considered to be proportional to the product of the length of the line and the estimated RMS angular error in the measurement of the position of the body. The dotted lines in Figure I-8B show this geometry with two additional planets. In this case the weighted least square position of the space vehicle is determined without ever performing a simple two-planet triangulation. The polyangulation automatically weights most heavily those sight lines which carry the least positional uncertainty. Thus, as a space vehicle travels from Earth to Mars it might happen that the position fix is dominated by data from the earth and the moon early in the flight; at mid-course the earth and Mars sight lines might have the heaviest weight; at the terminal phase, Mars and its moons, Phobos and

Deimos, will dominate the position calculation. (See Section I-B for an example of an Earth-Mars mission.)

B. Applications

One of the most important characteristics of the scanning camera navigation instrument is its versatility. For example, the device might be used to drift trim the gyros before injection into a transfer orbit to another planet, for mid-course navigation, for navigation after achieving a stable satellite orbit around the other planet, and for surface navigation after landing on the planet. In each case, the capability can be made completely self-contained.

Table I-2 summarizes a number of these applications. As the wide-angle optical system scans the sky, it will detect various targets, both stellar and those in the solar system. Usually the first data processing involves the collection of the slit scan time data to calculate the three axes of orientation of the vehicle. Next, this data may be used either to control the attitude of the vehicle to some predetermined orientation or to provide directional inputs to the computer for the solution of the navigation problem. Following this, and depending on the location of the vehicle, any one of the methods shown under B, C, D or E may be used. (Primary attention is given in this report to the crossed-slit configuration with the possible addition of a third slit for navigation in the vicinity of planets. As seen in Table I-2, however, other configurations are more advantageous in particular circumstances. A wide variety of slit structures is presented in Section II.)

1. Satellite Navigation

When the vehicle is in the vicinity of a body (i.e., largely within

TABLE I-2

APPLICATIONS OF SCANNING CAMERA TO SPACE NAVIGATION

A. ATTITUDE DETECTION & CONTROL

1. SPIN STABILIZED VEHICLE
If the SCANNING CAMERA instrument is rigidly mounted on a spin stabilized vehicle, a measurement of the time of appearance of 3 stars suffices to uniquely determine the orientation of the vehicle as a function of time.

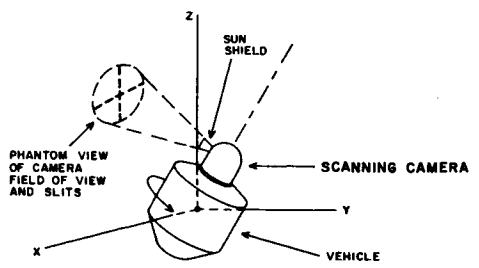

2. INERTIALLY STABLIZED VEHICLE
If the SCANNING CAMERA instrument is given a spinning motion relative to the vehicle, the three axes of orientation of the vehicle relative to inertial space can be determined and controlled.

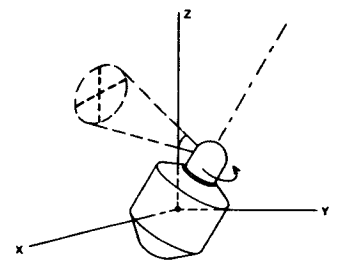

3. PLANET STABILIZED VEHICLE
If the scan field of the camera includes 2 non-parallel solar-system bodies, the orientation of the vehicle can be made perpendicular to the plane defined by Body No. 1, No. 2 and the vehicle. An operator can control the orientation about the yaw (z) axis to obtain the best viewing of one of the bodies - say the Moon in the instantaneous Earth-Moon-Vehicle plane.

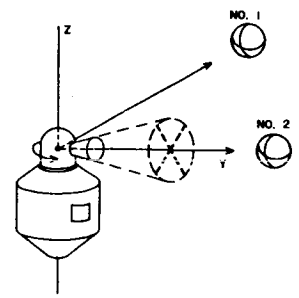

B. SATELLITE NAVIGATION

1. STADIMETRIC RANGING
By measuring the apparent diameter of a known (but not necessarily spherical) planet and measuring its direction relative to the stars, we can compute the position of the vehicle. To measure the diameter of the planet, a third slit must be added. This system is most advantageously used when the satellite altitude is between 1 and 10 planetary radii.

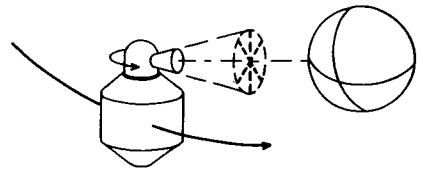

2. RADIAL (ROLL, PITCH) STABILIZATION
If the vehicle is radially stabilized by means of a horizon scanner and if the SCANNING CAMERA instrument is pointed radially outward, the satellite orbit can be determined by measuring the time at which stars cross the slits. The position of the vehicle is calculated indirectly by a dynamic method of orbit determination. In this case a circular slit can be used. This system is most advantageously used for low altitude satellites.

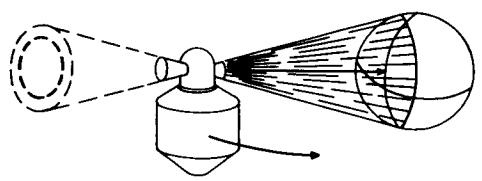

3. RADIAL (ROLL, PITCH, YAW) STABILIZATION
The vehicle can be roll and pitch stabilized relative to the instantaneous local vertical. It can be yaw stabilized relative to the orbit plane. In this case a dynamic orbit determination can be made similar to B-2. A crossed slit is preferable to a circular slit because of the resultant simplification of the equations for the orbit calculation.

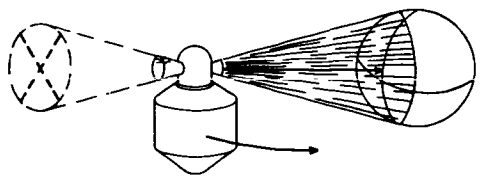

C. INTERPLANETARY NAVIGATION

1. TRIANGULATION
By measuring the positions of solar-system bodies relative to two known stars, it is possible to determine the position of the vehicle by simple triangulation. The greatest accuracy will be achieved if the closest nearly orthogonal solar-system bodies are used. Additional planetary targets will permit the use of a statistical technique (POLYANGULATION) in which a weighting factor proportional to the accuracy of each of the sight lines is used.

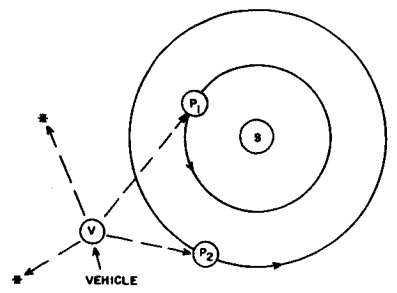

2. SOLAR-SYSTEM POSITION FIX
Without using star data, it is possible to accomplish a position fix from a measurement of the relative angles between 3 solar-system bodies.

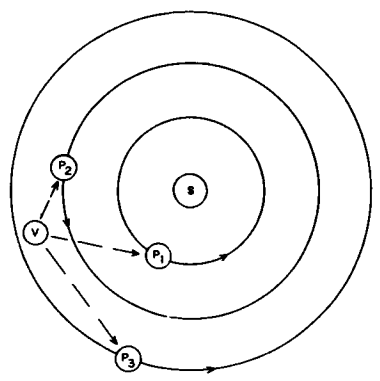

3. SOLAR-CENTERED (DYNAMIC)
If one axis of the vehicle is pointed toward the Sun and if the SCANNING CAMERA instrument is pointed in a diametrically opposite direction, then the measurement of the times at which 6 stars cross a circular slit suffices to calculate the position of the vehicle. Since this is a dynamic technique, the larger the motional arc in the heliocentric transfer orbit the greater will be the accuracy. No moving parts are needed for the application.

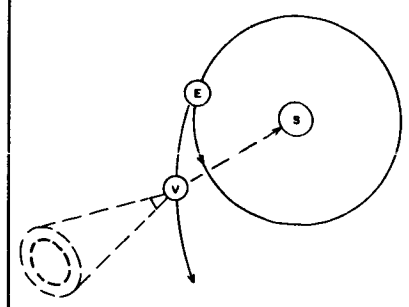

D. SURFACE NAVIGATION

1. LOCAL VERTICAL (NATURAL SCAN)
If the optical axis of the SCANNING CAMERA instrument is pointed outward in the direction of the gravity field and if the slit transit times for 2 known stars are recorded, the position of the vehicle can be computed. In this case the natural rotational motion of the planet provides the scanning motion. Depending on the distribution of bright stars and the planetary spin period, this method of position fixing might typically require 1 to 100 hours to complete.

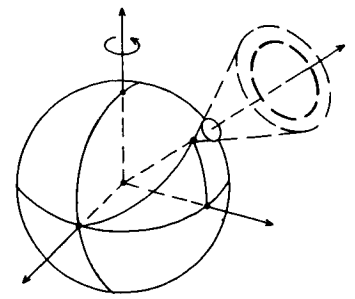

2. LOCAL VERTICAL (ARTIFICIAL SCAN)
This case is similar to D-1 except that the optical axis of the SCANNING CAMERA instrument is inclined at some unknown but comstant angle to the local vertical vector. By rotating the camera about the local vertical and measuring the slit scan times the position fix can be accomplished. This method of position fixing requires no longer than it takes to rotate the SCANNING CAMERA instrument through 3600, or typically 1 to 100 seconds.

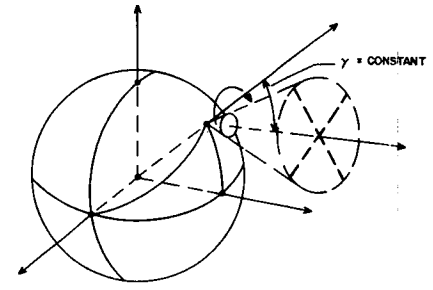

3. RANDOM ORIENTATION
If the vehicle carrying the instrumentation should be randomly oriented and lying on the surface of a solar-system body and if the SCANNING CAMERA instrument can detect star transits, then one can determine the direction and spin rate of the body. For example, one might have landed on the surface of a minor planet and wished to study its rotational motion or its orbital motion.

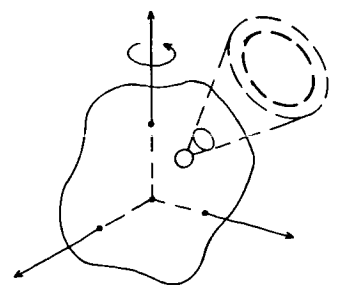

E. TRACK-WHILE-SCAN

1. RENDEZVOUS
As other space vehicles approach the vehicle on which the SCANNING CAMERA instrument is mounted, both bodies will increasingly be subjected to the same gravitational forces. To the extent that the differential accelerations are small, a passive ranging and position determination can be easily accomplished through the measurement of the angular position of the approaching vehicle on successive sweeps of the SCANNING CAMERA instrument.

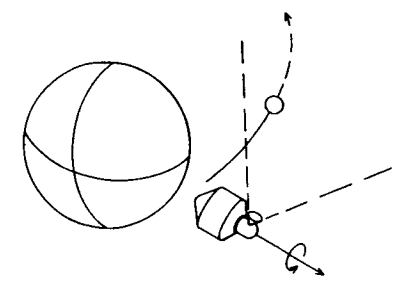

2. MULTIPLE TARGETS
In contrast with automatic tracking theodolites and similar devices with small fields of view, the SCANNING CAMERA instrument can monitor the positions of relatively large numbers of other space vehicles, ballistic missiles and the like. Provided sufficient solar reflection or self-illumination is available for accurate position measurement, their orbits can be calculated.

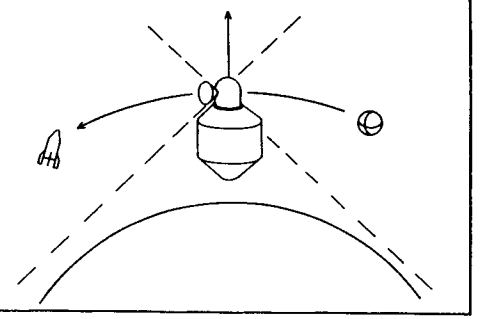

3. IMPACT AVOIDANCE
If the vehicle were to pass through a belt of asteroids, the problem of accidental impact presents itself. By calculations of the type described under E-1, it is possible to introduce impulsive changes in the orbit if a collision course with one of these minor planets is predicted by the computer.

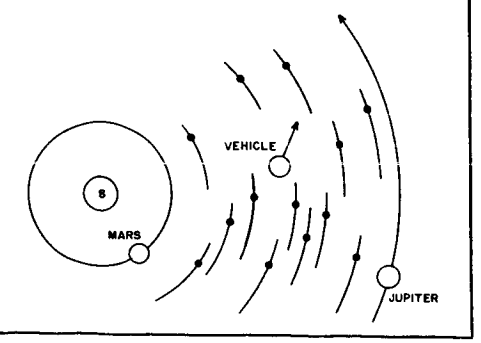

its gravitational control), there are two methods of navigation possible in addition to one similar to interplanetary position fixing. These are summarized in Figure I-9.

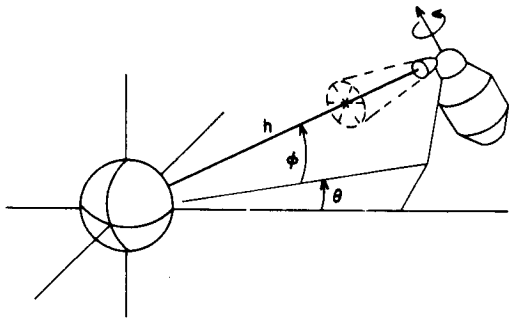

A. 3 SLIT METHOD ENABLES US TO MEASURE ANGULAR DIAMETER OF PLANET. STARS PROVIDE REFERENCE DIRECTION TO PLANET.

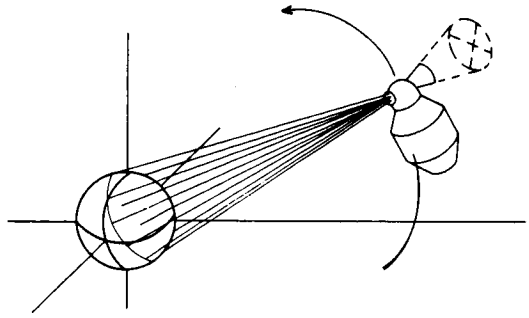

B. HORIZON SCANNER POINTS TOWARD LOCAL VERTICAL. TRACKER POINTS IN OPPOSITE DIRECTION AND MEASURES STELLAR SLIT SCAN TIMES.

Figure I-9. Methods of Satellite Navigation

The method shown in Figure I-9A involves the same operating mode as is used for triangulation except that a third slit is used to enable one to calculate the apparent angular diameter of the planet. Knowledge of the diameter suffices to determine the space vehicle distance from and direction to the planet after star reference data gives the necessary attitude. This method cannot be used at altitudes less than 1.44 planetary radii as is shown below. At altitudes greater than about 10 planetary radii the three-slit geometry intorduces errors which are greater than those resulting from two-body triangulation. Hence, the third slit

is useful over a limited range of altitudes or when the space vehicle is in the neighborhood of a planet.

The Three-Slit Method, or for that matter the Two-Slit Triangulation Method, breaks down after the space vehicle comes within a certain minimum distance from the planet. This occurs because the apparent image of the planet no longer can be made geometrically tangent to the two crossed slits. The minimum altitude may be written

$$h_m = R\left\{\sqrt{\left(\frac{\tan \alpha/2}{\sin \beta/2}\right)^2 + 1} - 1\right\} \qquad (1\text{-}1)$$

where the quantities in Equation (1-1) are as defined in Figure I-10. The

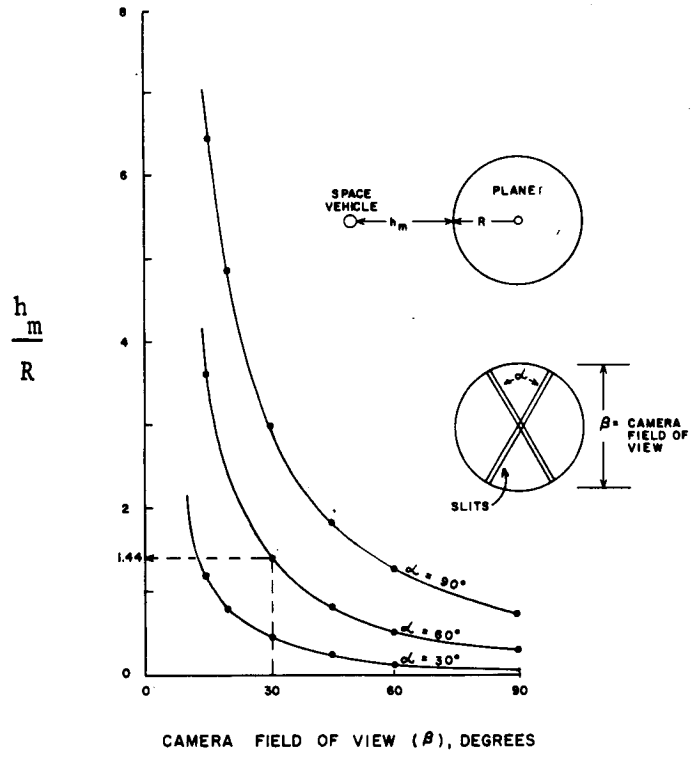

Figure I-10. Minimum Operational Altitude for Triangulation

dotted lines show that for the recommended optical design a minimum altitude of about 1.44 planetary radii can be achieved. The minimum altitude increases relatively rapidly as we cut down the field of view of the camera or as we increase the angle between the slits. Probably the lowest altitude one can hope to achieve with a high quality optical system (FOV = 50^{o}, slit angle = 30^{o}) is about .18 R. For the earth this implies a minimum altitude of 700 miles and the moon 200 miles.

The method shown in Figure I-9B involves essentially a different operating mode than does the triangulation technique or the direction-altitude technique and the minimum altitude considerations of Figure I-10 do not apply to this method. In this case it is assumed that an infrared horizon scanner continuously points the space vehicle at the planet center or more precisely radially inward. This is a natural operating mode when the space vehicle orbits about any celestial body and is frequently used on Earth satellites. The planet tracker is pointed opposite to the horizon scanner and measures the time of appearance of a minimum of three stars. From this data the orbital elements can be derived; from the orbital elements, the position of the space vehicle as a function of time can be calculated. This technique will work at any altitude where the vehicle orbit will maintain a reasonable amount of stability and at which the horizon scanner will return a continuous planetocentric orientation.

2. Interplanetary Navigation

To illustrate the use of the detection instrument for an inter-

planetary mission, an example was programmed on a Control Data 1604 computer. This example involves a rapid Earth to Mars transfer, a short waiting period at Mars and a slow return trip to Earth. The dates of departure and arrival are shown in Table I-3. This particular orbit was selected as a result of discussions with R. W. Gillespie using the criteria described by Breakwell, Gillespie and Ross,* and was made in order

1) to keep the duration of the round trip to approximately one year (rather than three years),
2) to achieve a minimum approach and departure velocity consistent with the one year round trip,
3) to launch at a time at which the orbit specifications are not changing rapidly,
4) to illustrate the triangulation geometry under a condition of rapid transfer (90 days) and relatively slow transfer (240 days), and finally
5) because it does not appear that a manned flight will be possible at an earlier date.

Had a 1965 launch date been assumed, a round trip of the order of 400 days would have resulted applying these criteria; had a 1971 launch date been assumed, a round trip of the order of 200 days could have been achieved. The selection of a ten day stayover at Mars was a matter of convenience

---

* Breakwell, J. V., Gillespie, R. W., Ross, S., "Researches in Interplanetary Transfer", American Rocket Society Journal, February 1961, pp. 201-208.

in using the ephemeris tables.

For these approximate trajectory computations it was assumed that the gravitational fields of the earth and Mars do not affect the transfer orbits. The inclination and eccentricity of the orbits were taken into consideration in these calculations.

TABLE I-3

SCHEDULE FOR INTERPLANETARY TRIP

	Date	Julian Day	Duration
Depart Earth	March 1, 1967	2439550	
			90 days
Arrive Mars	May 30, 1967	2439640	
			10 days
Depart Mars	June 9, 1967	2439650	
			240 days
Arrive Earth	February 3, 1968	2439890	

In Figure I-11 the positions of the earth, Mars and the vehicle are shown as a function of time. This figure is useful in studying the conditions for triangulation if one considers only the earth, Mars and the sun as possible target bodies. A more general presentation of the range and angle data is shown in Figures I-12 and I-13. Shown in dark lines are what appear to be the best targets for triangulation. However, as was described earlier, the position errors will be minimized if the least square polyangulation technique is used.

In making the decision as to which pair of planets might be most suitable for simple triangulation at any instant, the following three factors were considered:

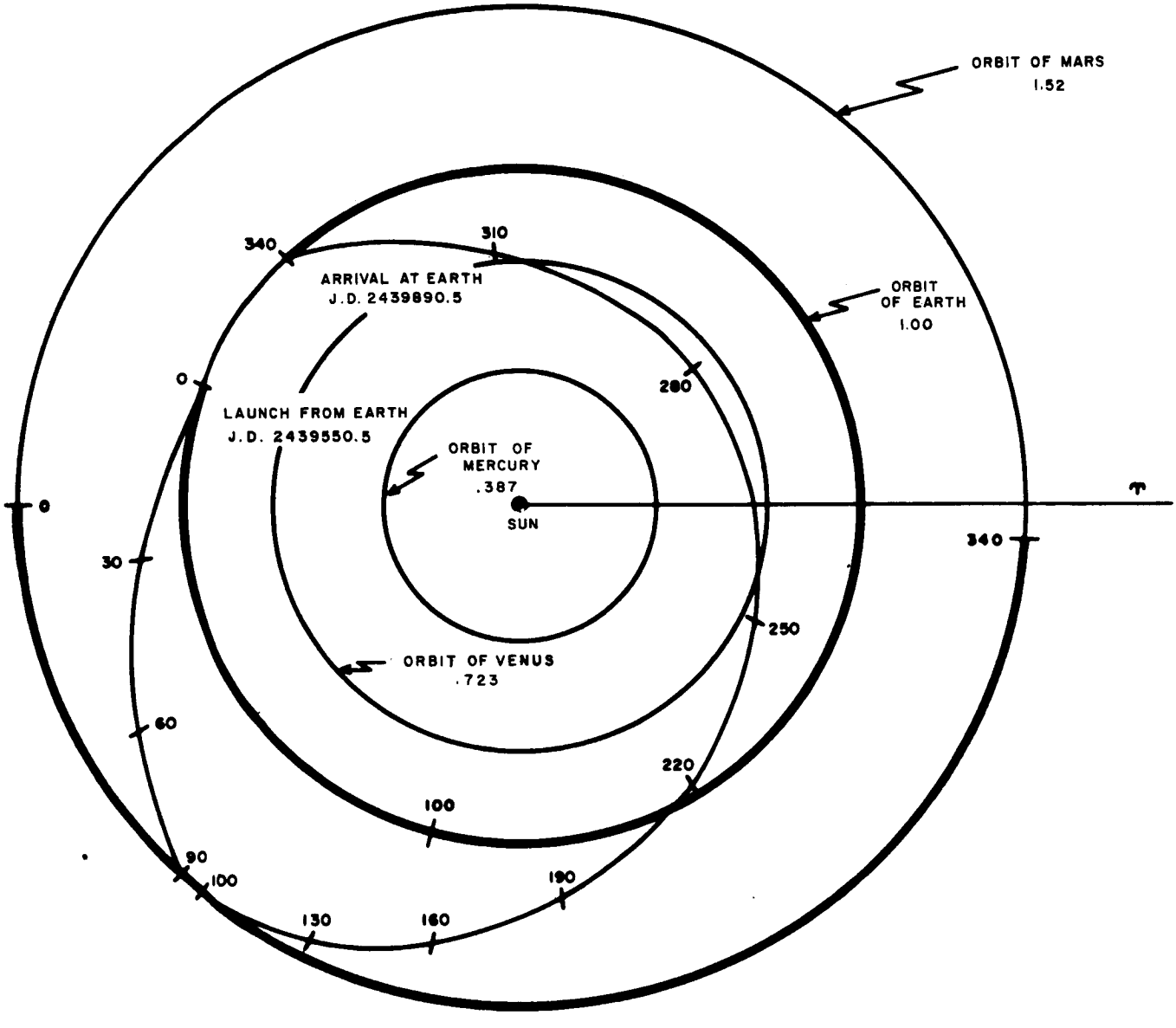

Figure I-11. Transfer Trajectories to and from Mars

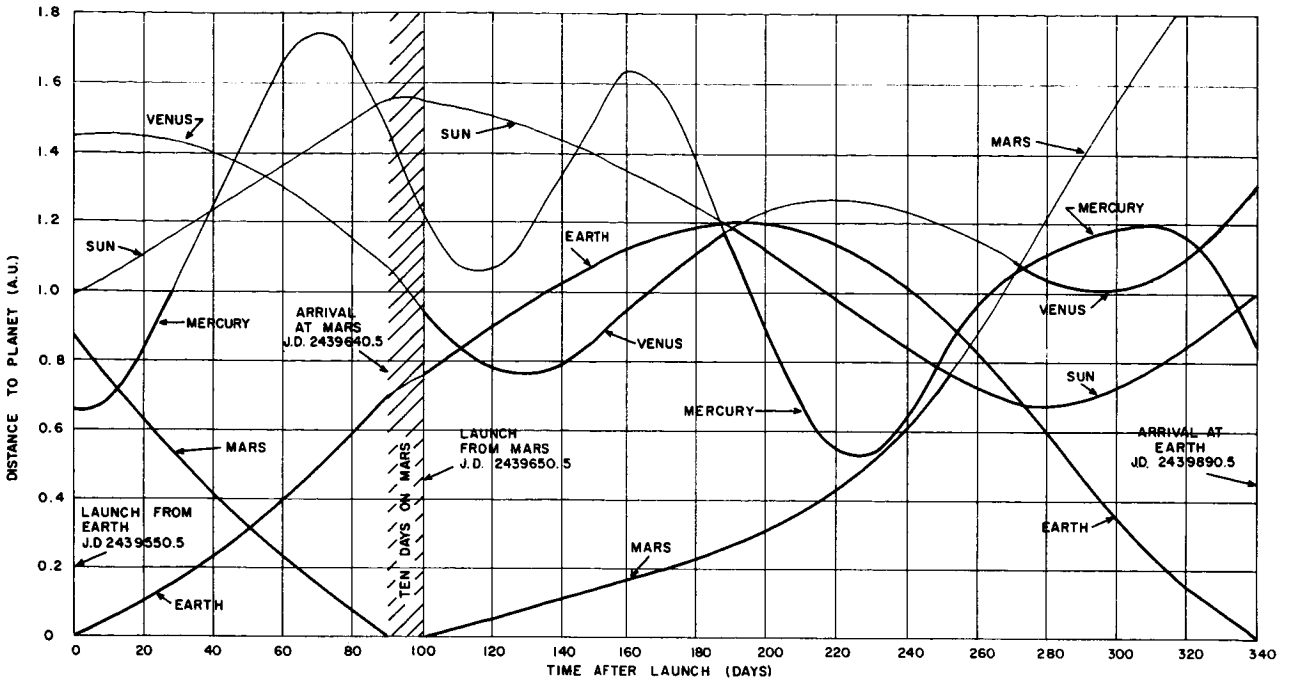

Figure I-12. Distance to Planets During Earth-Mars-Earth Transfer

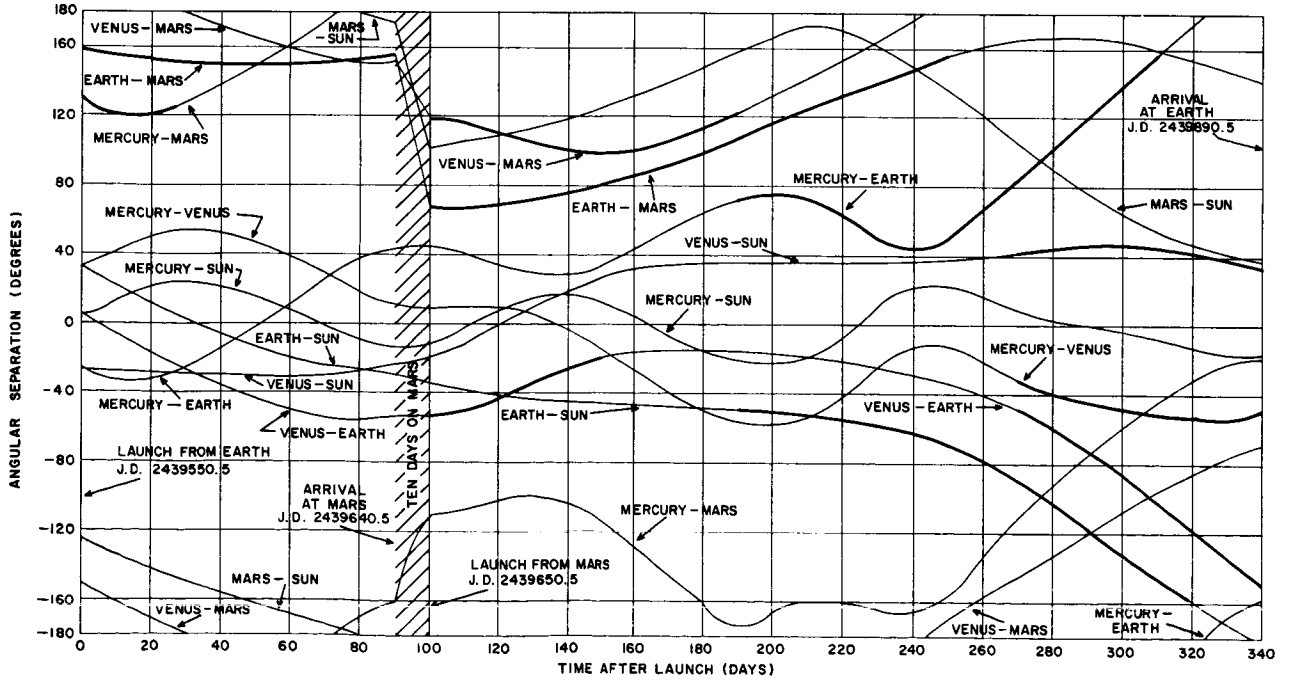

Figure I-13. Angular Separations of Planets During Earth-Mars-Earth Transfer

1) the included angle (angular separation)between the planets should be as close to 90^{o} as possible,
2) the range to the planets should be as small as posible, and
3) the angle between the planet and the sun should not be close to zero because of the background problem caused by sunlight entering the optical system.

3. Surface Navigation

After landing on the surface of a celestial body, there are three methods of employing the scanning camera for surface navigation. These are summarized in Figure I-14.

The first (Figure I-14A) utilizes a near-by body such as a moon in a manner similar to interplanetary navigation. The camera scans the sky in the region of the body and establishes a line of position. The observer's location is then the point of intersection of that line and the surface of the body on which the position is desired.

If the camera is pendulously supported as in Figure I-14B so that its rotational axis is parallel with the local vertical, and scanned conically about this vertical, it is possible to calculate the astronomic latitude and longitude of the observing station, as before, by measuring the slit scan times associated with at least two stars. Typically the optical axis is inclined upward at an angle of about 30^{o} to keep the scan region above the local terrain irregularities. The absolute elevation angle need not be accurately known during this operation; however, it is important that the scan axis be accurately aligned relative

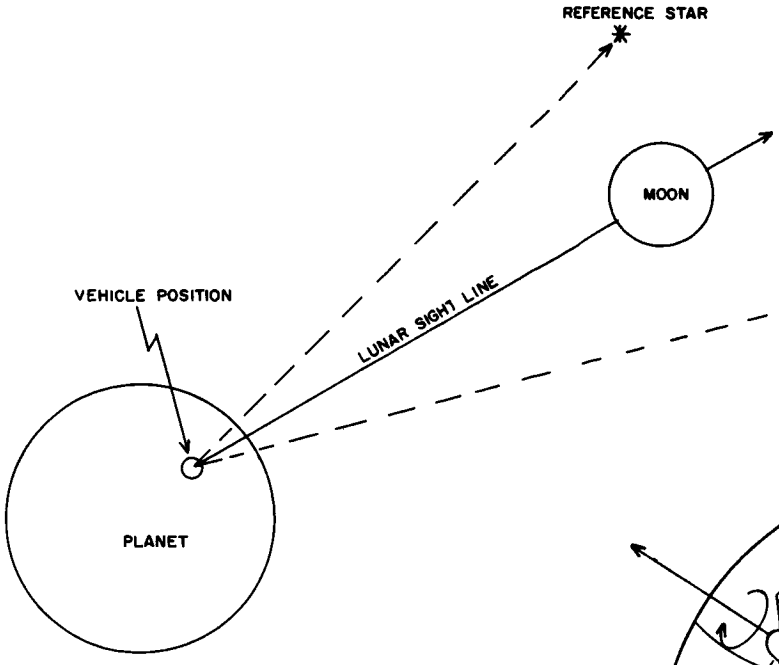

A. Surface Navigation Utilizing a Local Moon

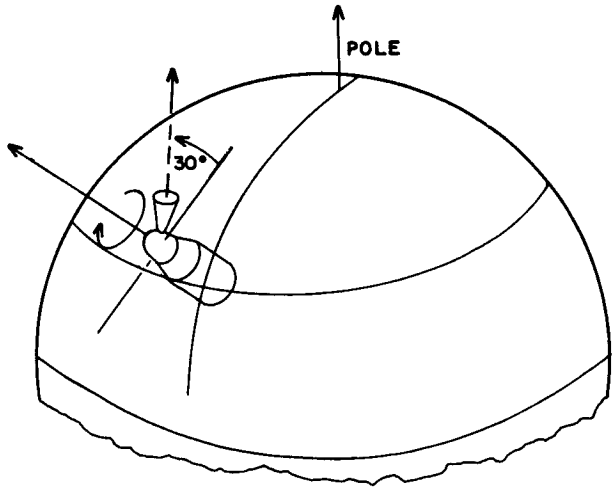

B. Scanning above Horizon

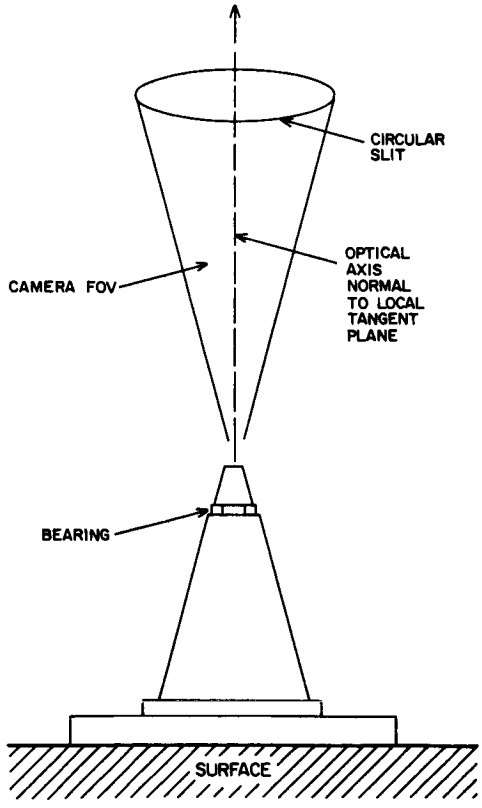

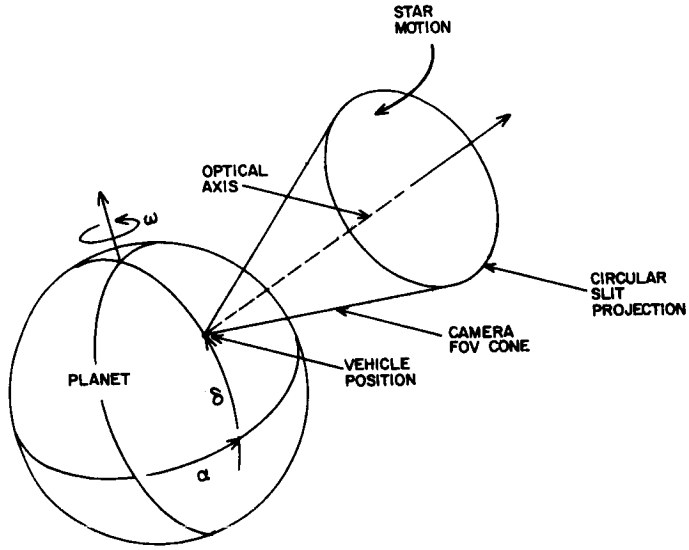

C. Scan Motion Provided by Body Rotation

Figure I-14. Application of Scanning Camera to Surface Navigation

to the local vertical. If the leveling errors can be kept small compared with the star transit time errors, an astronomic position measurement on the surface of the moon accurate to better than 100 meters could be achieved. A correction must be introduced because the rotational motion of the body changes the position of the stars during the period of one rotation of the camera. However, this correction is small for a body rotating as slowly as the moon.

A further variant is shown in Figure I-14C where the camera is stationary relative to the body and pointed vertically. The scanning motion is then provided by the rotation of the body itself, the transit times of stars being used to compute astronomic position as before.

4. Track-While-Scan Search

Thus far emphasis has been placed upon the use of the proposed instrument to measure the angular bearing of a limited number of targets whose positions are changing relatively slowly. In addition to these applications, the proposed instrument can be used to keep track of a multiplicity of targets which are distributed over a broad region of the sky and whose positions are rapidly changing. In fact, it is exactly in this type of operation that the proposed instrument finds its greatest advantage over a typical tracking theodolite with its narrow field of view and its inability to handle more than one target at a time.

If the camera were supplied with an elevation axis gimbal so that it could be used in a conical scan mode, it can perform a useful role in

rendezvous with other satellites and space vehicles. One assumes that the satellite on which the detector is mounted orients itself toward the sub-satellite point so that the scan region can be kept above the horizon.

C. Target Identification

The scanning camera measures both time of transit of the target across each slit and target magnitude. As mentioned previously, the times provide the basis for deriving accurate navigational information. In addition, the magnitudes are essential to permit the identification of the targets.

Since identification is a true example of data processing, a much more detailed discussion is presented in Section IV-B under Computer Requirements. We will give here, however, the main essentials and philosophy.

1. Technique of Identification

Assuming the scanning camera gathers data for several periods, there are three levels in the identification process. The first involves scan-to-scan correlation. It is planned that this will be accomplished by requiring that the two transit times (belonging to adjacent scan periods) be separated by one period to a high degree of accuracy, and that the magnitudes are comparable within a lesser accuracy requirement. Even with some precession, the data of adjacent periods should be accurately separated by one period, though data from widely diverse periods will not have an integral-period separation.

The next level of identification consists in matching the targets in one slit with those in another slit. This depends quite critically on the measured magnitude since the only general relation between the transit times of a single target across two slits is that the time difference

(corresponding to target elevation above or below the scan plane) cannot exceed some maximum value (achieved when the target transits the tips of the slits). To help at this level, we therefore only accept slit matches which are unambiguous, i.e., which do not involve more than one target in each slit.

The third level, the association of measured targets with actual targets in the catalog, is shown in sequence in Figure I-15. Of the unambiguously matched targets between the two slits, the three brightest are chosen and their mutual angular separations computed using the measured transit times.* The star catalog is then searched to find a triplet of stars having the same mutual separations. The search is based upon measured magnitudes, and can be visualized with the use of a "magnitude matrix" as shown in Figure I-15. This is merely an array whose columns and rows are labeled with the stellar catalog magnitudes and whose entries are the angular separations of star pairs belonging to the row-column intersections. Therefore, by using the measured magnitude of a particular star pair to enter the matrix, and then by comparing the measured angular separation with the matrix entry, one can tell, within limits, if the catalog pair matches the measured pair. If it does not, then the magnitude matrix is searched in the neighborhood of the measured magnitude pair until a match is found. When two targets have been tentatively so

---

* Since it is possible that some planets may appear to be stars (see Section I-D), these are combined with actual stars to form the 'star catalog' mentioned in this section . (See Section IV-B.)

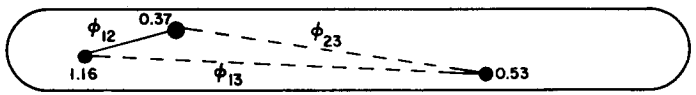

1. Discard all but brightest three stars of magnitude $\leq$ 0.0.

2. Calculate angular separation of brightest two stars (ϕ_{12}) based on instrument measurement.

3. Initiate search from star catalog. (Compare only those stars with magnitude comparable with measured magnitudes.)

4. Compare angular separation based on measured value with angular separation based on catalog value.

CATALOG MAGNITUDES

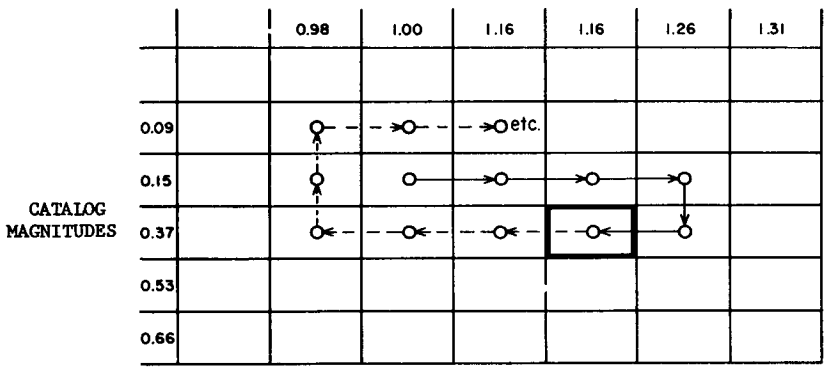

MAGNITUDE MATRIX

5. When angular separation compares with descrimination limit δ, the first two stars are assumed tentatively identified. (In the example, six pairs were searched before this happened.)

6. Next, the remaining target is paired with one of the others (say Star 3 is paired with Star 2) and steps 3 and 4 are repeated. (Star 2 is assumed to be already identified, so the search is only one dimensional.) If search region is exhausted, return to step 4 and continue search along dotted line.

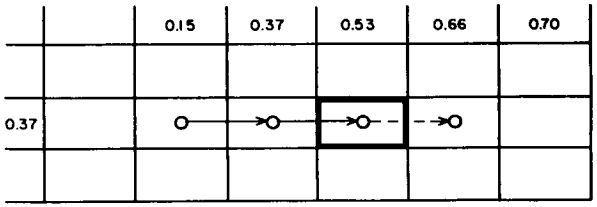

7. Finally, a consistency check is performed by comparing the measured angular separation ϕ_{13} with its catalog counterpart. If this passes, triplet is identified. If consistency check cannot be satisfied, go back to step 6 and continue search along dotted line.

Figure I-15. Sequence of Identification of Three Bright Stars

identified, the third measured target is paired with one of them and the process repeated. This time, only a row of the magnitude matrix need be searched since it is assumed that one star is already identified. If this search is also successful, then one checks to be sure that the remaining untested angular separation is in agreement. If it is, then the triplet is said to be identified and the identification of the remaining targets is easy (see Section IV). If at any stage, an inconsistency is found, or the searches exceed their limits, then the technique reverts to a continuation of the previous step. In this way, allowance is made for numerous mistakes, since the final triple match of all the angular separations is nearly impossible without the correct targets. Of course, it is always possible that no identification can be achieved in which case the navigator must exercise some judgment. However, this almost never happens as is seen from Section III-E where the results of a computer simulation of this very process are discussed.

2. Ambiguities

Some rationale for the identification technique discussed above can be derived from an examination of appropriate statistics of the brighter stars.* We have analyzed, via a simple computer program written for the Control Data Corporation 1604, the angular separations and magnitudes of the fifty brightest stars. There are $n(n-1)\frac{1}{2} = 1225$ such separations

* Experimental verification (dependent, of course, on achieved instrumental accuracies) is given in the simulation of Section III-E.

which are distributed between 0^{o} and 180^{o} as shown in Figure I-16. Theoretically, of course, the distribution is proportional to the sine of the angle which is also shown.

Figure I-17 is an approximate plot of the number of separations which are within a certain number of minutes of arc of each other. For example, if an angular separation of ten degrees is measured between a pair of stars, and it is expected that this measurement could be in error by as much as twenty minutes of arc, then there are two pairs which could give rise to this measurement. That is, two ambiguities in the identification of star pairs by their angular separation alone exist for a twenty minute of arc error at ten degrees separation. We see that on the average, an accuracy of ten minutes of arc will permit only four ambiguities.

Ten minutes of arc is large compared to the measurement accuracy of the camera--ten seconds of arc. The smaller value, however, relates to the ability to locate a target if attitude were known. Now during the identification process, the camera motion will be assumed to be one of uniform rotation about a stationary axis. This conforms with reality in the case where the camera is mounted on an inertial platform. Then the angular separation of two targets is given correctly by their apparent elevations and azimuths. If the camera is, however, freely spinning, then some small amount of precession may be present in which case the angular separation of two targets is not so simple. Thus we may be forced to accept a larger error in the approximate separations than might be implied by the camera accuracy. This, of course, does not degrade the final

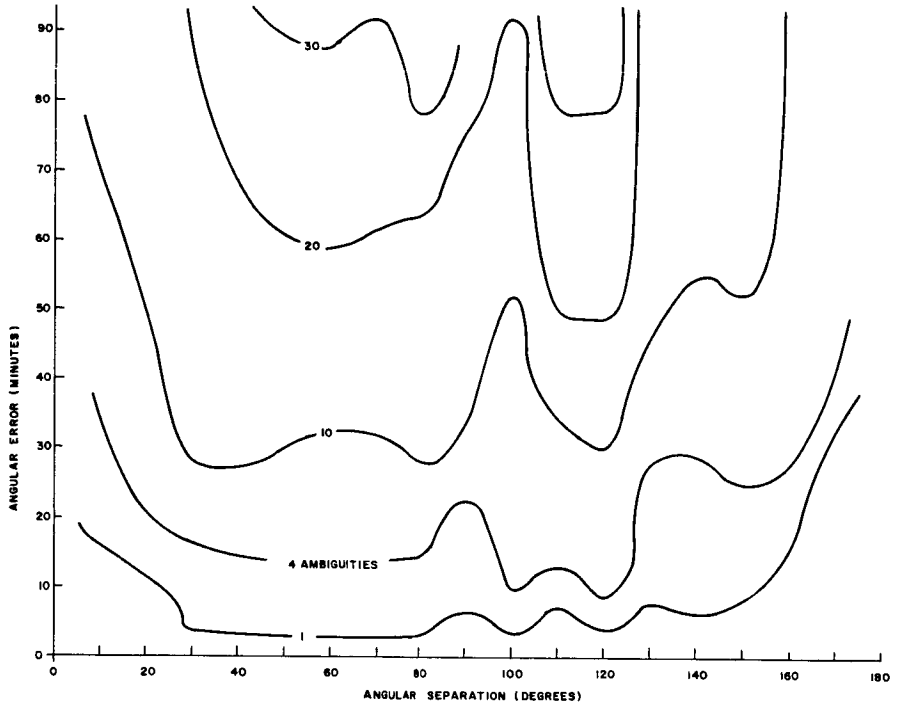

Figure I-17. Pair Ambiguities for Angular Separation Measurement Error

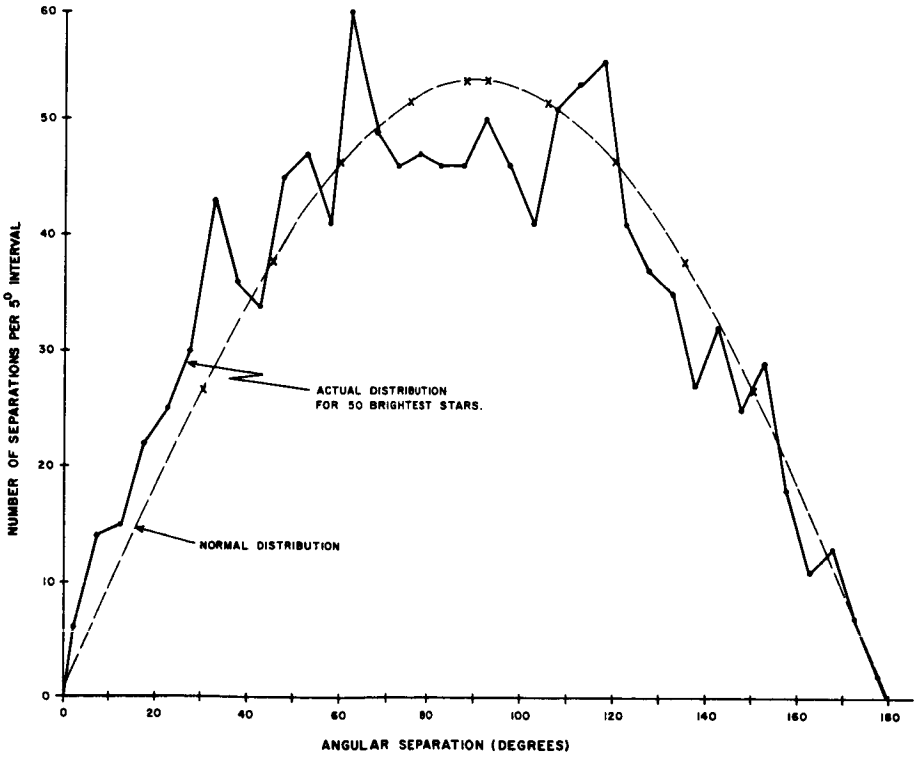

Figure I-16. Distribution of Angular Separations Between Fifty Brightest Stars

navigational accuracy of the system, but could prolong the identification process due to wide acceptance limits on the separation.

The star magnitude or intensity is also measured by the instrument. If the accuracy of this is $\pm$ .10 magnitude (10% in intensity), the remaining ambiguities are shown in Figure I-18. This figure indicates those pairs of angular separations (two separations, four stars) which differ by a small amount and at the same time have component magnitudes which are also close. For example, the point at .15 magnitude and 22 seconds of arc means that two pairs of stars have separations differing by only 22 seconds of arc, while all four magnitudes are within .15 magnitude of each other.

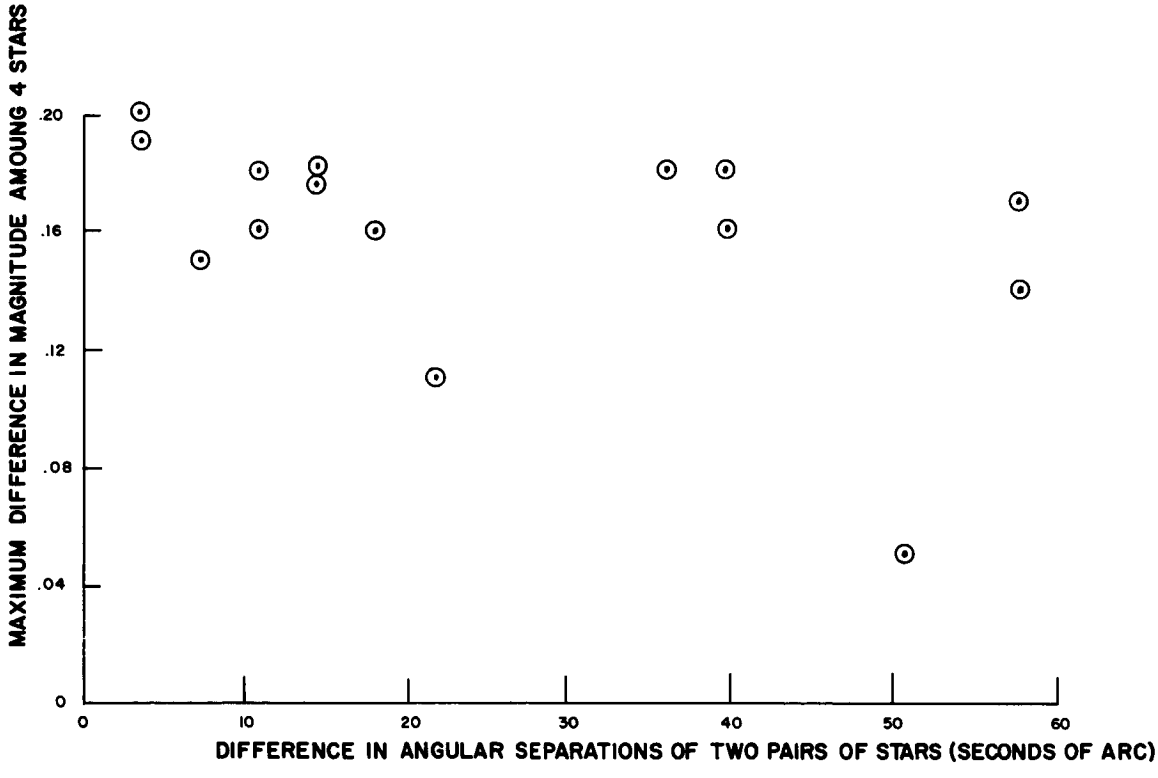

Figure I-18. Differences in Magnitude Between Star Pairs Having Similar Angular Separations

As a result, we may draw the following conclusion: if it is possible to measure angular separations to an accuracy of $\pm$ 10 seconds of arc and if it is possible to measure star intensities to an accuracy of $\pm$ .07 magnitude, then one can uniquely identify any of the star pairs arising from the fifty brightest stars which are needed for attitude determination. Since our calculations show that the contribution of the instrument error in the angular separation determination can be held to this value, and since it appears that we can measure intensity (or intensity ratio) to an accuracy of $\pm$ 10%, it appears that we can make a unique identification from only two stars for almost all of the cases encountered. Actually, this is not needed, because we require the existence of a third star for a consistency check, and as was shown in Figure I-15, if the consistency check is not satisfied it will only be necessary to revert to a previous step and continue the computer search. The existence of variable aberration, proper motion, variable star intensity, variable planet intensity and position will all tend to create conditions in which a mistaken initial identification of the first two stars can result. However, if the logical capability of the computer is properly used this will not result in a basic error in the identification but will merely cause a slight increase in the time required to achieve a unique identification.

The number of star angular differences increases an $n(n - 1)\frac{1}{2}$ where n is the number of stars. This raises the question as to whether the number of similar star angular differences which match within a discrimination limit δ, say one minute of arc, is more nearly proportional to $n^{3.5}$.

This means that any enlargement of the basic list of stars as a means of decreasing the field of view of the camera, or for some other reason, will result in a substantial increase in the difficulty of star identification.

To see why this occurs, consider the following. Figure I-16 shows the relation between the number of stars per unit angular interval versus the angular separation for the list of 1225 angular separations. Theoretically, one would expect this distribution function to follow a sinusoidal curve, as it does, with amplitude given by

$$A = \frac{1225}{2 \sum_{n=0}^{17} \sin 2.5\ (2n + 1)} \doteq \begin{array}{l}\text{53 star angular differences per } 5^{\circ} \text{ at the maximum of the sine curve.}\end{array} \qquad (1\text{-}1)$$

Since the expected number per unit interval is not a constant, one cannot apply the Poisson distribution in its simple form. However, most of the small differences in angular separation will occur in the central region where the angular separation is between 45° and 135°. Thus, if we deal with this interval we can write approximately

$$f(x) = \frac{m^{x}\ e^{-m}}{x!} \qquad (1\text{-}2)$$

where f(x) is the probability that x stars will fall within the interval y degrees. m is the average number of star angular differences per y degree interval. Since $m \doteq 50$ star differences per 5 degree interval (= 0.1 star difference per .01 degree interval), we may write

$$f(x) = \frac{0.1^{x}\ e^{-0.1}}{x!} \quad . \tag{1-3}$$

If we take a region which is 10^4, .01 degree intervals wide (100°), the expected number of cases in which two star pairs have similar angular separations within .01 degree is

$$E \approx 10^4\ \frac{0.1^{2}\ e^{-0.1}}{2!} \approx 50 \quad . \tag{1-4}$$

The cumulative value given on the basis of actual data in Figure I-16 is 78, so we know that this is the correct order of magnitude.

The value of $m = \frac{n(n-1)}{12250}$ is the number of star differences per .01 degree interval for any value of n. If we consider only those cases in which two pairs have similar angular separations (rather than 3, 4, etc.) we may write

$$E \approx 10^4\ \frac{m^{2}\ e^{-m}}{2} \quad . \tag{1-5}$$

If we take the ratio of the expected number of similar angular separations for n stars to that for fifty stars we obtain

$$\frac{E_n}{E_{50}} \approx \left(\frac{n}{50}\right)^4 \exp\left[\frac{-(n^2 - 50^2)}{1225 \times 10^4}\right] . \tag{1-6}$$

If $n \approx 50$, the effective value of the exponent is 4, if $n \approx 75$, the effective value of the exponent is about 3.5, if $n \approx 10^2$ the effective value

of the exponent is about 3.

D. Characteristics of Celestial Targets

To complete the general description of the scanning camera navigation system, some discussion of the types and characteristics of the targets to be used is necessary. These targets are divided into two classes: self-luminous bodies (stars, excluding the sun), and those which are detectable by reflected energy (planets, moons, asteroids, etc.). The stars are considered as point sources radiating in the optical region of the electromagnetic spectrum and relatively stationary against the celestial sphere. Their interesting characteristics are: magnitude as seen by the sensor, position, and motion. The planets and other solar system bodies reflect solar light by various means (atmospheric scattering, surface reflection), possess differing shapes, and in general have a great amount of relative motion. The interesting quantities here, then, are: orbits, shape, and albedo or reflectance (both absolute and also as a function of phase angle). It is not our intention here to present a set of finalized parameters but merely to indicate what should be considered in using celestial bodies for navigation.

1. Stars

The positions of stars are given in Right Ascension (hours, minutes, seconds) and Declination (degrees, minutes, seconds) relative to the first point of Aries and the earth's equator. For actual use in celestial navigation a catalog must be compiled listing these positions for some epoch.*

---

* For a review of the use of stars and planets in space navigation systems, see Naqvi, A. M. and Levy, R. J., "Some Astronomical and Geophysical

Along with this, the proper motion of the star, the direction of this proper motion, and the distance of the star from the solar system should also be included. These are needed for correcting the catalog positions as discussed in Section III-B.

The intensity or magnitude of each star as seen by the optical system-photomultiplier detector depends upon two factors: the spectral distribution of energy emitted from the star itself and the wavelength response of the sensor. Some representative stellar energy distributions are shown in Figure I-19 where it can be seen that most of the energy from A or B type distributions falls in the wavelength region 0.3 to 0.5 micron Figure I-20 gives the response for an S-4 detector which will be quite similar to that for the proposed system. We see that it matches the output of star types A and B quite well but will not respond to type K or M stars very strongly. Thus for a given total amount of emitted energy, a type A star will appear much brighter than a type K star to a system with an S-4 response.

Double stars do not cause difficulties in the proposed system for two basic reasons: (1) in most double star systems the magnitude of the secondary components is sufficiently far below the threshhold of the detector as not to be sensed, and (2) those which are of sensible intensity are closer to the primary than the resolution of the camera and so will constitute

---

Considerations for Space Navigation," IEEE Transactions on Aerospace and Navigational Electronics, September 1963, p. 154. A listing having the accuracies desired in space navigation systems is FK4-Vierter Fundamentalkatalog, Astronomisches Rechen-Institut, Heidelberg, Germany; 1961.

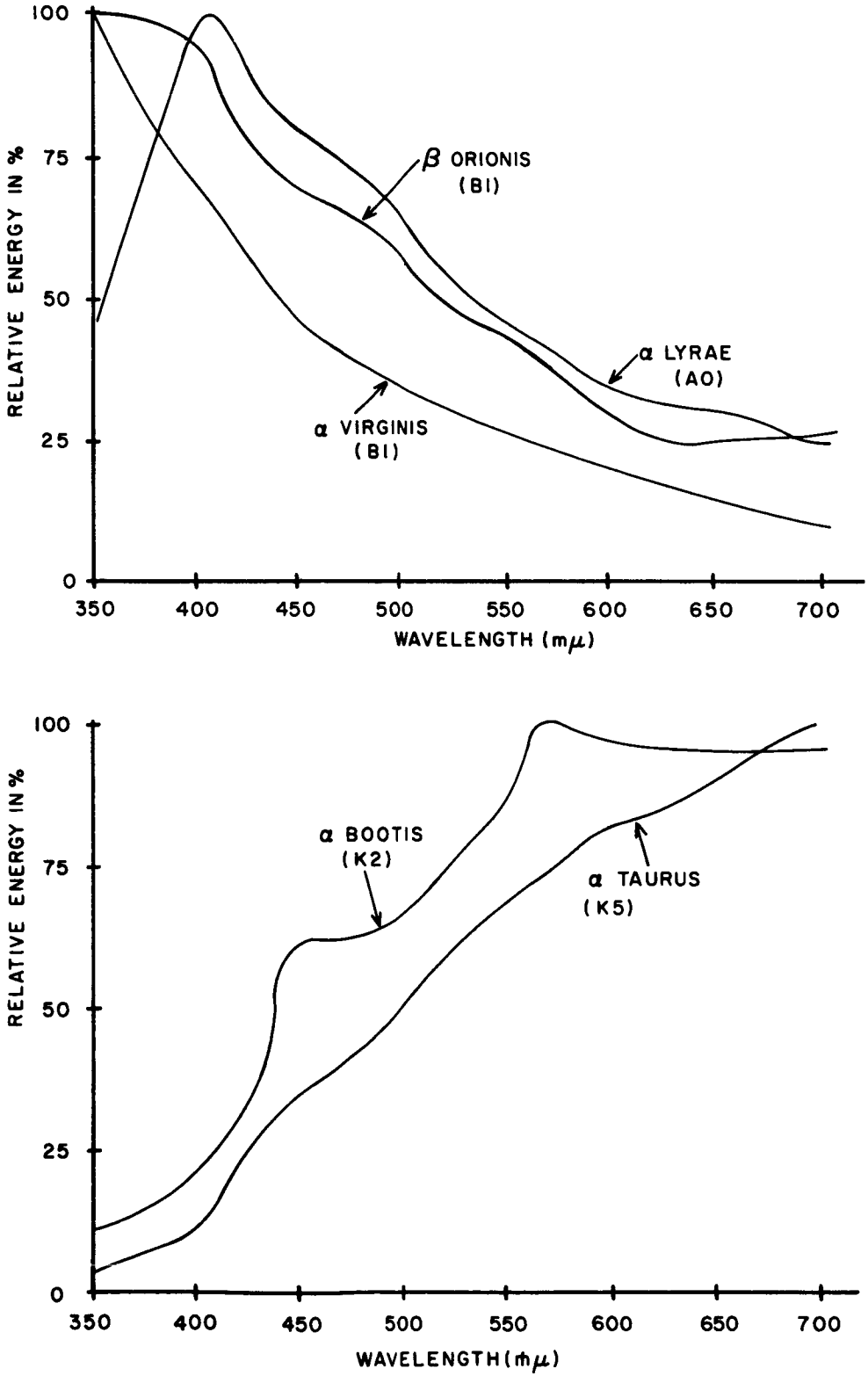

Figure I-19. Spectral Energy Distribution for Several Stars

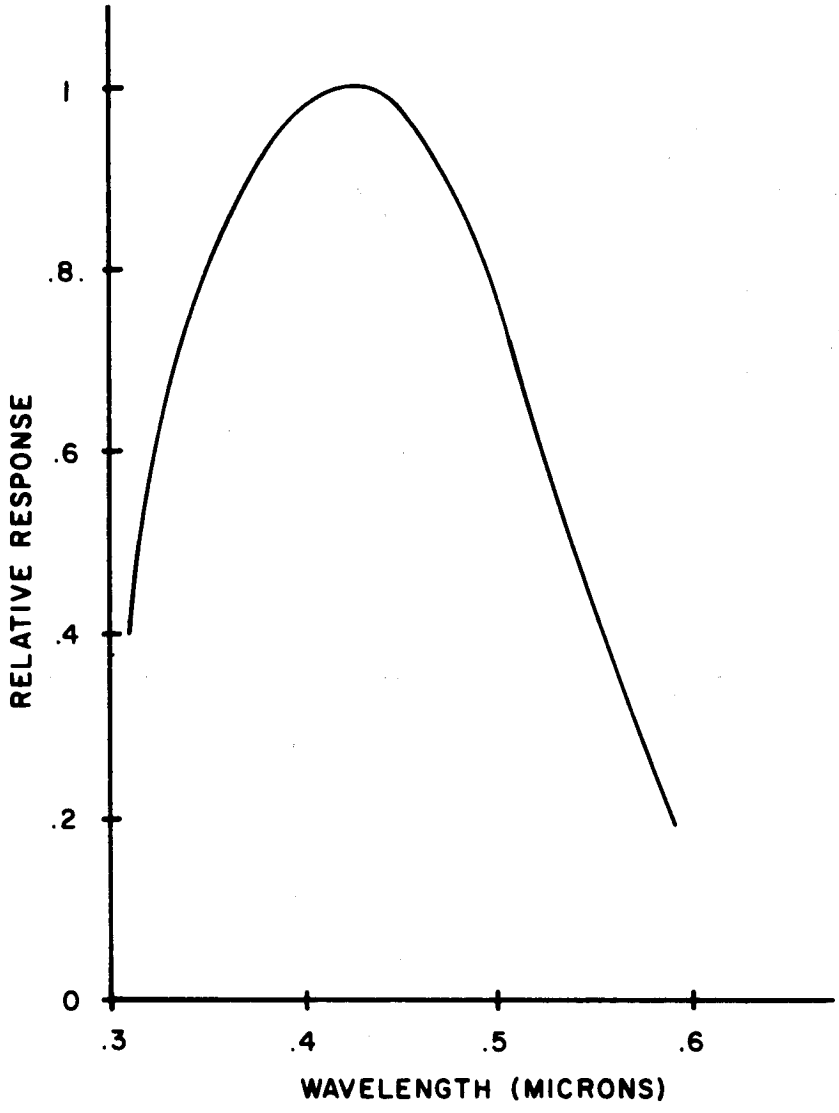

Figure I-20. Relative Response versus Wavelength for S-4 Photocathode Surface

a separate target. The principal aspects for which care must be taken are (1) orbital motion of the primary and (2) magnitude variation in the primary due to eclipse. Both of these are, however, well known quantities for the brighter more interesting stars and are hence easily incorporated as corrections.

2. Planets

"Planets" can be divided into two groups. The major planets are Mercury, Venus, Earth, Mars, Jupiter, Saturn, Uranus, Neptune, and Pluto. The minor planets include the moons, asteroids, etcetera.

Planets have several characteristics which are interestering. Table I-4 gives the equatorial radius, ellipticity, and the inclination of the equator to the orbit for the major bodies.* Also listed are the orbital characteristics of the planets showing their time dependence (T measured in centuries from 1900).** For actual use in space navigation, an ephemeris of the planets (or a set of equations from which one can be calculated) must be available to the on-board computer.

The relative size of the planets is a function of the distance of the observer. Figure I-21 shows the relative minimum and maximum sizes of the planets as they would appear to an observer at distance D from the sun with the planet at a distance r_p from the sun. (See sketch.) It is expressed in Equation (1-7)

$$\rho = \frac{R}{r} \times 2 \times 10^5 \text{ arc seconds} \qquad (1\text{-}7)$$

---

* Allen, C. W., Astrophysical Quantities, The Athlone Press, London, (1963), p. 142.

** Clark, Jr., V. C., et al., "Design Parameters for Ballistic Interplanetary Trajectories. Part 1. One-Way Transfers to Mars and Venus," Jet Propulsion Laboratory Technical Report No. 32-77, January 16, 1963, p. 12.

TABLE I-4

ORBITAL AND PHYSICAL CHARACTERISTICS OF PLANETS

Planet	Semimajor axis a, AU	Sidereal Period, Tropical Years	Mean Orbital Velocity, km/s	Eccentricity e	Inclination to ecliptic i, deg.	Longitude of ascending node Ω, deg.
Mercury	0.387099	0.24085	47.90	0.205625+0.000020T[a]	7.003819+0.00175T	47.737778+1.18500T
Venus	0.723332	0.61521	35.05	0.006793-0.000050T	3.394264+0.00125T	76.236389+0.90556T
Earth	1.000000	1.00004	29.80	0.016729-0.000042T	0	0
Mars	1.52369	1.88089	24.14	0.093357+0.000094T	1.849986-0.000639T	49.173611+0.77389T
Jupiter	5.2028	11.86223	13.06	0.048417+0.000164T	1.305875-0.005694T	99.948611+1.01056T
Saturn	9.540	29.45772	9.65	0.055720-0.000345T	2.490583-0.003889T	113.226806+0.87306T
Uranus	19.18	84.013	6.80	0.0471 +0.0002T	0.772792+0.000639T	73.726528+0.49861T
Neptune	30.07	164.79	5.43	0.00872 +0.00004T	1.774486-0.00953T	131.230833+1.09889T
Pluto	39.44	248.4	4.74	0.247	17.140000-0.00556T	109.633750+1.35806T

	Argument of perihelion ω, deg.	Planet at 1950 Jan 0.5 L	Radius (equatorial) R_e km	Ellipticity $\frac{R_e - R_p}{R_e}$	Inclination of Equator to Orbit
Mercury	28.937778+0.36944T	33°10'06"	2,420	0.0	-° -'
Venus	54.619305+0.50139T	31 34 19	6,100	0.0	23 ?
Earth	102.078056+1.71667T	99 35 18	6,378	0.0034	23 27
Mars	285.965000+1.06667T	144 20 07	3,380	0.0052	23 59
Jupiter	273.577222+0.59944T	316 09 34	71,350	0.062	3 05
Saturn	338.850694+1.08528T	158 18 13	60,400	0.096	26 44
Uranus	96.129028+1.11250T	98 18 31	23,800	0.06	97 55
Neptune	272.935934-0.43222T	194 57 08	22,200	0.02	28 48
Pluto	113.860694+0.03083T	165 36 09	3,000		

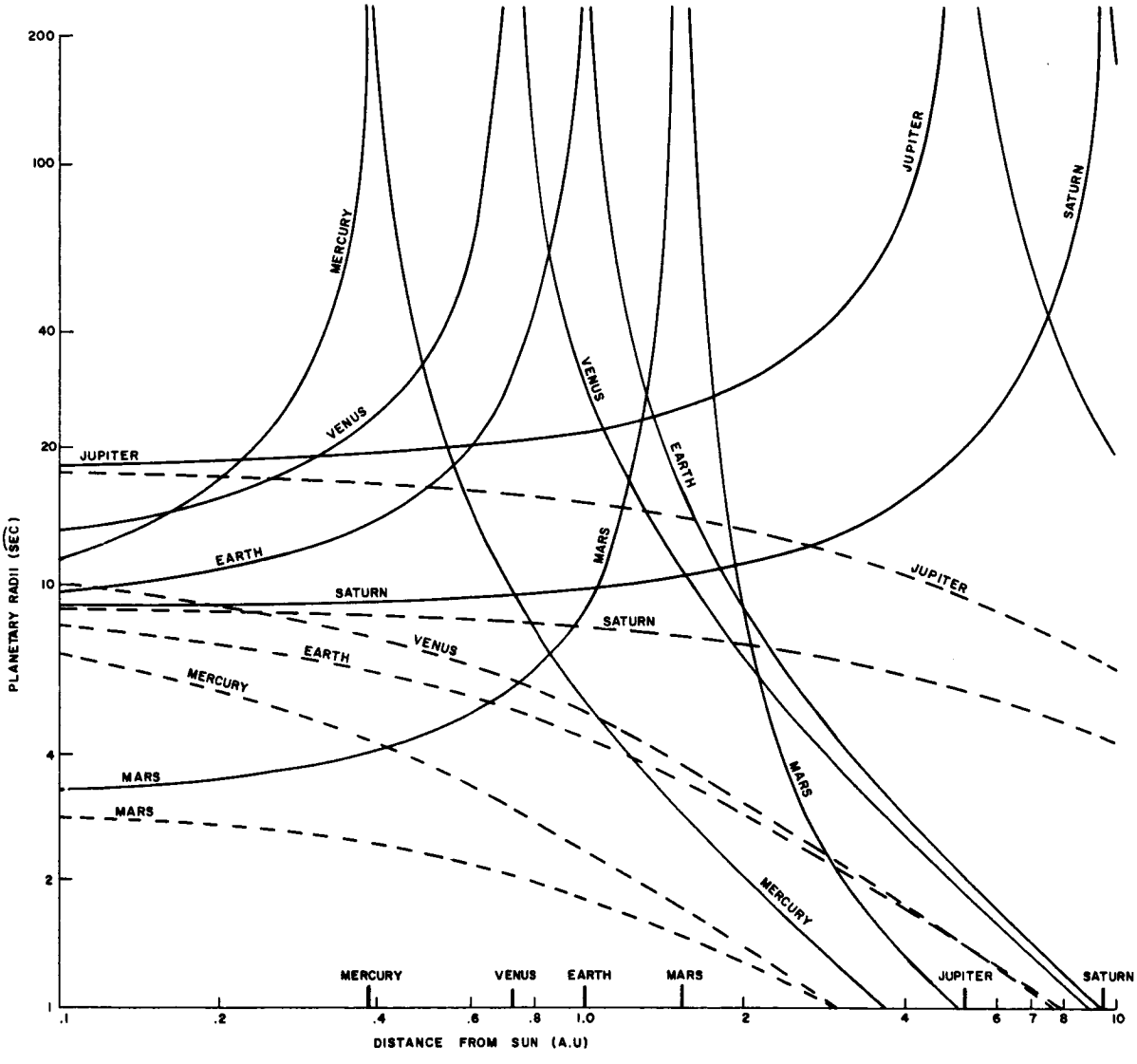

Figure I-21. Range of Planet Sizes as Function of Vehicle Distance from Sun

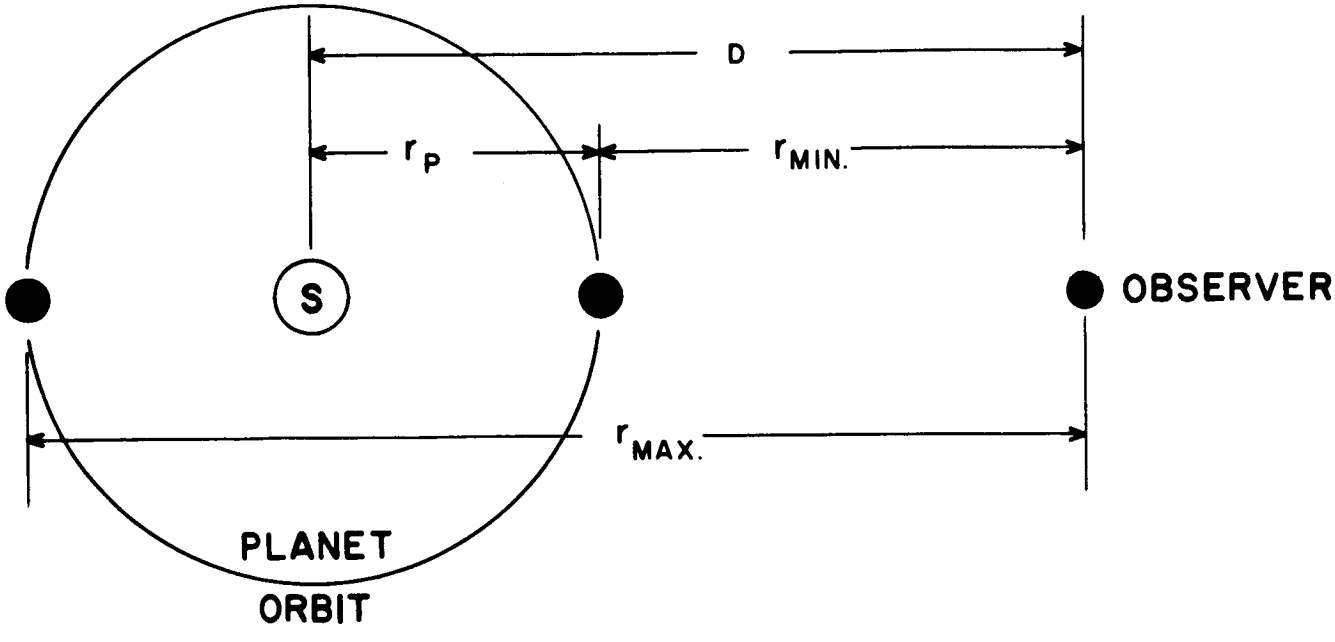

where $r = D \pm r_p$. Here ρ is the relative size of the planet in seconds of arc. The dotted lines represent the minimum size of the planet (i.e., where $r = D - r_p$) and the solid lines represent the maximum size ($r = D + r_p$).

Another planetary characteristic is that of illuminance or magnitude. The V magnitude (on the scale of Johnson and Morgan*) can be expressed as:

$$V = V(1, 0) + 5 \log r_p r + \Delta m(\alpha) \qquad (1\text{-}8)$$

where V(1, 0) is the magnitude of the planet when it is at unit distance from both the sun and the observer (see Table I-5),** r_p is the planet's distance from the sun, r is the planet's distance from the observer, and

---

* Johnson, H. L. and Morgan, W. W., "Fundamental Stellar Photometry," Astrophysical Journal, Vol. 117, (1953), p. 313.

** Planets and Satellites, edited by G. P. Kuiper and B. M. Middlehurst, University of Chicago Press, (1961).

TABLE I-5

MAGNITUDES OF THE PLANETS

Name	V(1, 0)	V (Observer at Sun)
Mercury	-0.36	-4.48
Venus	-4.29	-5.70
Earth	-3.87	-3.87
Mars	-1.52	+0.31
Jupiter	-9.25	-2.09
Saturn	-8.88	+0.92
Uranus	-7.19	+5.64
Neptune	-6.87	+7.91
Pluto	-1.01	+14.95

the solar phase angle, α, is the angular distance at the planet subtended by the observer and the sun. $\Delta m(\alpha)$ is the change in magnitude as a function of the solar phase angle ($\Delta m(0) = 0$).

Figure I-22 shows the maximum and minimum magnitude of the planets as seen by an observer located as in the above sketch. (The phase angle α is always assumed equal to zero.) The minimum magnitude is taken as the value when the planet and observer are on opposite sides of the sun. The maximum value occurs for the observer situated between the sun and the planet and is not presented when the observer passes beyond the planet. Thus no examination is made of phases near 180° for small vehicle-planet

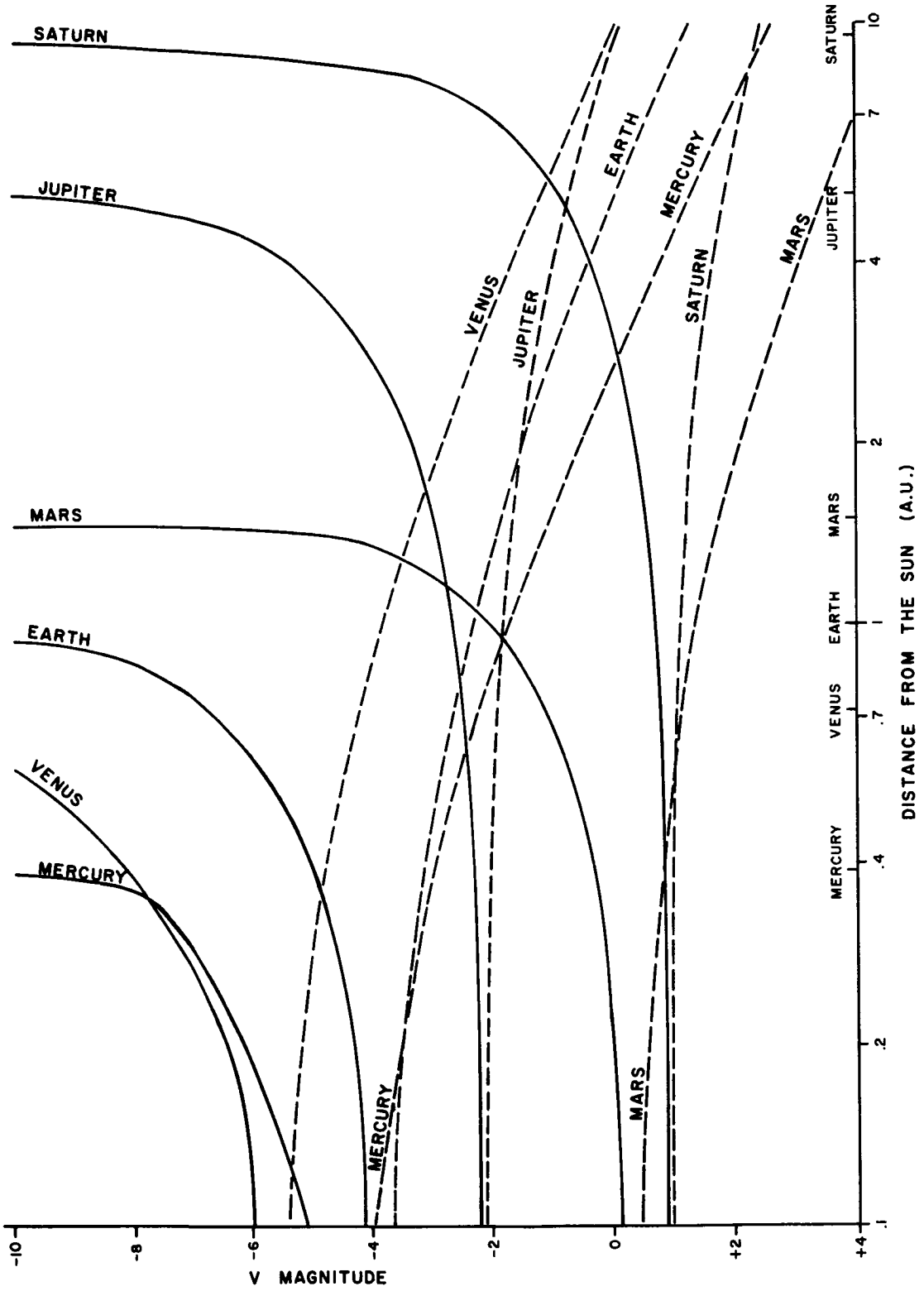

Figure I-22. Minimum and Maximum Planetary Magnitudes as a Function of Vehicle Distance from the Sun

separation.

Since all minor planets in our solar system cannot possibly be studied, a list of Selected Minor Planets is given in Table I-6.* The symbol m_{pg} at $r\Delta = 1$ is the magnitude of an asteroid, obtained by correcting the observed magnitude (m_{pg}) to unit solar and terrestial distance (r and $\Delta = 1$). As the eccentricity of some of the minor planets indicates, their paths are very elliptic relative to the orbits of the major planets.

* Allen, C. W., Astrophysical Quantities, The Athlone Press, London, 1963, p. 153. For some pictorial orbits of asteroids, see Rudaux, L. and De Vaucouleurs, G., Larousse Encyclopedia of Astronomy, Batchworth Press Limited, 1959, p. 205.

TABLE I-6

SELECTED MINOR PLANETS

Number and Name	Radius	m_{pg} at $r\Delta=1$	Orbital Data Period	a	e	i	Perihelion radius a(1-e)	Aphelion radius a(1+e)
	Km		d	AU		°	AU	AU
1 Ceres	350	4.0	1681	2.767	0.079	10.6	2.548	2.985
2 Pallas	230	5.1	1684	2.767	0.235	34.8	2.116	3.417
4 Vesta	190	4.2	1325	2.361	0.088	7.1	2.153	2.568
10 Hygiea	160	6.4	2042	3.151	0.099	3.8	2.839	3.462
15 Eunomia	140	6.2	1569	2.645	0.185	11.8	2.155	3.134
16 Psyche	140	6.8	1826	2.923	0.135	3.1	2.528	3.317
511 Davida	130	7.0	2072	3.182	0.177	15.7	2.618	3.745
3 Juno	110	6.3	1594	2.670	0.256	13.0	2.042	3.353
6 Hebe	110	6.6	1380	2.426	0.203	14.8	1.933	2.918
7 Iris	100	6.7	1344	2.385	0.230	5.5	1.836	2.933
51 Nemausa	40	8.6	1330	2.366	0.065	9.9	2.212	2.519
433 Eros	7	12.3	642	1.458	0.223	10.8	1.132	1.783
1620 Geographos	1.5	15.9	507	1.244	0.335	13.3	0.827	1.660
1566 Icarus	0.7	17.7	408	1.077	0.827	23.0	0.186	1.967
Apollo	0.5	18	662	1.486	0.566	6.4	0.644	2.312
Hermes	0.3	19	535	1.290	0.475	4.7	0.677	1.902
Adonis	0.15	21	1008	1.969	0.779	1.5	0.435	3.502

II. INSTRUMENTATION

There are two configurations in which the scanning camera may be used. In the first case the camera can be rigidly mounted on a spin stabilized vehicle (or perhaps more generally on a vehicle which is not inertially stabilized); or in the second case, the camera can be mounted on a vehicle which is inertially stabilized, in which case one rotational degree of freedom relative to the vehicle is necessary in order to provide the scanning motion. In this latter case, the accuracy of the system is not necessarily limited by the drift of the platform on which the camera is mounted. (If the drift is small and reasonably regular, it can be computed in the digital computer by comparing measurements made on successive rotations of the camera.)

Figure II-1 shows the various components of the navigation system. Case I shows the signal processing for a spinning or a tumbling vehicle where no moving parts are needed either in the camera or relative to the vehicle. Here a clock measures the time of appearance of the signal and feeds this information to the general purpose digital computer. As an aid in target identification and in pairing the signals, a digitized intensity measurement is also fed into the computer at the same time. The digital computer then selects the proper navigational program and computes the position and orientation of the vehicle.

In Case II of Figure II-1, the signal processing is shown for an inertially stabilized vehicle. It is assumed that an angle encoder measures the position of the camera relative to the vehicle whenever a sufficiently bright signal appears at the photomultiplier. This digitally encoded angle measurement is then fed to the computer. In other respects,

CASE I: MEASUREMENT OF CAMERA POSITION USING CLOCK ONLY

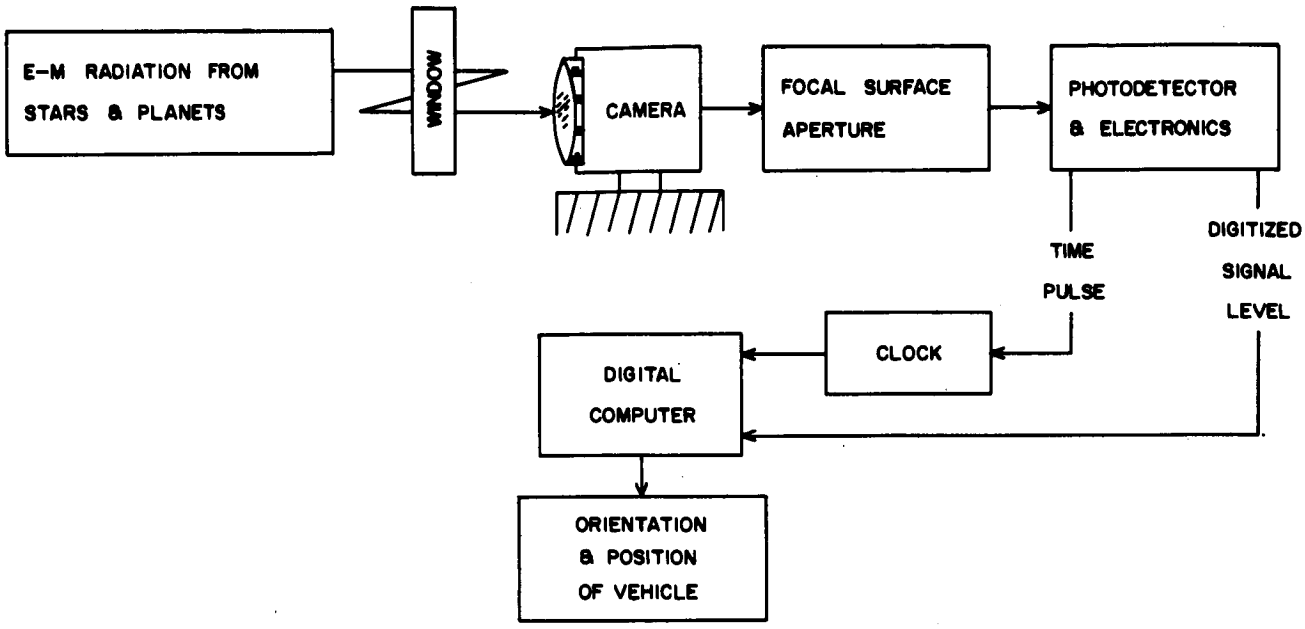

CASE II: MEASUREMENT OF CAMERA POSITION USING ANGLE ENCODER

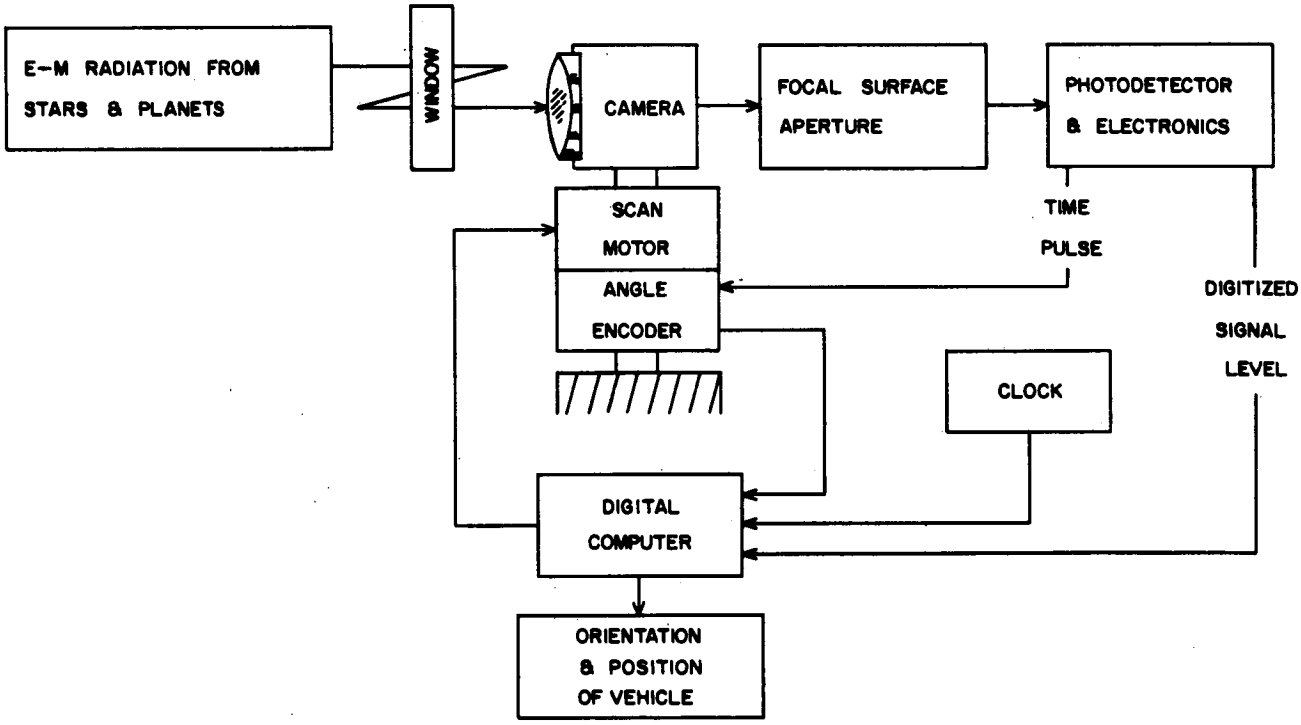

Figure II-1. Components of Navigation Instrument

Case II is similar to Case I.

A possible third case exists which is not shown in Figure II-1, but which deserves further study. This is the case in which we have an inertially stabilized vehicle and a scan motor which drives the camera at an extremely uniform rate. In this case an angle encoder is not needed because of the proportionality between angle and time, and the clock replaces the angle encoder as it did in Case I. This will simplify the instrumentation as well as the weight and power requirements but represents a difficult motor design problem.

The order of discussion of the navigation instrument which is given below is the same as the signal processing shown in Figure II-1. The optical, electrical, and mechanical features of the overall design form the three parts of this section.

A. Optical Design

The dominant factor affecting optical design is the requirement of a relatively wide field of view, about 30^{o}, in combination with a high image quality over the full field. We wish to measure the positions of the stars and planets to an accuracy lying between 10^{-4} and 10^{-5} radians, and thus require that the blur circle falls within this same range. In this section we will first of all describe the factors leading to the selection of a wide-angle Baker-Nunn type of camera design and then discuss the fiber optics and slits which make up the focal surface structure. Finally, a high energy target detector will be described which protects the photomultipliers while at the same time permits a more versatile application of the camera. The analysis of the optical system from the point of view of aberrations and transmissivity is deferred to Section III.

1. Selection of the Optical System

In trying to determine the type of instrument best suited to the scanning camera requirements a variety of optical designs and detection techniques were considered. A comparison of the characteristics of four possible instruments is shown in Table II-1. These instruments are described as follows:

1. WIDE-ANGLE CAMERA with crossed slits and fiber optics to direct light to the detector,
2. WIDE-ANGLE CAMERA with image tube at focus,

TABLE II-1

CHARACTERISTICS OF SEVERAL POSSIBLE INSTRUMENTS FOR SCANNING CAMERA

DESCRIPTION OF INSTRUMENT	ACCURACY OF ANGLE MEASUREMENT	TYPE OF DETECTOR	TYPE OF OPTICAL DESIGN	INSTANTANEOUS FIELD OF VIEW	IDENTIFICATION OF STARS	ELECTRONIC COMPLEXITY	MECHANICAL COMPLEXITY	MOVING PARTS NEEDED	SIZE AND WEIGHT	ESTIMATED OVER-ALL PERFORMANCE AS STAR ANGLE COMPARATOR
1. WIDE-ANGLE CAMERA, CROSSED SLITS WITH FIBER OPTICS TO DIRECT LIGHT TO DETECTOR 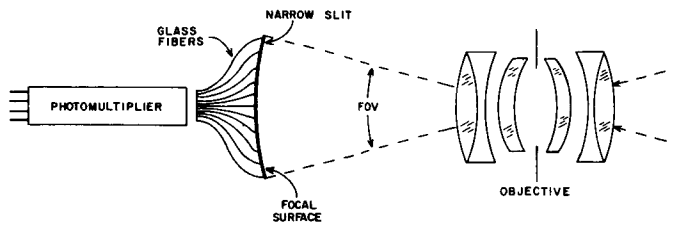	INTERMEDIATE from viewpoint of quality of optical image. BEST from viewpoint of resolution achievable over wide field of view. This is accomplished with accurately located slits in mask.	PHOTOMULTIPLIER	SUPER-SCHMIDT or WIDE-ANGLE ASTROGRAPHIC LENS	GOOD 20° - 40°	BEST. Photomultiplier permits pre-identification by intensity measurement. Accurate angular separation measurements remove all ambiguity.	VERY SIMPLE. Because of photomultiplication, preamps do not present a problem. Relies on capability of computer, since only time measurements are needed from detector.	VERY SIMPLE	NONE, except for small magnetically deflected spring-mounted shutter between ends of fibers and photomultiplier.	MINIMAL	BEST
2. WIDE-ANGLE CAMERA, IMAGE TUBE AT FOCUS 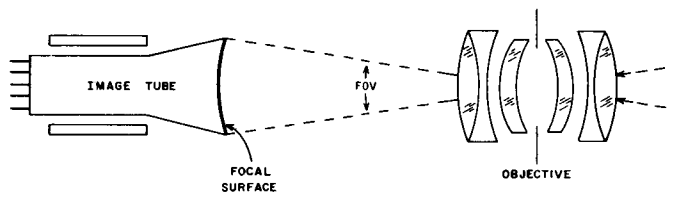	INTERMEDIATE from viewpoint of quality of optical image. INTERMEDIATE from viewpoint of resolution of image tube over wide angular field of view.	IMAGE ORTHICON OR VIDICON	SUPER-SCHMIDT or WIDE-ANGLE ASTROGRAPHIC LENS	GOOD 20° - 40°	INTERMEDIATE. If field of view is not too large accuracy of angular separations probably adequate. POOR. Due to variations in response across surface of image tube. Intensity measurements are not sufficiently accurate for identification.	RELATIVELY SIMPLE. Linearity of scan across face of image tube for accurate resoltuion of target position presents a problem. Scan voltages must be converted from analoy to digital form before transmission to computer.	VERY SIMPLE	NONE, except for sun shutter.	MINIMAL	INTERMEDIATE
3. CONCENTRIC OPTICAL SYSTEM, TRACK-WHILE-SCAN DETECTOR 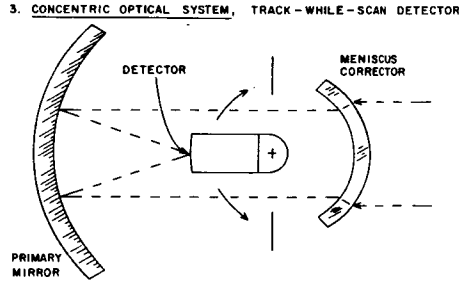	POOREST because of difficulty of gimbaling detector as is required to cover full field of view.	IMAGE TUBE	BOUWERS CONCENTRIC CATADIOPTRIC SYSTEM	EXCELLENT 40° - 100°	POOR. Neither angular separations nor star intensities can be accurately measured.	RELATIVELY COMPLEX. In addition to image tube electronics, drive system must be used to cover entire field of view.	RELATIVELY COMPLEX. Mechanism must be provided to scan field of view in two directions - otherwise blocking would prevent use of full field of view.	YES. Scan mechanism is needed to move detector over full field of view.	LARGE. Primary mirror must be very large and heavy in order to permit system to operate over large field of view.	INTERMEDIATE
4. STAR TRACKER, AZIMUTH AND ELEVATION AXES 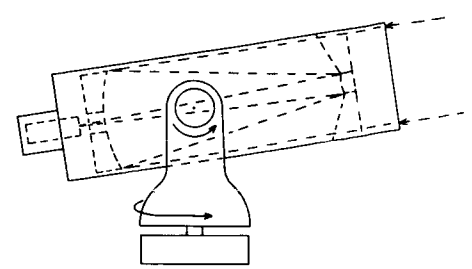	BEST from viewpoint of quantum limitations to locating center of gravity of star image and from viewpoint of optical image quality. INTERMEDIATE from viewpoint of angle encoders required to measure direction of pointing of telescope.	PHOTOMULTIPLIER	CASSEGRAIN TELESCOPE	POOR $\leq 4^{\circ}$	EXCELLENT. Angular separations can be accurately measured as can intensities.	VERY COMPLEX. In addition to detection electronics for error signal, a control system for driving telescope to correct angular position must be used.	RELATIVELY COMPLEX. Elevation and azemuth axes must be provided. Bearings must operate in space environment. Drive motors and angle encoders are needed for each axis.	YES. Entire telescope must be pointed toward star which is being tracked.	LARGE. Equipment needed to support, drive and measure position of telescope adds considerably to size and weight.	POOREST

3. CONCENTRIC OPTICAL SYSTEM with track-while-scan detection, and

4. STAR TRACKER with azimuth and elevation axes.

In reverse order, the gimballed star tracker, Number 4, has two primary disadvantages which make it unattractive as an instrument for lunar and interplanetary navigation. First, since the star tracker has a very limited field of view, it is not possible to search large fields of view for reacquisition of the target if a temporary malfunction occurs. Second, it is an extremely complex instrument both mechanically and electrically.

The concentric optical system, Number 3, offers by far the largest field of view of any of the instruments; however, a mechanism must be provided to move the detector across this field of view since the aperture blocking and the angular resolution are not acceptable when using a fixed detector. To cover a 100° field of view the primary mirror tends to become rather large and heavy in the Bouwers concentric optical design. Because of this large size, distortion of the mirror due to thermal gradients presents a serious design problem.

System Number 2, the wide angle camera with an image orthicon or vidicon at its focus, has a limitation of its instantaneous field of view which is imposed by the resolution of the image tube itself. Furthermore, it will be necessary to provide some method of searching the various regions of the sky. Assuming that the camera is mounted on an inertially stabilized platform, this means that a gimballing arrangement must be provided and that a separate angle encoder must be provided for

each pointing axis used.

System Number 1 is a wide-angle camera equipped with slits at the focus of the optical system. The light entering the slits is brought back to the detector by means of transparent dielectric fibers. Thus, the photomultiplier can be mounted at any convenient location. Typically, a field of view of 30 degrees is used and the design of these slits assumes a variety of forms. For simplicity, the optical system shown in Table II-1 is a Ross astrographic lens, whereas we will presently show that a Schmidt design is more desirable.

The wide-angle camera using slits is preferred to the wide-angle camera using an image tube for the following reasons:

a) Accuracy of Relative Angle Measurement. The slits on the focal plane can be positioned to an accuracy of about 10^{-4} inches, and the edges of these slits can be made uniform to an accuracy of about 10^{-5} inches. If the slits are two inches in length, the means an accuracy of at least 1/20,000 over the field of view of the wide-angle camera. In contrast, the resolution over the entire two inch face of an image will not be significantly better than one part in 2,000. Thus, the slit system has an accuracy advantage of about ten.

b) Accuracy of Star Intensity Measurement. Both for false target discrimination and for intensity preselection as a method of more easily identifying stars and

planets, it is advantageous to be able to make accurate photometric measurements. Since the sensitivity varies widely over the face of an image tube for small high-resolution star images, the image tube is not satisfactory as a method of intensity measurement. On the other hand, a photomultiplier if properly used and in the presence of sufficient radiation can provide an intensity measurement accurate to 1%. While the photomultiplier sometimes also has local variations in the sensitivity of its photocathode, it will be noted from Table II-1 that Instrument Number 1 has the photomultiplier located sufficiently far behind the ends of the fibers that the image of a single star is spread over a large portion of the photosensitive surface and thus averaging is achieved. In order to achieve an absolute intensity reference, a calibrated source is recommended. However, in certain cases the ratio of star intensities is a more significant parameter than their absolute magnitudes.

c) Need for Inertial Stabilization. Since the image tube continuously collects radiation, a rapid angular motion of the camera will tend to blur the image. The image tube (Number 2) therefore works

most efficiently when the camera is not moving in inertial space--thus the need for inertial stabilization. On the other hand, the device recommended in the present report can be made to function with equal accuracy when mounted on a tumbling space vehicle or on an inertially stabilized vehicle.

d) Electronic Complexity. In the case of the image tube an electrostatic or electromagnetic system for beam deflection must be provided. To achieve the utmost in resolution is a difficult circuit design problem and probably the heavier electromagnetic deflection system should be used. Also, the basic deflection system is analog in form and a conversion to a digital output is needed for the computer. On the other hand, the photomultiplier in System Number 1 only acts as a signal source for the clock which is naturally a digital device. Thus it would seem, at least for the systems compared here, that the scanning slits and photomultiplier combination lead to less electronic complexity.

e) Navigation Capability. Perhaps the most notable advantage over the instrument which used the image tube is the manner in which it can locate the positions of the moon or the planets for a lunar or interplanetary mission. This is achieved by measuring the position of

the planetary limb only. Thus, problems associated with variable solar aspect angle, a poorly defined planetary terminator, or variations of the albedo across the illuminated planetary surface are avoided.

Having thus chosen a wide-angle optical system with slits on the focal surface, we must determine the required field of view. Figure II-2 shows the relation between number of stars, n, scanned per rotation, and

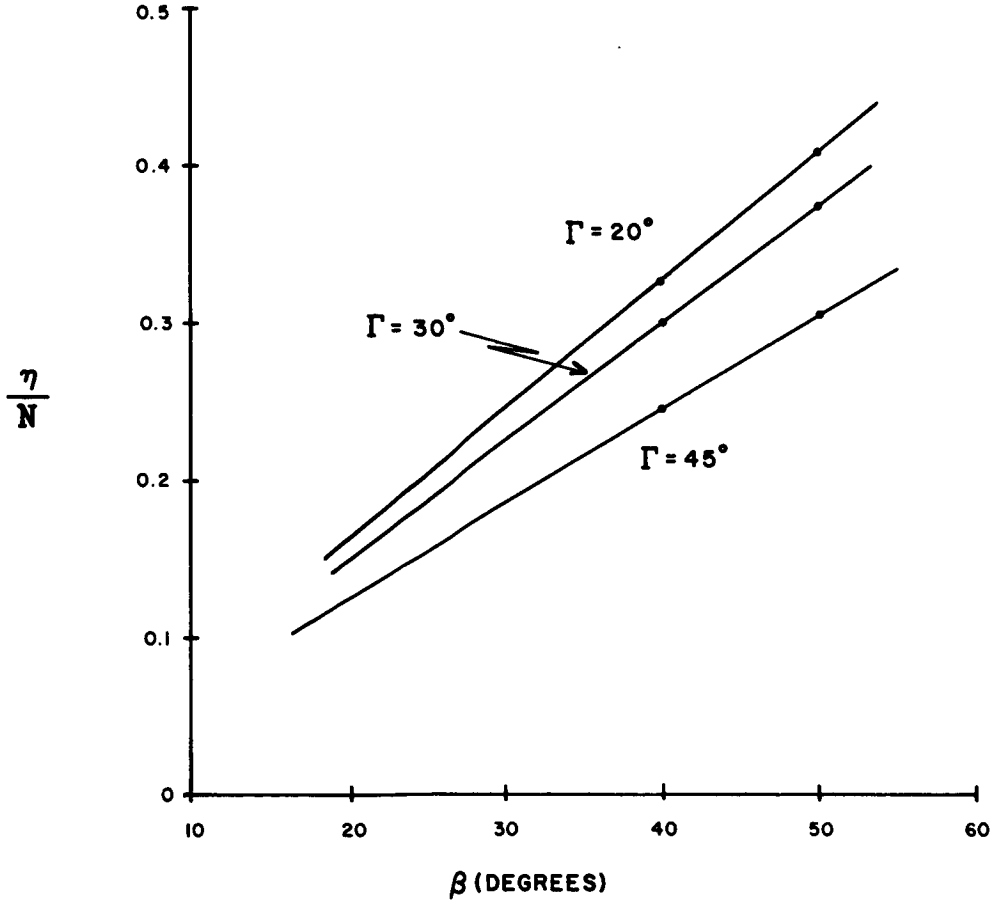

Figure II-2. Fraction n/N of Sky Scanned versus Field of View β and Half-Angle Between Slits Γ

the camera field of view, β, for a system of crossed slits. The effect of varying the angle Γ between the slits is also shown. The quantity N is the total number of stars in the sky (assumed uniformly distributed) brighter than a given magnitude. Supposing that N = 50, then for a slit angle of 30^{o} a field of view of at least 27^{o} is needed to detect ten stars during one rotation. Now, a simulation of the star identification technique (Section III-E) shows that at least three stars should be used to permit a check on the separation angle-magnitude comparison of pairs. Further requiring that this navigation capability be existent even for half of a scan (to account for planet obscuration), we require an equivalent of six stars for the entire scan. Finally, we have assumed the N stars to be uniformly distributed. To ensure, therefore, that every half-scan detects three stars, we will require than an even distribution give six stars or an equivalent of twelve stars over a complete scan. With this requirement, Figure II-3 shows the trade-offs between field of view, β, and the total number of stars, N. Also shown are the limiting magnitudes which will have to be detected. If the angle $\Gamma = 45^{o}$, the azimuth and elevation of each target will be equally well determined. However, for smaller Γ, more efficient use is made of the full field of view. The combination $\beta = \Gamma = 30^{o}$ seems to be a good compromise requiring a catalog of the fifty-four brightest stars down to a magnitude of about 2.35.

The types of wide-angle optical designs considered as having characteristics sufficiently close to our requirements are shown in Figure II-4.

They are:

1. The Ross wide-angle astrographic lens F/4.0, 20° FOV,
2. The Baker-Nunn satellite tracking camera, F/10., 30° FOV,
3. The Super-Schmidt meteor camera, F/0.67, 50° FOV.

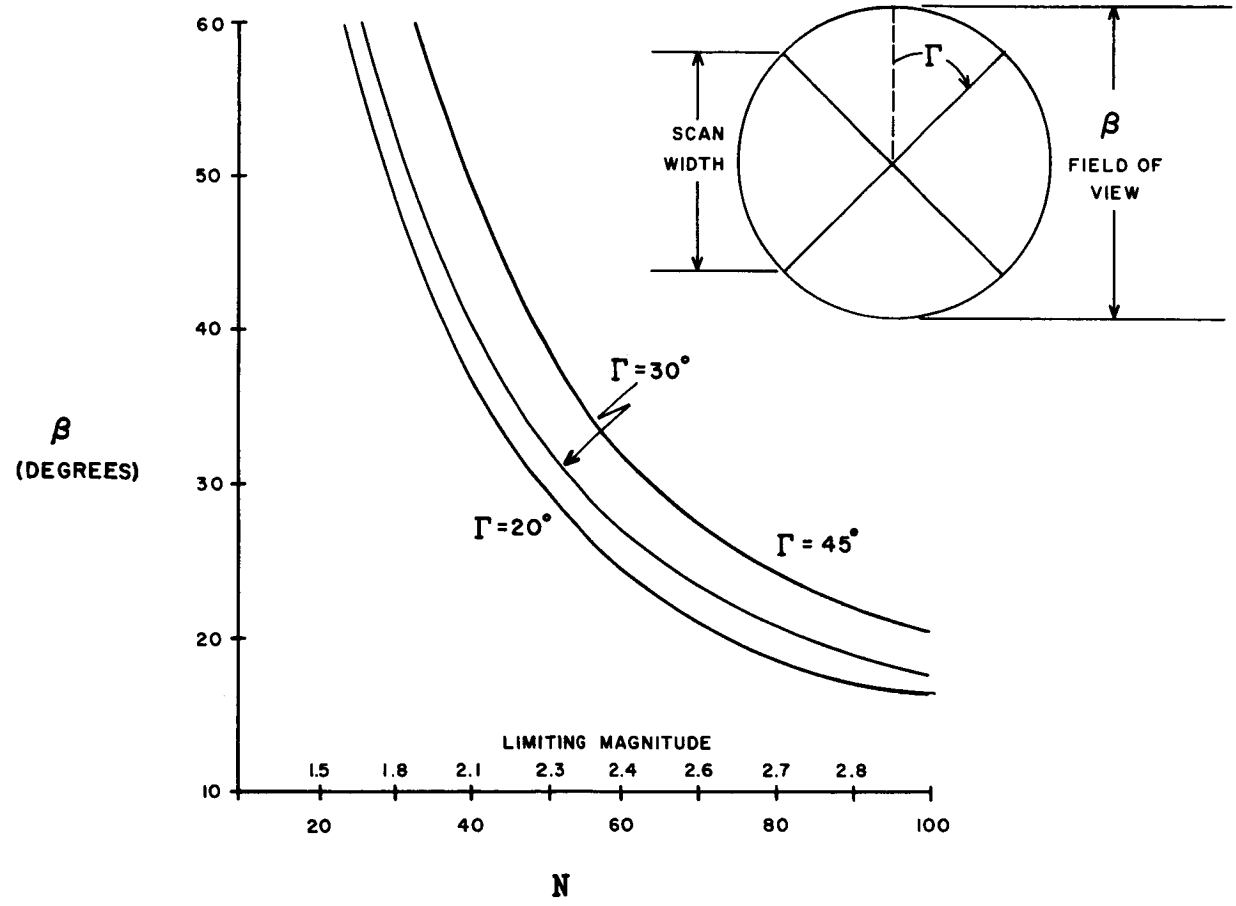

Figure II-3. Minimum Field of View β for N Brightest Stars over Sky

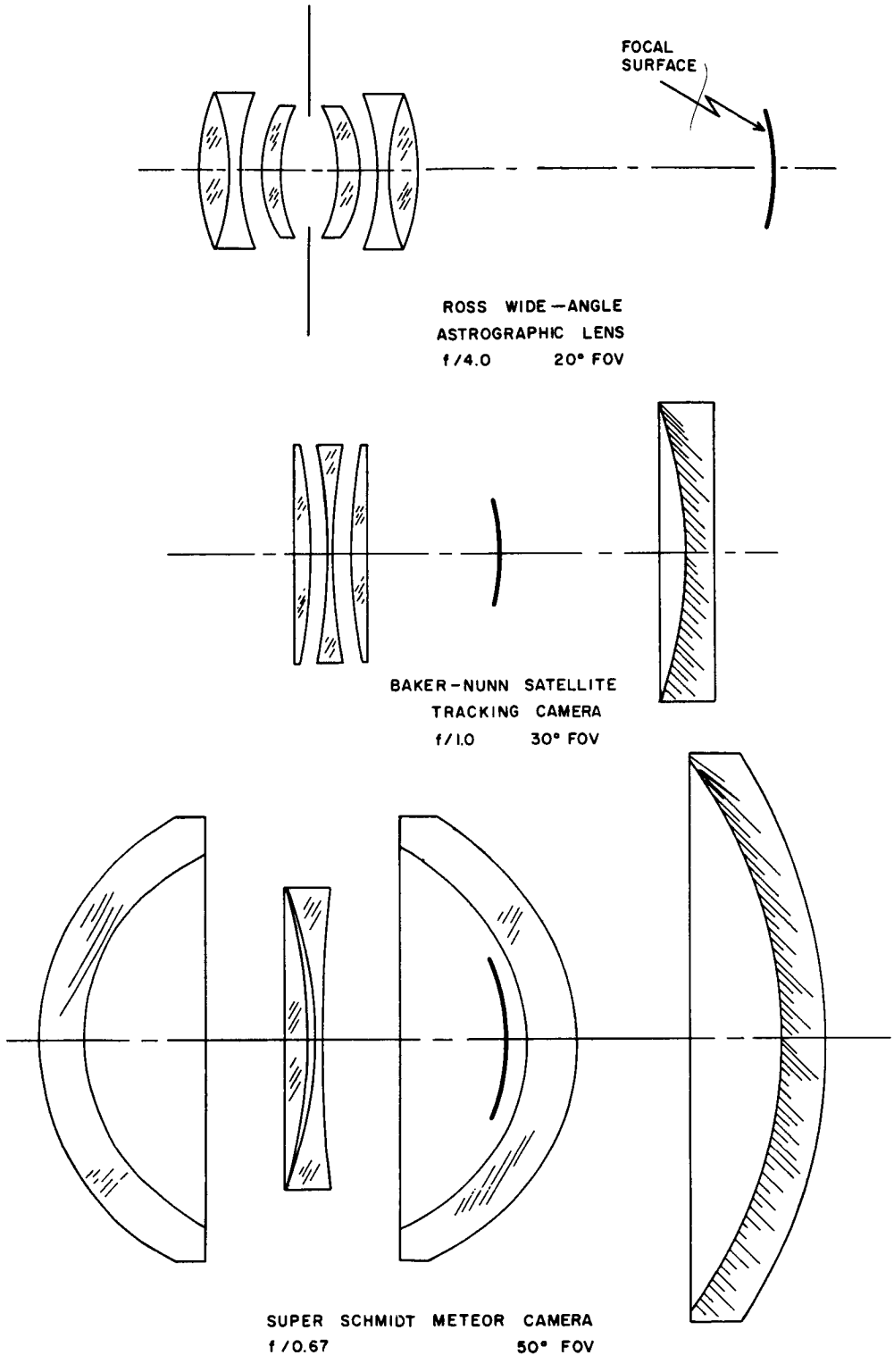

Figure II-4. Optical Designs Considered for Scanning Camera

The Baker-Nunn Satellite-Tracking Camera was constructed during the International Geophysical Year under the direction of the Smithsonian Astrophysical Observatory. It was conceived by F. L. Whipple and J. A. Hynek, while J. G. Baker supplied the detailed optical design and J. Nunn designed the mechanical components and mount. The camera is a modified Schmidt design featuring a three-element corrector system as shown in Figure II-4 which also includes some of the original dimensions. Baker's design placed 80% of the light within a 20 μ image (8.1 seconds of arc diameter) over a 30 degree field for all colors from red through violet. In practice, the finished cameras achieved minimum image diameters ranging from 20 μ to 30 μ (8.1 to 12.2 seconds of arc). Both the aperture and focal length are 20 inches, and Table II-2 lists the principal characteristics of each optical element. The back-up plate which defines the focal surface is figured to an accuracy of $\pm$ .0002 inches and is very nearly a sphere.

The Ross lens has the advantage that the focal surface is easily accessible for mounting the detector, while the other two Schmidt cameras have focal surfaces which are between the primary mirror and the corrector lenses and not so easily accessible. It is possible to avoid this problem to a considerable extent, however, by the use of fiber optics.

The two modified Schmidt cameras give a somewhat better quality image for the wide fields of view required. The super-Schmidt meteor camera might be worthy of consideration in certain cases where a field of view as large as 50° is desired. For a given aperture the weight of

TABLE II-2. IMPORTANT CHARACTERISTICS OF BAKER-NUNN CAMERA OPTICAL ELEMENTS **

No.	Name	First Surface		Type of Glass
1	Positive corrector	Spherical (501")*	Aspherical (shape A)	KzFS-2
2	Negative corrector	Aspherical (shape B)	Aspherical (shape B)	SK-14
3	Positive corrector	Aspherical (shape A)	Spherical (501")	KzFS-2
4	Mirror	Spherical (40")	---	Pyrex
5	Back-up Plate	Approx. spherical(20")	---	Pyrex

* Figures in parentheses give approximate radii of curvature.

the glass in this camera is rather large. Also, the 30° FOV is sufficient to track the earth or the moon when they subtend angles as large as 48° and therefore the larger field of view is not normally advantageous.

As a result of our 30° field of view requirement, it was decided that the Baker-Nunn satellite tracking camera be scaled down to a four inch aperture, while holding the blur circle to 20 seconds of arc. The characteristics of this optical design are shown in Table II-3.

One might think that the relatively short focal length, four inches, would present a limitation to accuracy. It does not, since the slits can be positioned on the more or less spherically curved focal surface to an accuracy of 10^{-4} inches. This is equivalent to an angle of $10^{-4}/4$ radians, or only five seconds of arc. The region between the slits is open and

** Henize, Karl G., "Tracking Artificial Satellites and Space Vehicles", Advances in Space Science, Vol. 2, edited by Frederick I. Ordway III, Academic Press, New York, 1960, pp. 117-142.

TABLE II-3

CHARACTERISTICS OF SCANNING CAMERA OPTICAL SYSTEM

Type of Camera	Baker-Nunn
Aperture	4 Inches
Field of View	30 Degrees
f Number	1.0
Effective Focal Length	4.0 Inches
Diameter of Primary	5.5 Inches
Diameter of Focal Surface	2.0 Inches
Diameter of Blur Circle	20 Seconds of Arc
Focal Surface	Slits can be made to conform to whatever surface minimizes optical aberrations.
Spectral Region	3600 Å to 7000 Å

thus causes no blocking. One can expect a certain amount of distortion for images which are near the edge of the field; however, the distortion is radial (that is, the images are displaced towards or away from the point where the axis intersects the focal surface) and therefore a correction factor can easily be included in the computation of transit times. Since coma and most of the other aberrations of the optical system will be symmetric about a radial line, our system of radial slits will eliminate their effects. The major aberration of the optical design shown in the middle of Figure II-4 is that of field curvature. However, by means of a system of slits curved to conform to the focal surface, this aberration

causes no difficulty.

2. Focal Surface Assembly

Three elements are involved in focal surface assembly:

Mask,

Fiber Optics,

Supporting Spider.

The mask provides a definition of the slit configuration which permits the derivation of navigational information from the scanned targets. The image is allowed to pass through the mask only at the slits. Immediately behind the slits in the mask are arranged a row of optical fibers--tiny strands of glass--with their axes normal to the focal surface. These fibers conduct the image energy, by means of internal reflections, out of the optical system and to the photomultiplier detector. The supporting spider is in the form of a thin cross and holds the fibers and mask in their correct relation to the main camera optics. The spider is attached to the outside of the camera and provides thereby, rigidity, means of aligning the slit structure, and means for supporting the fibers as they leave the optical system.

Figure II-5 shows some details of the focal surface and its supporting structure. (This figure should be read along with Figure II-1 and Figure I-2.) The line of fibers which forms each slit are overlapped to produce a thin rectangular shape as they leave the optical system. The final bundle at the terminus can be in the form of a cylinder or any other convenient shape.

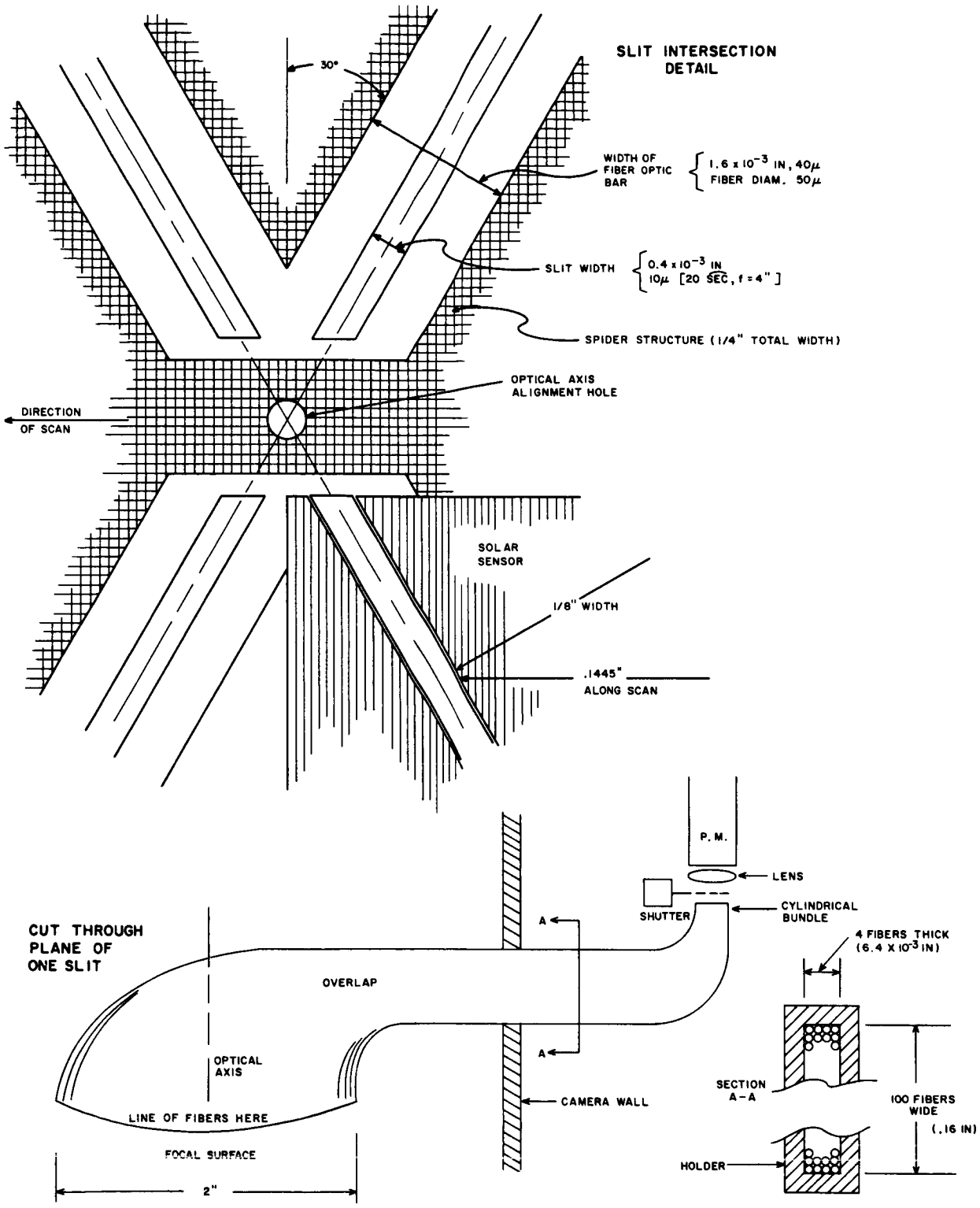

Figure II-5. Focal Surface and Support Details

At the focal surface, the fibers are fused together to form a narrow bar upon which the slit rests. This will eliminate possible losses which could result if the fibers were left cylindrical. (If the image were to fall on a fiber intersection, some of the energy would be transmitted to the potting compound and become lost.) Away from the focal surface and after being formed to the desired contours, the fibers are to be cemented together and enclosed in the supporting spider. The focal surface is then ground to the desired shape and the slits either attached or scribed to this surface.

Two methods have been suggested for the mask itself. In one scheme the focal surface is coated with a metal which is in turn covered with wax. The focal assembly is then fixed in a jig so that it can be rotated about its center of curvature. A diamond scribe can then remove the wax in an even and precise line. Acid applied to the slit then slowly dissolves the metal, the process being monitored under a microscope and stopped when the slit width reaches the desired 0.4 mil thickness.

The second technique is to similarly scribe a flat surface which is then transferred and glued to the focal assembly. This is certainly cheaper, though requires more care and is probably not as repeatable as the direct scribe method.

While chiefly concerned with the crossed-slit system, there are many other shapes which would also yield navigational information. These apertures in the focal surface mask may range from that of a single point to the complete removal of the mask itself. Each pattern of holes, slits

and surface openings has its own peculiar advantages. In Table II-4, a summary of focal surface apertures is shown in which the following classification is used:

1. Point L^0
2. Line L^1
3. Surface L^2
4. Volume L^3
5. Time $T \cdot L^n$ $(n = 0, 1, 2, 3)$

Point apertures find their greatest use when scanning targets of extended luminosity such as planets. They provide an opportunity for considerable statistical refinement by using a multiplicity of points.

Line, or slit, apertures can be used to measure the positions of point targets (stars) as well as extended targets and are therefore particularly attractive for space navigation where the orientation of a vehicle is determined from the stars and its position from the planets.

Open regions in the focal surface mask (surface apertures) can to some extent provide a measure of target positions, but because of their large exposed areas background noise becomes a problem. The primary use of exposed surfaces is that of measuring the intensities of very bright targets.

By the word "volume", we mean the ability of the system to extract information from the change in response characteristic as the position of the mask is moved along the optical axis. For example, if one had a mask with several "point" apertures, the signal build-up will be different if

TABLE II-4

SHAPES OF APERTURES IN FOCAL-SURFACE MASK

APERTURE SHAPE	Dimension[1]	Examples[2]	Statistical Techniques[3]	Types of Measurements								Primary Advantages	Primary Disadvantages
				Angular Measurement		Integrated Brightness Meas.		Distance Meas.		Temporal Brightness Meas.			
				Point Targets	Extended Targets	Point Targets	Extended Targets	Point Targets	Extended Targets	Point Targets	Extended Targets		
1. Point	$[L^0]$	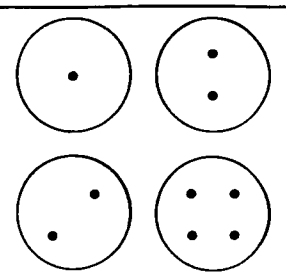	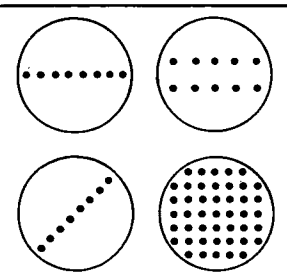		X							Measurement of position of extended targets which have relatively uniform perimeter. Statistical advantage can be obtained with very little increase in background noise by using a multiplicity of detection points.	Cannot measure positions of point (star) targets because of vanishingly small probability of "point" detection element coinciding with "point" target.
2. Line	$[L^1]$	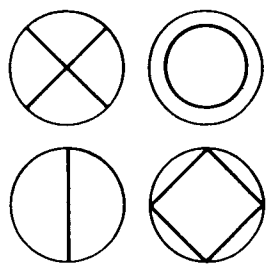	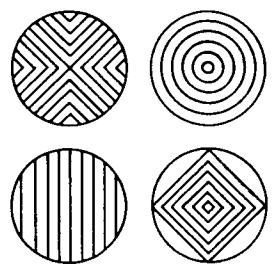	X	X							Can be used to determine both vehicle orientation and position because of ability to detect point and extended targets.	Unless separate photomultipliers are used for each line element, or unless one switches from one line to the next as the scan progresses, statistical advantage can not be fully realized because total area of slits allows too much star background noise to contaminate signals.
3. Surface	$[L^2]$	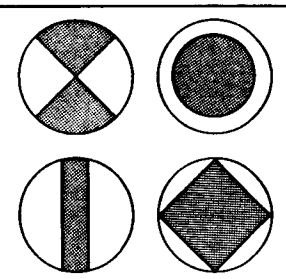	Statistical refinement not possible	X	X	X	X					Large exposed surface makes it possible to accurately measure brightness of extended targets.	Because of large exposed region, one can only accurately measure signals from very strong targets.
4. Volume	$[L^3]$	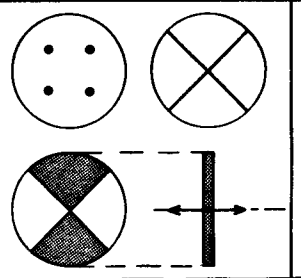	Same as 1 and 2, except that means are provided to translate mask along optical axis.	X	X	X	X	X	X			Can be used as passive ranging technique, however this technique is applicable only when target is very close to camera (as during the completion of a rendezvous operation).	Mechanism needed for "focusing" in order to determine range to target.
5. Time	$[T \cdot L^n]$ $n = 0, 1, 2, 3$	Can use any of forms shown in 1, 2, 3 or 4.	Temporal statistical techniques may also be used. Those given above in this column are spatial.	X	X	X	X	X	X	X	X	Time variation of signal level provides further data on shape of luminous region of body being viewed.	Degradation of accuracy of angular position measurement will probably result from attempt to perform multiplicity of functions.

1 L = length; T = time.

2 Under 3. SURFACE, darkened area represents cutaway (open) area of mask.

3 Repeated measurement during a single scan by a multiplicity of apertures will yield statistical improvement in angular position measurement.

the mask is out of focus than if it is in focus. Conversely, if a target is relatively close to the camera, its image surface will be displaced and a measurement of this displacement provides a means of calculating the distance of the target. This technique has been adequately considered in the past, and probably has a very limited use here. However, if the scanning camera were provided this capability, it could be used near the terminal phase of a rendezvous operation as a passive means of determining target range.

Finally, in any one case the temporal variation of intensity can be measured as a method of deriving more information about the target. This measurement could provide such diverse information as that used for a communication system, or it could provide a measure of the inclination of a planetary satellite orbit relative to the sun-planet vector, or it could be used in a system which estimates the distance of a space vehicle by the measurement of the intensity of the sun. For the present, none of these applications seems particularly deserving of further analysis for a navigation system. However, they are described as a part of a general evaluation of capabilities which might be developed with the proposed instrument.

3. Fiber Optics

As is well known, a transparent dielectric fiber of constant diameter will conduct light along its length due to multiple internal reflections.*

* Kapany, N. W., Fiber Optics, Appendix N, Concepts of Classical Optics, J. Strong, W. H. Freeman and Company, 1958.

Little loss of energy occurs and geometrical optics is sufficient for analysis if the fiber diameter is many times the wavelength of light. When the diameter is small, diffraction plays a role, and the fibers act as wave guides. Fiber diameters in the range 10 μ to 250 μ (4×10^{-4} to 0.01 inch) are standard.

The optical fibers used for the scanning camera would be from two to four inches in length and would be 50 μ to 65 μ in diameter (four to five times the slit width). They would be glass coated for protection against surface contamination during handling and cementing or potting of the fiber bundles. The coating material is usually of glass and is of lower index of refraction than that of the core. Even the slightest amount of surface contamination absorbs light and causes significant reduction in transmissivity along the fiber. Furthermore, the coating forms a barrier between the reflection surface and the potting compound which would otherwise produce light loss at each surface reflection.

The maximum angle, with respect to the fiber axis, of a ray of light striking the end of a glass fiber, which will be transmitted by total reflection within the fibers is dependent on the refractive indices of the core and coating materials. This angle may be computed from

$$\sin i = \sqrt{N_1^2 - N_2^2} \qquad (2\text{-}1)$$

where

N_1 = index of refraction of core

N_2 = index of refraction of coating

i = incident angle of ray

For example a camera having a f/1 objective lens would have an angle of 28° subtended by the objective lens, the vertex being at the focal plane. In order to transmit the light by total reflection within the fiber, 2i must be greater than 28° to allow for manufacturing tolerances and variation in refractive indices of the fiber materials. Figure II-6 shows the relationship between maximum angle of incident light which will be transmitted by total reflection within a fiber for various differential indices of refraction of core and coating materials.

One practical selection of refractive indices for core and coating materials is 1.58 and 1.52 respectively. With this combination 2i becomes 50° which is more than sufficient to accomodate the 28° cone angle of light impinging on the fiber end and still allow for generous manufacturing tolerances.

4. High Intensity Detector

Since the scanning camera will sample large regions of the celestial sphere, it is very possible that the sun or some other high intensity targets may pass across the slit structure. If this were to occur, an excessive amount of current would be drawn from the photomultiplier with possible permanent damage. To protect against this, the area near the slits is continually monitored by a separate detection system. If a target whose intensity may cause damage to the photocathode enters the field of this detector, a shutter is actuated automatically to block off light

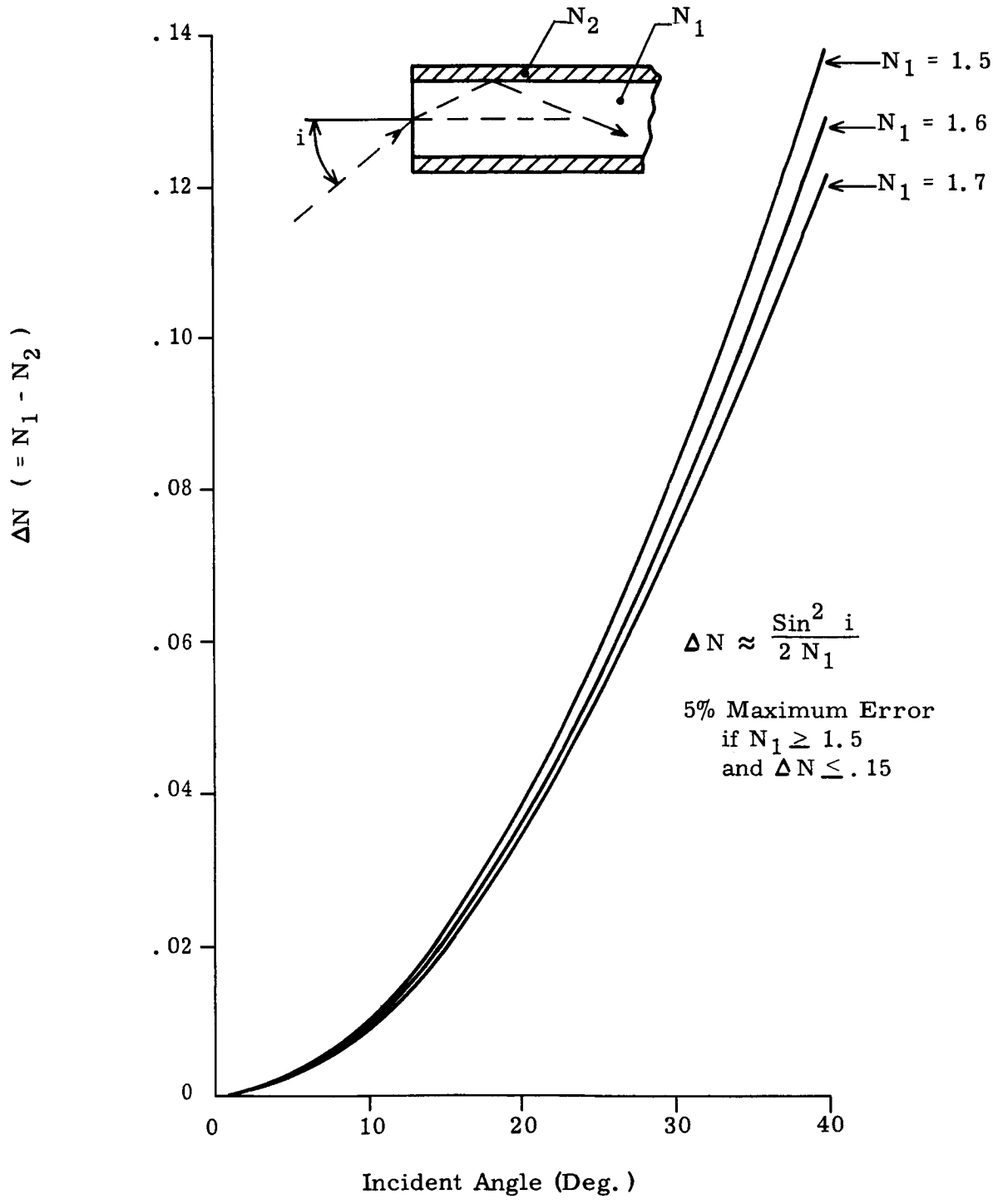

Figure II-6. Maximum Incident Angle of a Ray of Light Which Will be Transmitted by Total Reflection within a Fiber for Various Differential Indices of Refraction of Core and Coating Materials

to one of the photomultipliers, depending on which slit the bright target is approaching. During this time if no target of excessive intensity exists in one of the remaining fields, the camera is free to detect transits in these fields. Schematically, the relation between the camera slits and the larger slits of the high intensity detector are shown in Figure II-7. The effective slits of the detector are 4^{o} wide and their projected centerlines are coincident with the projected centerlines of the camera slits, (4.6^{o} in direction of camera motion).

The mechanical configuration of the high intensity detector can take two forms. The first is shown in Figure II-5 where solar cells have been placed (or deposited) in close physical proximity to the camera slits on the focal surface. These cells then actuate a shutter placed between the ends of the fibers and the photomultipliers. A second configuration is shown in Figure II-8 which is completely separate from the principle optical system. The entire detector may be very small with solid state components for sensory elements themselves. In each design it is easy to note the sectionalization of the slits. This permits operation of the camera very close to bright objects with only a ¼ to ½ reduction in efficiency.

The design of the shutter is shown in Figure II-9. Assuming that the camera spin period is ten seconds and that the photodiode detects the high intensity target ($\frac{1}{2}^{o}$ for sun or moon for camera near the earth) one millisecond after the target is in the field of the detector, the remaining time for shutter operation is 50 milliseconds.

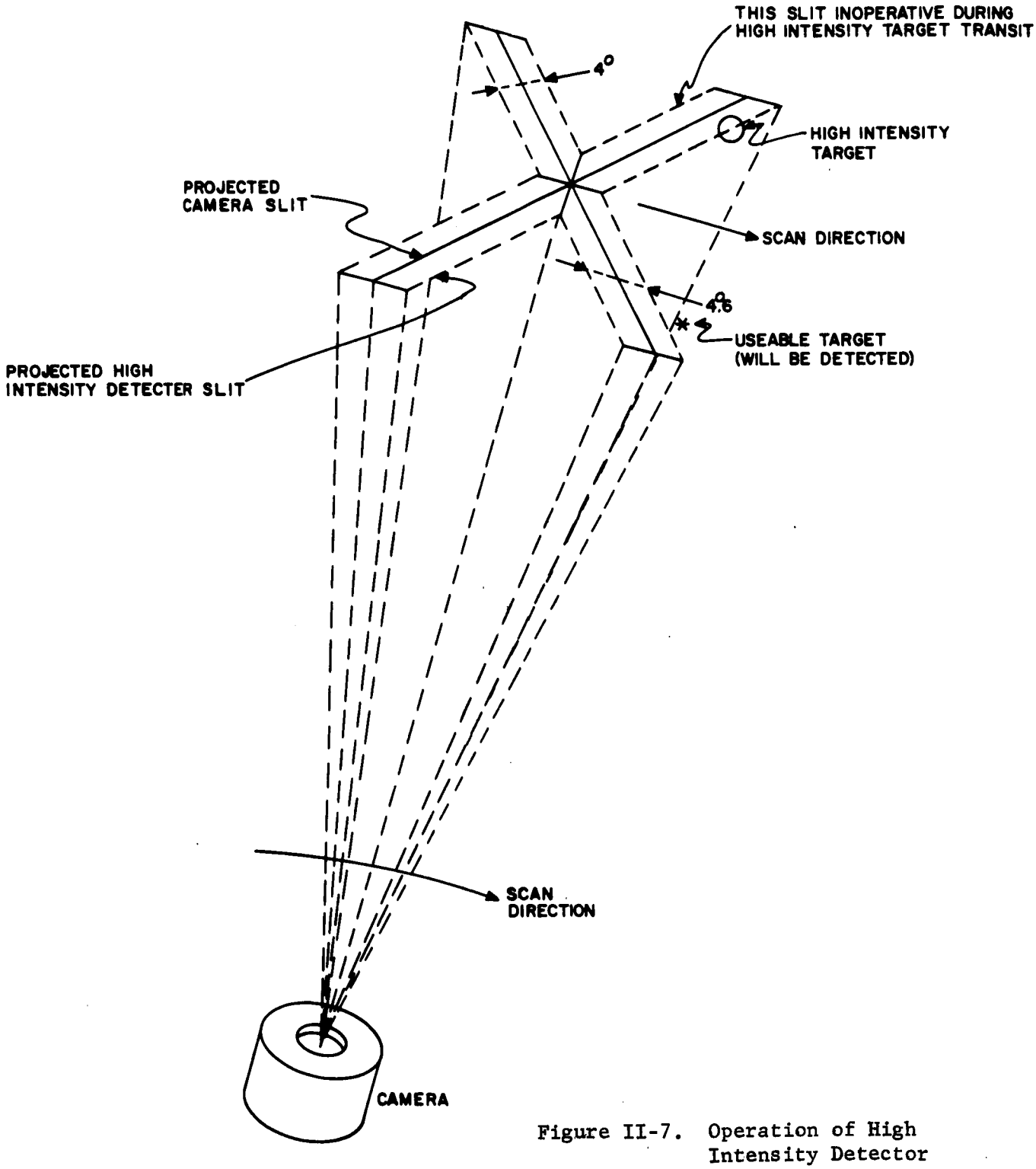

Figure II-7. Operation of High Intensity Detector

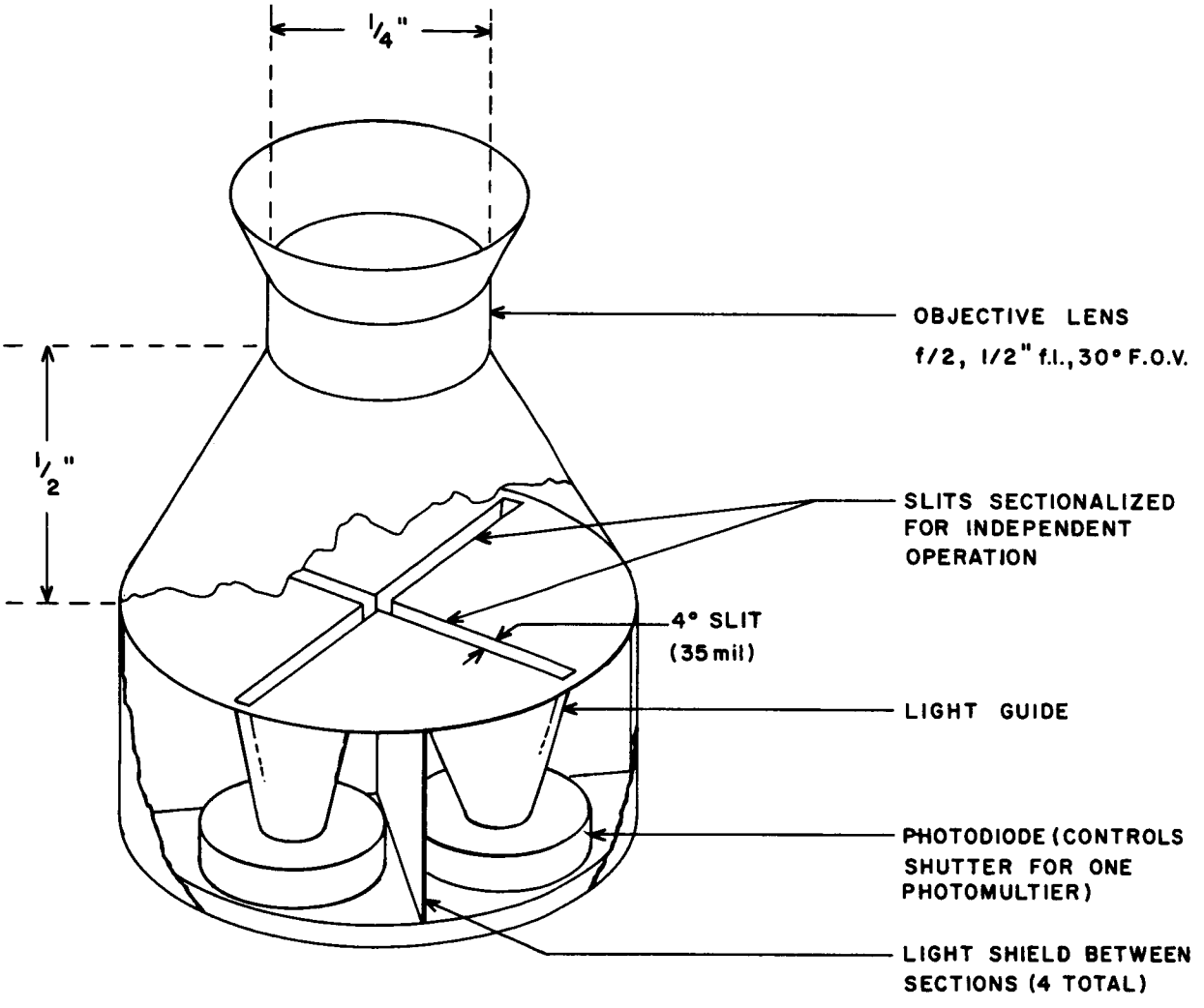

Figure II-8. Basic Design of Independent High Intensity Detector

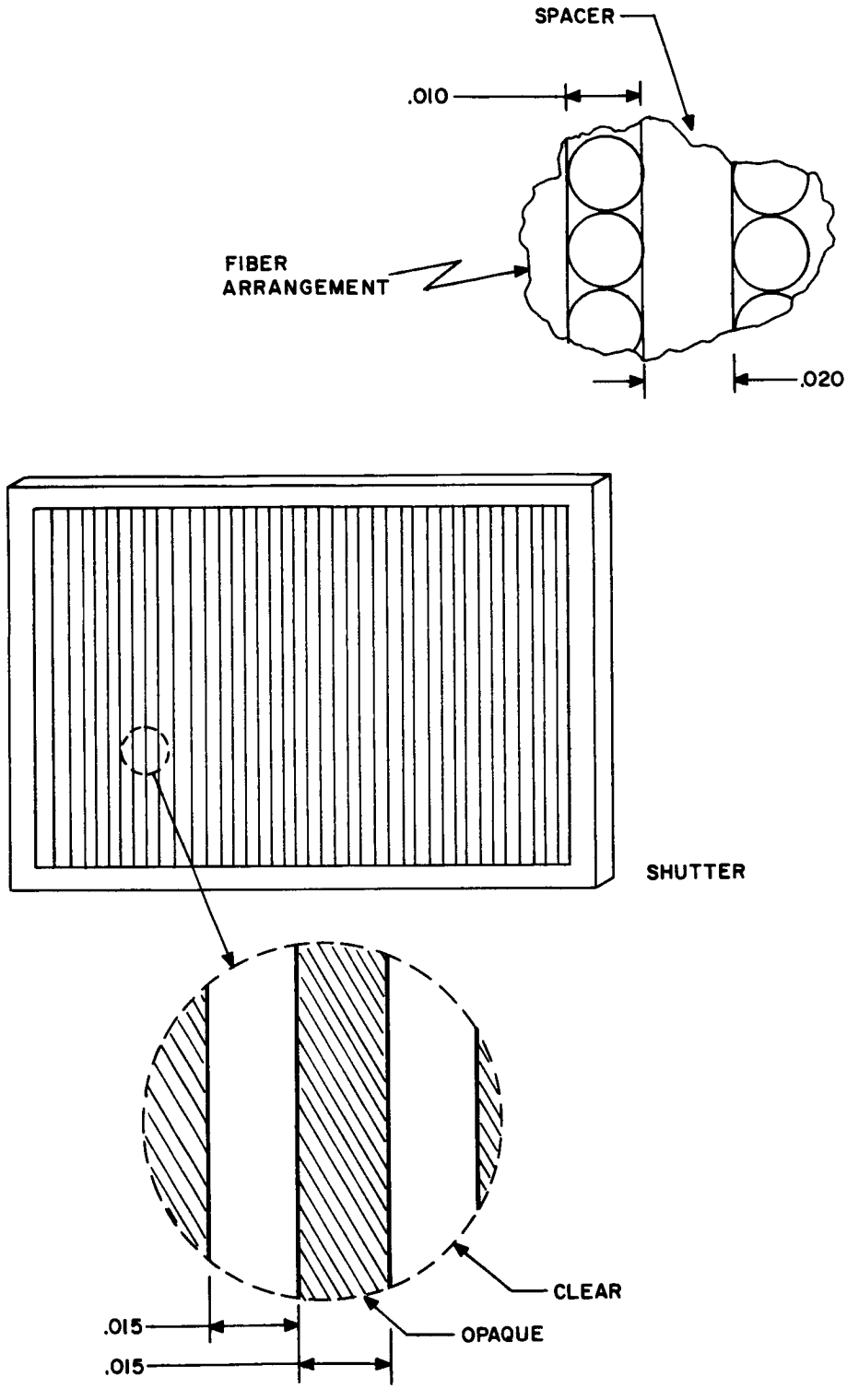

Figure II-9. Shutter and Fiber Arrangement at Photomultiplier

In order to minimize the time for shutter operation, the shutter mass and travel should be held to a small value. To facilitate this, the shutter design takes the configuration shown in Figure II-9. In this case the optical fiber diameter is shown as .010 inch. The shutter would then have to shift but .015 inch within 50 milliseconds of time which would require a relatively small amount of power if the mass of the shutter components are minimized.

B. Electronics

After the light passes through the dielectric fibers shown in Figure II-5 it impinges on the face of the photomultiplier. Suitable circuits must be developed to amplify this signal, measure the time at which it reaches a predetermined intensity level, measure the intensity itself, and transmit these values in digital form to the computer. In this section we discuss the photomultiplier, electronics to process the signals, and logic to form the data words.

1. Selection of Photomultiplier

The particular photomultiplier chosen depends upon

Cathode Size,

Gain,

High Voltage,

Ruggedness, and

Dark Current Noise.

The size of the cathode is not a restriction in our case since the fibers coming from the slit can be formed into a bundle at least smaller in area than the cathode. Photomultipliers with high gain ($\sim 10^6$) are desirable since the signal then becomes so great that noise sources in the amplifier and following electronics do not have a significant effect. One does not desire that an excessively high voltage be required by the tube because of power limitations in a space environment. Similarly for ruggedness of the phototube structure. The principle feature for the detection of scanned targets, is the size of the dark current noise. This

is caused by thermionic emission from the cathode and dynodes and also by fluctuations in the leakage current. From the discussions in Section III-D, where the general problem of detection accuracy and noise receive attention, it is shown that two photomultipliers which meet the dark current noise criteria are: RCA 1P21 and EMI 9502S. Neither of these are ruggedized though many corporations are currently expending effort in this area. For example, RCA is developing "an extremely rugged 9-stage photomultiplier intended for use in the detection and measurement of very low light levels and in critical applications involving high mechanical stress".* This will be a side-on tube having overall dimensions of ½ inch in diameter and 1.31 inches in length.

2. Photomultiplier Electronics

Because of the requirement that the phototube detect both stars and planets, some very bright objects may be observed. To permit detection of targets with wide ranges in intensity, it is planned that the gain will be changed to maintain the anode current constant (logarithmic feedback). Thus the multiplier voltage will be a measure of the magnitude of the target while the fast rise and fall times of the phototube anode current will be used for transit time measurements. Figure II-10 shows an example of both the multiplier voltage and anode current as a function of target magnitude. The zero signal voltage on the tube, E_o, is about 1900 volts so that an 1150 volt pulse will be generated for a 1st magnitude

* Proposed Technical Objective sheet for RCA developmental type C70129B, May 27, 1963.

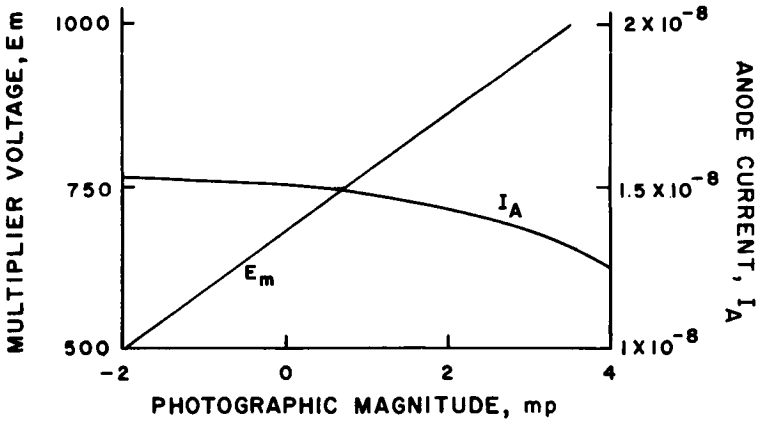

Figure II-10. Representative Phototube Output Current and Multiplier Voltage as a Function of Target Magnitude Using Logarithmic Feedback

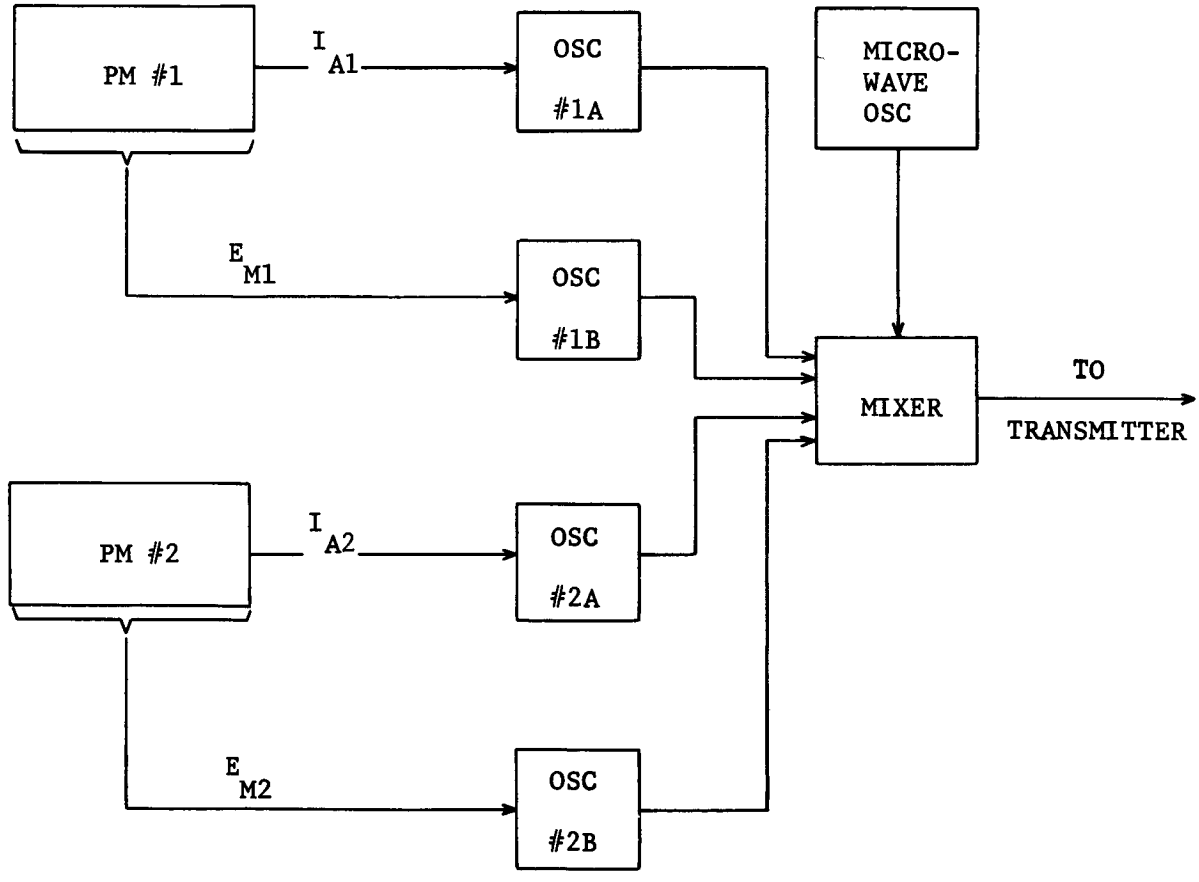

Figure II-11. Schematic of Electronics in Capsule

star. The E_m curve has a slower rise time than the anode current curve. The latter is therefore more useful for time measurements while the former can be measured for magnitude and at the same time protect the tube from excessive current damage.

The electronic instrumentation between the photomultipliers and the computer is necessarily divided into two parts. Because the detector will be separate from the space vehicle and not coupled to it by anything which might disturb its (the detector's) motion, information must be transmitted from the detector to the vehicle, a distance between six inches and four feet.

To minimize the instrumentation in the detector capsule, both the anode current and multiplier voltage pulses are to be sent immediately to the mother vehicle for analysis. This does not require four separate transmission channels but can be done by modulating a carrier frequency as shown schematically in Figure II-11. For example, the current pulse, I_{A1}, from photomultiplier number 1 changes the frequency of the output of oscillator number 1A which in turn amplitude modulates a master micro-wave oscillator. The master carrier is then transmitted to the mother vehicle for processing. All four outputs of the two photomultipliers similarly shift their respective oscillator frequencies. The signal transmitted has, then, a bandwidth twice the value of the highest modulator frequency and is centered on the master oscillator frequency.

The electronics required in the space vehicle itself are schematically shown in Figure II-12. There the signal transmitted from the capsule is

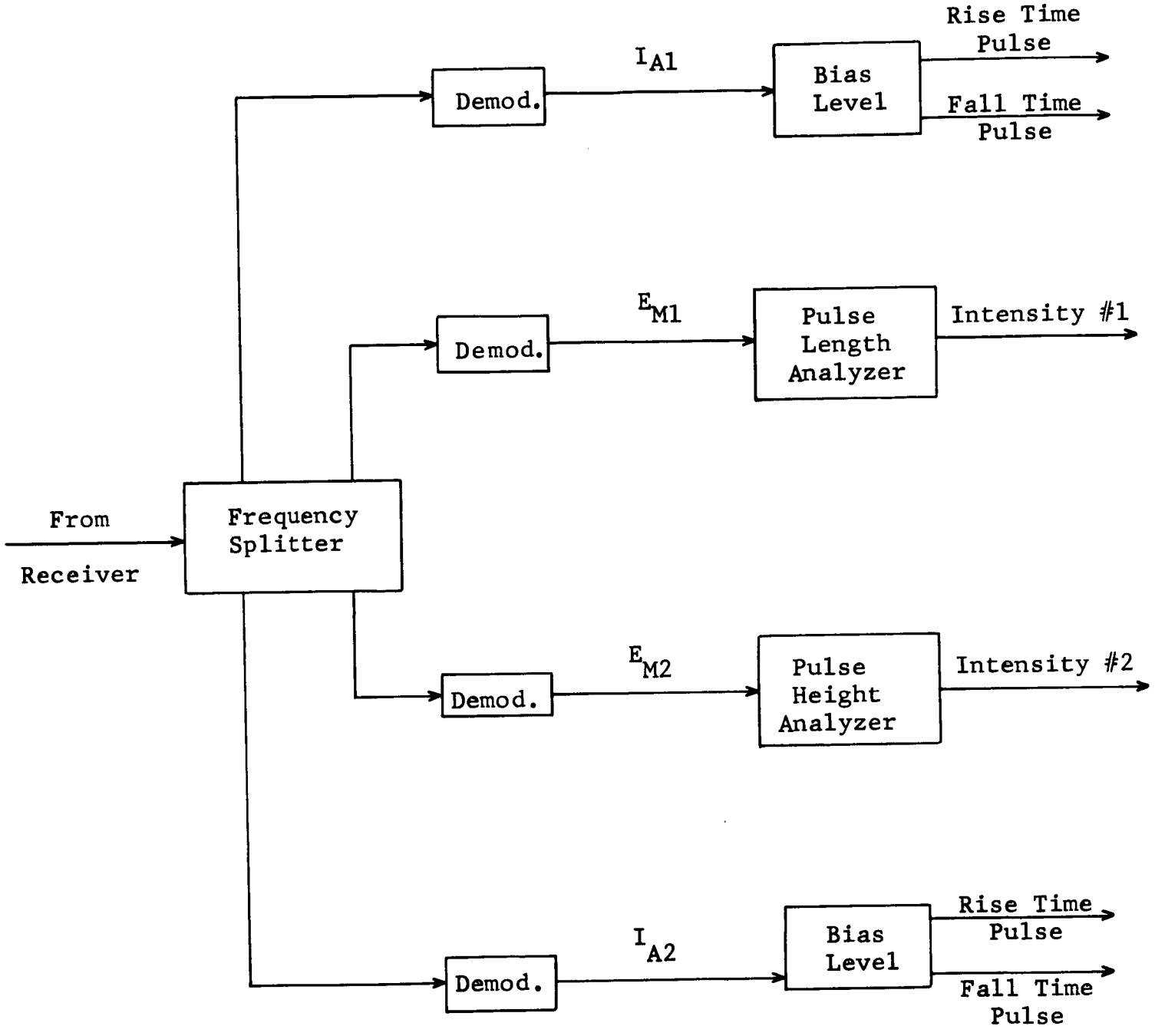

Figure II-12. Schematic Representation of Vehicle Electronics Prior to Data Formation Logic

received and split as to frequency into its four information components. These are each demodulated resulting in the original anode currents and multiplier voltages.

Each anode current is then used to measure the times that the pulse rises above and falls below a given bias level. The average value of these two times is what constitutes the target transit time.

The multiplier voltage measures the target intensity using some device such as a pulse-height analyzer. Six bits, or 63 levels, could be resolved which would be about equal to the expected correlation of measurement to reality.

3. Data Logic

It is planned to construct two 24-bit words for each target transit of a given slit. The method of construction is shown in Figure II-13. Three registers, each 24 bits long, are shown. The first ("Elapsed Time Register") contains at any instant, the count (in 10 μsecond intervals) of the time from the start of the measurement sequence. This count is accumulated from 10 μsecond pulses generated by an external clock. The register will hold up to 168 seconds of time, well enough to encompass ten scan periods of ten seconds each, and will be able to resolve angles as small as one second of arc.

When the anode current from the photomultiplier rises above a given bias level, a pulse is generated which gates the contents of the first register into the second ("Rise Time Register"). This latter then contains the time at which the anode current exceeds the bias.

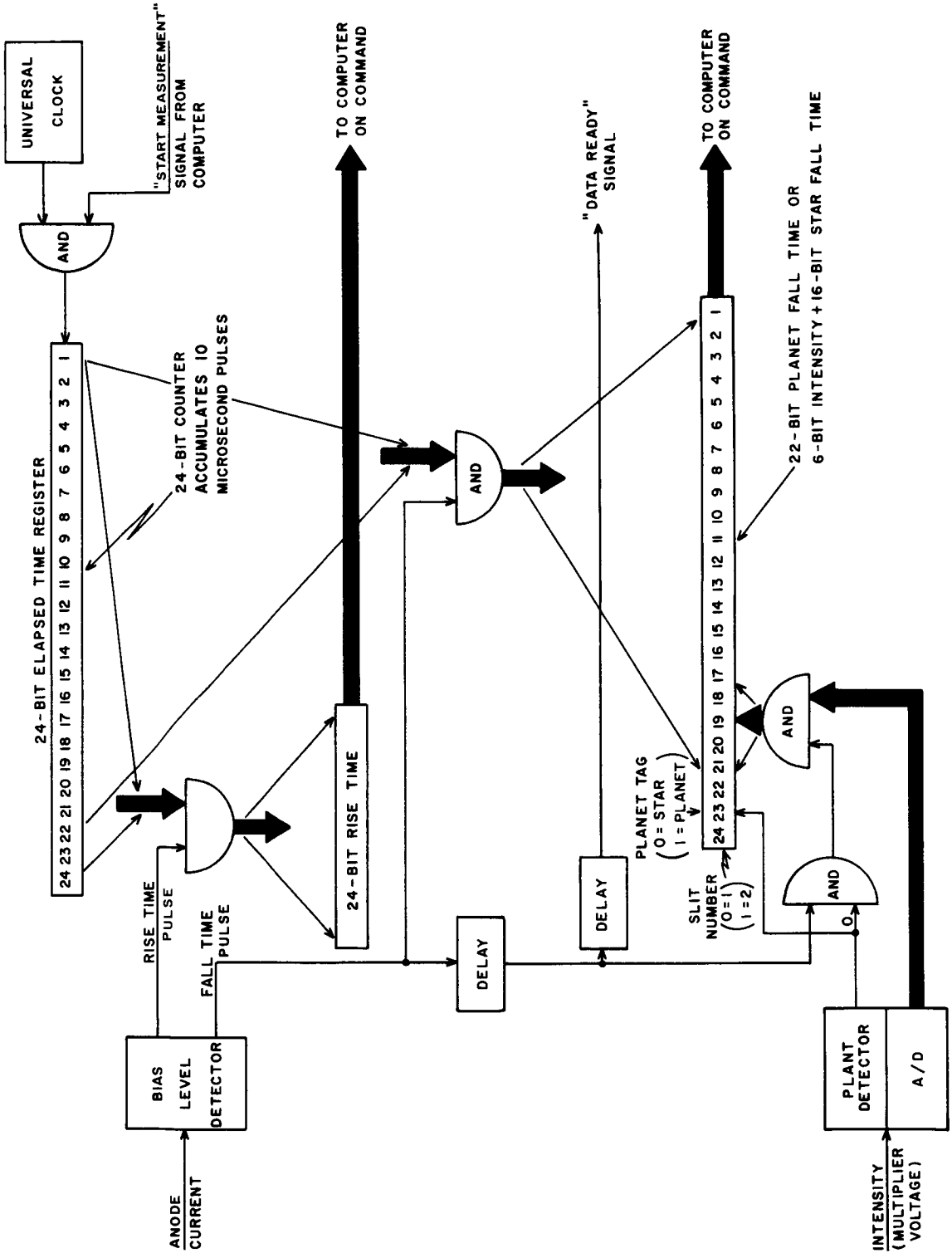

Figure II-13. Block Diagram for Transit Data Formation

The third register accumulates several quantities and its contents depend on the type of target detected. The reason for this is that planets are extended bodies, and in some cases the trailing edge rather than the leading edge of the planet will be measured. ("Trailing" and "leading" refer to the manner in which the slit approaches the planetary disk.) Since it is not known beforehand which is desirable, both the rise time (denoting the entrance of the leading illuminated portion of the planet into the slit) and the fall time (denoting the exit from the slit of the trailing illuminated portion) need to be recorded.

The largest size of a planet, due to the slit configuration chosen, is 60^{o} in diameter. Thus it is possible that one slit is illuminated for one-sixth of a period or 1.667 seconds (ten second period) by a full disc planet. Using a 10 μsecond count resolution, such a dwell time would consume $1.667/10^{-5}$ = 166,700 counts and could fill just over one-half of an 18-bit register.

For a planet, then, the second data word has its lowest eighteen bits identical to the lowest eighteen bits of the Elapsed Time Register at the anode current fall time.* Since intensity data is not needed for a

---

* It is to be noted that these eighteen bits are not used to count the dwell time; they merely reproduce the Elapsed Time Register at the fall time. Thus it is possible for this number actually to be less than the number represented by the lowest eighteen bits of the Rise Time Register. Such an event would mean that the nineteenth bit of the Elapsed Time Register had changed between the rise and fall times. One is only concerned, therefore, in preventing this bit from changing more than once. This is ensured if $2^{18} - 1 >$ expected maximum number of counts. That is, the eighteen bit counter can never overflow twice (regardless of where it begins the count) if the expected maximum number of counts is less than could be contained in such a register.

planet, only two more bits are used: one denoting the slit number (0 means Slit #1, 1 means Slit #2) and one for a target tag (0 for stars, 1 for planets or any extended target).

The number of bits needed, therefore, is only twenty while Figure II-13 shows a 24-bit word. This has been done merely to simplify the situation. The total number of bits produced is 24 + 20 = 44 which would fit in two words each 22 bits long. However, the computer will accept data equal to its word length, which we feel has a high probability of being in the 24 to 30 bit range. Furthermore, to retain the rise time in one unit, a 24-bit input is required; complicating the hardware by using words of different sizes seems unnecessary. For planets, then, the second word contains: a one-bit slit tag, a one-bit target tag, and the 22-bit lower portion of the Elapsed Time Register at fall time.

So much for planets and other extended targets. Stars are much simpler in that, being almost point sources, they remain no longer than about 368 μseconds in the slit. To measure fall time, then, no more than six bits would be needed for counting. In order not to complicate the hardware, however, it is suggested that the 22-bit lower portion of the Elapsed Time Register be transferred to the second word upon receipt of the fall time pulse in the manner identical to that used for planets. In addition, after a short delay, bits 17 through 22 of this word are overwritten with the intensity code. The anode current rise time pulse, of course, transfers 24 bits between the Elapsed Time Register and the Rise Time Register as is also done for planets. For stars, then, the

second word contains: a one-bit slit tag, a one-bit target tag, a six-bit intensity code, and a sixteen-bit fall time. Again the sixteen bits are way in excess of what's needed, but compatibility with the planet detection procedure and uniformity of word length suggests these values.

In any event, shortly after fall time, the computer is informed that data is ready whereupon the two words are transferred either directly into the computer or into an intermediate buffer. (The reader is directed to Section IV-A if he wishes to follow the history of the data words into the computer.)

C. Mechanical Design

Among the considerations involved in the mechanical design are the following: (1) choice of a system and parameters of the system which will provide a motion of the camera which is either known or computable, (2) design of a system which will constrain or allow for retrieval of the camera, (3) design of structural characteristics.

In regard to the second feature, numerous methods of retrieval or constraint of the camera are feasible and the comparative advantages depend on the situation imposed. In some situations the camera would be constrained to the vehicle so that the problem of retrieval would not exist. Again, the operator may have the capability to move about away from the vehicle, in which case retrieval would not be a problem. In other situations a mechanical system may be required to either constrain or retrieve the camera. Because of the undefined nature of the specific application at the present time, not a great deal of attention was devoted to this problem.

In regard to item (3), the mechanical demands on the structure will be small since the camera will be operated in a low force environment and it has no delicate parts. Hence a design compatible with normal criteria such as weight and size can also be expected to satisfy the structural criteria. In relation to the optical design, of course, structure is of great importance; here, too, however, normal design care appears to be sufficient.

The description of the motion of the camera (Item (1)) is of prime importance since it provides

the reference frame in which the measurements are made and hence must be known accurately. In order to achieve the desired system accuracy the orientation as a function of time must be known within the order of ten seconds of arc. If the camera is a rigid body, its motion can be described by an intricate mathematical model, or in an effort to avoid the intricate model, the parameters can be chosen so that part of the motion is diminished. Another method to avoid the intricate mathematical model would be to make the body non-rigid in a way that would cause a simplified motion.

1. The Motion of a Rigid Camera

The motion of a rigid body can be described if the moments of inertia and the initial angular rates are known. However, unless two of the moments of inertia are nearly equal and unless the initial angular rate vector is nearly equal to a certain prescribed vector, the mathematical model will not be simple, and indeed, if the moments of inertial are greatly different, the model will be quite complicated. So, with a rigid body, the success of the system can be achieved in two ways, (1) the use of an intricate mathematical model, (2) the provision of near equality in the values of two moments of inertia and the nearness of the initial angular rate vector to a certain prescribed vector (i.e., a vector parallel to the principal axis of the body).

The nutation of a rigid body can be made small enough to be removed from the mathematical model by making the precession angle small. This task is formidable. If the nutation amplitude is to be less than ten seconds of arc, for example, and if the moments of inertia are equal to

within one part in one thousand, the initial angular rate perpendicular to the scan axis must be of the order of one hundredth the scan rate. This would require an elegant system which would spin the camera about the desired axis (the principal axis along $\hat{k}_4$) while compensating for the angular rate of the vehicle to within one hundredth the scan rate and then release the camera with a negligible torque perpendicular to the spin axis. It would also be required that sophisticated tests be made to determine the moments of inertia. The nutation amplitude as a function of the difference in the moments of inertia and the initial angular rate perpendicular to the spin axis is shown in Figure II-14 which is based on the analysis of Appendix A.

Rather than use a system to reduce the initial angular rate, ω_o, the first term in the nutation could be included in the mathematical model. In such a method the error in θ would be of order S where

$$S = \tfrac{1}{4}\left[\frac{I_2 - I_1}{(I_2+I_1)}\right]^2 \frac{I_3^2}{(2I_3 - I_1 - I_2)^2}\left[\frac{I_1\,\omega_o}{I_3\,\nu_s}\right]$$

If, as in the previous example, the moments of inertia are equal to one part in one thousand, the initial angular rate perpendicular to the scan rate can be of the order of one hundred times the scan rate. This is a trivial task. If the moments of inertia were less well controlled, i.e., equal to one part in one hundred, then the angular rate must be of the order of the scan rate. This can be done, and since this accuracy of the moments of inertia (one part in one hundred) can be achieved, it is feasible that

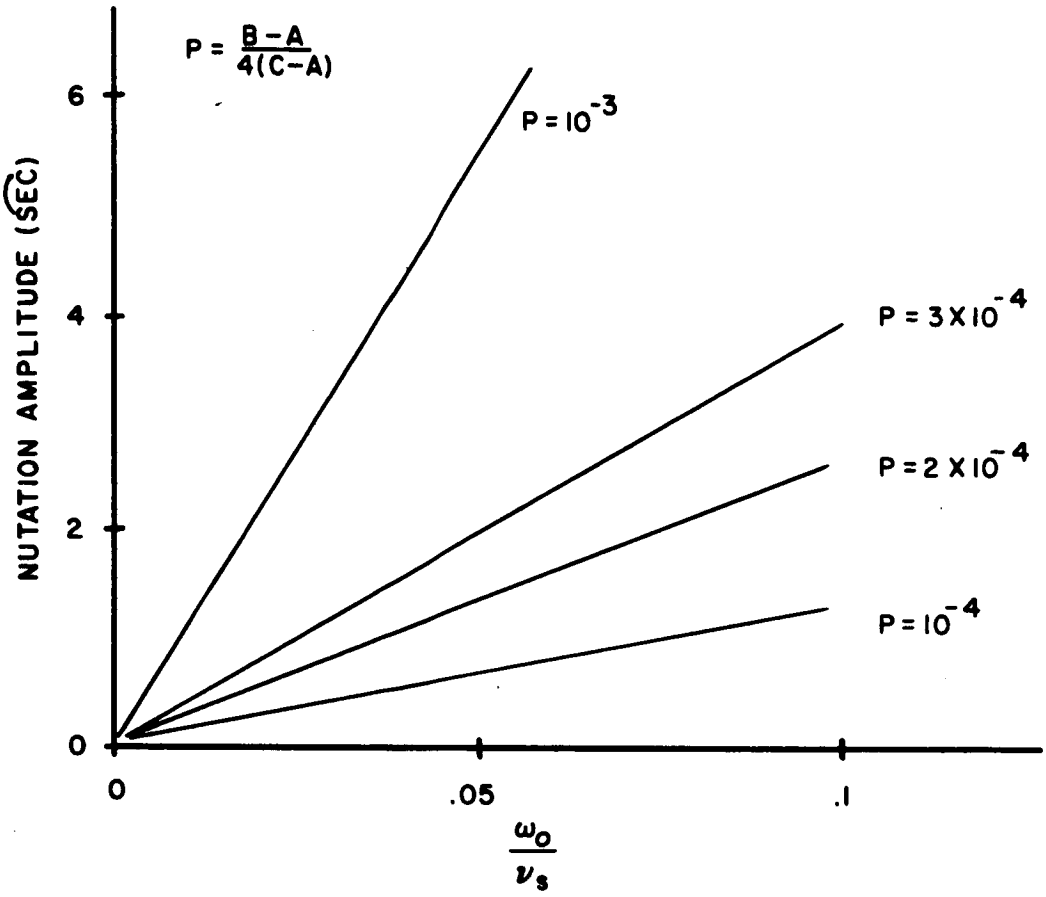

Figure II-14. Nutation Amplitude vs. $\frac{\omega_o}{\nu_s}$ for a Rigid Body

a mathematical model which includes the precession and the first harmonic of the nutation will represent the motion within ten seconds of arc.

In the second order solution, ϕ contains a term which must be included but it is of the form of a constant times time so it can be added to a term in the first approximation and thus it does not contribute a complication to the mathematical model.

So then, it can be concluded that the motion of the rigid camera can be represented accurately only if, (1) the initial angular rate perpendicular to the spin axis is very small, or if (2) the mathematical model includes the first harmonic of the nutation and a second order term in the model of ϕ, and if the moments of inertia are equal to an order of one part in one hundred.

2. The Momentum Wheel

The momentum wheel concept was investigated and appears to be a practical method of eliminating the nutation from the mathematical model and even presents the possibility of causing all motion to be small enough so that it could be represented by an angular rate equal, in magnitude, to the scan rate and in a fixed direction. (See Figure II-15.)

The basic thought involved in the momentum wheel concept is that a swiftly spinning wheel will provide a large momentum even if the camera has only a slow angular rate. This large momentum can be expected to cause the amplitudes of the camera motion to be small and thus allow the motion to be represented by a simple mathematical model. In addition to providing a large angular momentum the momentum wheel system provides

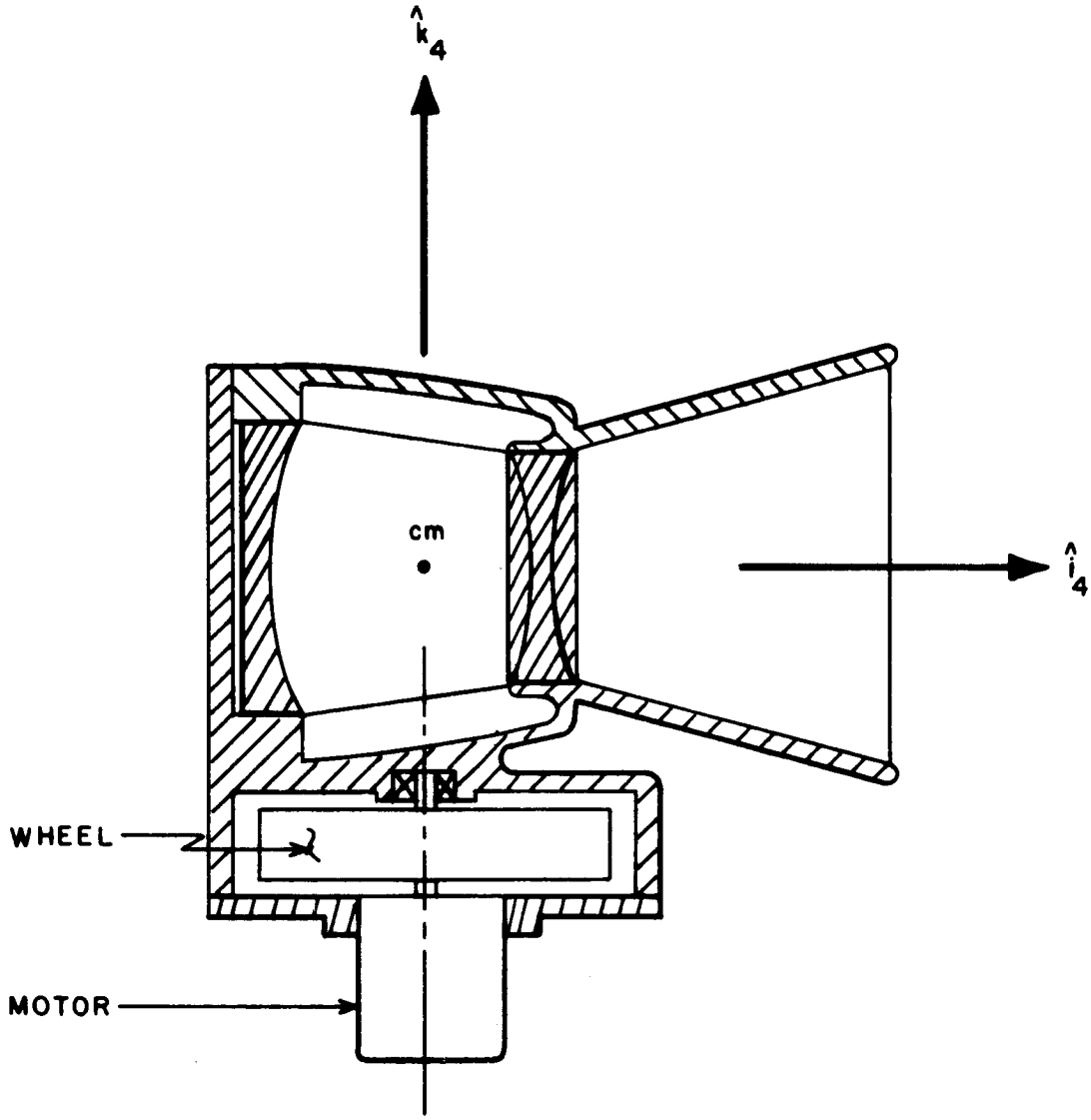

Figure II-15. Camera with Momentum Wheel

a means of changing the scan rate through application of a torque between the wheel and the camera, and thus allows the operator to release the camera with zero angular rate. It is expected that this is easier than releasing a spinning body and that this method will allow a minimum of undesired angular rate.

An approximate analytical representation of the motion was derived to determine the effects of the initial angular rate, the differences in the moments of inertia, and the products of inertia (which includes the distance between the centers of mass of the wheel and the camera). This derivation is shown in Appendix G. The influences of the several parameters are shown in Figures II-17, II-18, and II-19.

Figures II-17, II-18 and II-19 show the amplitude of the several parts of the motion. The motion is made up of a cone defined by the angle γ, a precession cone θ_o, and the nutation, which is a change in θ (see Figure II-16 The values of γ, θ_o and the nutation are dependent on ν_s, ψ_1, ω_o, I_{xz}, I_{xy}, I_1, I_2, I_3, A_1, and C_1. These parameters are defined in Appendix G.

These figures show, for example, that if $\dot{\psi}_1 = 1000$ rad/sec

$$\omega_o = .05 \text{ rad/sec}$$

$$\frac{I_1 + A_1}{C_1} = 2$$

$$\sqrt{\left(\frac{I_{xy}}{I_1 + A_1}\right)^2 + \frac{1}{4}\left(\frac{I_2 - I_1}{I_1 + A_1}\right)^2} = \frac{1}{10} \quad ,$$

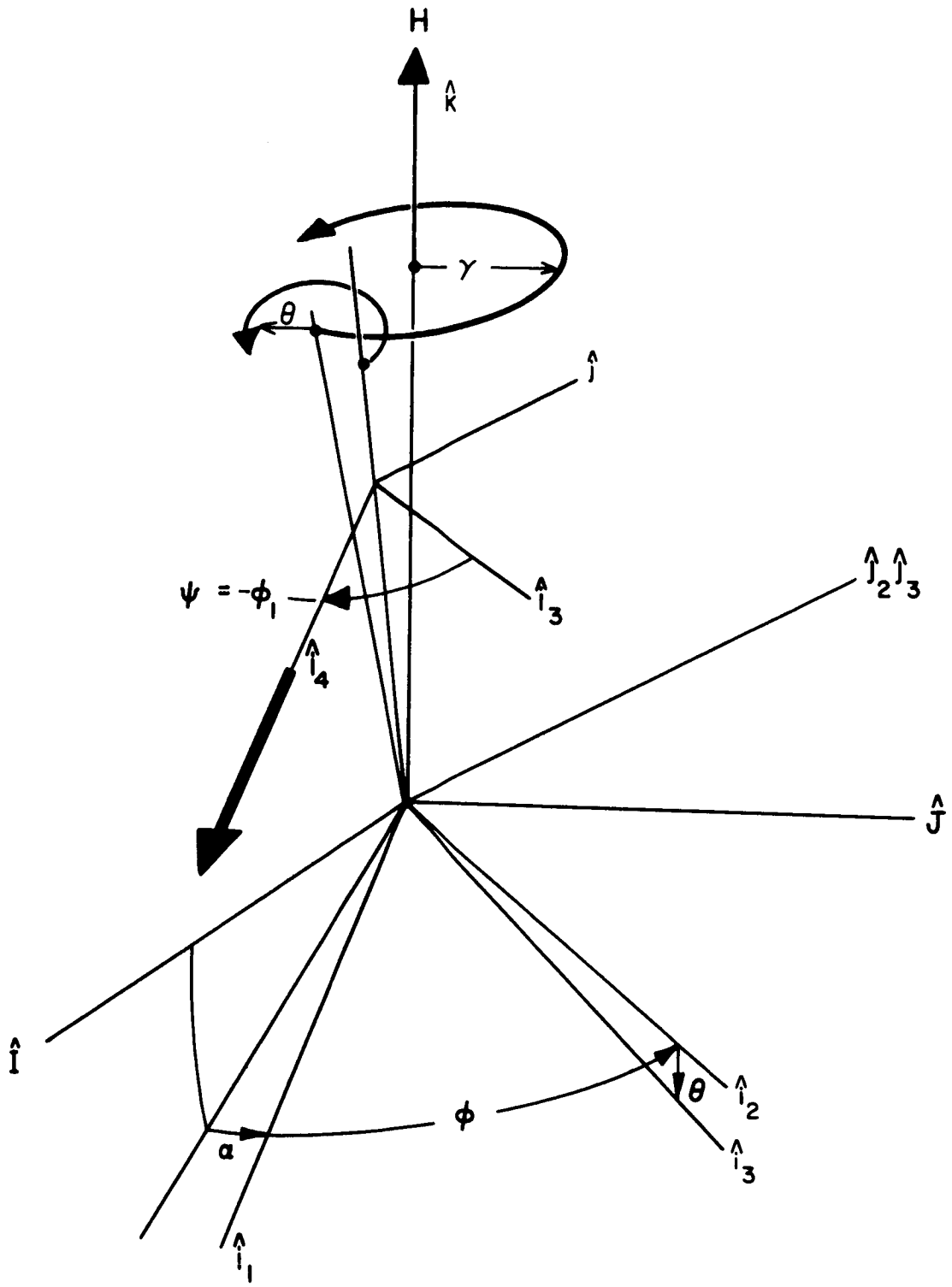

Figure II-16. The Motion of the Camera (with Momentum Wheel)

that the precession, θ_o, would be 10^{-4} rad. and the nutation would be $.5 \times 10^{-5}$ rad. In this case the mathematical model would need to include the precession angle but the nutation could be discarded. Also in this case, if

$$\frac{I_{xz}}{C_1}$$

were of order 1/10 and if the scan rate, ν_s, were one rad/sec, the angle γ would be or the order $1/10^4$. The mathematical model would then have to include γ.

Figures II-17, II-18, and II-19 show that it is indeed possible, with the momentum wheel to have a motion which is described by a rotation vector which remains within ten seconds of arc of a constant vector. This motion, of course, would provide the simplest model. In order to maintain the rotation vector within ten seconds of arc, the parameters could be chosen to be:

$$\dot{\psi} = 1000 \text{ rad/sec}$$

$$\nu_s = .3$$

$$\frac{I_{xz}}{c_1} = \frac{1}{3} \times 10^{-1}$$

$$\omega_o = 10^{-2} \text{ rad/sec}$$

$$\frac{I_1+A_1}{c_1} = 3$$

This is all quite reasonable and suggests that the momentum wheel provides a convenient method of obtaining a known reference frame in which to make the measurements.

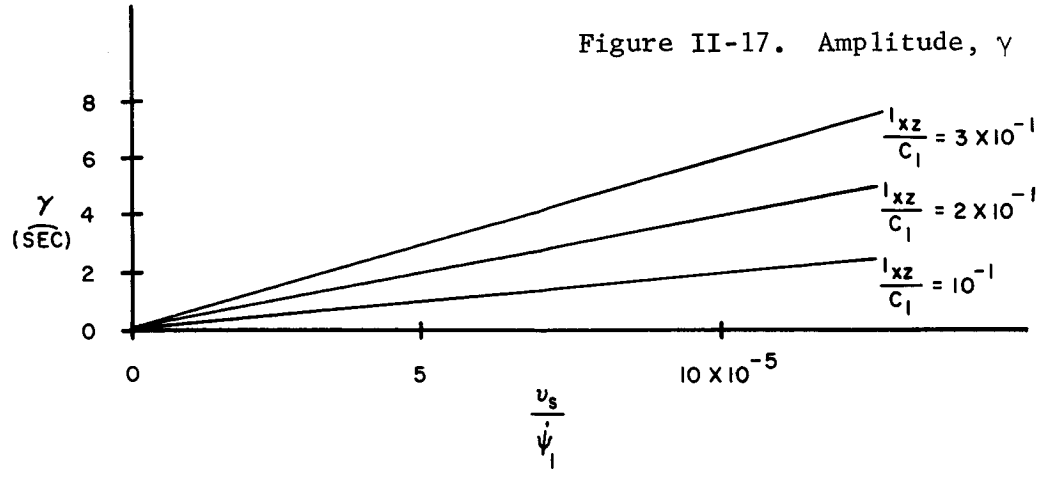

Figure II-17. Amplitude, γ

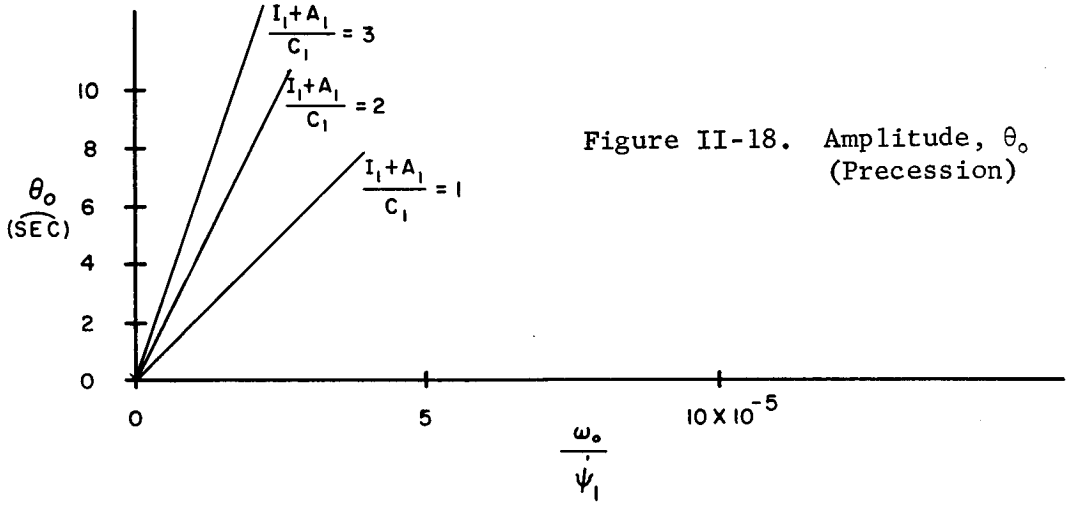

Figure II-18. Amplitude, θ_o (Precession)

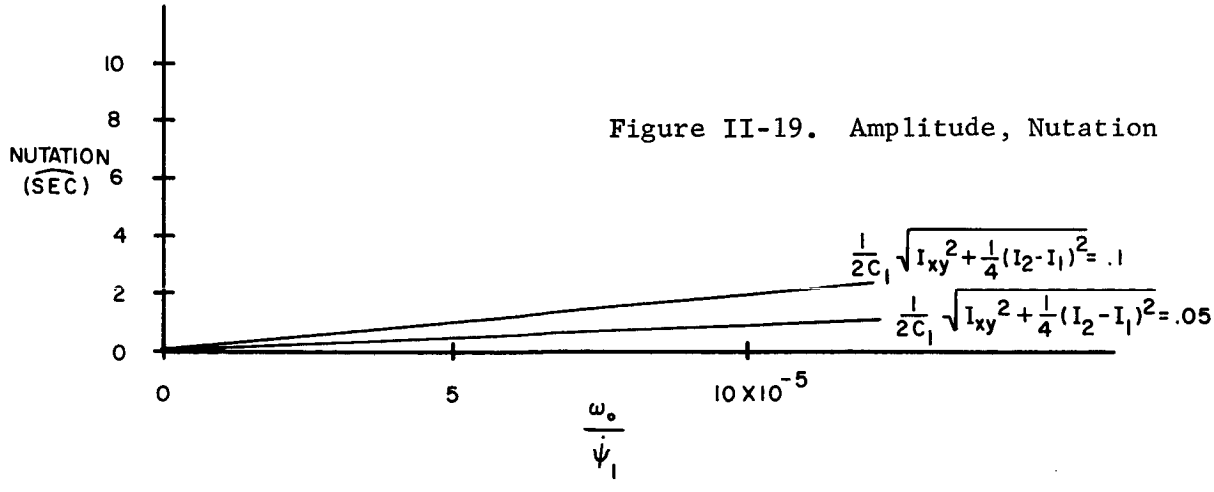

Figure II-19. Amplitude, Nutation

III. SYSTEM ANALYSIS

The present section is divided into five parts. The first derives the equations basic to the scanning camera navigation concept. Symmetric body motion (i.e., rotation about an axis which is in turn uniformly precessing about a constant angular momentum direction) is assumed with extensions to more complex motions given in Appendix A. Following this is an analysis of the corrections to be made to the catalogued positions of celestial targets necessitated by the effects of parallax, proper motion, aberration, and the finite velocity of light. The transmissivity of the scaled-down Baker-Nunn optical design is followed by an examination of the measurement errors related to noise (photon noise, background noise, detector noise). Closing the section is a presentation of the results of some simulations of the navigation concept. This was done both to test the accuracy of interplanetary navigation and to evaluate the technique of target identification proposed in Section I-C and detailed in Section IV-B.

A. Mathematical Analysis

Analyzing the scanning camera navigation system from a mathematical point of view involves generating an equation (or set of equations) which relates the transit time of a known target across a particular slit to the position and attitude of the camera, and then generating the equations for computing this position and attitude from an entire

set of measured transit times. We now proceed to each of these in that order.

1. Transit Time Equation

Let us choose as our principle coordinate system the astronomical frame (X, Y, Z) in which the position of a star is specified by its right ascension, α, and declination, δ. This reference frame is shown in Figure III-1a. Two more coordinate references are also shown in Figure III-1: the angular momentum frame (x', y', z') rotated as in Figure III-1b from the astronomical frame by τ and ξ, and the instrument frame (x, y, z) fixed in the camera and related to the angular momentum frame by the angles θ (angle of precession), ϕ (angle to the line of nodes), and ψ as shown in Figure III-1c. In this latter reference system, x extends along the camera optical axis and z along the spin axis. These frames are chosen to simplify the notation describing the motion of the scanning camera. Since the angular momentum vector points along z', the angles τ and ξ are constant. Furthermore, for a symmetric rotating body, the angle θ remains constant while ϕ and ψ are both linear functions of the time, t: $\phi = \Omega t + \phi_o$, $\psi = \mu t + \psi_o$ where Ω and μ are rates and ϕ_o, ψ_o phase angles. (See Appendix A for a more general formulation of the motion in terms of expansions of elliptic functions.)

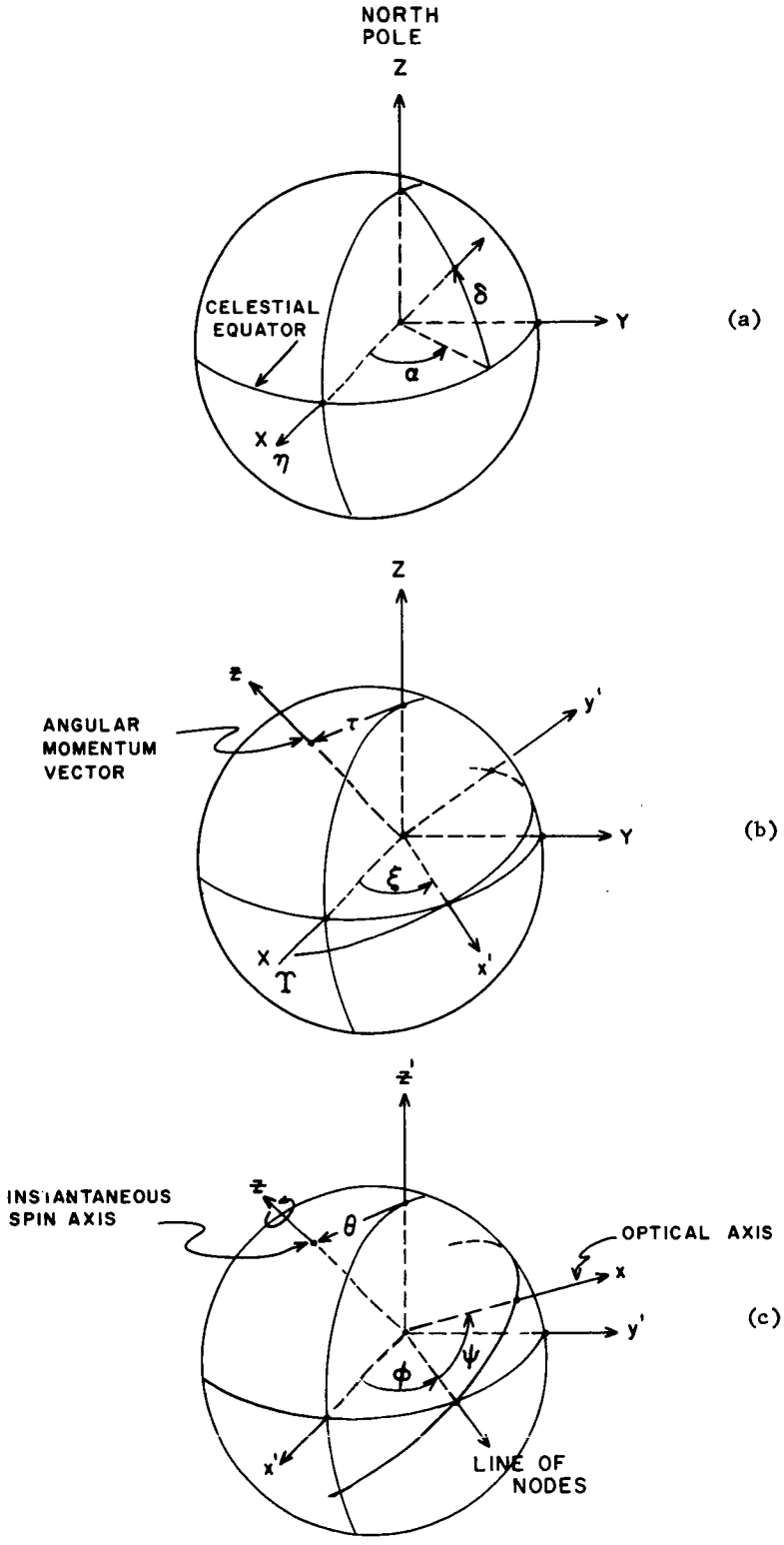

Figure III-1. Relations Between Various Coordinate Systems

Let the position of any object relative to the camera be given by the vector $\overline{V}$ in the astronomical frame and $\overline{v}$ in the instantaneous instrument frame. The relation between the components of these vectors is then just

$$\overline{v} = E \cdot H \cdot \overline{V} \tag{3-1}$$

where E is the Euler matrix

$$E = \begin{pmatrix} \cos\psi\cos\phi - \cos\theta\sin\phi\sin\psi \,, & \cos\psi\sin\phi + \cos\theta\cos\phi\sin\psi \,, & \sin\psi\sin\theta \\ -\sin\psi\cos\phi - \cos\theta\sin\phi\cos\psi \,, & -\sin\psi\sin\phi + \cos\theta\cos\phi\cos\psi \,, & \cos\psi\sin\theta \\ \sin\theta\sin\phi \,, & -\sin\theta\cos\phi \,, & \cos\theta \end{pmatrix} , \tag{3-2}$$

and H is a similar matrix

$$H = \begin{pmatrix} \cos \xi & \sin \xi & 0 \\ -\cos \tau \sin \xi & \cos \tau \cos \xi & \sin \tau \\ \sin \tau \sin \xi & -\sin \tau \cos \xi & \cos \tau \end{pmatrix} . \qquad (3\text{-}3)$$

H, of course, transforms $\bar{V}$ into the angular momentum frame and E transforms the result into the instrument frame.

Now at the instant of measurement, the target coincides with the projection of a camera slit. We assume that the slits are portions of great circle arcs passing through the optical axis as shown in Figure III-2. Denoting the angular distance between the optical axis and the target direction by η, the position vector $\bar{v}$ of the target relative to the camera is

$$\bar{v} = v \begin{pmatrix} \cos \eta \\ \sin \eta \sin \Gamma \\ \sin \eta \cos \Gamma \end{pmatrix} , \qquad (3\text{-}4)$$

where $v = |\bar{v}| = |\bar{V}|$, η is measured positively towards the spin axis, and Γ is the angle between the optical axis-spin axis plane and the slit plane (= Γ for Slit #1, = $-\Gamma$ for Slit #2, = 0 for Slit #3).

The transit time equation can now be derived very simply. Let x, y, z be the components of $\bar{V}$ in the astronomical reference frame. Combining Equations (3-4) and (3-1), we eliminate the unwanted variable η by dividing the second component of (3-1) by the third. Rearranging the result gives

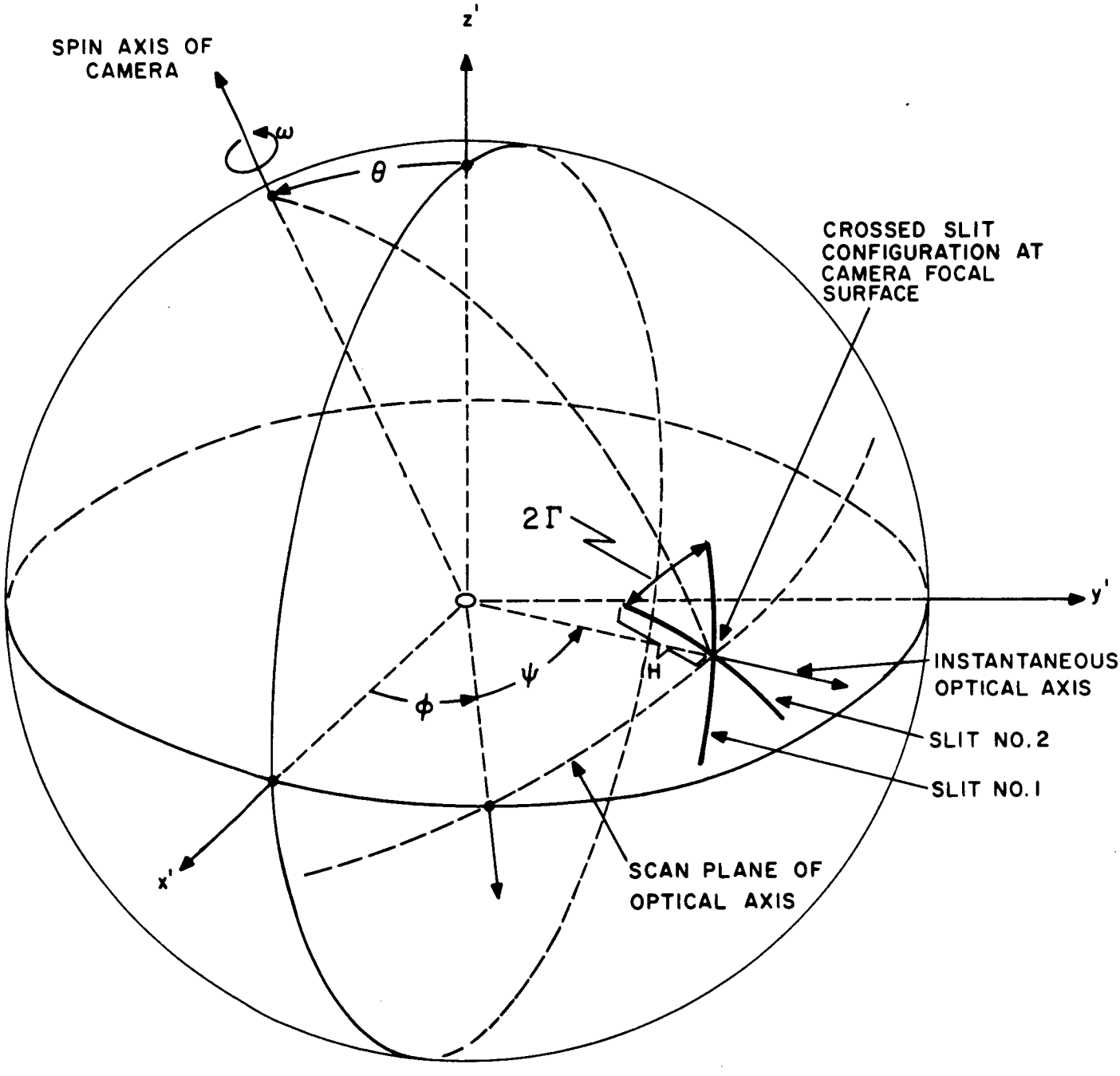

Figure III-2. Relationship of Camera Reference System to Angular Momentum Frame

$$X\left[A_1 - A_2 \tan \Gamma\right] + Y\left[B_1 - B_2 \tan \Gamma\right]$$

$$+ Z\left[C_1 - C_2 \tan \Gamma\right] = 0 \qquad (3\text{-}5)$$

where

$$A_1 = \cos \xi \left[- \sin \psi \cos \phi - \cos \theta \sin \phi \cos \psi\right]$$

$$- \cos \tau \sin \xi \left[- \sin \psi \sin \phi + \cos \theta \cos \phi \cos \psi\right]$$

$$+ \sin \tau \sin \xi \cos \psi \sin \theta \ , \qquad (3\text{-}6)$$

$$B_1 = \sin \xi \left[- \sin \psi \cos \phi - \cos \theta \sin \phi \cos \psi\right]$$

$$+ \cos \tau \cos \xi \left[- \sin \psi \sin \phi + \cos \theta \cos \phi \cos \psi\right]$$

$$- \sin \tau \cos \xi \cos \psi \sin \theta \ , \qquad (3\text{-}7)$$

$$C_1 = \sin \tau \left[- \sin \psi \sin \phi + \cos \theta \cos \phi \cos \psi\right]$$

$$+ \cos \tau \cos \psi \sin \theta \ , \qquad (3\text{-}8)$$

$$A_2 = \cos \xi \sin \theta \sin \phi + \sin \theta \cos \phi \cos \tau \sin \xi$$

$$+ \sin \tau \sin \xi \cos \theta \ , \qquad (3\text{-}9)$$

$$B_2 = \sin \xi \sin \theta \sin \phi - \cos \tau \cos \xi \sin \theta \cos \phi$$

$$- \sin \tau \cos \xi \cos \theta \ , \qquad (3\text{-}10)$$

$$C_2 = - \sin \tau \sin \theta \cos \phi + \cos \tau \cos \theta \ . \qquad (3\text{-}11)$$

Equation (3-5) applies to all three slits but is considerably simplified for Slit #3 where $\Gamma = 0$. It is the solution of this equation for both: (a) the target transit time in terms of an assumed position and attitude, and (b) the camera position and attitude in terms of a set of measured transit times, that forms the basis of the scanning camera navigation system. Case (a) takes place during the target identification procedure described in Section IV-B, while Case (b) generates the navigation information and forms the second part of the present section.

If the target is a star, Equation (3-5) becomes rather insensitive to the position of the vehicle within the solar system. Assuming, then, that the catalog position coordinates α and δ are corrected for aberration and parallax using the approximate position and velocity of the vehicle, the components X, Y, and Z of the vector $\bar{V}$ need only be specified by

$$\bar{V} = \begin{pmatrix} X \\ Y \\ Z \end{pmatrix} = v \begin{pmatrix} \cos\delta \cos\alpha \\ \cos\delta \sin\alpha \\ \sin\delta \end{pmatrix} . \qquad (3\text{-}12)$$

We see that the distance to the star, v, can be cancelled easily from Equation (3-5) and so is of no account. Substituting this into Equation (3-5) gives the basic equation for stellar targets:

$$\cos\alpha \left[A_1 - A_2 \tan\Gamma\right] + \sin\alpha \left[B_1 - B_2 \tan\Gamma\right]$$

$$+ \tan\delta \left[C_1 - C_2 \tan\Gamma\right] = 0 \qquad (3\text{-}13)$$

wherein v, the distance to the star, has been cancelled out.

In the case of planets, Equation (3-5) depends heavily on the relative position of the camera in the solar system. In addition, planetary (and no doubt vehicle) positions will be specified in the ecliptic coordinate system, rotated through an angle ϵ (obliquity of the ecliptic = 23°27'8".26)* about the negative X axis from the astronomical frame. Thus, if in the ecliptic system, the position of a given planet is specified by the vector $\bar{p}$, and that of the vehicle by the vector $\bar{r}$, then the relative position vector $\bar{V}$ in the astronomical frame is

---

* Allen, C. W., Astrophysical Quantities, University of London, Athlone Press, London, England, p. 18; 1955.

$$\bar{V} = \begin{pmatrix} X \\ Y \\ Z \end{pmatrix} = \begin{pmatrix} 1 & 0 & 0 \\ 0 & \cos\epsilon & -\sin\epsilon \\ 0 & \sin\epsilon & \cos\epsilon \end{pmatrix} \begin{pmatrix} p_x - r_x \\ p_y - r_y \\ p_z - r_z \end{pmatrix} \qquad (3\text{-}14)$$

where the subscripts x, y, and z denote components in the ecliptic system. Combining this with Equation (3-5) and rearranging, we have the basic equation for planetary targets:

$$(p_x - r_x)\left[A_1 - A_2 \tan\Gamma\right]$$

$$+ (p_y - r_y)\left[(B_1 - B_2 \tan\Gamma)\cos\epsilon + (C_1 - C_2 \tan\Gamma)\sin\epsilon\right]$$

$$+ (p_z - r_z)\left[-(B_1 - B_2 \tan\Gamma)\sin\epsilon + (C_1 - C_2 \tan\Gamma)\cos\epsilon\right] = 0 \qquad (3\text{-}15)$$

We now pass to discussing the solution of Equations (3-13) and (3-15) for navigational information given that a number of transit times of various bodies have been measured.

2. Navigation Computations

The ability of the scanning camera to detect a multitude of targets immediately permits a determination of the desired unknowns by some smoothing technique such as least squares.* In addition to this, however, the basic Equations (3-13) and (3-15) are highly non-linear in both the

* Bartlett, D. P., Method of Least Squares, Rumford Press, Boston; 1945.

measured transit times and the attitude parameters, but not in the vehicle position.

Thus let us first formulate the navigation computation on the following general lines. Let $f_k(x_1, x_2, \ldots x_n; t_k) = 0$ represent p functions ($k = 1, 2, \ldots, p$), connecting the measurable parameter t_k and the unknowns x_j, $j = 1, 2, \ldots, n$. Because of the non-linearity of f_k in the variable t_k and perhaps in some of the unknowns, we first linearize the function using assumed values x_j' and t_k':

$$f_k' + \sum_{j=1}^{n} \left(\frac{\partial f_k}{\partial x_j}\right)' \Delta x_j + \left(\frac{\partial f_k}{\partial t_k}\right)' \Delta t_k = 0 \qquad (3\text{-}16)$$

where the primes denote evaluation at x_j' and t_k' and the true values are $x_j = x_j' + \Delta x_j$, $t_k = t_k' + \Delta t_k$. Let p measurements of t_k now be made, one measurement for each $k(k = 1, 2, \ldots, p)$, yielding values t_{km}.* The expectation of any of these values is just the solution of Equation (3-16); i.e., a linear function of the incremental unknowns Δx_j:

$$E(t_{km}) = t_k' - \frac{f_k' + \sum_{j=1}^{n} \left(\frac{\partial f_k}{\partial x_j}\right)' \Delta x_j}{(\partial f_k/\partial t_k)'} \qquad (3\text{-}17)$$

The Gauss-Markoff theorem** states that the best unbiased linear least

---

* This is slightly different from the usual problem in which one measurable quantity is measured many times. Here, f_k is a different function for each k and therefore each t_k will also be different.

** Trumpler and Weaver, Statistical Astronomy, Dover Press, New York, p. 182; 1953.

squares estimates Δx_j are those values of the Δx_j that minimize the sum of squares

$$S = \sum_{k=1}^{p} (t_{km} - E(t_{km}))^2 \, w_k^2 \qquad (3\text{-}18)$$

where w_k is a weighting function dependent on the variance σ_k^2 of t_{km}.*

Now, as described in Section III-D, the RMS transit time error σ_k is dependent on the camera aperture, spin period, and target magnitude. All targets have the first two effects in common. Hence we shall take

$$w_k = 10^{-.133 m_k} \qquad (3\text{-}19)$$

where m_k is the magnitude of the target. Furthermore, for lack of any better estimate, we let $t_k' = t_{km}$. That is, we evaluate the function and its partials at the measured value t_{km} since this represents a highly accurate approximation to the true t_k.

---

* The usual least squares analysis is based on minimizing the sum of the squares of the residuals of a function. This is not in general, however, the procedure for computing the "best" values of the unknowns when the measured quantity is buried in a nonlinear manner in the function as it is in our case. Physically, one expects that if the measured values are believed to be normally distributed about the true value as mean, then the values of the computed unknowns should cluster about a value corresponding to that mean. By minimizing the sum of the squares of the function residuals, one is finding values of the unknowns which correspond to the mean of the function residuals, and these are not necessarily the same values as would correspond to the mean of the measured values. Said in other words, one certainly acts correctly in minimizing the sum of the squares of the residuals of the measured quantities, but there can arise some question as to the validity of this result when the same procedure is applied to the resiguals of a function connecting the measured and unknown quantities.

The equations from which the Δx_j are calculated come from minimizing S with respect to the unknowns:

$$\frac{\partial S}{\partial \Delta x_j} = 0 , \quad j = 1, 2, \ldots, n. \tag{3-20}$$

This is a system of n algebraic equations linear in the n unknowns Δx_j. The coefficients are all constants since evaluated using assumed values of the parameters. Carrying out the indicated differentiations, the solution is given by a matrix inversion:

$$\tilde{\Delta X} = M^{-1} B \tag{3-21}$$

where $\tilde{\Delta X}$ is a n x 1 column vector whose elements are the Δx_j, M is an n x n square matrix with elements m_{ij}:

$$m_{ij} = \sum_{k=1}^{p} \frac{(\partial f_k/\partial x_i)'(\partial f_k/\partial x_j)'}{(\partial f_k/\partial t_k)'^2} w_k^2 \tag{3-22}$$

and B is an n x 1 column vector whose elements are b_i:

$$b_i = - \sum_{k=1}^{p} \frac{f_k'(\partial f_k/\partial x_i)'}{(\partial f_k/\partial t_k)'^2} w_k^2 . \tag{3-23}$$

Let us now be more explicit. To compute the attitude parameters of the scanning camera, only the stars will be used. Thus the function f_k given by Equation (3-13) will not contain the position coordinates of the

vehicle, but will be nonlinear in the seven attitude variables:

τ, ξ	These angles define the direction of the angular momentum vector relative to the astronomical frame.
θ_o, ϕ_o, ψ_o	These Euler angles define the orientation of the instrument frame with respect to the angular momentum frame at some zero time.
μ	Spin rate
Ω	Precession rate

Appendix B gives the explicit forms for the functions and derivations appearing in Equations (3-22) and (3-23) for the case of symmetric body motion. To attack the more general case of the motion of a slightly unsymmetric body, the equations of Appendix A are to be used. Equations (3-22) and (3-23), together with Equation (3-19) and the measured transit times of identified targets are sufficient to compute the deviations of the attitude parameters from their assumed values for one iteration.

The computation of vehicle position $\bar{r}$ is somewhat similar except that f_k given by Equation (3-15) is linear in the unknowns. (Since attitude will be determined first, the attitude parameters here are considered known.) It can thus be written:

$$f_k = r_x a_k + r_y b_k + r_x c_k + d_k = 0 \qquad (3\text{-}24)$$

where the (constant) coefficients are given explicitly in Appendix C.

At first sight a significant improvement might seem possible due to this linearity. This is not so because of the dependence of the coefficients a_k, b_k, c_k, and d_k on the measured transit time t_k. Since

we desire to minimize the residuals of this measured quantity, an attempt to compute the full position rather than the increments in position will result in a quadratic or worse in the unknowns.

To escape this complexity and still compute the position directly, we will use assumed values of r_x, r_y, r_z for the function $\partial f_k/\partial t_k$ in the denominators of Equations (3-22) and (3-23), but retain these variables and unknowns in the numerators. In the form (3-24) we note that $\partial f/\partial r_x = a$, $\partial f/\partial r_y = b$, $\partial f/\partial r_z = c$ so that on substituting into (3-22) and (3-23) the vehicle position becomes

$$\begin{pmatrix} r_x \\ r_y \\ r_z \end{pmatrix} = M^{-1} B \qquad (3\text{-}25)$$

where M is a symmetric matrix with elements

$$m_{11} = \sum_{k=1}^{p} \frac{a_k'^2}{(\partial f_k/\partial t_k)'^2} w_k^2 \qquad (3\text{-}26)$$

$$m_{22} = \sum_{k=1}^{p} \frac{b_k'^2}{(\partial f_k/\partial t_k)'^2} w_k^2 \qquad (3\text{-}27)$$

$$m_{33} = \sum_{k=1}^{p} \frac{c_k'^2}{(\partial f_k/\partial t_k)'^2} w_k^2 \qquad (3\text{-}28)$$

$$m_{12} = \sum_{k=1}^{p} \frac{a_k' \; b_k'}{(\partial f_k/\partial t_k)'^2} \; w_k^2 \qquad (3\text{-}29)$$

$$m_{13} = \sum_{k=1}^{p} \frac{a_k' \; c_k'}{(\partial f_k/\partial t_k)'^2} \; w_k^2 \qquad (3\text{-}30)$$

$$m_{23} = \sum_{k=1}^{p} \frac{b_k' \; c_k'}{(\partial f_k/\partial t_k)'^2} \; w_k^2 \qquad (3\text{-}31)$$

$$m_{ij} = m_{ji} \qquad (3\text{-}32)$$

and B is a column vector with elements

$$b_1 = - \sum_{k=1}^{p} \frac{d_k' \; a_k'}{(\partial f_k/\partial t_k)'^2} \; w_k^2 \qquad (3\text{-}33)$$

$$b_2 = - \sum_{k=1}^{p} \frac{d_k' \; b_k'}{(\partial f_k/\partial t_k)'^2} \; w_k^2 \qquad (3\text{-}34)$$

$$b_3 = - \sum_{k=1}^{p} \frac{d_k' \; c_k'}{(\partial f_k/\partial t_k)'^2} \; w_k^2 \; . \qquad (3\text{-}35)$$

B. Corrections to Target Positions

The targets of principle interest for space navigation are stars and planets. To realize the accuracy potential of the scanning camera instrumentation, the positions of these bodies must be known to at least that accuracy. For the purposes of this section, two accuracy levels will be chosen: it is desired that all targets be locatable to within two and ten seconds of arc respectively. The first represents a highly accurate system while the second permits some relaxation of the computer requirements.

The positions of stars are normally given by entries in a catalog such as the Atlas Coeli* while the positions of planets can be similarly determined using an ephemeris** or through computation with their orbital elements. These positions are usually not of sufficient accuracy, however, when considering space missions of ten years duration or more and distances from the sun out to 40 A.U. (near the orbit of Pluto). On the other hand, it is possible to make corrections to the published positions which will reduce the position error to tolerable limits with only a nominal amount of effort. Stated in another way, the catalog and ephemeris positions are sufficiently accurate that only small corrections need be applied to reduce the errors below two or ten seconds of arc.

---

* Atlas Coeli - II Katalog - 1950.0, Antonin' Becvar, Praha, 1960.

** Planetary Coordinates for the Years 1960-1980, H. M. Stationery Office, London, 1958.

It is the purpose of this section to point out the need for such corrections and then to derive the equations and parameters necessary to make the corrections.

1. Need for Position Corrections

We will assume mission lengths up to ten years, camera scan periods of 10-100 seconds and required target location accuracies of 2-10 seconds of arc. Star positions suffer from proper motion, parallax, and aberration. Planetary positions, if computed from an ephemeris for the exact time of measurement, need only be corrected for aberration (which includes the effects of the finite velocity of light). The finite velocity of light poses no problem here because the catalog star positions include this effect already. That is, these are catalogs of the apparent star positions as seen from a stationary observer located at the center of the solar system.

Proper Motion

Proper motion is the real tangential velocity of the star relative to the solar system. It is designated by μ and usually given in seconds of arc per year. For the one hundred brightest stars the largest proper motion* is 3.68" per year and only four of these stars have values greater that 1" per year (see Figure III-3). Quite obviously such values have no effect during a single measurement period of 100 seconds or less, but

* Allen, C. W., Astrophysical Quantities, Althone Press, University of London, 1963, p. 229.

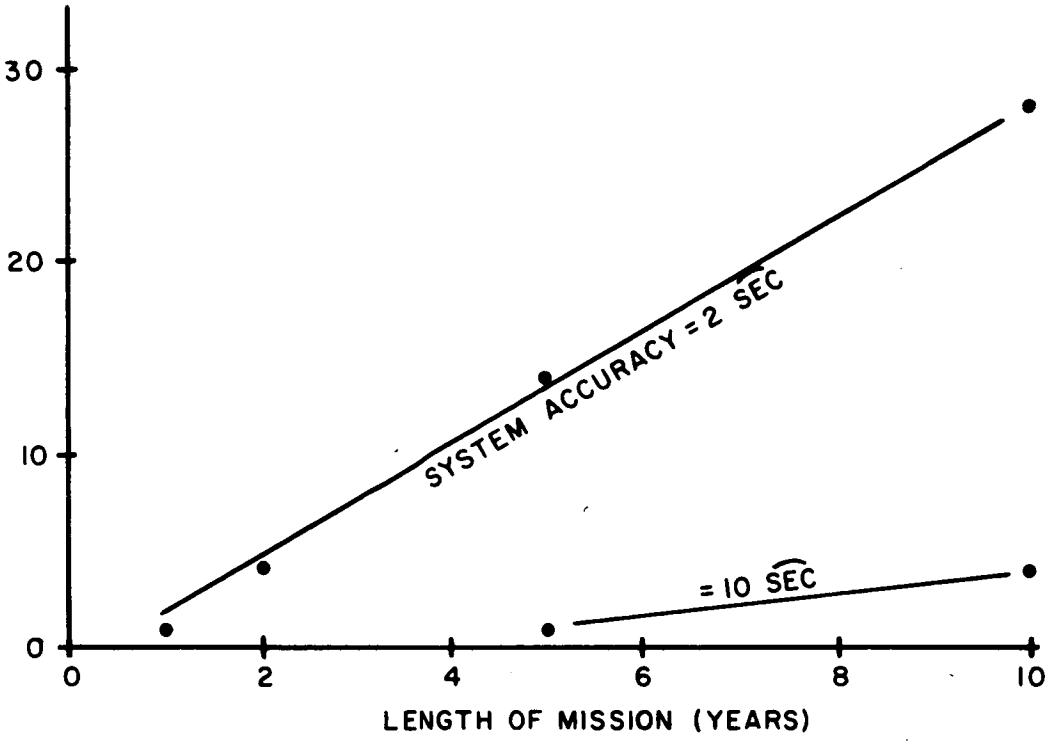

Figure III-3. Number of Stars Requiring Correction for Proper Motion

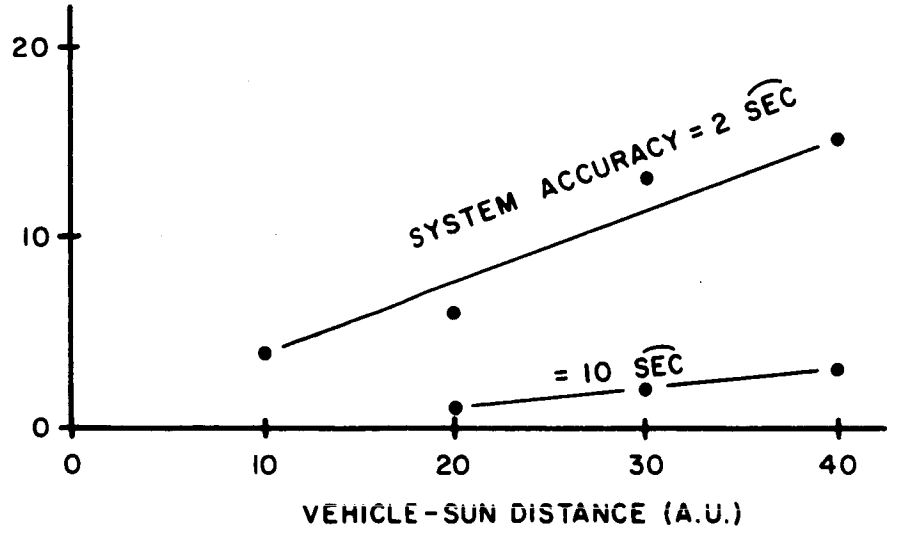

Figure III-4. Number of Stars Requiring Correction for Parallax

for long missions the positions of some stars will have to be updated. For example, if a mission of ten years takes place, and position accuracies of two seconds of arc are desired, then, of the 100 brightest stars, 28 of them will have to undergo corrections. If ten seconds of arc is required, only four stars are affected.

Parallax

Parallax denotes the apparent angular displacement of the closer stars due to the observer not being at the solar system center. Its symbol is π and is given in seconds of arc per astronomical unit. It can also be found from the stellar distances given in parsecs since $pc \cdot \pi = 1$. If we consider missions not farther away from the sun than Pluto (40 A.U.) and require accuracies of two seconds of arc, then stars closer than 20 parsecs or those whose (Earth) parallax is greater than 0".05 must include corrections for vehicle position. As seen from Figure III-4, this includes 16 of the 100 brightest stars. (Fifteen of these also require proper motion correction over a ten year period.) For a ten second of arc system accuracy, only three stars require correction.)

Aberration

This is a phenomenon dependent on vehicle velocity tending to shift all targets (angularly) in the direction of the velocity vector. The angle of shift or aberration angle, is denoted by α and given by $\sin \alpha = v/c$ where v is the vehicle speed and c the speed of light. Since the vehicle will usually be moving along with a planet or itself be in orbit about

the sun, we can expect velocities in the range 5 to 50 kilometers per second. Therefore we can expect aberration angles in the range 3 to 30 seconds of arc, or sufficient to require correction.

Measurement Period

All other corrections may be computed for the approximate time of measurement. The measurement itself, however, can take up to 100 or more seconds. During this time a planet may very well have moved a sufficient amount to require further correction. For example, the earth moves about 30 kilometers per second, so if we are about 1 A.U. away from it and in a direction perpendicular to its velocity, a 100 second measurement period finds the earth moved by four seconds of arc.

All planets suffer from this problem, especially when the vehicle motion about the planet need also be taken into account. To circumvent this difficulty, the positions need merely be computed for the instant of transit of the target across the slits.

Finite Velocity of Light

A measurement made at time t will not find the planet where the ephemeris says it is at that time. This is due to the fact that an ephemeris gives the true position at time t while measurement gives the true position at time t - r/c where r is the planet-observer range and c the velocity of light. That is, the target always lags behind where it really is. Taking a range of 1 A.U., a planet whose velocity is thirty kilometers per second (observer perpendicular to this velocity)

will lag twenty seconds of arc behind its ephemeris position. This is large enough to require correction. This is exactly the same as aberration, however, and is so treated in the subsequent equations.

2. Correction Equations

It is assumed that the tabulated spherical coordinates of the light source on the celestial sphere are given with respect to a right-handed coordinate system whose origin is at the center of mass of the solar system and whose x, y plane is in the plane of the celestial equator with the x axis in the direction of the first point of Aries.*

Furthermore, the following information is in the computer memory:

(1) the right ascensions and declinations of the light sources in tabulated form (or in the form of equations for solar system objects).

(2) the distance from the origin of the coordinate system to the light source,

(3) the approximate velocity and position of the vehicle with respect to the coordinate system, and

(4) the velocity of the light source when it is a planet and the proper motion of the light source when it is a star.

With the above information, the observer in the vehicle can compute the

---

* See Section III-A or a standard work on celestial mechanics such as Smart, W. M., Text-Book on Spherical Astronomy, Cambridge University Press, 1960.

corrections needed to make the stored coordinates and measured positions agree.

The equations for the corrections due to proper motion for a star are for right ascension

$$\Delta\alpha(t) = \dot{\alpha}(t - t_o) \quad , \tag{3-36}$$

and declination

$$\Delta\delta(t) = \dot{\delta}(t - t_o) \quad , \tag{3-37}$$

where $\dot{\alpha}$ is the angular velocity of the star about the polar axis of the celestial sphere, where $\dot{\delta}$ is the angular velocity of the star on its hour circle, and where $t - t_o$ is the difference in time from the last known tabulated values of α and δ at time t_o. Note that $\dot{\alpha}$ and $\dot{\delta}$ are assumed to be constants over the time interval of $t - t_o$.

The equations for the corrections due to parallax are for right ascension

$$\Delta\alpha = \frac{\bar{R} \cdot \hat{\alpha}}{(\bar{R} \cdot \hat{s} - \lambda) \cos\delta} \quad , \tag{3-38}$$

and declination

$$\Delta\delta = \frac{\bar{R} \cdot \hat{\delta}}{(\bar{R} \cdot \hat{s} - \lambda)} \quad , \tag{3-39}$$

where $\hat{s}$ is a unit vector in the direction of the light source from the origin, $\hat{\alpha}$ is a unit vector in the direction of increasing α at the point α, δ on the celestial sphere, $\hat{\delta}$ is a unit vector in the direction of increasing δ at the point α, δ on the celestial sphere, $\bar{R}$ is the position vector of the vehicle, and λ is the distance from the origin of the coordinate system to the light source. Note that $\hat{s}$, $\hat{\alpha}$, and $\hat{\delta}$ form an orthogonal set of unit vectors on the celestial sphere at the point α, δ. All of the vectors and scalar quantities for the parallax corrections are illustrated in Figure III-5.

The equations for the corrections due to the aberration of light are for right ascension,

$$\Delta\alpha = \frac{\bar{V}_{sv} \cdot \hat{\alpha}}{c \cos \delta} \quad , \tag{3-40}$$

and declination

$$\Delta\delta = \frac{\bar{V}_{sv} \cdot \hat{\delta}}{c} \quad , \tag{3-41}$$

where $\bar{V}_{sv}$ is the relative velocity vector of the vehicle with respect to the light source, c is the velocity of light, and $\hat{\alpha}$ and $\hat{\delta}$ are defined above. $\bar{V}_{sv}$, the relative velocity of the vehicle with respect to the light source is given by the equation

$$\bar{V}_{sv} = \bar{V}_v - \bar{V}_s \tag{3-42}$$

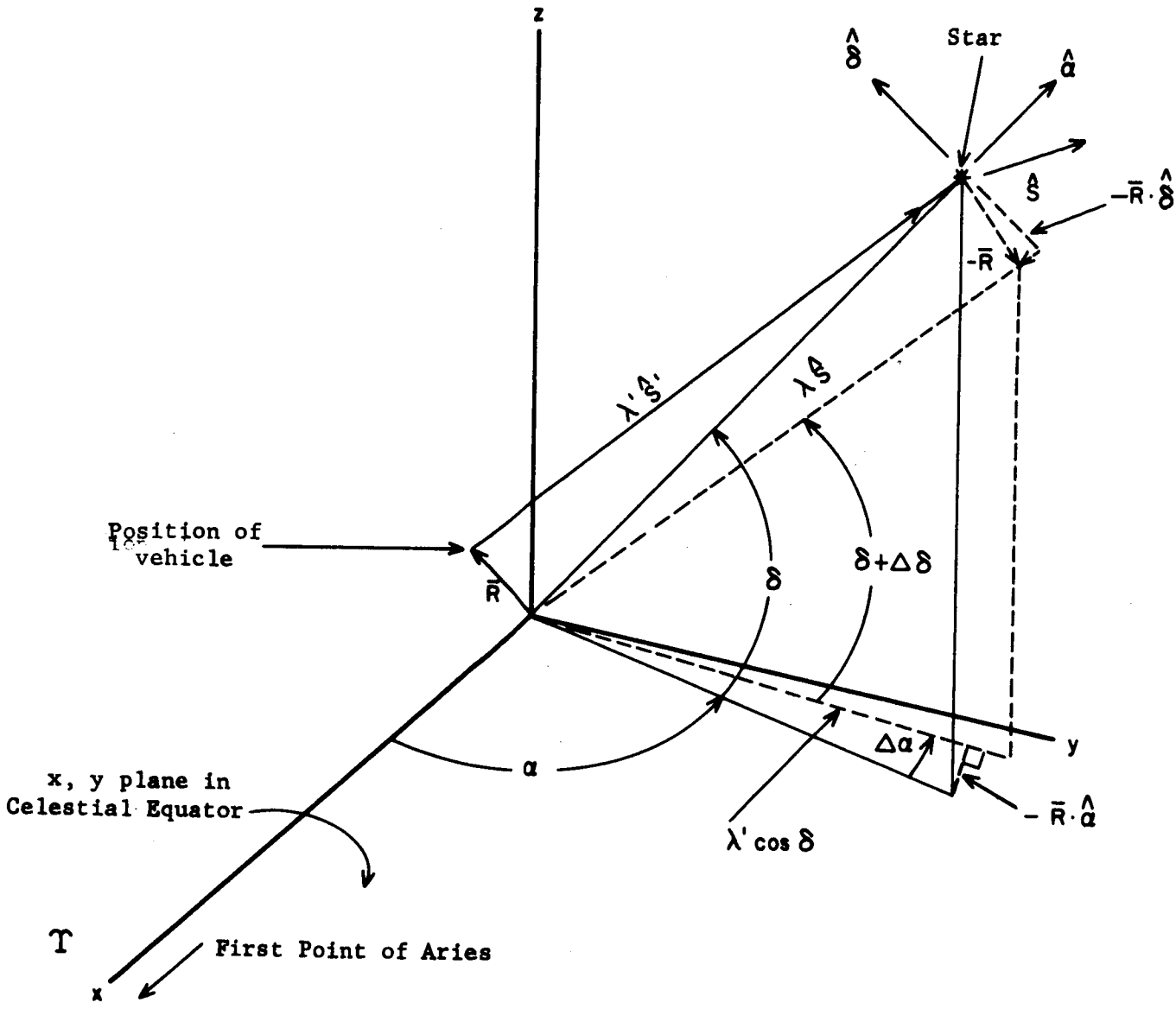

Figure III-5. Diagram Illustrating the Effect of Parallax (Due to parallax star is shifted by $-\bar{R}$ to a new position on the celestial sphere.)

where $\overline{V}_v$ is the velocity of the vehicle with respect to the origin, and $\overline{V}_s$ is the velocity of the source with respect to the origin. If the light source is a star, then $\overline{V}_s$ is negligible and $\overline{V}_{sv} \doteq \overline{V}_v$. If the light source is a planet, then $\overline{V}_s$ is not negligible and must be included in the computation. All vectors and scalar quantities in the aberration correction are illustrated in Figure III-6.

The remainder of this section contains the derivatives of these equations.*

Proper Motion Corrections

For stars, the proper motion corrections given by Equations (3-36) and (3-37) need no derivation once the motions are assumed linear over the time scale (ten years) of interest. For planets, proper motion has no significance since positions are computed from orbit equations which contain the orbiting motion.

Parallax Corrections

The parallax corrections can be derived in the following manner. First, compute the distance from the observer to the light source; second, compute the components of $-\overline{R}$ (the negative position vector of the vehicle) in the α and δ direction; then third, compute the corrections using small angle approximations.

---

* For similar work see A Compendium of Spherical Astronomy, by S. Newcomb, Dover, New York, 1960.

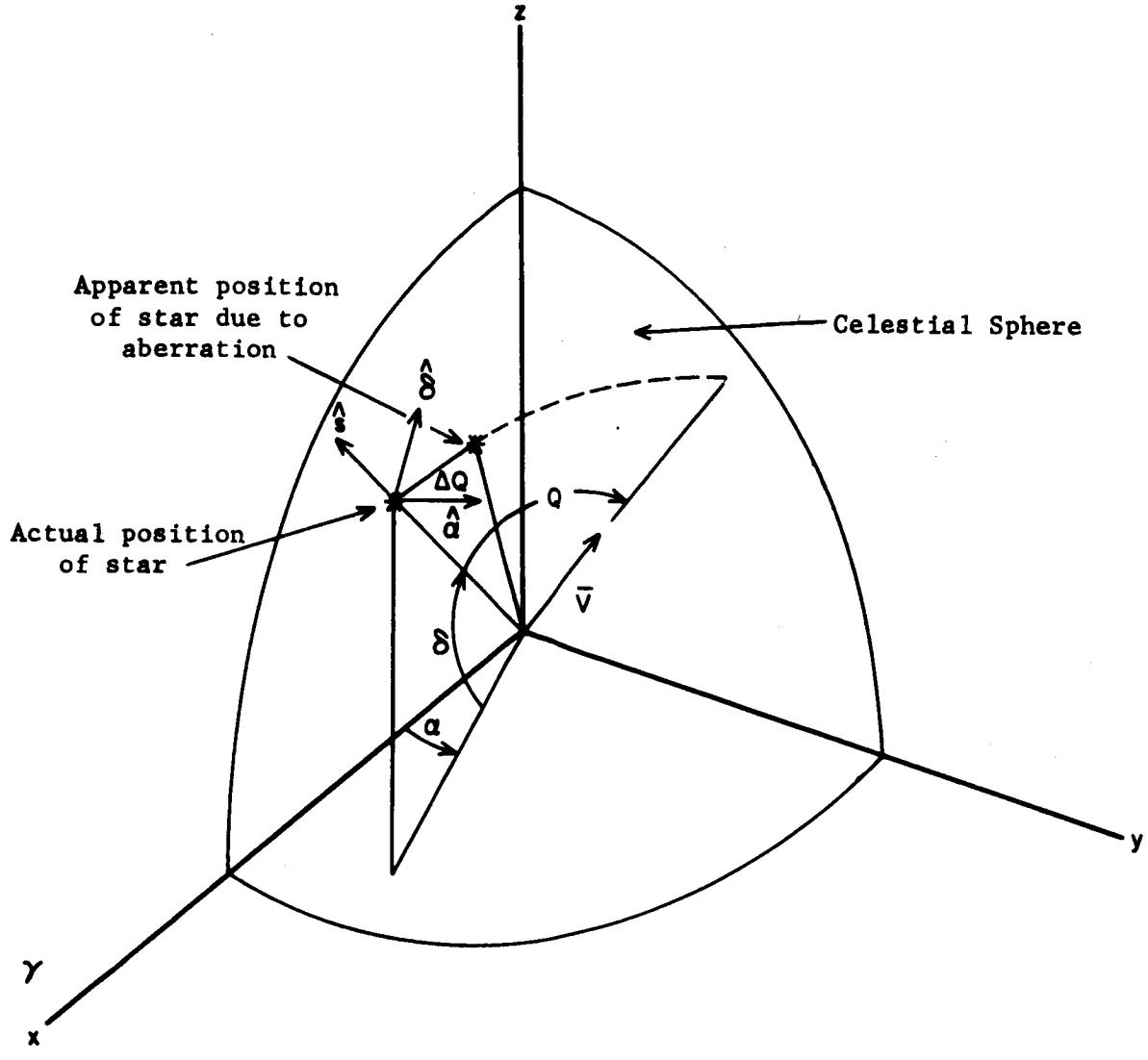

Figure III-6. Diagram Illustrating the Effect of Aberration (x, y plane in Celestial Equator. Star is displaced towards the point on the celestial sphere towards which the observer is moving.)

The vector $\lambda'\hat{s}'$ to the light source from the vehicle is

$$\lambda' \hat{s}' = \lambda \hat{s} - \bar{R} \tag{3-43}$$

where λ, $\hat{s}$, and $\bar{R}$ are defined as given previously, λ' is the distance from the vehicle to the light source, and $\hat{s}'$ is a unit vector from the vehicle to the light source. Doting the vector $\lambda'\hat{s}'$ into itself, yields for λ'

$$\lambda' = \lambda \left[1 - \frac{2\bar{R} \cdot \hat{s}}{\lambda} + \frac{r^2}{\lambda^2} \right]^{\frac{1}{2}} , \tag{3-44}$$

where r is the magnitude of $\bar{R}$.

The parallax correction can be thought of as shifting the star position by $-\bar{R}$ where $\bar{R}$ is the position vector of the vehicle. The direction of the vector $\lambda\hat{s} - \bar{R}$ will determine the new spherical coordinates of the star. The change in α and δ due to the change in the direction of the vector $\lambda\hat{s}$ to $\lambda\hat{s} - \bar{R}$ will be proportional to the scalar quantities obtained by doting $-\bar{R}$ into the unit vectors $\hat{\alpha}$ and $\hat{\delta}$ at α, δ. The parallax angular corrections will then be

$$\tan(\Delta\alpha) = - \frac{\bar{R} \cdot \hat{\alpha}}{\lambda' \cos \delta} , \tag{3-45}$$

and

$$\tan(\Delta\delta) = - \frac{\bar{R} \cdot \hat{\delta}}{\lambda'} . \tag{3-46}$$

If small angle approximations are made for the tangents of the above angles and if the magnitude of r is considered to be very small compared to λ, then the above equations can be approximated by Equations (3-38) and (3-39) given above.

This, of course, only applies to stars. To compute the apparent right ascension and declination of a planet, one uses Equation (3-43) directly.

Aberration Corrections

The light source of a star will appear to an observer in a moving vehicle to be shifted slightly towards the point on the celestial sphere towards which an observer is travelling. The magnitude of the angular shift ΔQ, or the aberration, is given by the equation

$$\Delta Q = \frac{V_V}{c} \sin Q \qquad (3\text{-}47)$$

where V_V is the speed of the vehicle with respect to the coordinate system, c is the speed of light, and Q is the angle between $\hat{s}$, the unit vector to the star, and $\overline{V}$, the velocity of the vehicle.

The relationship between ΔQ and $\Delta\alpha$, and between ΔQ and $\Delta\delta$ can be derived by an examination of the spherical triangle formed on the celestial sphere by the north pole, the actual position of the star, and the apparent position of the star due to aberration. This spherical triangle is illustrated in Figure III-7. From this triangle using the Law of Cosines and the Law of Sines, the following relationships are established:

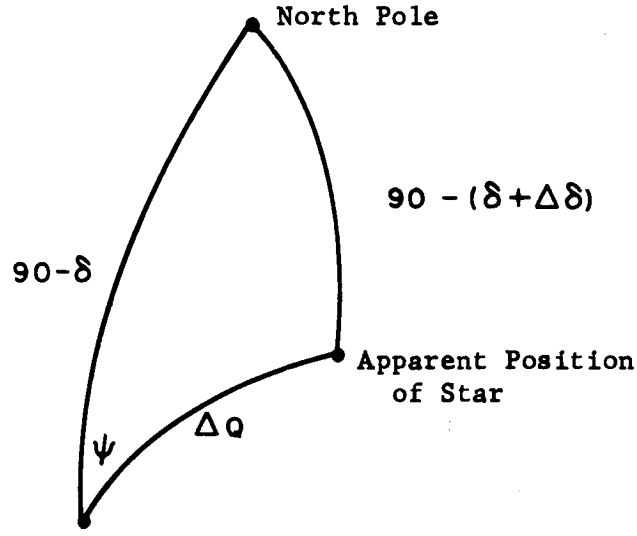

Figure III-7. Spherical Triangle Used in Aberration Calculations

$$\cos[90^\circ - (\delta + \Delta\delta)] = \cos(90^\circ - \delta)\cos\Delta Q + \sin(90^\circ - \delta)\sin\Delta Q\cos\psi \quad , \tag{3-48}$$

and

$$\frac{\sin\Delta\alpha}{\sin\Delta Q} = \frac{\sin\psi}{\sin(\delta + \Delta\delta)} \quad , \tag{3-49}$$

where ψ is the angle between the great circle ΔQ and the hour circle on which the star lies. Using small angle approximations, the above equations can be reduced to

$$\Delta\alpha = \frac{\Delta Q\cos(90^\circ - \psi)}{\cos\delta} \tag{3-50}$$

and

$$\Delta\delta = \Delta Q\cos\psi \quad . \tag{3-51}$$

These equations, in turn, can be reduced to

$$\Delta\alpha = \frac{V_V \sin Q\cos(90^\circ - \psi)}{c\cos\delta} \tag{3-52}$$

and

$$\Delta\delta = \frac{V_v \sin Q \cos \psi}{c} \tag{3-53}$$

where the expression for ΔQ in Equation (3-47) is substituted into Equations (3-50) and (3-51).

If a unit vector $\hat{t}$ is defined as

$$\hat{t} = \frac{\hat{s} \times \bar{V}_v}{|\hat{s} \times \bar{V}_v|} \tag{3-54}$$

then the following relationships can be established from the basic definitions of the vector and dot products of two vectors:

$$V_v \sin Q = |\hat{s} \times \bar{V}_v| \quad , \tag{3-55}$$

$$\cos \psi = (-\hat{\alpha}) \cdot \hat{t} \quad , \tag{3-56}$$

and

$$\cos(90^o - \psi) = \hat{t} \cdot \hat{\delta} \quad . \tag{3-57}$$

Substituting the above three expressions for $V_v \sin Q$, $\cos \psi$, and $\cos(90^o - \psi)$ into Equations (3-52) and (3-53) yields

$$\Delta\alpha = \frac{|\hat{s} \times \bar{V}_v| \ (\hat{t} \cdot \hat{\delta})}{c \cos \delta} \ , \tag{3-58}$$

and

$$\Delta\delta = \frac{|\hat{s} \times \bar{V}_v| \ (\hat{t} \cdot (-\hat{\alpha}))}{c} \tag{3-59}$$

The velocity vector $\bar{V}$ of the vehicle can be written as a vector sum of the three orthogonal unit vectors $\hat{s}$, $\hat{\alpha}$, $\hat{\delta}$:

$$\bar{V}_v = (\bar{V}_v \cdot \hat{s})\ \hat{s} + (\bar{V}_v \cdot \hat{\alpha})\ \hat{\alpha} + (\bar{V}_v \cdot \hat{\delta})\ \hat{\delta} \ . \tag{3-60}$$

When $\hat{s} \times \bar{V}_v$ is now computed using the rules for the vector product of orthogonal unit vectors, the unit vector $\hat{t}$ is found to be given by the equation

$$\hat{t} = \frac{(\bar{V}_v \cdot \hat{\alpha})\ \hat{\delta} + (\bar{V}_v \cdot \hat{\delta})(-\hat{\alpha})}{|\hat{s} \times \bar{V}_v|} \ . \tag{3-61}$$

From Equation (3-61), the dot products $(\hat{t} \cdot \hat{\delta})$ and $(\hat{t} \cdot (-\hat{\alpha}))$ can be derived as

$$\hat{t} \cdot \hat{\delta} = \frac{\bar{V}_v \cdot \hat{\alpha}}{|\hat{s} \times \bar{V}_v|} \ , \tag{3-62}$$

and

$$\hat{t} \cdot (-\hat{\alpha}) = \frac{\bar{V}_v \cdot \hat{\delta}}{|\hat{s} \times \bar{V}_v|} \quad . \tag{3-63}$$

When Equations (3-62) and (3-63) are substituted into Equations (3-58) and (3-59), the results are

$$\Delta\alpha = \frac{\bar{V}_v \cdot \hat{\alpha}}{c \cos \delta} \quad , \tag{3-64}$$

and

$$\Delta\delta = \frac{\bar{V}_v \cdot \hat{\delta}}{c} \quad . \tag{3-65}$$

If the light source is moving with respect to the coordinate system with constant angular speeds of $\dot{\alpha}$ and $\dot{\delta}$ where both $\dot{\alpha}$ and $\dot{\delta} > 0$, the aberration corrections for time t will be

$$\Delta\alpha = \frac{\bar{V}_v \cdot \hat{\alpha}}{c \cos \delta} - \dot{\alpha} \tau \quad , \tag{3-66}$$

and

$$\Delta\delta = \frac{\bar{V}_v \cdot \hat{\delta}}{c} - \dot{\delta} \tau \quad , \tag{3-67}$$

where τ is the time it takes for a light ray to travel from the star to the vehicle. τ, however, is given as

$$\tau = \frac{\lambda'}{c} \tag{3-68}$$

and Equations (3-66) and (3-67) are thus

$$\Delta\alpha = \frac{\bar{V}_v \cdot \hat{\alpha}}{c \cos \delta} - \frac{\dot{\alpha}\, \lambda'}{c} \quad , \tag{3-69}$$

and

$$\Delta\delta = \frac{\bar{V}_v \cdot \hat{\delta}}{c} - \frac{\dot{\delta}\, \lambda'}{c} \tag{3-70}$$

The velocity of the light source with respect to the coordinate system can be written as

$$\bar{V}_s = \dot{\lambda}'\, \hat{s} + \lambda'\, \dot{\alpha}\, \hat{\alpha} \cos \delta + \lambda'\, \dot{\delta}\, \hat{\delta} \quad . \tag{3-71}$$

From Equation (3-71), $\dot{\alpha}\, \lambda'$ and $\lambda'\, \dot{\delta}$ can be determined as given by equations

$$\dot{\alpha}\, \lambda' = \frac{\bar{V}_s \cdot \hat{\alpha}}{\cos \delta} \quad , \tag{3-72}$$

and

$$\dot{\delta}\, \lambda' = \bar{V}_s \cdot \hat{\delta} \quad . \tag{3-73}$$

Substituting Equations (3-72) and (3-73) into (3-69) and (3-70) yields the Equations (3-40) and (3-41) as was to be shown.

C. Optical System Transmissivity

Included in considerations for transmissivity are:

1. 6 lens air-glass interface reflection losses,
2. mirror reflection loss,
3. 2 air-glass interface losses for the shutter,
4. 2 air-glass interface losses for fiber optics, and
5. absorption losses in fiber optics.

The follow parts of this section gives a breakdown of transmissivity functions for the various system components.

1. Objective Lens

The transmissivity of the objective lens will depend primarily on the number of interfaces formed by the lens elements, low reflectance lens coating, and air. Assuming that the absorption loss within the lens elements and the reflection loss between elements cemented together is negligible, the transmissivity of one coated interface is 99% when the indices of refraction at the coated interface are 1.0, 1.38, and 1.55 for air, coating, and glass respecitvely. If the coating thickness were equal to one quarter wavelength at the center of the visible spectrum and the indices of refraction were of proper values to give zero reflectance at the center of the spectrum, the reflectance at the two ends of the visible spectrum would be 0.6%. Based on this we will use an average value of 98.7% for transmissivity of each coated interface. We then have for the transmissivity of the objective lens

$$T_L = 0.987^n \tag{3-74}$$

where n = number of coated interfaces. The scanning camera lens has a total of six such interfaces; including the lens between the shutter and photomultiplier gives n = 8 or T_L = 88%.

2. Mirror Reflectivity

A mirror will be required for folding the camera optical system as explained previously. The aluminized spherical surface will provide reflection of the rays at relatively high efficiency. The efficiency of such a surface is wavelength dependent. Figure III-8 shows the percentage of normal incident light reflected from a polished aluminum surface as a function of wavelength. As an additional consideration reflection from a steel surface was included.

It is possible that a reflector could be made from a steel flat. However as indicated by Figure III-8 the reflectivity would be much lower resulting in a reduction of system transmissivity.

3. Transmissivity of Optical Fibers

The transmissivity of a glass fiber is given by the expression*

$$T(i) = (1 - \alpha')^{\eta} \cdot \exp\left[\frac{-LN_1}{N_1^2 - \sin^2 i}\right] \tag{3-75}$$

* Kapany, N. S., Jour. of the Optical Society of America, Vol. 49, no. 8, p. 783.

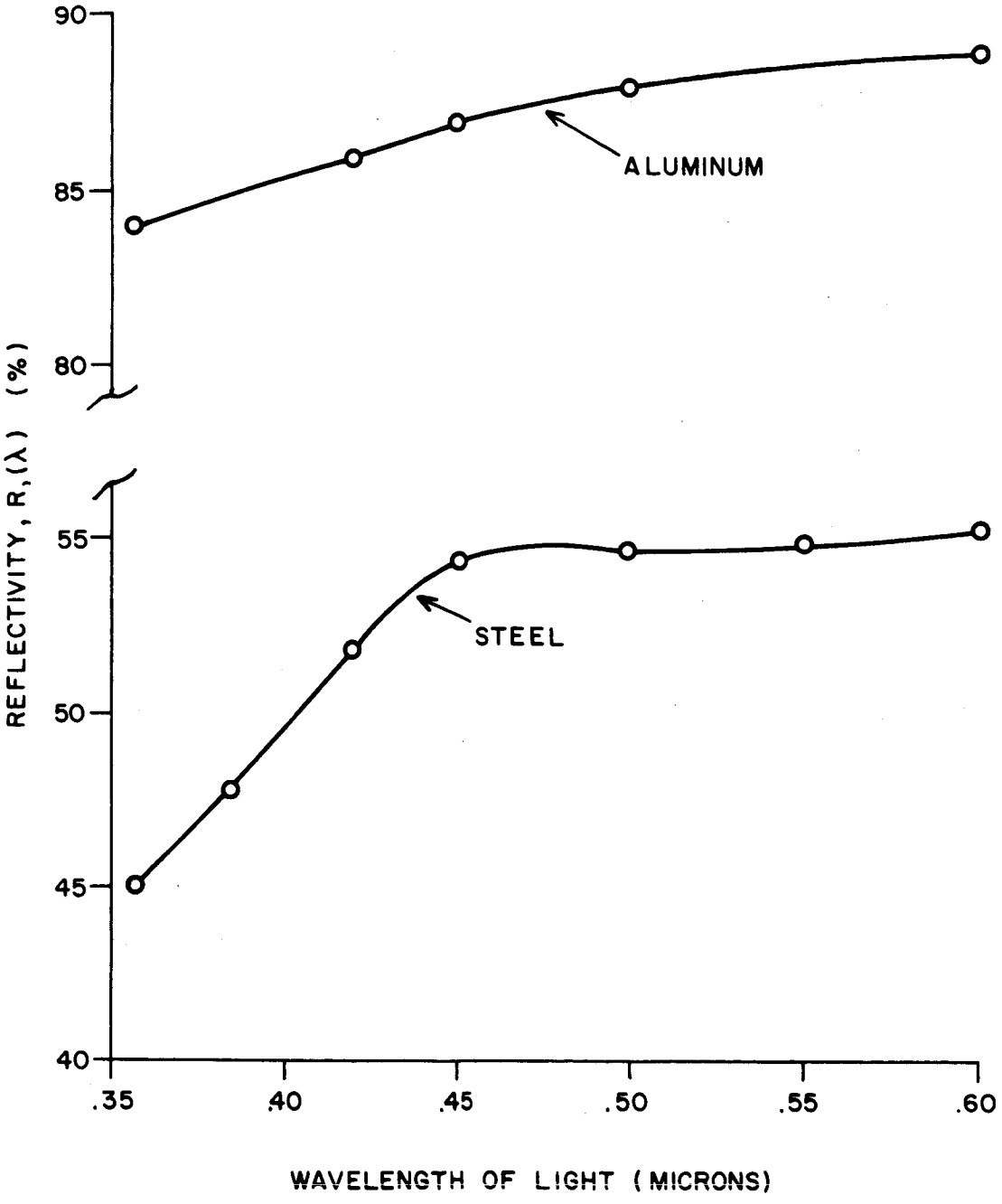

Figure III-8. Percent Reflection from a Polished Metal Surface Versus Wavelength of Incident Light

where

$$\eta = \frac{L \sin i}{d\sqrt{N_1^2 - \sin^2 i}} \qquad (3\text{-}76)$$

and

α = absorption coefficient of fiber core = $f(\lambda)$

α' = percentage of light loss at each reflection on fiber wall

d = fiber diameter

L = fiber length

N_1 = index of refraction of fiber core.

A freshly drawn clean glass fiber closely approximates the condition for $\alpha' = 0$ in the above expression. It is assumed that the same expression holds for a glass coated fiber since the interface between the core and coating is not exposed to handling or undesirable environmental conditions after manufacture.

For the conditions where $\alpha' = 0$, $\alpha = 8\%/\text{inch}$, $i \leq 30^{\circ}$, $N_1 \geq 1.5$ and $L \leq 8$ inches, which cover design conditions for the camera using coated fibers, an approximation of the expression for T(i) is given by

$$T(i) \approx e^{-\alpha L} = T(\alpha) \qquad (3\text{-}77)$$

The curves in Figure III-9 were plotted with Equation (3-77) and have a maximum error of less than 5%.

The absorption characteristics of two types of optical glass, which

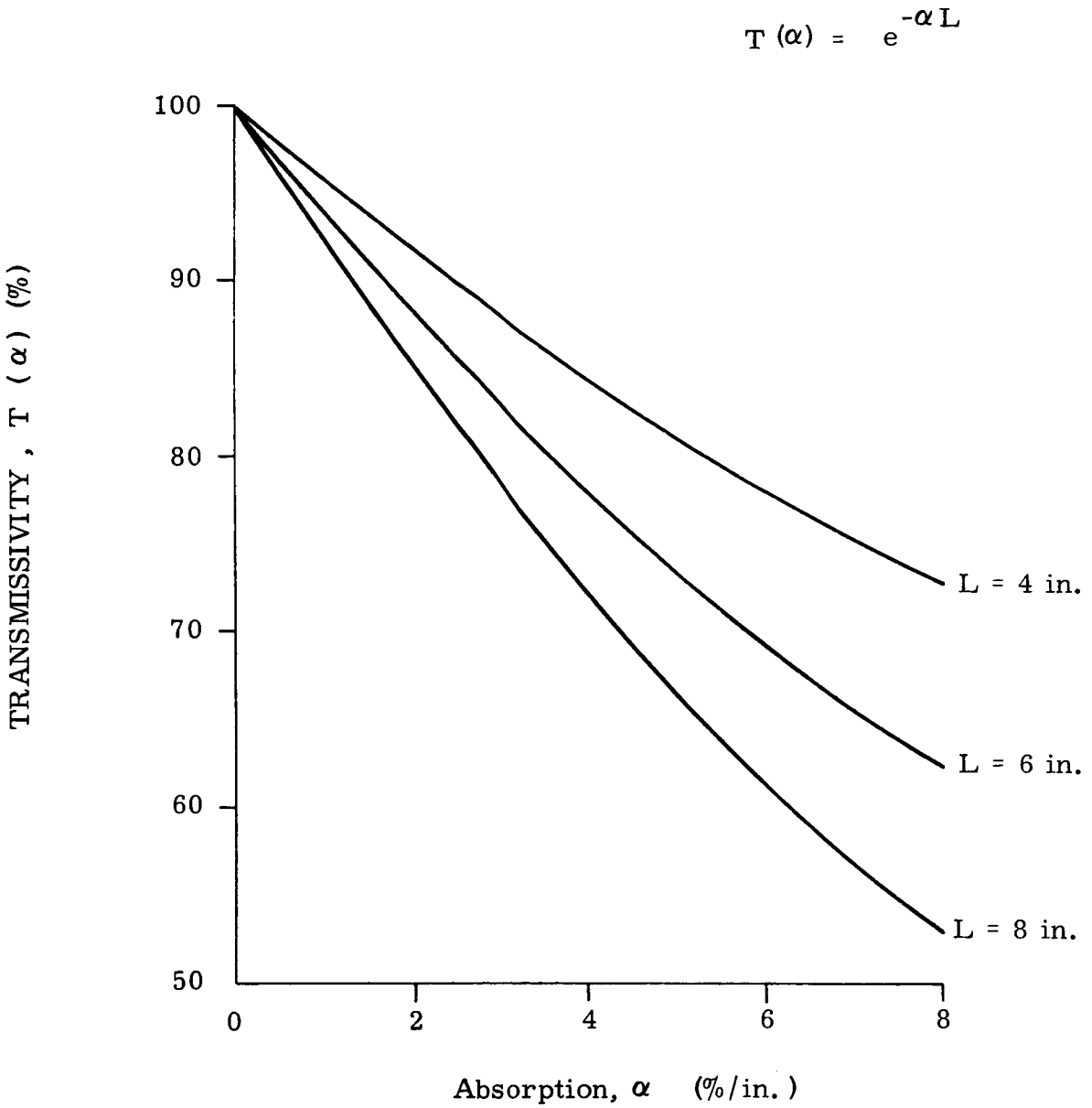

Figure III-9. Transmissivity in a Clean Glass Fiber

may be used as core material for fiber optics are shown in Figure III-10.

4. Interface Reflectance

The reflectance at an interface between two media of different refractive indices is given by

$$R = \frac{1}{2}\left[\frac{\tan^2 (i - r)}{\tan^2 (i + r)} + \frac{\sin^2 (i - r)}{\sin^2 (i + r)}\right] \qquad (3\text{-}78)$$

where

i = angle of incidence

r = angle of refraction

This reflectance constitutes a loss to the optical system and the resulting transmissivity through an interface becomes (1 - R). A simplification of Equation (3-78) may be made for our application. If $i \leq 30^{o}$

$$R = \left[\frac{N_1 - N_2}{N_1 + N_2}\right]^2 \qquad (3\text{-}79)$$

where N_1 and N_2 are indices of refraction of the materials forming the interface.

Figure III-11 shows the percent reflectance at a glass-air interface for a ray of light striking the interface at various incident angles. The solid curves show the reflectance if the incident ray is in glass.

Obviously, if a plate of glass has parallel sides as shown in the following sketch, the reflectance loss will be the same at the first and second face.

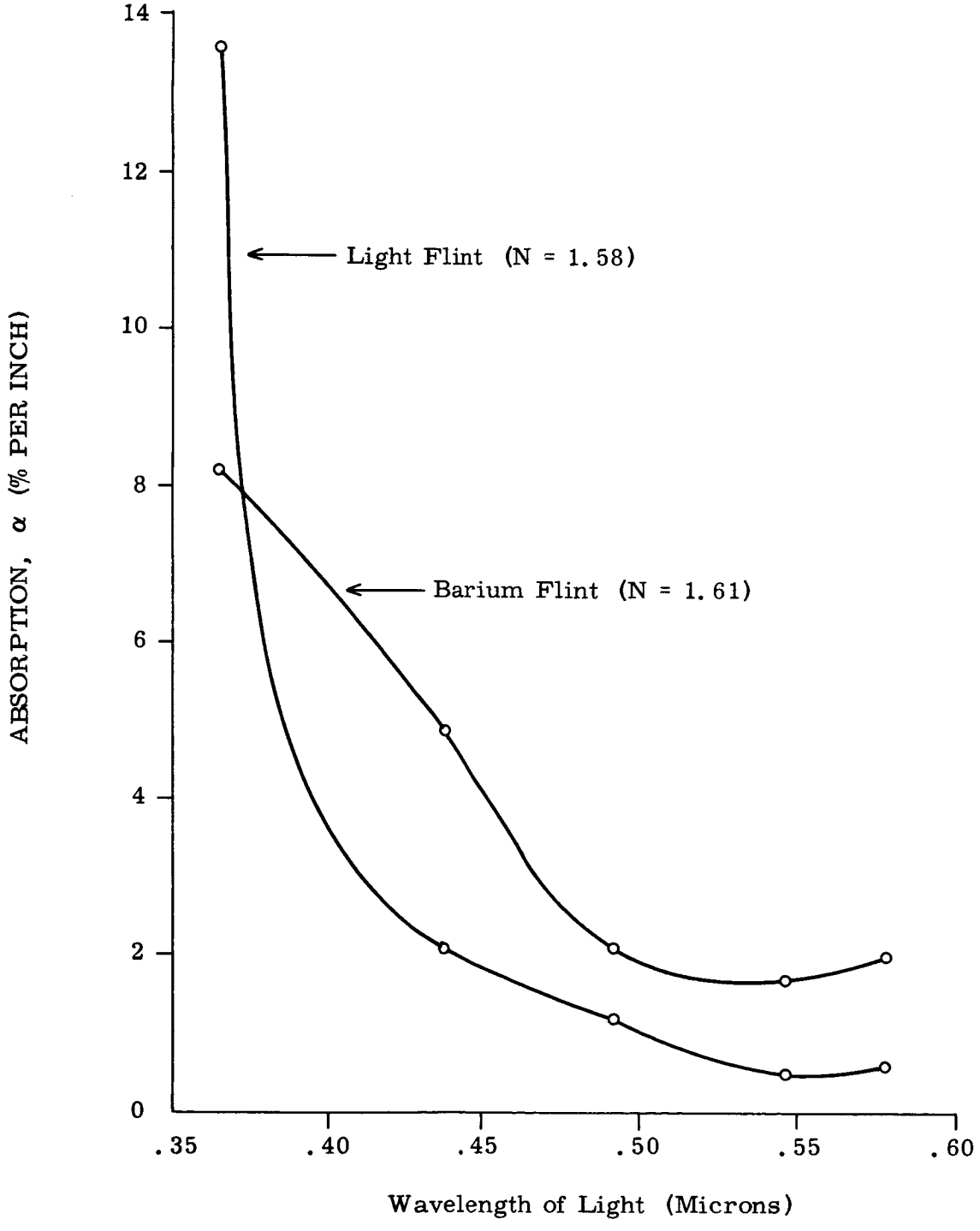

Figure III-10. Light Absorption Characteristics of Two Typical Types of Optical Glass (Points taken from "Laboratory Instruments" by A. Elliott and J. Home Dickson, page 208, published by Chemical Publishing Co., Inc., New York, N.Y.)

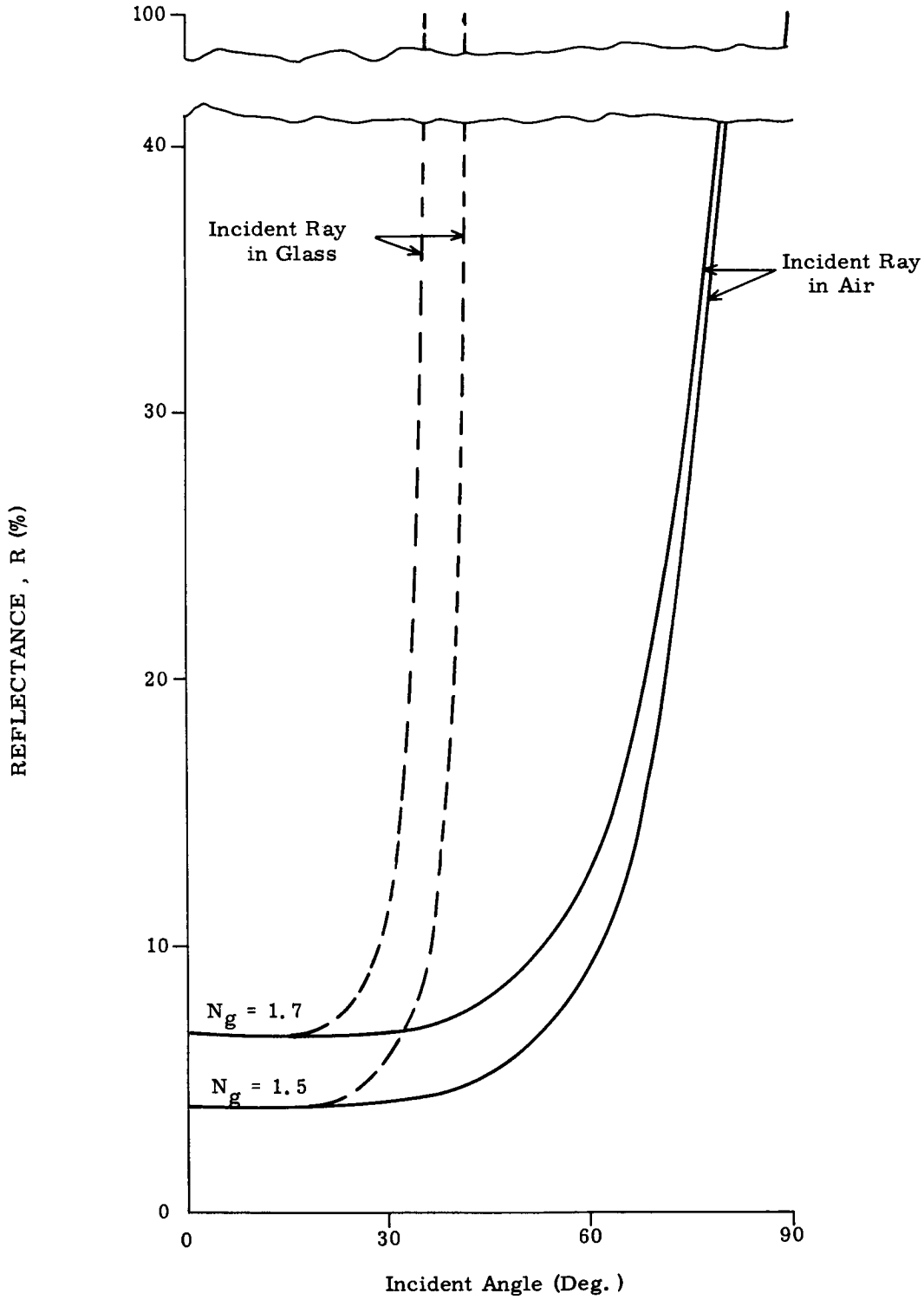

Figure III-11. Reflectance at a Glass-Air Interface

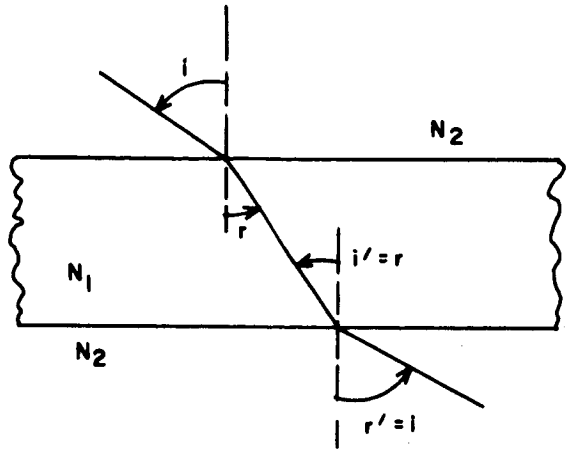

However, if the faces are not parallel the reflectance loss at the second face may be greater than that at the first as indicated by the following sketch and by reference to Figure III-11.

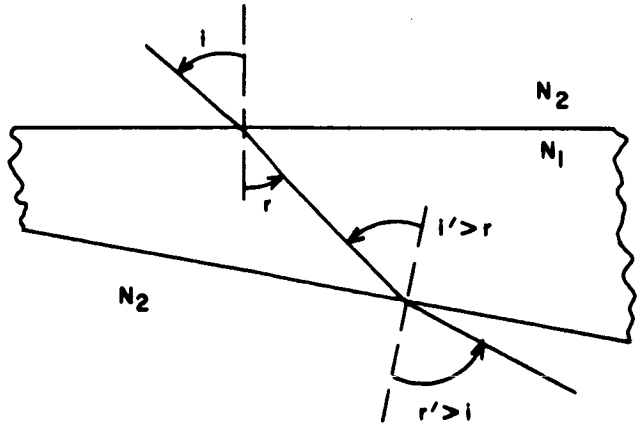

The angle with respect to the fiber axis, of a ray transferred through a fiber under proper conditions will be the same at the last wall reflection as at the first. If the faces of the fiber at both ends are in a plane perpendicular to the fiber axis the reflectance loss at both ends will be the same. However, if they are not perpendicular to the fiber axis additional loss may be encountered as shown above. For this reason proper orientation of fiber entrance and exit faces, fiber axis and light cone transmitted must be maintained so that unnecessary losses will not result, especially when transmitting relatively large cones of light.

5. System Transmissivity

The preceeding paragraphs give a breakdown of the transmissivity of the individual optical components. The percentage of light reaching the photomultiplier will be the product of the individual transmissivities. For the Baker-Nunn camera system and based on assumptions made in previous paragraphs we have

$$T = 0.987^{n} \cdot R_1(\lambda) \cdot \left[1 - \left(\frac{N_1 - 1}{N_1 + 1}\right)^2\right]^2 \cdot e^{-\alpha L} \qquad (3\text{-}80)$$

where

n = number of coated air-glass interfaces of objective lens

$R_1(\lambda)$ = reflectivity of aluminized mirror

N_1 = index of refraction of fiber optic core material

α = absorption coefficient of fiber optic core material

L = length of glass fibers

Equation (3-80) was used to plot curves in Figure III-12.

$$T = 0.987^{n} \cdot R_1(\lambda) \cdot \left[1 - \left(\frac{N_1 - 1}{N_1 + 1}\right)^2\right]^2 \cdot e^{-\alpha L}$$

Values assigned: n = 8, L = 4 inches

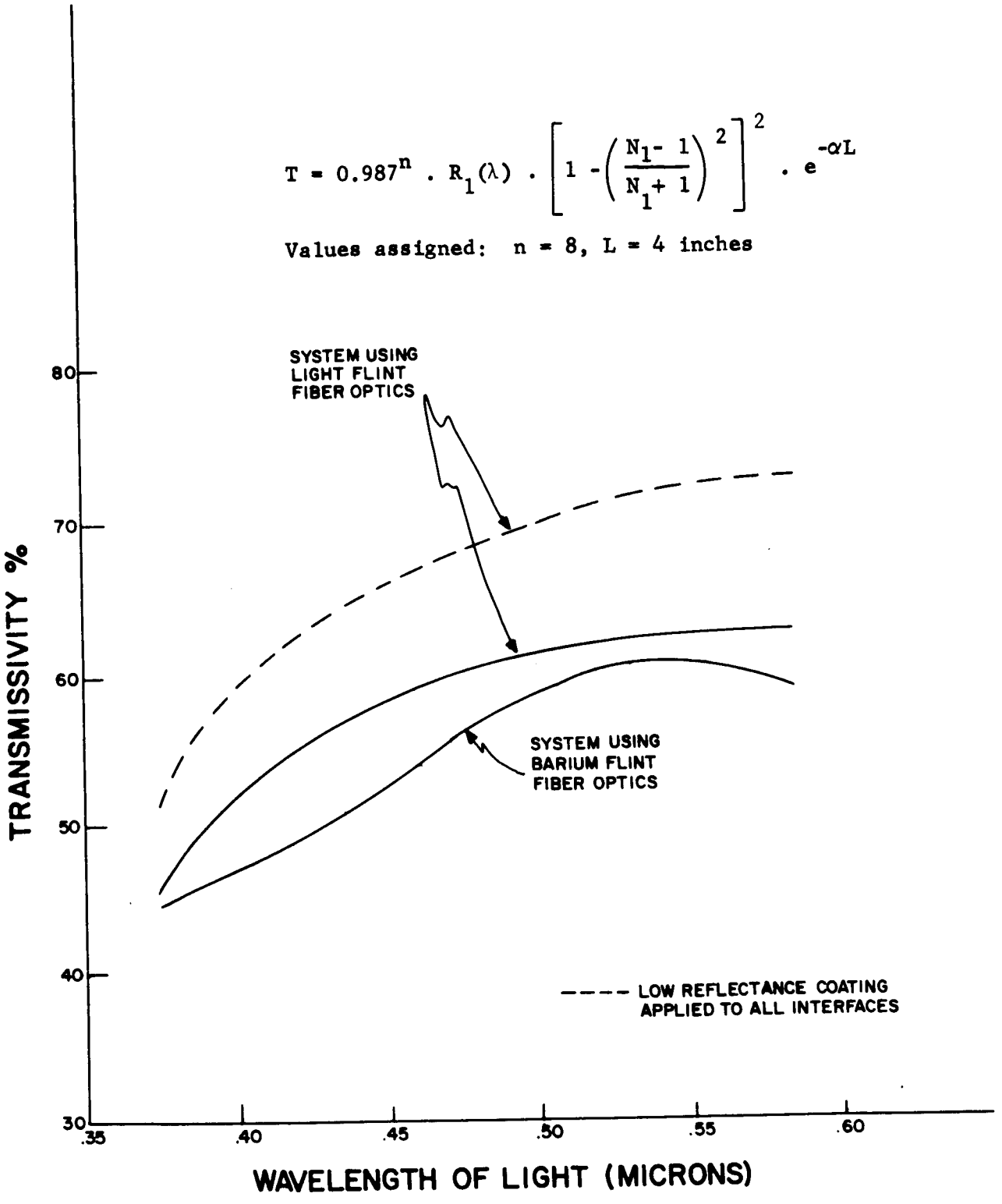

Figure III-12. Transmissivity of Scanning Camera Optical System

D. Noise and Detection Accuracy

The limitations in scanning instruments lies in their comparatively short dwell time on the target in relation to tracking-only devices. It is the purpose of this section to investigate the fundamental limitations to accuracy of the single slit scanning camera. This is to be contrasted with the mechanical and geometric sources of error which are not the subject here.

There would be no error in scanning systems were the signal, the background, and the instrument spurious currents constant or only slowly variable. The cause of this is that the passage of the target across the slit occurs rapidly thereby permitting the use of a frequency filter to eliminate low frequency signals. In fact, however, there are noise sources which have frequencies in the range of interest and which therefore can very easily contribute error during an attempt to measure the times of signal rise and fall. Noise creates two other problems: the occasional miss of a true target and the occasional "detection" of a false target. These three noise effects: miss probability, false target probability, and RMS time error, are the major subjects of the present section which closes with a determination of the accuracy of detection of the target.

For practical wide angle optical systems, the common situation is one in which it is not possible to obtain the required optical resolution over the full field of view. The width of the detection slit is therefore made equal to the diameter of the optical blur circle and it becomes necessary to interpolate this slit by measuring target intensity in order

to achieve the desired system accuracy. If the interpolation factor becomes appreciable (one-sixth or better of the slit width), the false and missed transit probabilities become negligible and the only consideration is RMS intensity error and its conversion to time or angle error.

The interpolation factor of one-sixth means that the signal-to-dominant noise ratio is six or better. If this is true, then the bias level can be placed down from the mean signal value three times the RMS noise level which ensures that at least 99.87% of all the true targets are detected.* At the same time, the bias level is still three times RMS noise level above zero. Since we have chosen the dominant noise source, no other source is larger and hence the false target probability is no more than 1.3×10^{-3}.*

To compute RMS time error due to system noise, let us assume that essentially all light from a star is focussed uniformly into an angular diameter α which is also the slit angular width. Rather than calculate an actual rate of signal change under these assumed conditions we further assume a linear rise from zero to maximum in a scanning angle α (slit width). Maximum signal current, with all efficiency corrections included but translated back to the photomultiplier cathode, is then

$$I_s = n_1 H_p S_p \frac{\pi D^2}{4} \qquad (3\text{-}81)$$

---

* Burington and May, Handbook of Probability and Statistics with Tables, Handbook Publishers, Inc., Sandusky, Ohio, 1958, p. 82.

where

I_s = photocathode signal current (amp),

n_1 = optical efficiency,

D = optical aperture (cm),

S_p = photocathode sensitivity (amp watt^{-1}), and

H_p = star irradiance (watts cm^{-2}).

This average output is disturbed by a noise current of RMS value

$$I_n\sqrt{B_n} \tag{3-82}$$

where

I_n = dominant or total noise current per unit bandwidth (amp sec$^{\frac{1}{2}}$)

B_n = equivalent noise bandwidth (cycles sec^{-1}).

To avoid both missed and false transits, detection of a limiting magnitude star must be accomplished near the 50 percent level, but this does not affect angular accuracy directly. The fractional RMS accuracy in intensity measurement is simply the ratio of RMS noise to peak signal. For a linearly rising signal, this is easily convertible to angle or time accuracy since it represents the fractional error in the slit width α:

$$\frac{I_n\sqrt{B_n}}{I_s} = \frac{\sigma}{\alpha}\cos\Gamma \tag{3-83}$$

where $\frac{\pi}{2} - \Gamma$ is the angle at which the slit is inclined to the scan direction ($\Gamma = 30^\circ$) and σ is the angular error due to the noise I_n.

Elsewhere* we have chosen

$$B_n = \frac{\pi\sqrt{5}}{4\sigma T} \tag{3-84}$$

where T is the scan period. To maintain an angular accuracy of σ or better, the general relation

$$n_1 H_p S_p \frac{\pi D^2}{4} \frac{\sigma}{\alpha} \cos \Gamma \geq I_n \left[\frac{\pi\sqrt{5}}{4\sigma T}\right]^{\frac{1}{2}} \tag{3-85}$$

must therefore be satisfied.

We now proceed to investigate the dominant sources of noise which must be considered in evaluating instrument performance: (1) star or planet photon noise, (2) background light photon noise, and (3) detector dark current noise. Choice of a photomultiplier detector effectively eliminates amplifier and resistor noise from consideration due to high signal gain in the tube itself. An additional component of background noise appears due to scanning. For a reasonable slit field of view, however, probability of detecting more than one star of sixth magnitude or less simultaneously is very small. Thus only stars above sixth magnitude need be considered as background. We do not consider this noise source here as its frequencies will be close to the scanning frequency and therefore out of range of the detected frequencies.

The remaining noise sources are restricted by the same bandwidth, so that this factor can for the moment be neglected. Furthermore,

* Harrington, D.C., "Noise Error Analysis of an Optical Star and Planet Scanner," presented at NAECON meeting, May 1963, Dayton, Ohio.

the comparisons of these noise sources has been accomplished in the last reference and here we wish only to present the curves somewhat differently. Let us first compare signal photon noise and photomultiplier dark current noise. Their ratio is:

$$\frac{I_{sn}}{I_{dn}} = \frac{E_1 D}{I_{dn}} \left[e\, n_1\, H_p\, S_p \frac{\pi}{4} \right]^{\frac{1}{2}} \qquad (3\text{-}86)$$

where

E_1 = photomultiplier noise enhancement factor (~1.3),

D = aperture diameter in centimeters,

e = electronic charge (1.6×10^{-19} coulombs),

n_1 = optical efficiency (~68% from Figure III-12),

S_p = mean photocathode sensitivity (~.04 amp/watt for S-4 surface), and

H_p = star irradiance

$= 3.57 \times 10^{-13} \times 10^{-.4m_p}$ watts cm^{-2} (m_p = photographic magnitude).

Photomultiplier dark current noise I_{dn} is a measured quantity. Some typical values are given in the following Table III-1. Writing Equation (3-86) in terms of the remaining variables gives

$$\frac{I_{sn}}{I_{dn}} = 4.54 \times 10^{-17} \frac{D}{I_{dn}} \times 10^{-.2m_p} \qquad (3\text{-}87)$$

which is plotted in Figure III-13 for several cases. We see that for a four inch aperture, phototubes with noises similar to the 1P21 or 9502S tubes should be chosen to minimize the influence of this effect on

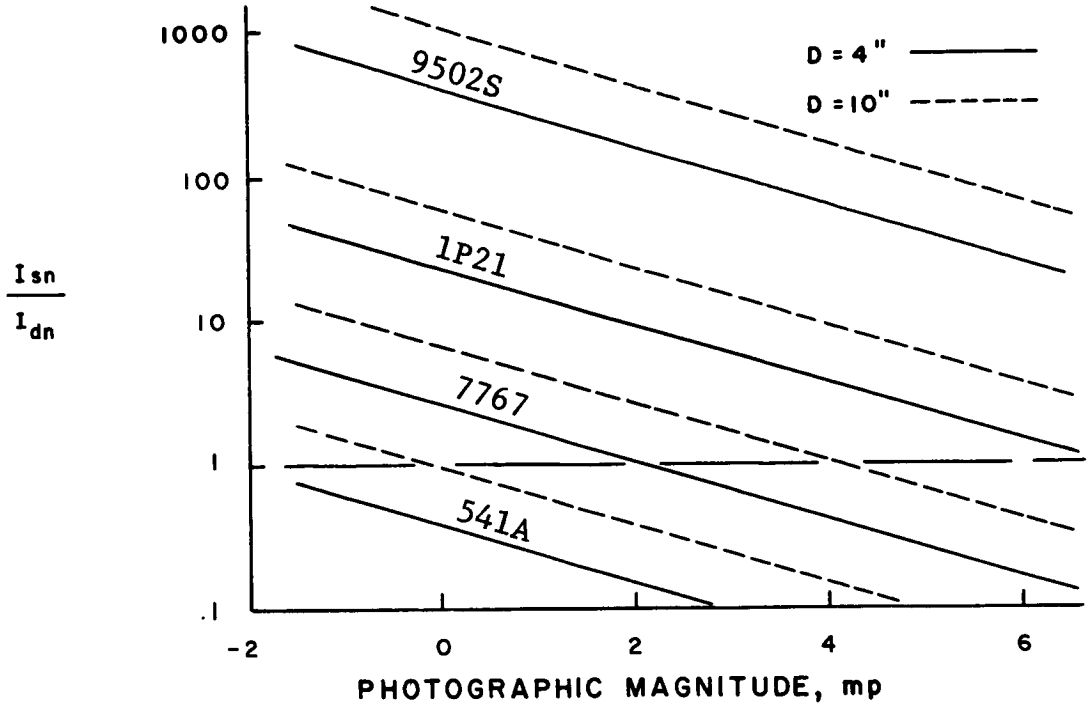

Figure III-13. Comparison of Signal Photon Noise and Photomultiplier Dark Current Noise

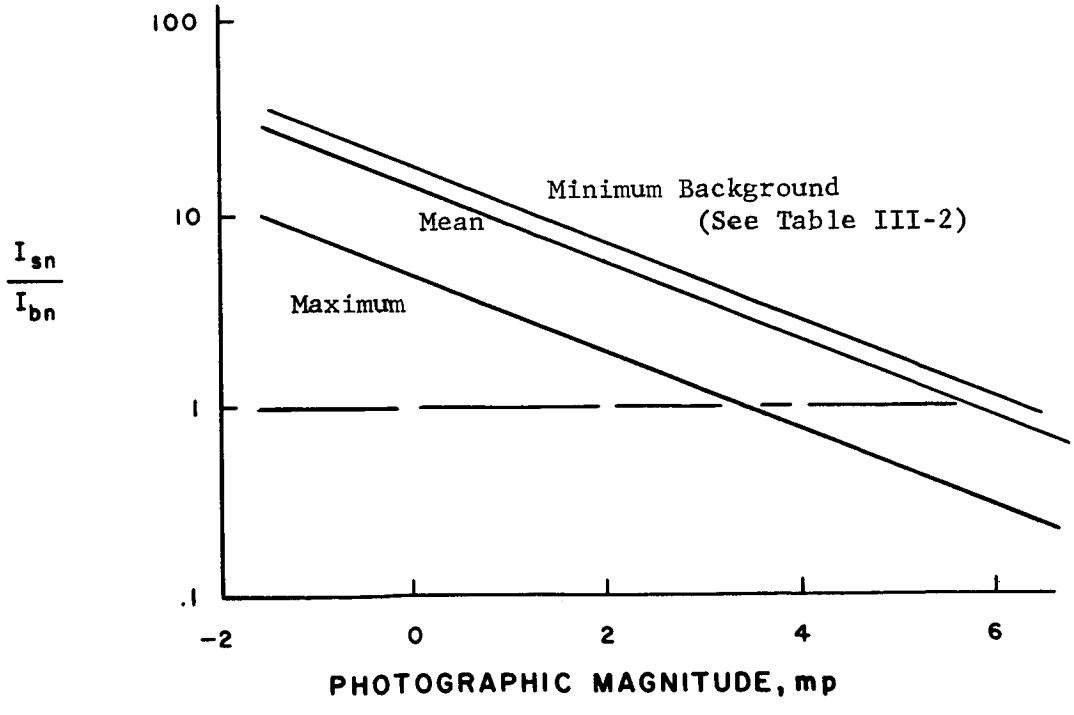

Figure III-14. Comparison of Signal Photon Noise and Background Photon Noise

TABLE III-1

TYPICAL PHOTOMULTIPLIER CHARACTERISTICS

Photomultiplier Type	Classification	Peak Radiant Sensitivity Amperes/watt	RMS Dark Current Noise Amp-sec$^{\frac{1}{2}}$
7767	Miniature	.048	1.8×10^{-16}
RCA 1P21	Miniature Low noise	.040	2×10^{-17}
EMI 9502S	Low noise	.040	1.1×10^{-18}
ASCOP 541A	Ruggedized	---	1.2×10^{-15}

system accuracy.

If this is done, the errors are then contributed by photon noise in either the signal (I_{sn}) or background (I_{bn}). The ratio of these effects is

$$\frac{I_{sn}}{I_{bn}} = \left[\frac{H_p}{2BJ_{bg}} \right]^{\frac{1}{2}} \qquad (3\text{-}88)$$

where

B = slit area in square degrees

$= 30^{o} \times \frac{20}{3600} = 1/6$ square degree.

Table III-2 shows some representative background conditions which form the basis for the curves of Equation (3-88) in Figure III-14. In the region of interest ($-2 > m > 2.5$) we again see that signal photon noise is dominant, though the background photon noise can be substantial near the sun.

The signal photon noise is given by

TABLE III-2

TYPICAL BACKGROUND CONDITIONS

Source*	Number of 10^{th} Mag. Photographic Stars Per Square Degree	Radiant Intensity,** J_{bg} watts/deg^2/cm^2
Faint stars, m > 6 (mean sky)	48	1.87×10^{-15}
Faint stars, m > 6 (gal. equator)	140	5.45×10^{-15}
Non-star galactic light	20 ?	7.8×10^{-16}
Zodiacal light		
30° elongation	1000	3.9×10^{-14}
150° elongation	80	3.12×10^{-15}
Minimum	40 ?	1.56×10^{-15}
Approximate Totals		
Minimum	88	3.43×10^{-15}
Mean	148	5.76×10^{-15}
Maximum	1160	4.52×10^{-14}

* Allen, C. W., Astrophysical Quantities, Athlone Press, London, 1963, p. 135, p. 159.

** Star, $m_v = 10$, outside earth's atmosphere has illuminance = 2.65×10^{-14} phot $\approx {}^{v}3.9 \times 10^{-17}$ watt/cm^2, (Ibid., p. 25, 26.)

$$I_{sn} = \frac{E_1 D}{2} \left[en_1 H_p S_p \pi \right]^{\frac{1}{2}} . \qquad (3\text{-}89)$$

Substitution into the angular accuracy Equation (3-85) thus produces the relation

$$\left[n_1 H_p S_p \frac{\pi D^2}{4} \right]^{\frac{1}{2}} \frac{\sigma}{\alpha} \cos \Gamma = E_1 \left[\frac{e \pi \sqrt{5}}{4 \sigma T} \right]^{\frac{1}{2}} \qquad (3\text{-}90)$$

or

$$3.47 \times 10^{-2} \times 10^{-.2 m_p} DT^{1/2} \sigma^{3/2} = 1 \qquad (3\text{-}91)$$

using the values

$n_1 = .68$,

$S_p = .04$ amp/watt,

$\alpha = 10^{-4}$ radians (20 seconds of arc),

$\Gamma = 30^{\circ}$,

$E_1 = 1.3$, and

$e = 1.6 \times 10^{-19}$ coulombs.

In Equation (3-91) the angular RMS accuracy σ is in seconds of arc, aperture diameter D in inches, and spin period T in seconds of time. The equation is plotted in Figure III-15 for a second magnitude star. We see that a spin period of ten seconds and an aperture of four inches diameter produces an RMS angular error in the target transit across one

of the camera slits of 3.5 seconds of arc. If the spin period is reduced to one second, the aperture diameter would have to be increased to ten inches or so to maintain the same RMS angle accuracy.

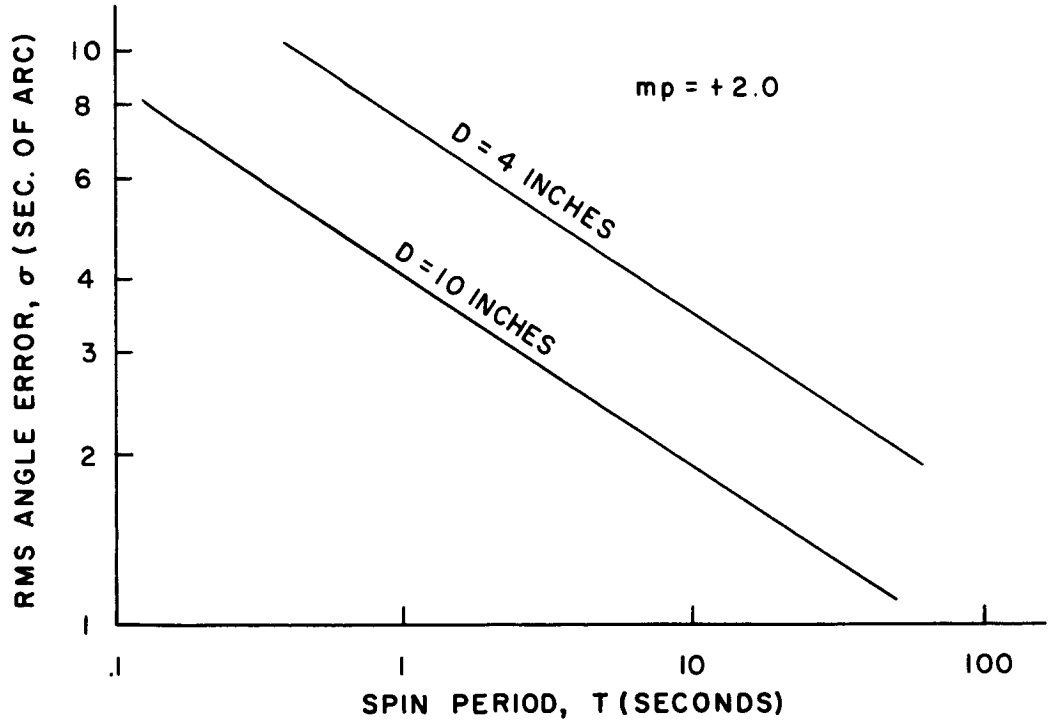

Figure III-15. Angular Error in Location of Target Due to Signal Photon Noies

E. System Simulation

This section will describe the results of two computer programs written in FORTRAN for the Control Data 1604 which simulate the operation of the scanning camera and hence permit an evaluation of its performance for space navigation. Time did not permit a complete simulation of all phases: scan motion, data input, target recognition, and solution of the navigational equations. However, the two programs here have, we hope, singled out two very important areas. The first is a program which recognizes targets from data which contains varying amounts of simulated measurement error. The second program utilizes the 'errored' data to computer vehicle position and attitude.

In both programs the 'Monte Carlo' technique is used. That is, the same problem is solved many times, each time using a different values for the applied errors. The errors themselves are samples taken from a gaussian distribution with mean zero and a given standard deviation. By examining the results of the many 'Monte Carlo' runs, the effect of the given error pattern on the identification task or on the position and attitude accuracy can be ascertained.

The particular stars used in both programs are listed in Table III-3 together with their General Catalog Number, photographic magnitude, and equatorial coordinates: Right Ascension and Declination. Assuming that the planets are point targets rotating in circles about the sun and that their orbital planes all coincide with the ecliptic, Table III-4 lists their pertinent characteristics for these programs.

TABLE III-3. 100 BRIGHTEST STARS*

GENERAL CATALOGUE NUMBER	RIGHT ASCENSION** (1970.0 EQUATOR) h	m	s	DECLINATION** (1970.0 EQUATOR) °	'	"	VISUAL MAGNITUDE
8833	6.	43.	49.5	-16.	*40.	*24.	-1.44
8302	6.	23.	17.1	-52.	*40.	*44.	-.72
19728	14.	37.	32.8	-60.	*42.	*47.	-.27
19242	14.	14.	17.6	19.	20.	17.	-.05
25466	18.	35.	55.3	38.	45.	17.	.03
6427	5.	14.	28.1	45.	58.	12.	.09
6410	5.	13.	5.6	-8.	*14.	-5.	.11
10277	7.	37.	43.9	5.	18.	12.	.36
1979	1.	36.	35.8	-57.	*23.	*19.	.49
18971	14.	1.	41.3	-60.	*13.	*46.	.63
7451	5.	53.	32.8	7.	24.	12.	.40
27470	19.	49.	19.2	8.	47.	15.	.77
5605	4.	34.	11.7	16.	27.	1.	.80
16952	12.	24.	54.8	-62.	*56.	-.	.83
22157	16.	27.	33.8	-26.	*22.	-2.	.94
18144	13.	23.	36.5	-11.	-.	*20.	.97
32000	22.	55.	59.7	-29.	*46.	*54.	1.16
10438	7.	43.	29.0	28.	6.	1.	1.15
28846	20.	40.	24.3	45.	10.	21.	1.25
17374	12.	45.	57.3	-59.	*31.	*31.	1.29
13926	10.	6.	46.5	12.	6.	52.	1.34
9188	6.	57.	26.8	-28.	*55.	*48.	1.48
10120	7.	32.	41.3	31.	57.	20.	1.56
23769	17.	31.	34.0	-37.	-5.	-2.	1.60
6668	5.	23.	31.3	6.	19.	28.	1.63
6681	5.	24.	23.6	28.	35.	2.	1.65
12764	9.	12.	52.9	-69.	*35.	*36.	1.68
17052	12.	29.	29.3	-56.	*56.	*45.	1.68
6960	5.	34.	41.3	-1.	*13.	*10.	1.70
30942	22.	6.	21.0	-47.	-6.	*27.	1.75
17518	12.	52.	42.9	56.	7.	21.	1.78
7089	5.	39.	14.7	-1.	*57.	*25.	1.79
4041	3.	22.	10.2	49.	45.	22.	1.80
25100	18.	22.	10.8	-34.	*24.	-3.	1.81
15185	11.	1.	53.5	61.	54.	49.	1.81
11105	8.	8.	36.5	-47.	*14.	*50.	1.85
9443	7.	7.	10.3	-26.	*20.	*39.	1.85
18643	13.	46.	21.5	49.	27.	44.	1.86
23857	17.	35.	9.6	-42.	*58.	*51.	1.86
7543	5.	57.	19.6	44.	56.	49.	1.89
8633	6.	35.	58.8	16.	25.	35.	1.93
12069	8.	43.	52.6	-54.	*35.	*53.	1.93
22558	16.	45.	28.2	-68.	*58.	*32.	1.93
28374	20.	23.	17.0	-56.	*50.	-.	1.94
11463	8.	21.	54.0	-59.	*24.	*45.	1.94

* Allen, C. W., Astrophysical Quantities, Athlone Press, 1963, p. 229.

** Computed by linear extrapolation from 1950.0 coordinate (Atlas Coeli, 1960) using Annual Variation.

GENERAL CATALOGUE NUMBER	RIGHT ASCENSION (1970.0 EQUATOR)			DECLINATION (1970.0 EQUATOR)			VISUAL MAGNITUDE
	h	m	s	°	′	″	
8223	6.	21.	22.6	-17.	*56.	*23.	1.96
2538	2.	5.	28.5	23.	19.	17.	2.00
2796	2.	17.	49.6	-3.	-6.	*47.	2.00
2243	1.	50.	7.1	89.	7.	40.	2.02
14177	10.	18.	19.3	19.	59.	39.	2.02
865	.	42.	5.0	-18.	-9.	-3.	2.04
20029	14.	50.	46.3	74.	16.	41.	2.04
13044	9.	26.	6.8	-8.	*31.	*39.	2.05
7264	5.	46.	20.0	-9.	*40.	*43.	2.06
127	.	6.	49.8	28.	55.	30.	2.07
23837	17.	33.	32.3	12.	34.	50.	2.07
19033	14.	4.	54.5	-36.	*13.	*24.	2.07
1400	1.	8.	2.7	35.	27.	44.	2.07
25941	18.	53.	24.3	-26.	*20.	-9.	2.09
16953	12.	24.	55.5	-62.	*56.	-2.	2.09
3733	3.	6.	12.6	40.	50.	30.	2.10
18133	13.	22.	43.4	55.	4.	53.	2.12
16189	11.	47.	31.8	14.	44.	24.	2.13
1117	.	54.	52.7	60.	33.	17.	2.15
17262	12.	39.	51.1	-48.	*47.	*44.	2.16
2477	2.	2.	2.8	42.	11.	13.	2.16
31685	22.	40.	53.0	-47.	-2.	*32.	2.16
6847	5.	30.	28.4	.	20.	58.	2.19
792	.	38.	47.5	56.	22.	23.	2.20
24432	17.	55.	54.4	51.	29.	30.	2.21
20947	15.	33.	25.0	26.	48.	52.	2.22
28338	20.	21.	8.9	40.	9.	34.	2.22
10947	8.	2.	31.8	-39.	*55.	-3.	2.23
12623	9.	6.	53.5	-43.	*18.	*38.	2.23
12831	9.	16.	17.3	-59.	-8.	*56.	2.24
147	.	7.	33.8	58.	59.	5.	2.26
22640	16.	48.	13.0	-34.	*14.	*26.	2.29
21489	15.	58.	33.3	-22.	*32.	*16.	2.32
18458	13.	37.	58.3	-53.	*18.	*53.	2.34
15145	11.	.	2.7	56.	32.	37.	2.36
519	.	24.	48.2	-42.	*28.	-9.	2.37
30431	21.	42.	42.7	9.	44.	11.	2.38
23988	17.	40.	24.5	-39.	-1.	-1.	2.39
19656	14.	33.	35.5	-42.	-1.	*38.	2.39
19856	14.	43.	40.6	27.	11.	58.	2.39
9886	7.	22.	54.4	-29.	*14.	*36.	2.42
16268	11.	52.	15.6	53.	51.	42.	2.43
29848	21.	17.	51.8	62.	27.	30.	2.43
23158	17.	8.	39.3	-15.	*41.	*23.	2.44
12938	9.	21.	11.1	-54.	*52.	*56.	2.45
28959	20.	44.	59.8	33.	51.	25.	2.46
32149	23.	3.	15.9	15.	2.	37.	2.49
19774	14.	39.	55.3	-47.	*15.	*40.	2.50
32135	23.	2.	19.0	27.	55.	10.	2.50
21609	16.	3.	41.3	-19.	*43.	*31.	2.52
3643	3.	.	42.6	3.	58.	23.	2.53
15438	11.	12.	30.9	20.	41.	18.	2.55
22332	16.	35.	30.1	-10.	*30.	*29.	2.56
26161	19.	.	42.3	-29.	*55.	*31.	2.57
16740	12.	14.	15.7	-17.	*22.	*32.	2.58

TABLE III-4

PLANETARY CHARACTERISTICS USED IN SIMULATION PROGRAMS

Planet Name	Radius of Circular Orbit, a_k (A.U.)*	Longitude on Jan. 14, 1970** (degrees)
Mercury	0.387099	116.466
Venus	0.723332	287.035
Earth	1.000000	113.130
Mars	1.52369	27.598
Jupiter	5.2028	203.412
Saturn	9.540	37.934
Uranus	19.18	185.532
Neptune	30.07	238.487
Pluto	39.44	184.608

The position of the k^{th} planet at any time t is given by

$$\bar{r}_k = a_k \begin{pmatrix} \cos \lambda_k \\ \sin \lambda_k \\ 0 \end{pmatrix} \tag{3-92}$$

where

$$\lambda_k = \lambda_{0k} + 86400 \frac{\sqrt{MG}}{a_k^{3/2}} (t - T_o) \tag{3-93}$$

and $t - T_o$ is the number of days from the Julian Date T_o = 2440600.5 (January 14, 1970), M = 1.99×10^{33} gm is the mass of the sun, and G = 1.996×10^{-47} $(A.U.)^3/sec^2$, gm is the universal gravitational constant.

1. Error Generation

We have assumed that all of the errors are purely random (i.e., no

---

* Allen, C. W., Astrophysical Quantities, Athlone Press, 1963, p. 142.

** Planetary Coordinates for the Years 1960-1980, H. M. Stationery Office, 1958.

systematic errors exist) and normally distributed about zero. Only two parameters, then, are needed to find the 'measured' value of a quantity q: the mean (true) value q_o, and the standard deviation $\sigma(q)$ of the 'measured' value about the 'true' value. ($\sigma(q)$ must either be specified prior to program execution or computed from other specified parameters.)

The 'measured' value is given by

$$q = q_o + \Delta q \tag{3-94}$$

where Δq is the measurement error. To compute Δq we make use of a subroutine entered in the Control Data CO-OP library as G5 CODA RNGN. This routine will generate random numbers R uniformly distributed in the range $0 \leq R \leq 1$. To construct a normal distribution of errors, we use a table of the values of the cumulative normal distribution function $F_N(t)$.* Such a table constructed for values of $t \equiv (q - q_o)/\sigma(q)$ from -3.4 to +3.4 in increments of 0.1 is searched until a value t_R is found such that

$$F_N(t_R) \leq R < F_N(t_R + 0.1) \quad . \tag{3-95}$$

The value of t which corresponds to R is given by a linear interpolation:

$$t = t_R + \left[\frac{R - F_N(t_R)}{F_N(t_R + 0.1) - F_N(t_R)} \right] \times 0.1 \quad . \tag{3-96}$$

* Burington, R. S. and May, D. C., Handbook of Probability and Statistics with Tables, Handbook Publishers, Ohio, 1958, p. 82.

The error Δq is then

$$\Delta q = \sigma \cdot t \tag{3-97}$$

and the 'measured' quantity is

$$q = q_o + \sigma \left[t_R + \frac{R - F_N(t_R)}{F_N(t_R + 0.1) - F_N(t_R)} \times 0.1 \right] \tag{3-98}$$

Since $-3.4 \leq t \leq +3.4$ then $-3.4\sigma \leq \Delta q \leq 3.4\sigma$; i.e., the assumption is made that all errors are within the 3.4 sigma range, or in other words that we are dealing with 99.94% of the possible cases. This is certainly not a serious restriction.

Figure III-16 shows a test of the gaussian distribution generator using mean zero and standard deviation 10. Figure III-16(a) indicates the distribution of sample means as a function of the number of points in each sample. Figure III-16(b) shows a similar plot for sample standard deviation. One sees that generally the points fall within one sigma of their intended values. Hence the error generating routine may be considered to be producing random values with the proper normal distribution.

2. Simulation of Target Identification

This program follows the general flow diagram of Figure III-17 and is described in much greater detail in Appendix D. For a given vehicle

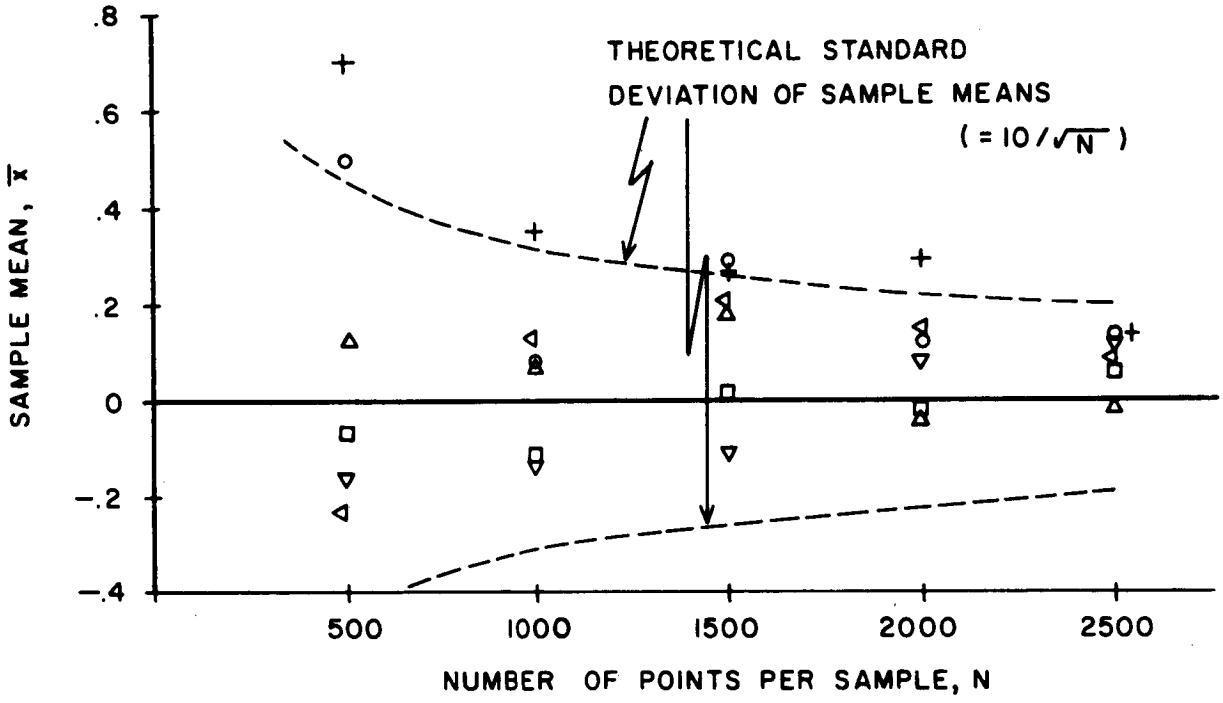

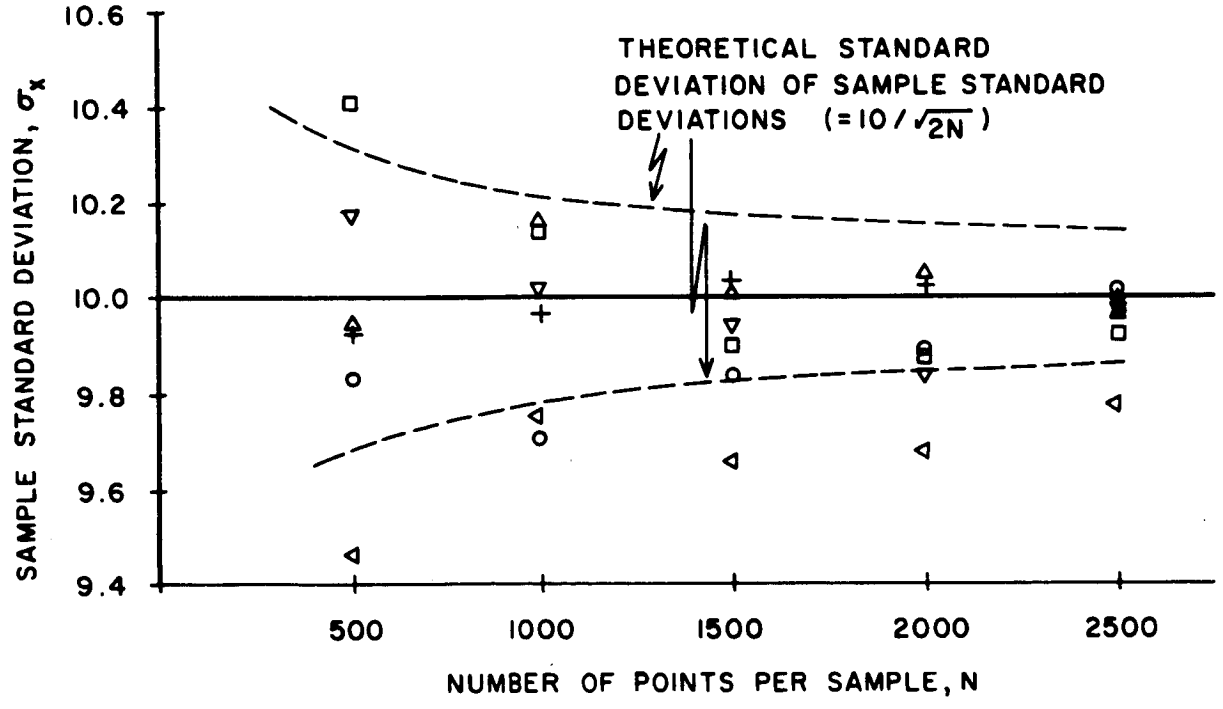

Figure III-16. Experimental Results of Gaussian Random Number Generator (case for mean zero and standard deviation 10; similar symbols indicate that previous points are included in determination.)

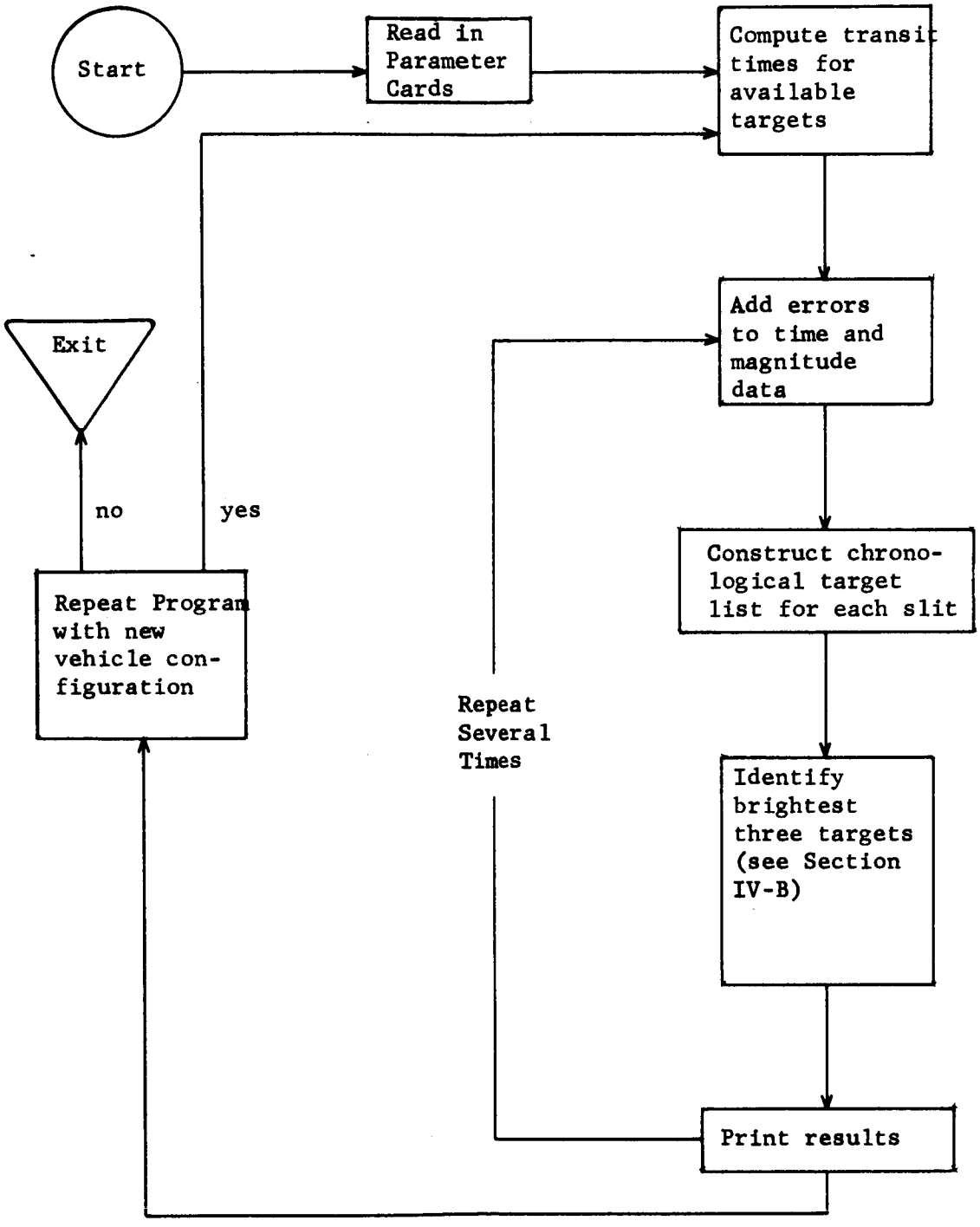

Figure III-17. Flow Diagram for Simulation of Target Identification

position and attitude, the available targets (those which will appear as point objects to the scanning camera) are determined and their true transit times computed. Errors are then added according to the preceeding section and a chronological list (one for each slit) of the targets detected is presented to the identification routine. The identification is carried out along the lines presented in Section IV-B. Essentially, the brightest targets in Slit #1 are paired in Slit #2 and then the star catalog is searched for a match with true targets.

The simulation program here attempted identification using both the brightest targets in the chronological list and also using those targets dimmer than the fifth brightest. This latter task was necessary in order to test the identification among stars only. That is, several planets, though they appeared as point targets (see Section I-D), had a large intensity. Since there were so few of them, identification was easy. To test the technique on stars only, therefore, the routine would also start with the sixth brightest target in Slit #1 and would thus skip most of the bright planets in this instance.

The basic characteristics of this program are:

1) only those planets appear as point sources which are less than 20 arc seconds in radius,
2) the planets rotate in circles about the sun; their orbits are coplanar and all lie in the ecliptic,
3) the camera both precesses (slightly) and spins as it scans the celestial sphere,

4) transit time errors depend upon the target intensity according to

$$\sigma(t) = \sigma_o \ 10^{.133m_p}$$

where σ_o is the assigned error for a zero magnitude target.

Table III-5 shows the two cases for which identification simulation results are presented. Also shown are the RMS angle and intensity errors applied to the true values for the Monte Carlo runs.

In general, for the range of RMS angle errors chosen no noticeable effect was observed. That is, all of the results show a dependence on the applied intensity error, but not on the applied angle error. That is undoubtedly due to the relatively small range of angular errors relative to the total angles measured.

There are two main steps in the identification procedure: (a) slit-

TABLE III-5

TWO CONFIGURATIONS FOR WHICH THE RESULTS OF THE IDENTIFICATION SIMULATION ARE PRESENTED

	Case #1	Case #2
Scan Region Orientation	Along Ecliptic	Inclined 45° to the Ecliptic
Number of Targets Detected	10 stars 4 planets	11 stars 0 planets
RMS Angular Errors in Target Location	10, 20, 50, 100 Seconds of Arc	
RMS Intensity Errors in Target Intensity	7, 14, 21, 28 % of Target Intensity	

to-slit matching by means of intensity, and (b) final identification with true targets through the matrix search. The results of the identification simulation then manifest themselves as the answers to three questions:

1. What percentage of the time did the matching fail and thus prevent an identification attempt?
2. What is the probability of a false identification?
3. How difficult was it to complete the identification? (i.e., what is the total number of tests required?)

The answer to Question #1 is given in Table III-6. For each entry

TABLE III-6

PERCENTAGE OF CASES IN WHICH LESS THAN THREE SLIT-TO-SLIT UNIQUE INTENSITY MATCHES OCCURRED

% Intensity Error	Case #1		Case #2	
	0 Start	6 Start	0 Start	6 Start
7	0	0	0	30¼
14	0	3/4	4	76
21	0	1½	10¾	81
28	0	6-3/4	14½	87

400 Monte Carlo runs were attempted and those which matched less than three targets between slits could not proceed to the identification. Thus in Case #1 where four planets were observed, the matching process which started with the brightest targets (three of the planets) always succeeded and even when starting with the sixth brightest usually proceeded to the actual identification. However, when only stars were in the scan region

(Case #2) the matching was not so easy, especially when only the dimmer stars were used. (Since there are more dim stars per unit magnitude than bright ones, a given intensity error overlaps more and hence tends to foil a unique matching attempt.) The general conclusion of Table III-6 is that a measurement of intensity to within 20% will be sufficient for matching in almost all of the instances if the brightest detected targets are used.

Once matching was achieved, the identification was either a success or a failure. Table III-7 gives the number of wrong identifications compared to the number attempted and estimates a relevant probability. The totals

TABLE III-7

FALSE IDENTIFICATION RESULTS

	Case #1		Case #2	
	0 down	6 down	0 down	6 down
Total Number of Identifications Attempted	1600	1381	999	93
Total Number of Wrong Identifications	3	3	2	0
Probability of Identification Failure	1.9×10^{-3}	2.2×10^{-3}	2×10^{-3}	$<10^{-2}$

are taken over all angle and intensity errors used and are displayed only as a function of scan orientation and whether or not the brightest targets were matched. In general we can probably conclude that the identification,

once the matching is achieved, fails in only one out of 500 attempts. Furthermore, when intensity was measured to 20 percent or better, there were not failures.

The answer to the third question--difficulty of identification--is shown in Figure III-18. There the total number of matrix locations in the search pattern (see Section IV-B for the details of the search and the magnitude matrix) is plotted along the vertical axis and RMS intensity error along the horizontal axis. Intersection of the vertical axis at three occurs because this is the minimum number of tests which must be made even when all the measurements are perfect. The points are simulation results and the continuous lines merely drawn through them. One sees that it is not unusual for a large number of tests to be executed before identification is completed.

3. Interplanetary Navigation Analysis

The second program constructed to simulate the scanning camera actually computes the vehicle position and attitude from 'noisy' measurements and compares these with their true values. In this way the effect of transit time measurement errors on the accuracy of the navigational concept can be ascertained.

The program follows the general diagram shown in Figure III-19 and is given explicitly in Appendix E. As with the target identification program this error analysis is an application of the 'Monte Carlo' technique. Errors are added to otherwise perfect measurement data (transit times) from which the navigational information is then obtained. Repeating the

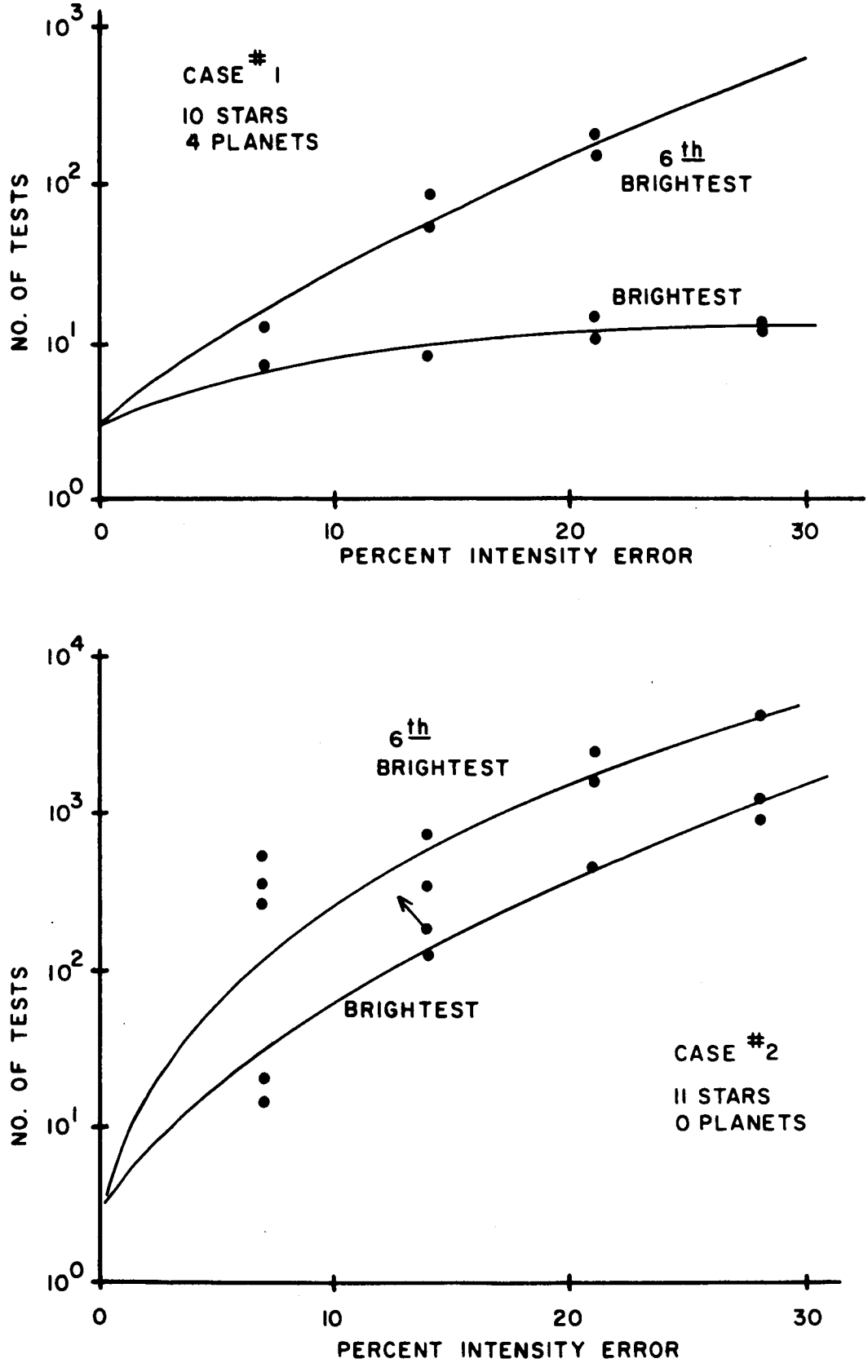

Figure III-18. Number of Tests Required to Complete Identification

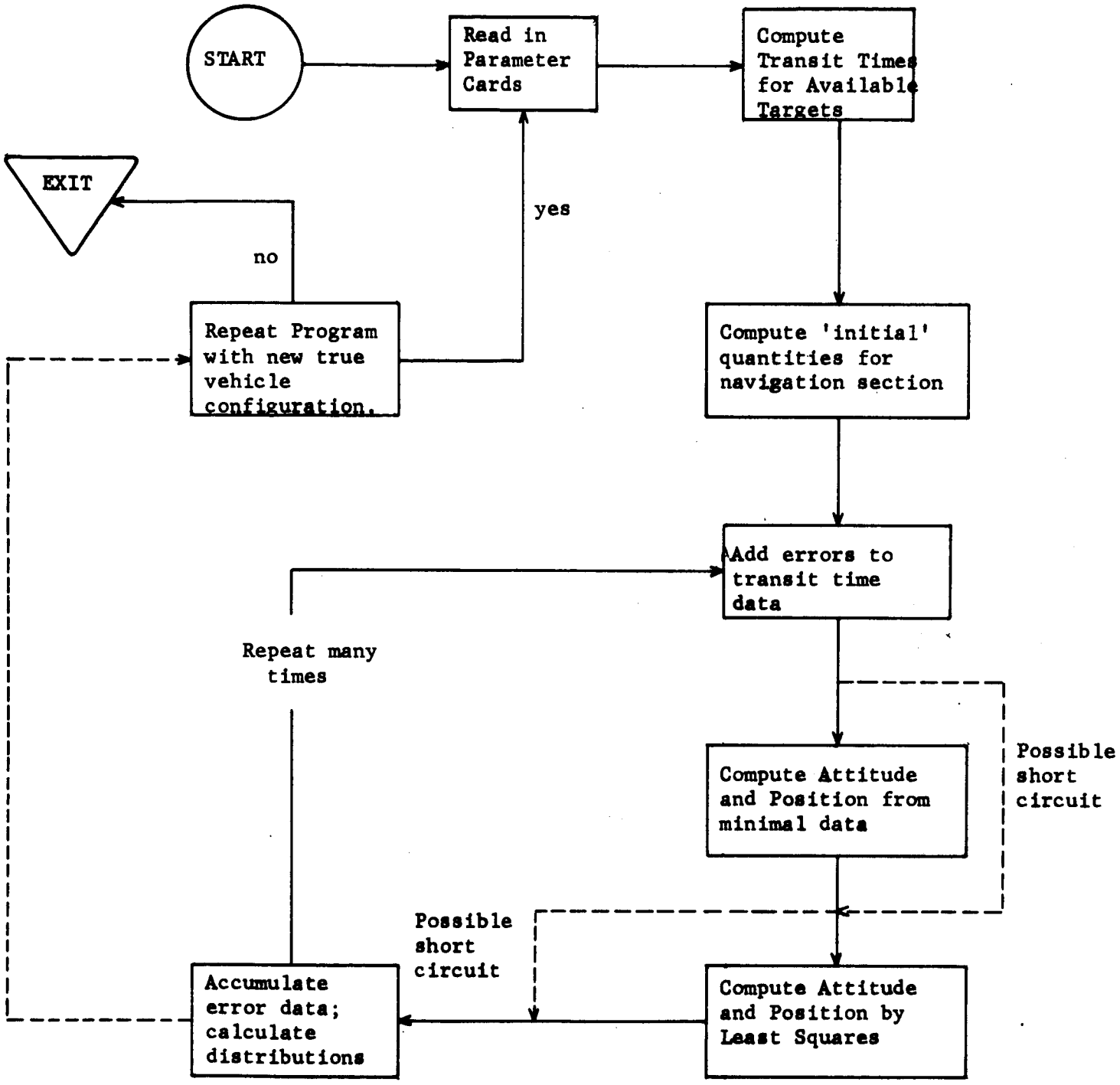

Figure III-19. General Flow Chart for Program ABLE

computation many times, each time using a different set of measurement errors (RMS value is same for each set), gives one a pattern of outputs grouped in some fashion about the true desired value. The comparison of these output patterns with the error patterns added to the perfect data is what in this case constitutes the 'error analysis'.

One begins as shown in Figure III-19 by reading the instruction cards for each particular program on which are recorded the true vehicle position and attitude plus various decision parameters. All of the 100 brightest stars and nine planets are then surveyed to test their availability to to the camera field of view. If they can be used, their transit times are computed using the equations of Section III-A. Following this, all quantities in the navigational calculation which do not depend on the individual transit times are computed. This saves computing them each time the following sequence is executed.

The first step in the Monte Carlo process consists of generating transit time errors and adding them to the true transit times. Then the position and attitude of the camera are computed from the 'measured' transit times by employing the equations of Section III-A. To start any iterative procedures here, the true values are taken as the initial iteration values. (Hence the ability to compute many of the quantities prior to the Monte Carlo process.) Finally, the position and attitude changes from their true values are accumulated. When the Monte Carlo process has been repeated a number of times, the standard deviation in these changes for each of the position and attitude parameters is computed and

printed on the line printer.

Several assumptions have been made to simplify the program. They are:

a) stars and planets are point sources, the planets revolving in circles in the ecliptic, and the stars fixed in the 1950.0 celestial sphere,

b) the camera rotates at a constant and known rate about a spin axis fixed in inertial space,

c) RMS time errors are the same for all targets and are equivalent to RMS angle errors of ten seconds of arc,

d) the 100 brightest stars and nine planets are the only targets and they have already been identified, and

e) the stars were used to determine attitude while the planets were used for position; the errors in attitude were no allowed to propagate into position deviations (i.e., during computation of position, the attitude was assumed free from error).

The program does not take into account, then, such sophistications as (1) corrections for target positions due to aberration, proper motion, target size, etc., (2) general rigid body motions of the camera system, (3) future interplanetary trajectories, and (4) a more physical simulation of the camera detection process. It was felt that in order to facilitate immediate progress on the program, and also to obtain a 'first order' picture of the error patterns to be expected in the more complex cases, such steps were warranted. We do not feel that any essential features were omitted which

in a future more correct error analysis, might significantly alter the present conclusions.

Of course, a true vehicle position and attitude at a certain time must be provided to the program. Figure III-20 shows the most investigated case. This is a scale drawing of the solar system on January 14, 1970 (J.D. 2440600.5) with the vehicle shown situated at (x, y, z) = (.9, 1.0, 0) in astronomical units and relative to the ecliptic coordinate frame. The attitude parameters employed are $\tau = 10^{o}$, $\xi = 45^{o}$, $t_o = 0$ seconds of time as shown in the sketch in the lower portion of the figure.

Using this vehicle state, the next six figures show the results of the error analysis when the number of targets and the angle τ are varied. Figure III-21a is a plot of the dependence of the spin axis pointing direction error on the total number of stars available for measurement. This is defined as

$$\sigma_{SD} = [\ \sigma^2(\tau) + \sin^2 \tau \ . \ \sigma^2\ (\xi)\ ]^{\frac{1}{2}}$$

where $\sigma(\tau)$ and $\sigma(\xi)$ are the RMS deviations in τ and ξ respectively. For example, if the sensor bias level is set to detect the fifty brightest stars in the sky (limiting magnitude about 2.0), it will actually see twelve during a complete scan for the given attitude and the spin axis direction error is approximately seven seconds of arc. If one hundred stars are available 22 are detected and the error has reduced to five seconds of arc.

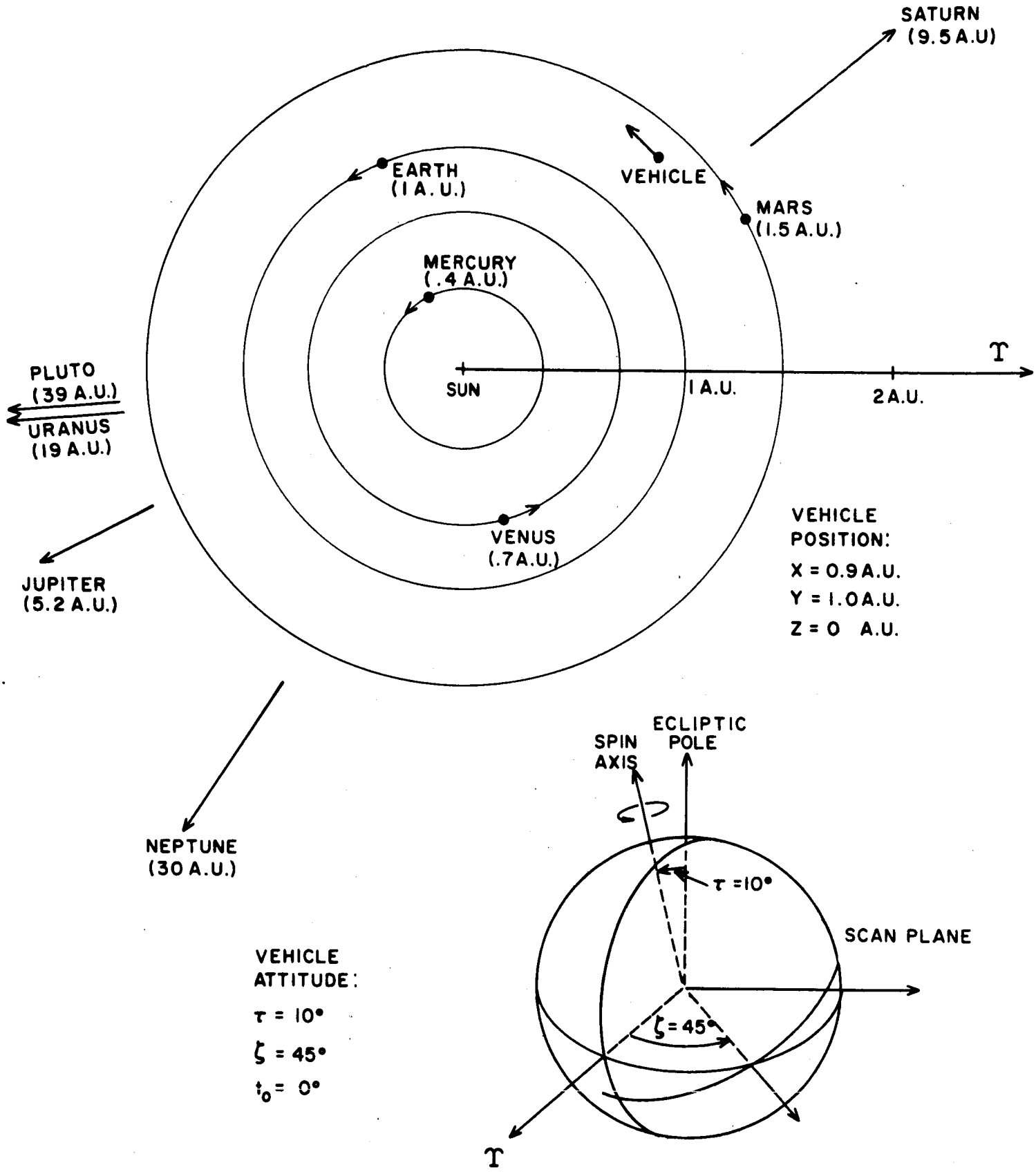

Figure III-20. Solar System on J.D. 2440600.5
(Jan. 14, 1970)

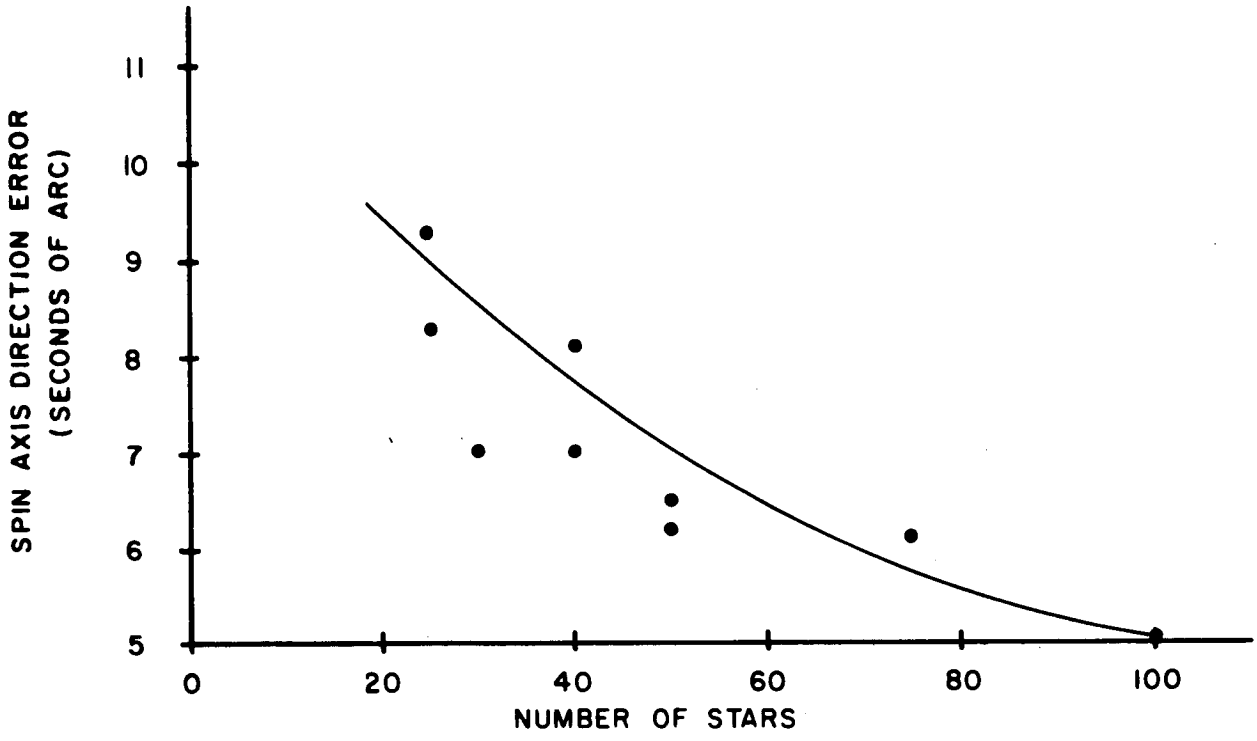

(a)

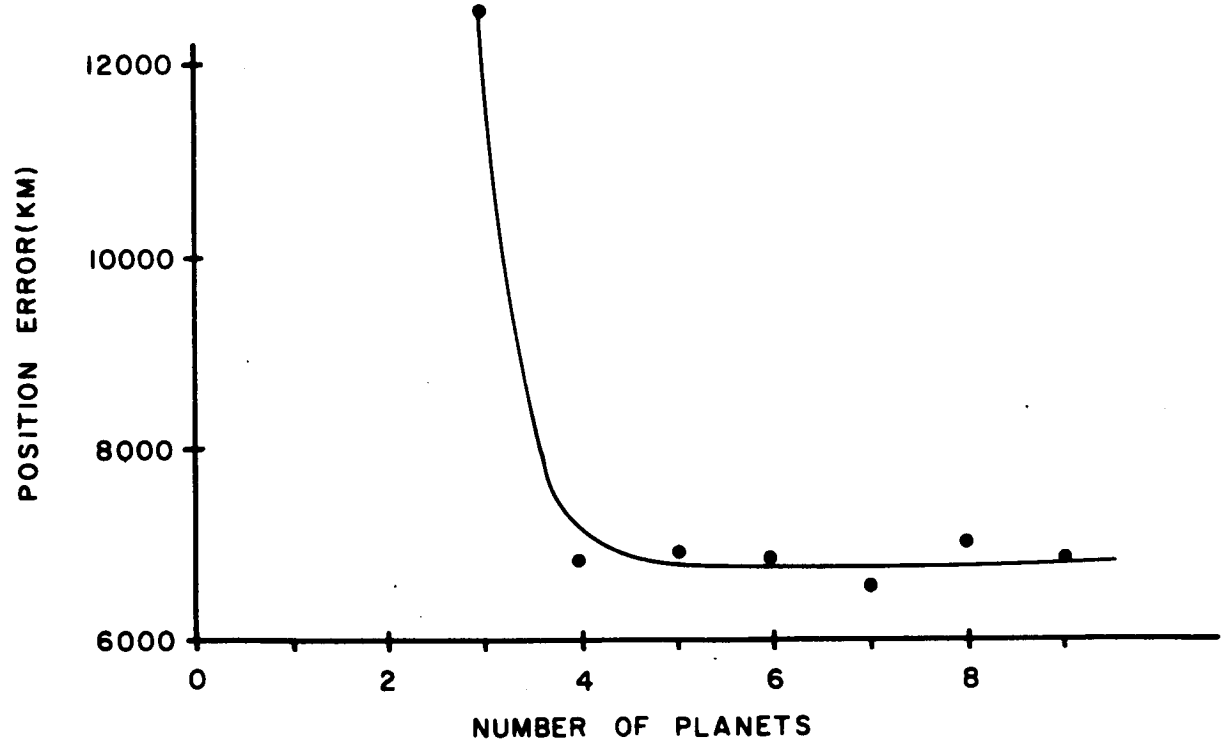

(b)

Figure III-21. Dependence of Spin Axis and Position Errors on Number of Targets Detected

Figure III-21b shows a similar dependence of position error on the number of planets used. Some care must be exercised in interpreting the horizontal axis. That is, if the number of planets is four, this means that the inner four planets (Mercury, Venus, Earth, Mars) are used to compute position. We see that for the vehicle position chosen, the addition of planets beyond Mars affects the position error not at all. This is due, of course, to the fact that Jupiter, Saturn, etcetera are at such a great distance compared to Mars and the other inner planets.

Figure III-22 and III-23 show the effect on the various errors of varying the angle τ between the spin axis and the angular momentum vector. As this angle approaches zero, the determinations of ξ and t_o become very bad (Figure III-22), but the spin axis direction error remains stable (Figure III-23a).

In the lower portion of Figure III-23 the effect on the position error is shown. There is, of course, no continuous effect and there should not be one since, in effect, one is merely varying the coordinate system. However, at about $\tau = 14^o$, a loss of two key planets (Earth and Mars) occurs which immediately increases the position error.

So far the results have been for a particular vehicle and planetary configuration. Figure III-24 shows how the position error behaves at two positions as time elapses. The right portion has the vehicle at its usual position while in the left portion of this figure the position is taken along the y-axis at a negative ½ A.U. Both the average error and the variation in the error are larger for the first case where the

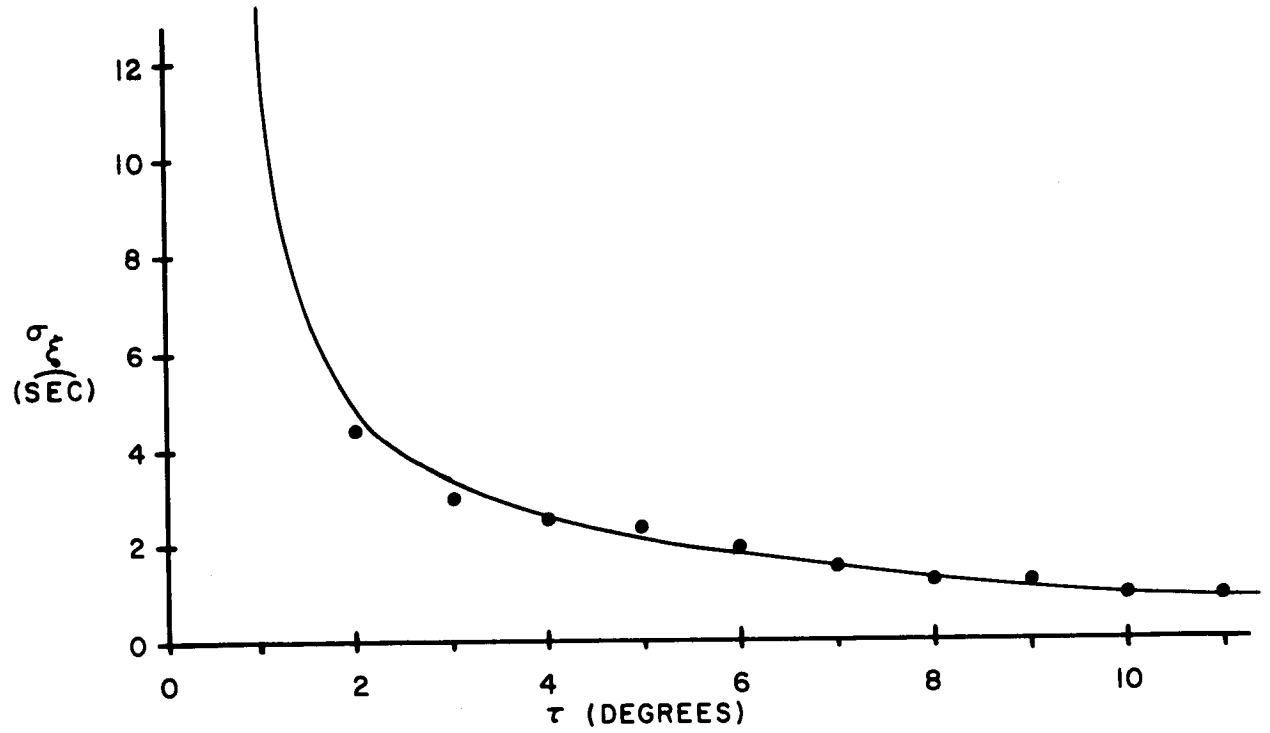

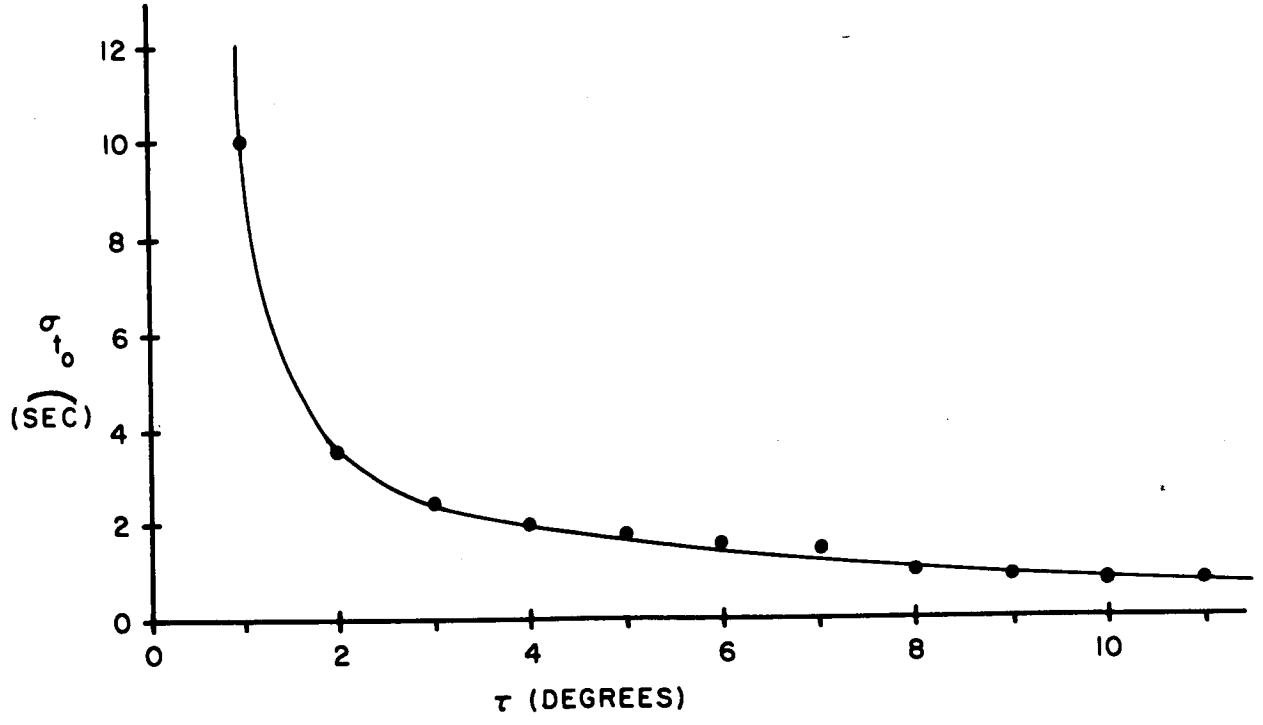

Figure III-22. Dependence of ξ and t_o Errors on Angle τ between Spin Axis and Angular Momentum Vector

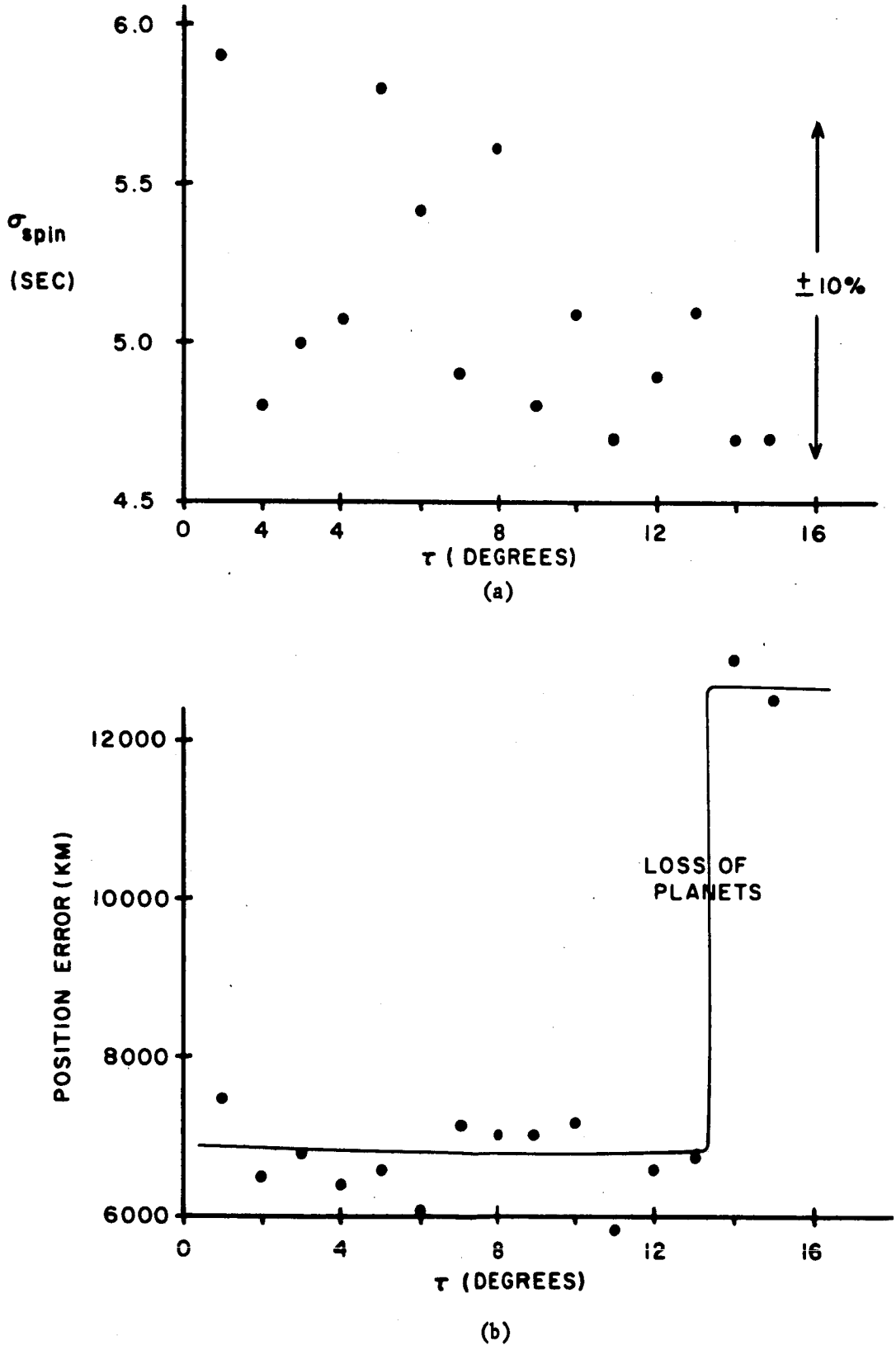

Figure III-23. Dependence of Spin Axis and Position Errors on the Angle τ

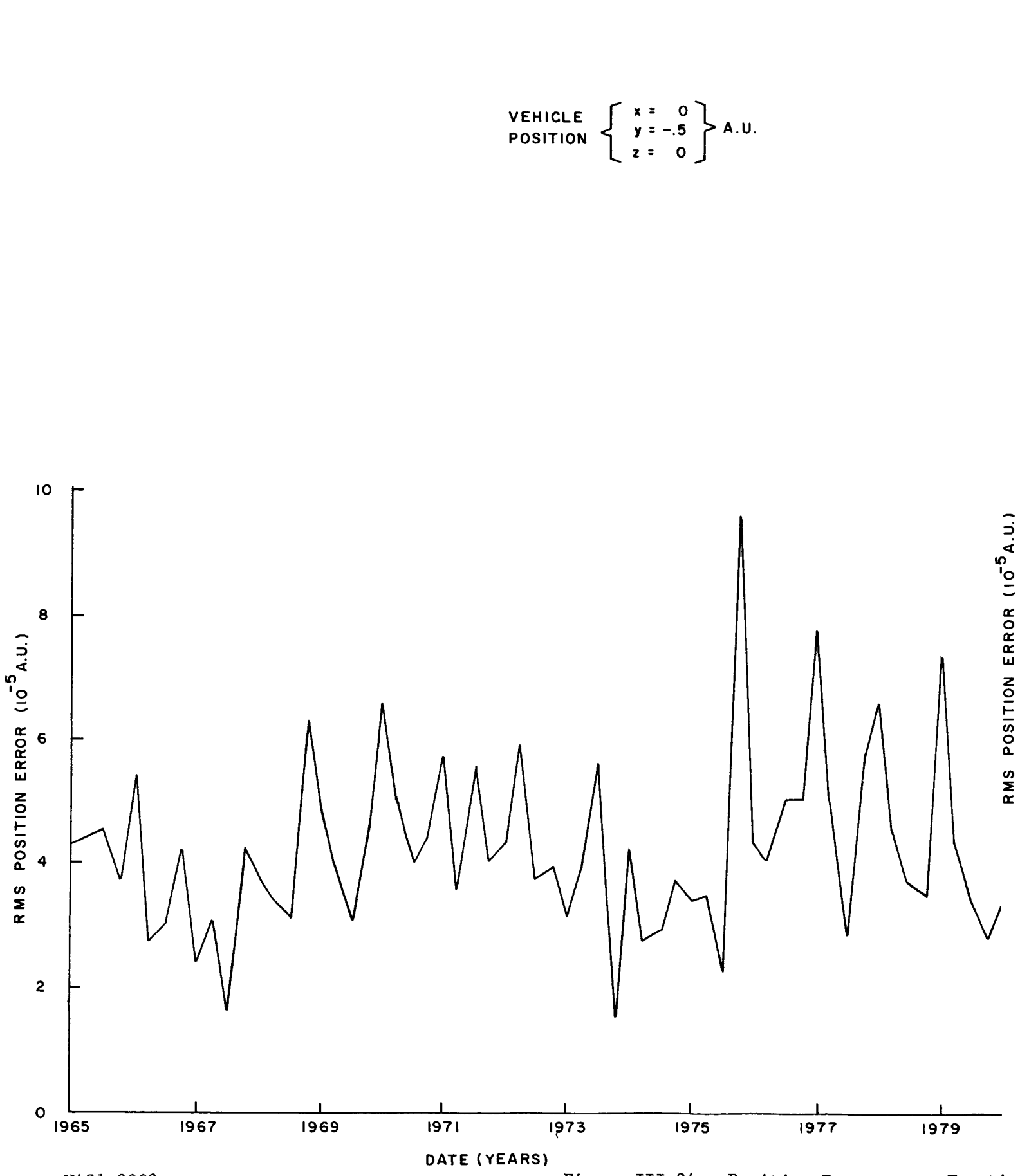

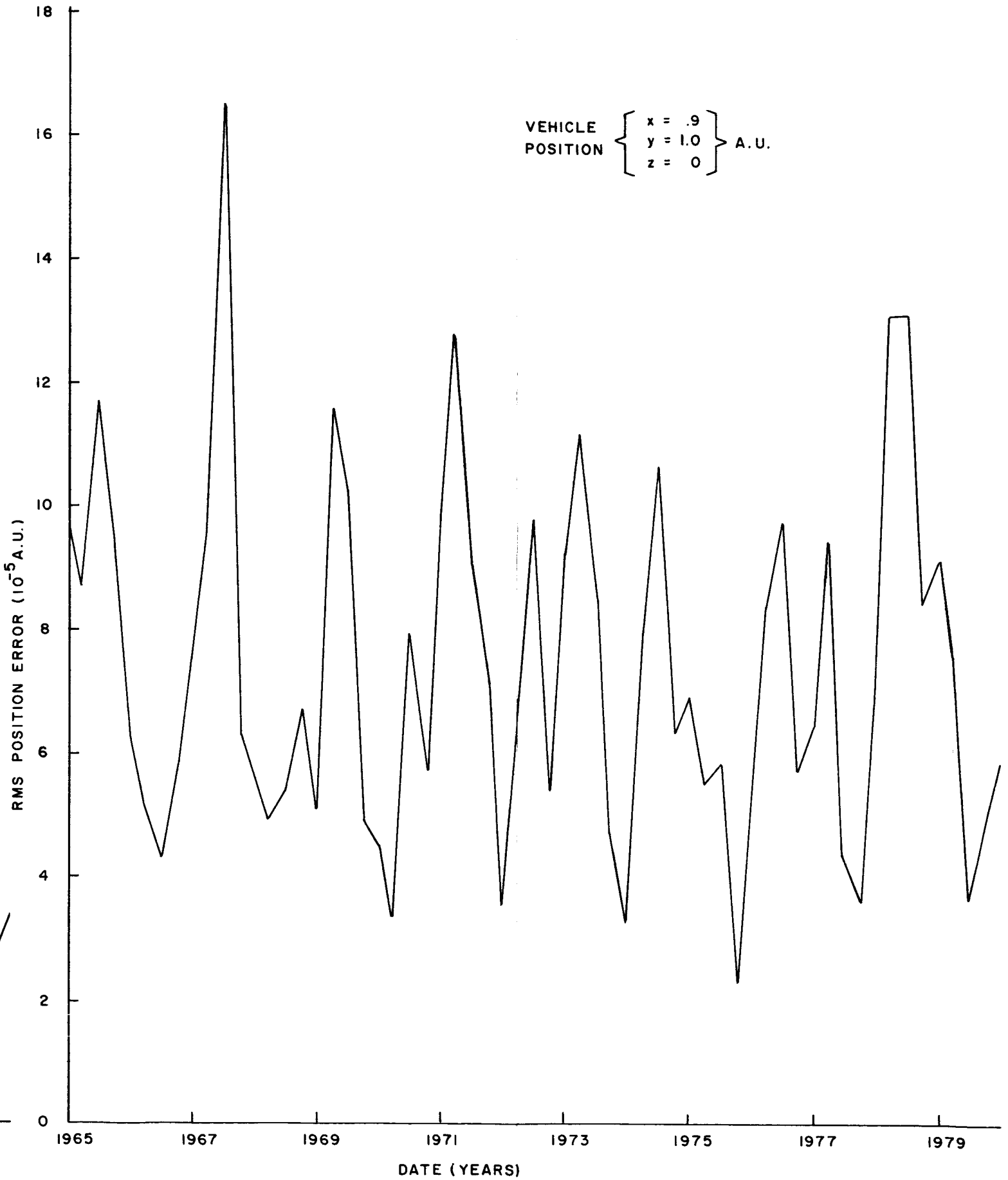

NAS1-2902

Figure III-24. Position Errors as a Function of Time for Two Vehicle Positions

vehicle was at a greater distance from the 'mean' planetary position (the sun).

Finally, Figures III-25 and III-26 show the effect of vehicle position. The view is one looking down on the ecliptic plane from above as in Figure III-20. Shown are lines of constant error for positions in the ecliptic plane (units are 10^{-6} A.U.). In Figure III-25 one sees that the error contours are approximately circular in the inner portion of the solar system but become large as one proceeds out towards either Jupiter or Saturn. This occurs because the inner planets become clustered together (in an angular sense) as one proceeds away from them. Furthermore, on the line between Jupiter and the sun, the planet does not aid in the position definition along the line. Thus, until one comes close to Jupiter, the position errors build up to a value near 400 x 10^{-6} A.U. or 30,000 kilometers whereas closer to the sun the errors are more like 7500 kilometers.

Figure III-26 is a detail of the previous figure and shows quite well the effect of the planetary geometry. Along this line formed by Venus, Mercury, and Earth the position determination is poorer than in other areas. The best areas are near Earth or Mercury where the lines to the various planets are perpendicular and relatively short.

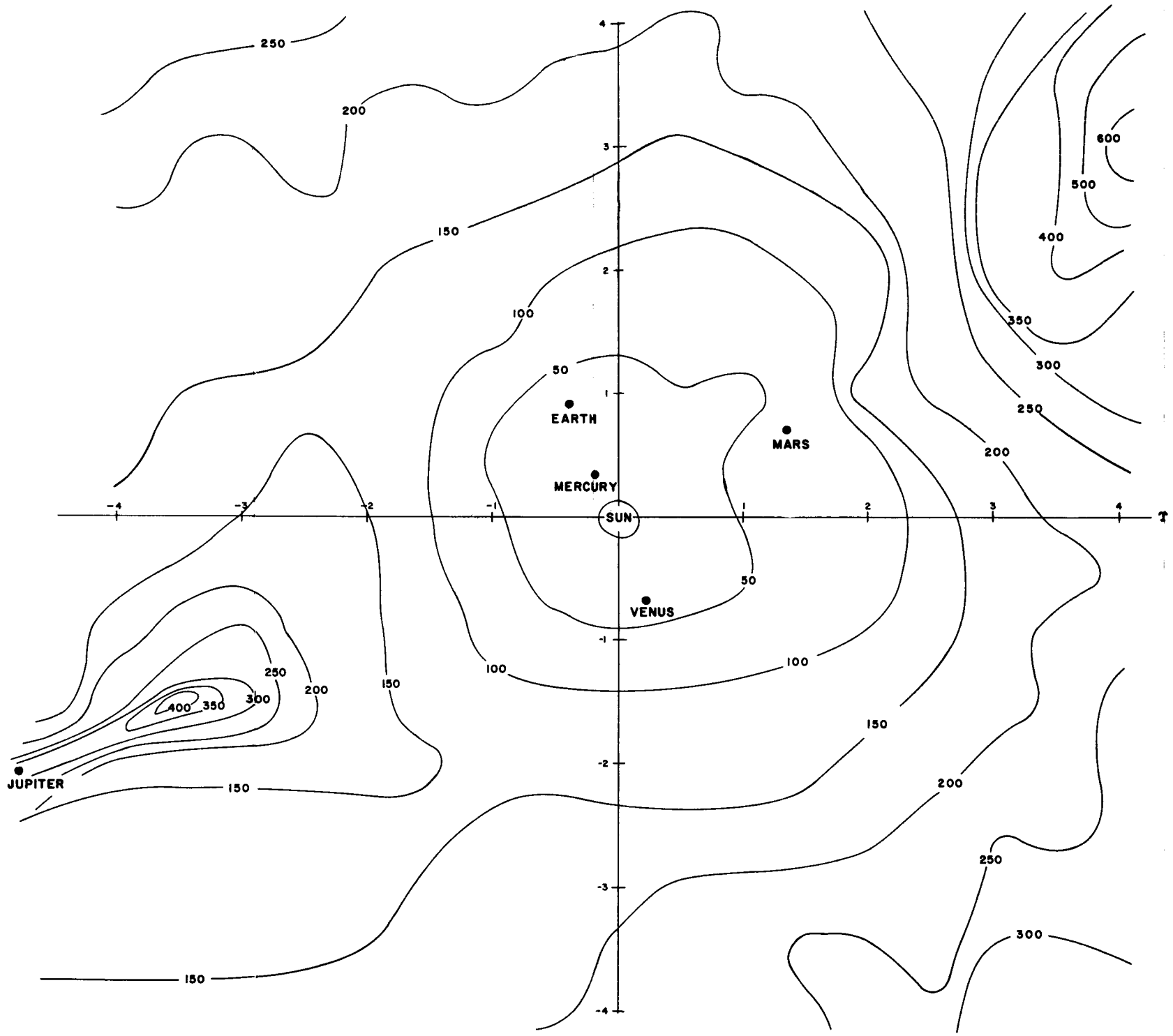

Figure III-25. Constant Error Contours in the Ecliptic Plane for J.D. 2440600.5 (σ = 10 seconds)

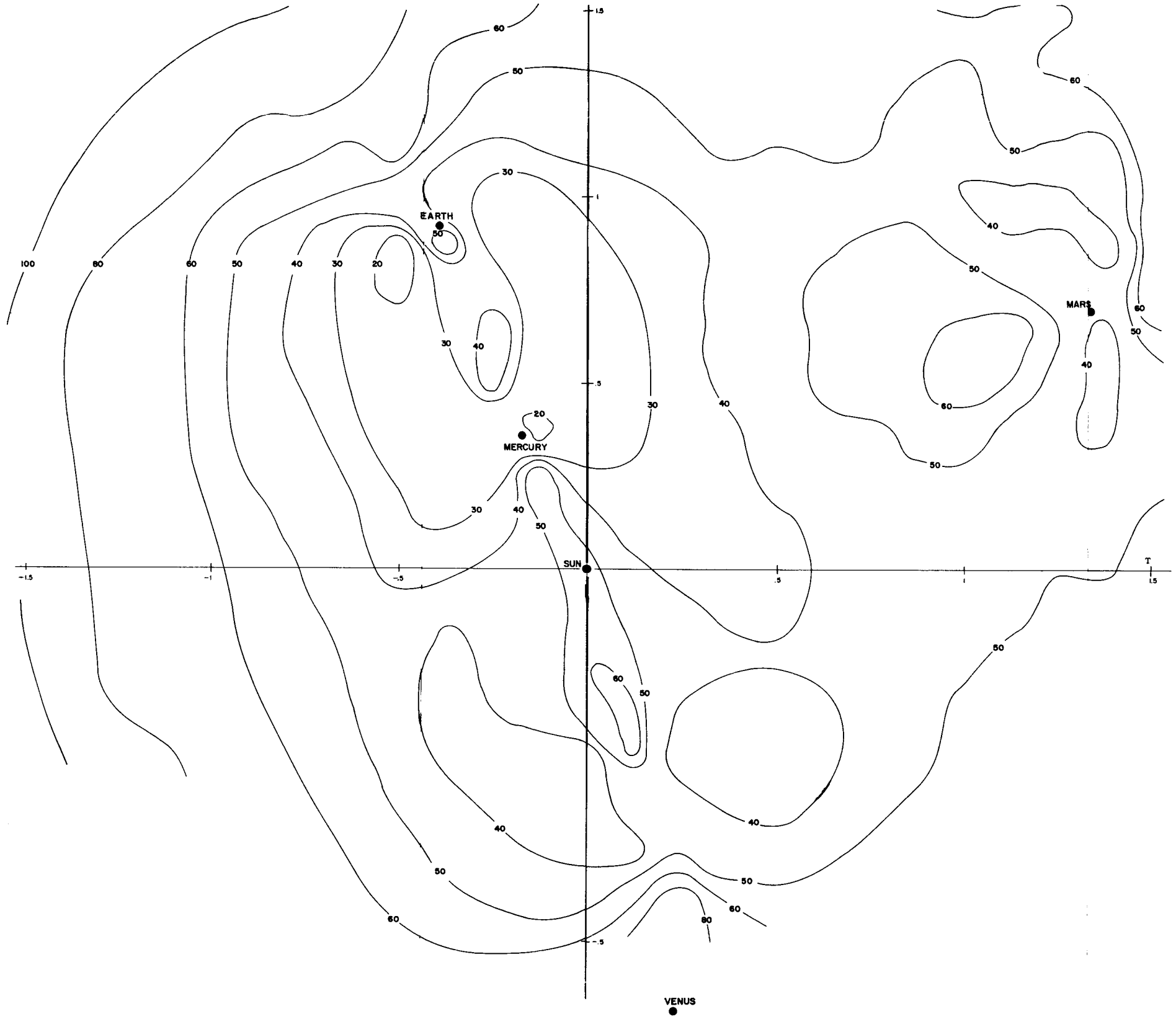

Figure III-26. Constant Error Contours in the Ecliptic Plane for J.D. 2440600.5 (σ = 10 seconds)

IV. COMPUTER REQUIREMENTS

In this section we present the discussions and results of studies mainly concentrated on the problem of processing the scanning camera data to derive navigational information (attitude and position). That is, we will be most concerned with the computer program which inputs data, identifies the targets, and solves the navigation equations. We make an attempt to estimate two quantities: (a) the number of storage locations required for the program, (taken in the sense of one instruction per location), and (b) the time taken in executing the program.

To estimate storage requirements, we do not include such subroutines as sine, cosine, and tangent since these will undoubtedly form part of the standard library in the computer repertoire of subroutines. Matrix inversion, however, because this is specialized for our particular problem, will be included (in the equation solution routine). For execution time, on the other hand, all of the functions encountered are taken into account. Furthermore, we state the time as the number of equivalent additions. In this manner, a specification of the add time for a particular computer (in microseconds) immediately produces the program execution time. A perusal of the operation times for standard computers shows that the following time equivalents are probable:

multiply	4½ additions
divide	7 "
sine, cosine, tangent, arcfunctions	55 "

and these are the numbers used in this section.

There are two broad assumptions we will follow both for definiteness and, in the first case, simplicity, in deriving these requirements. The first of these relates to the problem of fixed versus floating point operations in the computer. We have based our estimates upon fixed point arithmetic while fully realizing that some of the more involved mathematical processes will require floating point to maintain accuracy. Examples of the latter are: transcendental functions, divisions, and matrix inversion. On the other hand, a great deal of the processing problem involves mere housekeeping: incrementing index registers, loading, storing, branching, testing, etc. These are operations in which fixed point arithmetic is fully adequate. Now the neglect of floating point considerations will tend to increase both the storage requirements and execution times from those estimated here. In addition, however, it must be remembered that the present estimates are just that. They can undoubtedly be reduced by from 10% to 25% by the careful programming of a competent person. These two effects thus tend to cancel one another and so should not be the source of too great an error. In any case the contract goal is to demonstrate feasibility and we feel that the estimates do give one a good basis for judging.

The second major assumption warranting attention at this point has to do with the camera motion. We are supposing here that the camera capsule forms a symmetric rigid body and rotates in a force-free manner about an axis near to its symmetry axis. All of the computer estimates are based on this premise. Now if a system is to be imagined in which the

camera is mounted on a stabilized platform and driven about in the scan mode, angles being measured by an encoder rather than time, then all of the mathematics become considerably simplified with a consequent reduction in storage and speed requirements. Conversely, if the capsule be assumed assymatric, the equations of motion lead to elliptic functions as their solution thus complicating the computer program with obvious results. Perhaps, then, in this area we have chosen what is more or less a compromise in the complexity of the equations to be solved.

Table IV-1 is a summary of the computer requirements as estimated in this section. We see that some 5400 instruction are needed and that the execution time runs from 0.1 to 1.5 million equivalent adds. A computer possessing a 5 microsecond add time would then complete this task (beyond the time required for measurement) in from ½ to 7½ seconds. We must, of course, be careful about accepting such estimates too readily. Some parts were examined quite carefully, others merely programmed in FORTRAN on the Control Data 1604 and still others only approximated.

Overall, however, the execution time is well under any reasonable requirements and could be 10 to 1,000 times longer for extended space missions without becoming excessive. The storage requirements also are not too large, though here it is more desirable to be able to minimize.

The remaining parts of this section examine in greater detail the individual computer tasks of data input, target identification, and solution of the equations. Closing the section is a discussion of desirable computer

TABLE IV-1

SUMMARY OF COMPUTER REQUIREMENTS FOR
PROCESSING SCANNING CAMERA NAVIGATION DATA

PROGRAM	NUMBER OF REQUIRED STORAGE LOCATIONS	EXECUTION TIME (equivalent adds)		
		min.	aver.	max.
Data Input (Interrupt)	272	47	221	240
Pre-Processing	660	-	3.5×10^3	-
Triplet Identification	1450	3.1×10^4	4.8×10^4	9.2×10^4
Attitude and Verification	980	-	4×10^4	-
Solution of Navigation Equations	935	4.9×10^4	5×10^5	1.28×10^6
Data Lists and Ephemeris	1051			
TOTAL STORAGE	5347	8×10^4	5.9×10^5	1.4×10^6
		Total Execution Time (after measurement ceases)		

characteristics (interrupt, buffer, word length, add time, external memories, instruction repertoire, etc.) for processing the scanning camera data in particular and space mission data in general.

A. Data Input

The processing of camera data by the computer, especially in the input stage, depends upon the exact form of that data. We therefore take the discussion of Section II-B as our starting point. There it was shown that each detected event produced via the camera electronics two 24-bit "words" containing a variety of information about the target. This data is stored in a buffer (see Section IV-D) until the computer can accept it.

Since the data will arrive rather slowly in comparison to the computer's ability to process it, the latter will probably be engaged in other pursuits. To prevent data pile-up, the computer also possess an "interrupt" feature (see Section IV-D) which is activated in such a case as this. It is the aim of the present discussion to present an interrupt program which empties the buffer, sorts the information, and stores it appropriately for use later by the identification procedure.

First, however, let us show what the form and content of the incoming data is. We will use only the 2-slit camera for simplicity. The addition of the third vertical slit would not effect any changes if its information entered the computer via a different channel having its own interrupt procedure.

As shown in Section II-B and IV-D, the computer buffer stores words sequentially as received and can hold, say, up to sixteen words. Each event generates two words which are entered in the buffer in a particular order. Let us designate by BIE a counter which is part of the buffer (but accessible to the computer) and which contains the buffer location number

wherein the next data word is to be entered. This counter is increased by one each time such a word enters and automatically reads "1" after the sixteenth word has been entered.* Such a counter permits both the electronics to know where data is to be stored and the computer to know if more data is still in the buffer (by comparing BIE to a similar counter BII which is internal to the computer and designates the location from which the next data word is to be extracted).

The first word of information belonging to each event contains the time that the photomultiplier anode current becomes greater than the bias level. This "rise time" is in units of 10 microseconds and hence can tell time up to $(2^{24}-1) \times 10^{-5} = 167.8$ seconds, long enough to encompass ten scans of ten seconds each.

The structure of the second 24-bit word depends upon the target:

STAR

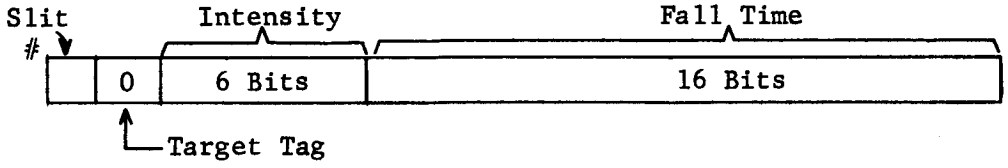

PLANET

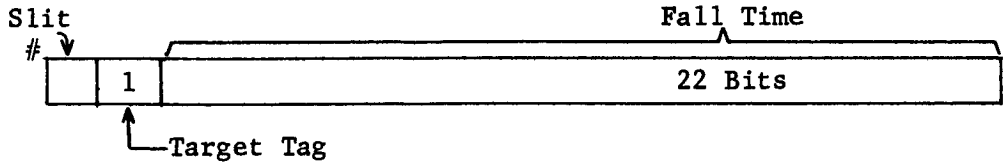

* This is easily accomplished using a 4-bit word with end-around carry. When it reads 1111 (= 16), an addition of 1 in the lowest bit makes the counter 0000. The end-around carry then produces 0001.

The first two bits in each case contain similar information: bit #1 - slit number (0 = #1, 1 = #2), bit #2 - target tag (0 = star, 1 = planet). The last twenty-two bits of the second data word contain, for extended targets such as planets, the time that the photomultiplier anode current falls below the bias level. The least bit here also measures ten microseconds so that $(2^{22}-1) \times 10^{-5} = 41.9$ seconds can be contained, more than sufficient for even the largest planets. The "fall time" is required in case measurements are desired on the trailing edge of a planet. To keep instrumentation to a minimum, the same fall time gating is used for stars. However, a 6-bit intensity code overwrites the upper portion of this fall time.

The tasks of the interrupt routine and the general order of execution of this routine are shown in Figure IV-1. (A detailed scheme is given in Appendix F.) The lists mentioned are shown in Figure IV-2. For planets, a true fall time is computed and both rise and fall times stored in the Planet Data List of Figure IV-2c. Stars are treated in a much more sophisticated manner since the identification of them is crucial. Targets which have adjacent transit times and too similar magnitudes are relegated to the Odd Target List (Figure IV-2b) to avoid ambiguities in the searches during identification. To accomplish this, no target data is stored until the next data enters. This permits the "similarity" comparison and explains the notation "Previous" and "Present". One expects that no more than four targets (out of an expected 15 or 20) will be lost due to precession and a similar number gained. Allowing for two fast-moving targets, the number of odd targets (or rather number of such detections) will not exceed

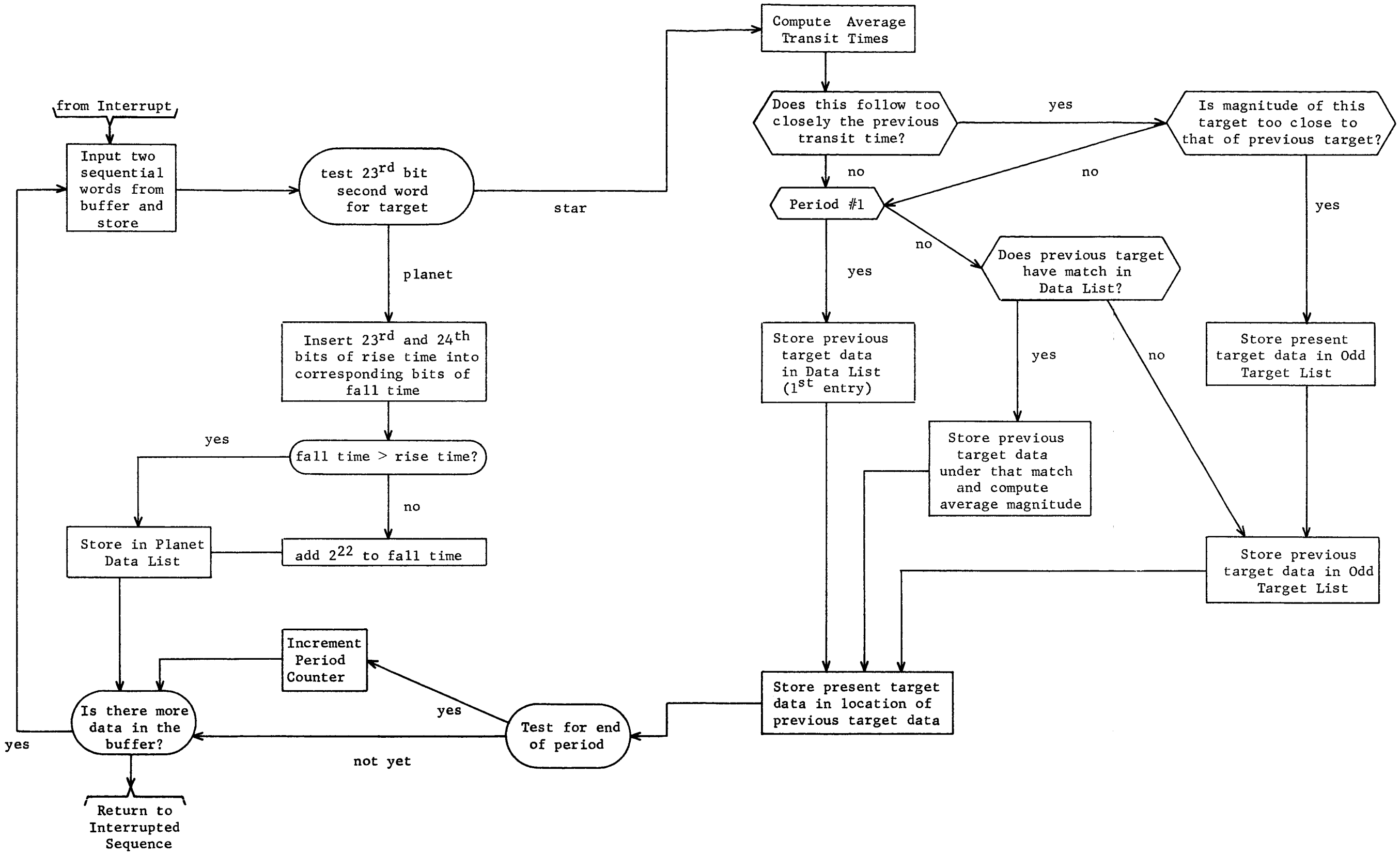

Figure IV-1. Flow Diagram for Data Interrupt Sequence

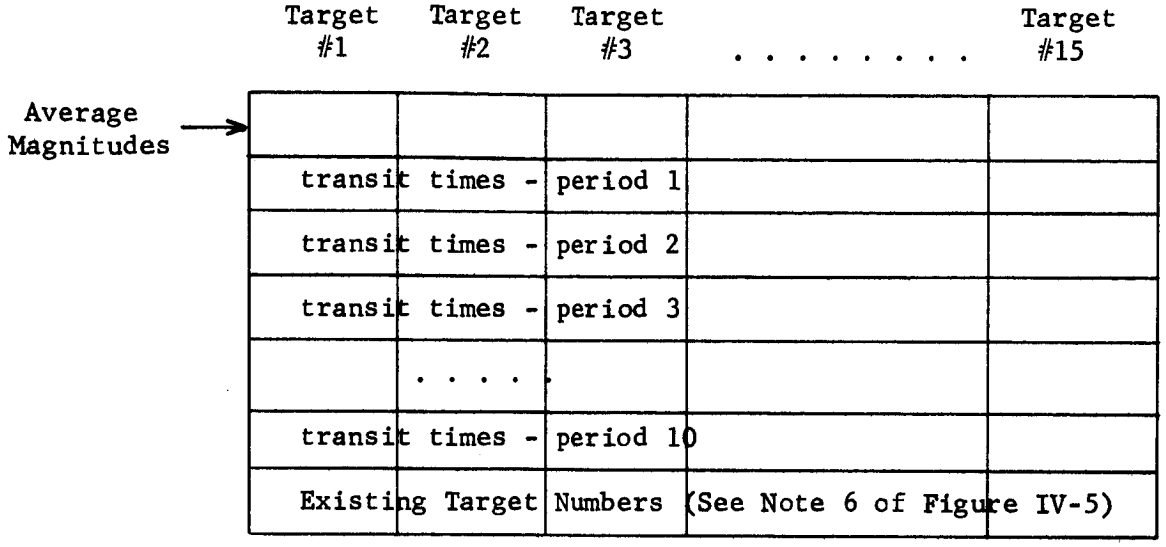

(a) Data List - one for each slit

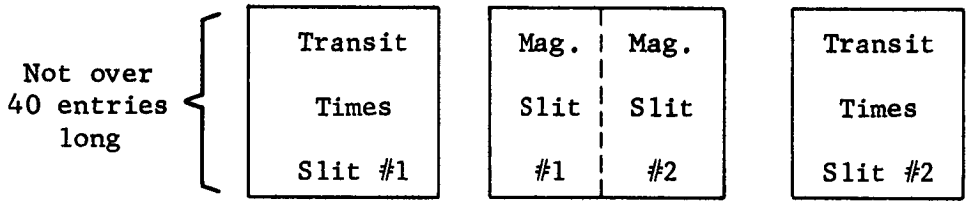

(b) Odd Target List

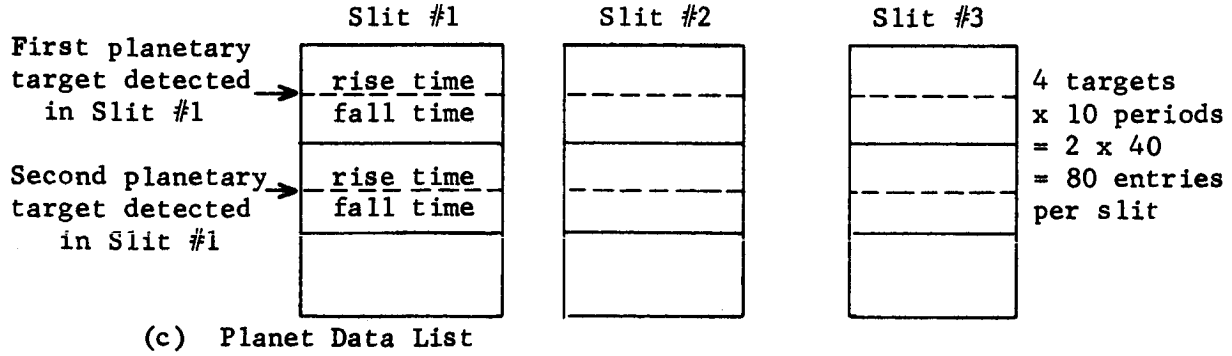

(c) Planet Data List

Figure IV-2. Data Lists Affected by Input Routine

4 x 10/2 + 2 x 10 = 40 pieces of data per slit. (The 10/2 factor means that these four targets only become new on the average of half-way through the ten periods of measurement.)

The main task of the interrupt program is to construct the Data List (Figure IV-2a) from star-like transits, and this is done differently depending upon whether it is the first or subsequent periods of camera rotation.

(a) First Period - For a given slit, columns in the Data List are assigned consecutively to the incoming targets. Thus (we neglect from here on considerations of 'similar' targets) the first target to enter slit #1 has its magnitude stored in row 1, column 1 of the Data List for slit #1 and its transit time in row 2, column 1. The second target gets stored similarly in column 2 and so forth. Slit #2 is treated in an exactly comparable manner. Up to fifteen targets per slit will be allowed; the remainder, if any, being relegated to the Odd Target List. The incoming targets are continually paired with the column 1 target to check for period change. (This also permits an accurate evaluation of the period.)

(b) Second and Subsequent Periods - For periods after the first, each target is matched in the Data List to find its counterpart in the previous period. That is, its transit time should be almost exactly one period later and its magnitude similar. If a match is found, say with the k^{th} target in the Data List

(k^{th} column), then the transit time is stored also in the k^{th} column and in the row corresponding to the period. (2^{nd} row for period 1, 3^{rd} row for period 2, etc.) Furthermore, the magnitude is averaged with the magnitude at the top of the k^{th} column by the formula

$$m_{av} = \frac{(n - 1)\, m_k + m}{n} \qquad (4\text{-}1)$$

where m_{av} is the new average, m_k the previous average, m the new magnitude, and n the total number of entries (including the present one) in the k^{th} column. If a match cannot be found, the data is sent to the Odd Target List. It should be evident now why "similar" targets are discouraged from entering the Data List.

The obvious advantage to the above technique is the collection under their respective targets of almost all of the incoming data. Thus when the measurement is completed, the identification of a target carries with it all of the data also belonging to it. Furthermore, the magnitude of any target is now far more accurate (about three times better if ten periods are measured) than any individual determination. This will prove of great help in pairing targets between slits.

The disadvantage is that dependence is placed on the first period. If these targets disappear or additional ones appear (due to precession), no new columns are started. This is probably not an insurmountable problem

and can be remedied by a more sophisticated analysis.

As mentioned before, Appendix F contains a detailed program of Figure IV-1. Merely counting the number of instructions and estimating equivalent adds, the following Table IV-2 compiles the computer requirements implied by the program. We have divided it into five sections for more critical examination. Some of the sections (Input, Decision, Return) are executed

TABLE IV-2

MEMORY REQUIREMENTS AND EXECUTION SPEEDS FOR DATA INPUT INTERRUPT ROUTINE

Program Section	Memory Locations	Execution Speeds (est) (equivalent add's)	
Input	15	13	each time
Decision	8	5	each time
Star Data Processing	197	213	90% time
Planet Data Processing	24	19½	10% time
Return	9	9	each time
Temp. Store	7	Min.	Average / Max.
Masks	4		
Indexes	8	46½	220¾ / 240
Program Total	272		
List Storage:			
Data List	360		
Odd Target List	120		
Planet Data List	160		
List Storage Total	640		

each time the interrupt is called while Star and Planet Data Processing are only accomplished when such targets are seen. It appears from our studies and simulations that about ten stars (of the fifty brightest) and four planets will be sighted, but not over two of the latter (as shown in Section I-D) will have sizes large enough to be distinguished as such. Thus 90% of the time that the interrupt program is called, the target will be processed as a star.

The data lists occupy a considerable amount of storage, but they have been estimated on a ten-period basis. It is also evident that the Star Data Processing problem consumes the greatest amount of program storage and causes much of the longest running time. This is also evident from a perusal of Figure IV-1. It is felt that competent programming could reduce both the running time and required locations by maybe 25%. As it stands, however, a computer with, say, an add time of five microseconds would take anywhere from 232 microseconds to 1.2 milliseconds with an average in the neighborhood of 1.1 milliseconds. Now this is long compared with the approximately 300 microseconds required to construct the data (see Section II-B). But no loss of information occurs when a buffer capable of retaining the data from several consecutive targets is available (see Section IV-D).

B. Target Identification

When the data from the scanning camera has begun to enter and accumulate in the computer, the identification process can begin. The purpose of this section is to describe the procedures to be used in identifying the targets.

Two philisophical aspects of the procedure presented bear immediate mentioning. The first is that stars (and small planets) form the basis of the identification and large planets are only noted once our footing is secure. This has been done to avoid the range of sizes and magnitudes to be expected from planets. The second general comment is that to a large extent, the procedure uses expected quantities. That is, before a measurement is even made, many possibilities are eliminated using the approximate position of the vehicle. For example, those targets which will appear large can be noted while small planets which will appear as stars are made ready to appear as such. Again, the motion of the capsule is assumed simple--no more complicated than small angle precession.

More sophistication and a wider range of possibilities will undoubtedly significantly change the stated procedure. Time does not permit the investigation of such luxuries at the present, however.

The reader is warned that not every pitfall is investigated in these pages, but for the sake of success versus completeness, the main problems are outlined and methods of attack described. It is hoped that no essential feature has been neglected or that those that have are amenable to solution.

The identification of detected targets will follow the general diagram

of Figure IV-3. Upon loading the entire navigation program into the computer memory and torquing the capsule up to its desired spin rate, the measurements can begin. Data formed by the electronics is accepted and stored by an interrupt program called each time a target is detected. The main program begins as in Figure IV-3 by first digesting the data coming in and subjecting it to a number of qualitative and quantitative tests. It is suggested that this take place until all data has been gathered. (About ten periods at ten seconds apiece implies 1½ minutes for the entire measurement.) Then several of the star-like targets are selected and an attempt is made to identify three of them with three stars (or planets) by means of angular pair separation and magnitude. Accomplishing this, an approximate attitude is determined and the remaining targets merely have their presence verified. There will, of course, sometimes remain odd targets such as a fast moving (in an angular sense) asteroid or near space vehicle. These are the last to be identified (or perhaps classified if unidentifiable).

Having identified all (or a sufficient number) of navigational targets, the program passes on to the solution of the navigational equations (the subject of Section IV-C and Section III-A2).

1. Pre-Processing

As the measurements proceed, the incoming data from the scanning camera will be analyzed as to compatibility before an attempt is made to identify the targets and use them for navigation. Figure IV-4 shows a possible flow diagram for this program. Such things as expected number of

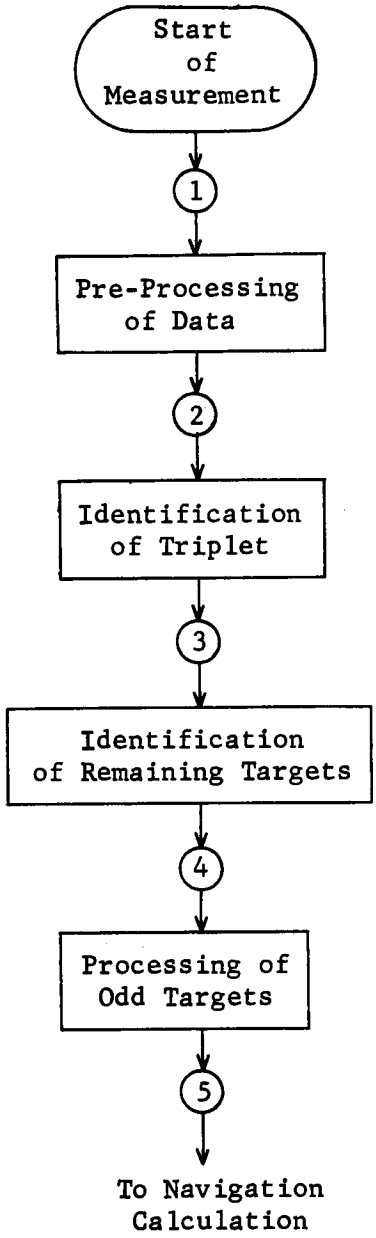

Figure IV-3. General Identification Procedure

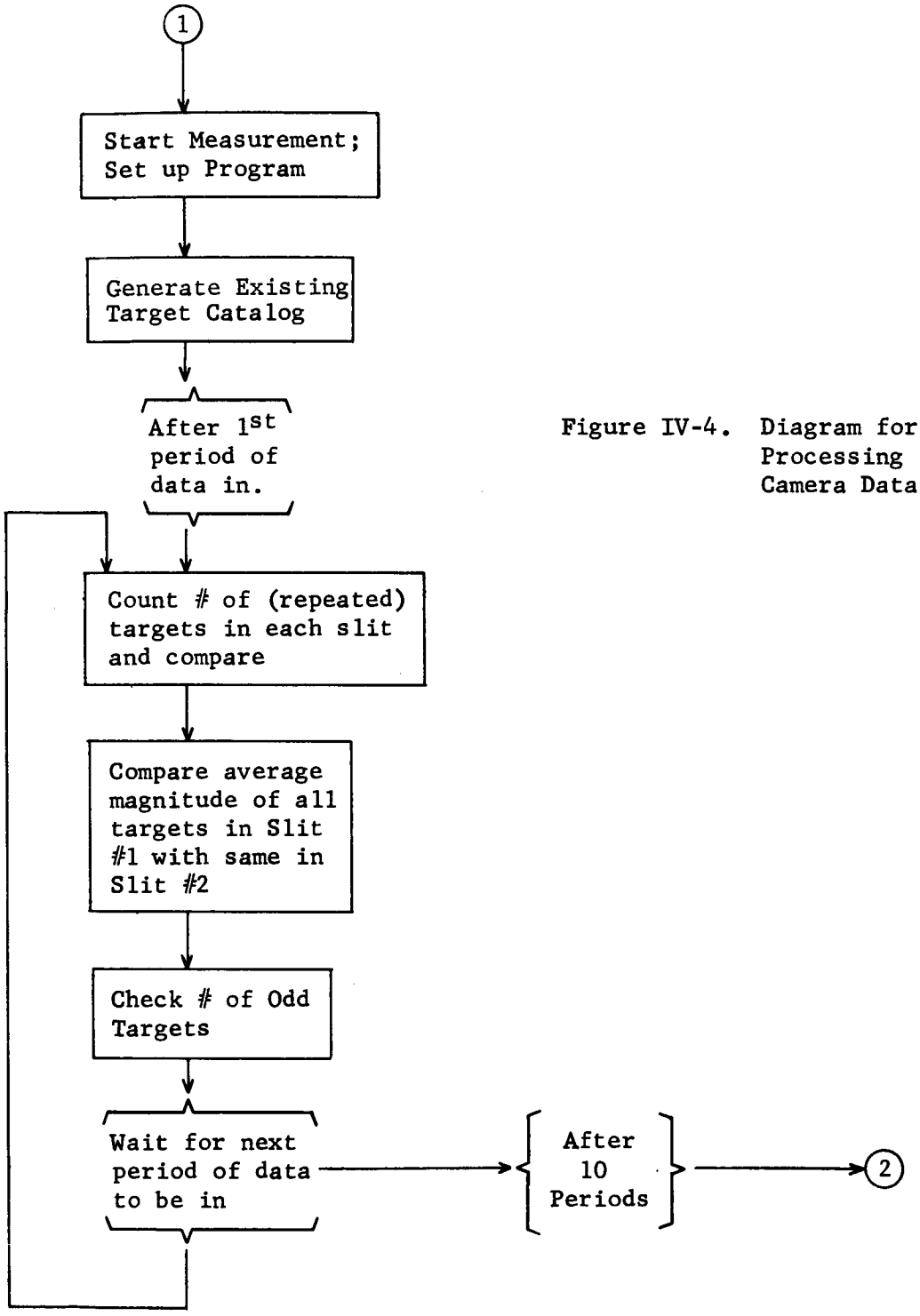

Figure IV-4. Diagram for Pre-Processing of Camera Data

targets, expected range of intensities, period and slit repeatability, etc. are monitored. If serious deviations are detected (one slit having brighter targets than the other, an excessive amount of false or missed targets, not enough or too many targets, etc.), the navigator is notified and he can then decide on an appropriate course of action. In the case of an unmanned system, a study would have to be made to permit more sophistication in this portion of the program. Perhaps bias levels could be changed, or the vehicle itself re-oriented for better viewing, or even re-start the spin of the capsule. In any case, all of the periods are so processed and checked before passing to the Target Identification sequence.

Part of the Pre-Processing task will be to generate, for use during target identification, an Existing Target Catalog. This is a list consisting mainly of stars, but also includes all other known bodies which might appear as stars to the camera optical system. The planets, for example, are reviewed to determine which will appear as such (i.e., have a relatively long pulse time in the slits) and which are so small as to appear as stars (angular radius less than about 20 seconds of arc). For those resembling stars, the approximate vehicle position is used in conjunction with the planetary ephemerides to compute their apparent right ascensions. declinations, and magnitudes. This data is then combined with that of a standard star catalog,* and the whole ordered according to magnitude.

---

* Corrected for proper motion, parallax, aberration, and slow magnitude variations as discussed in Section I-D. That is, the standard catalog contains all the appropriate parameters from which the Existing Target Catalog (for this particular measurement time) is constructed.

In regions where the vehicle might encounter them, moons, coments, asteroids and other targets are similarly treated. Thus is built up a list of targets as they should appear to the optical system. It can be pictured as having the following structure:

EXISTING TARGET CATALOG

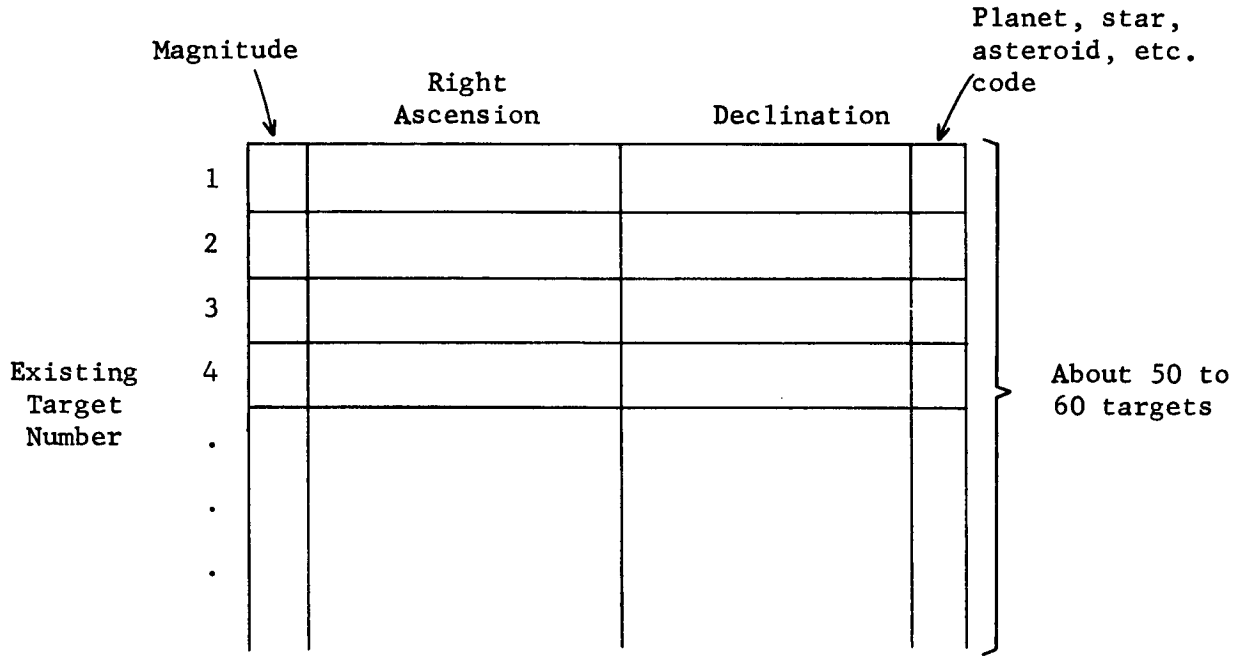

The computer requirements for Pre-Processing, summarized in Table IV-3, center mainly about the ephemeris lists and the generation of the Existing Target Catalog. To obtain estimates, let us assume that six orbital elements, radius, and albedo are stored for each of six planets. The last two can be stored in one word, so these "ephemerides" occupy 6 x 7 = 42 locations. For each of the fifty brightest stars, right ascension, declination, two components of proper motion, magnitude, and parallax are required, the last four being stored in two words and the total using 50 x 4 = 200 locations. The Existing Target Catalog itself, of course,

TABLE IV-3

STORAGE REQUIREMENTS FOR PRE-PROCESSING SEQUENCE

Tables:	
Planetary Ephemerides	42 locations
Stellar Catalog	200 locations
Existing Target Catalog	168 locations
Program:	
Construction	600 locations
Remainder of Pre-Processing	60 locations
Total.....	1070 locations
Execution Time: Sequence operable during entire measurement process.	

contains 56 targets with four pieces of data apiece, or 56 x 3 = 168 locations (magnitude and code can occupy one word). Ephemeris lists, therefore, occupy 410 locations altogether.

The generation of the Existing Target Catalog is estimated from a simulation (see Section III-E and Appendix E) to require about 600 storage locations. The remainder of the Pre-Processing program does not appear to be significant. The total number of required locations, including the various catalogues, is thus about 1070. The running time is not significant here since this part of the program remains in operation during the entire measurement sequence. It is estimated, however, that to generate the Existing Target Catalog would take 17 milliseconds on a computer with a 5 μsecond add time.

2. Identification of Three Stars

As the first part of the identification sequence, an attempt will be made to identify three stars (or planets) using the scheme blocked out in Figure IV-5. This figure, together with the accompanying notes is hoped to be self-explanatory. However, the following brief summary may be of help.

(a) First, four targets in Slit #1 (starting with the brightest) are paired with four targets in Slit #2.

(b) Then, various combinations of these targets (taken three at a time) are compared as to angular separation and intensity with a table of actual stars (including planets expected to look like stars. See Note 4).

(c) If a match for the triplet is found, the program proceeds to the identification of all the targets.

(d) If a match cannot be found among the four combinations, another star-like target is paired between the slits (as in (a)) and this takes the place of the brightest of the original four. The process then repeats from (b).

Six targets are so tried and there are several places where the logic gives up and exits to the navigator. Again, for an automatic system, an additional degree of sophistication may have to be inserted.

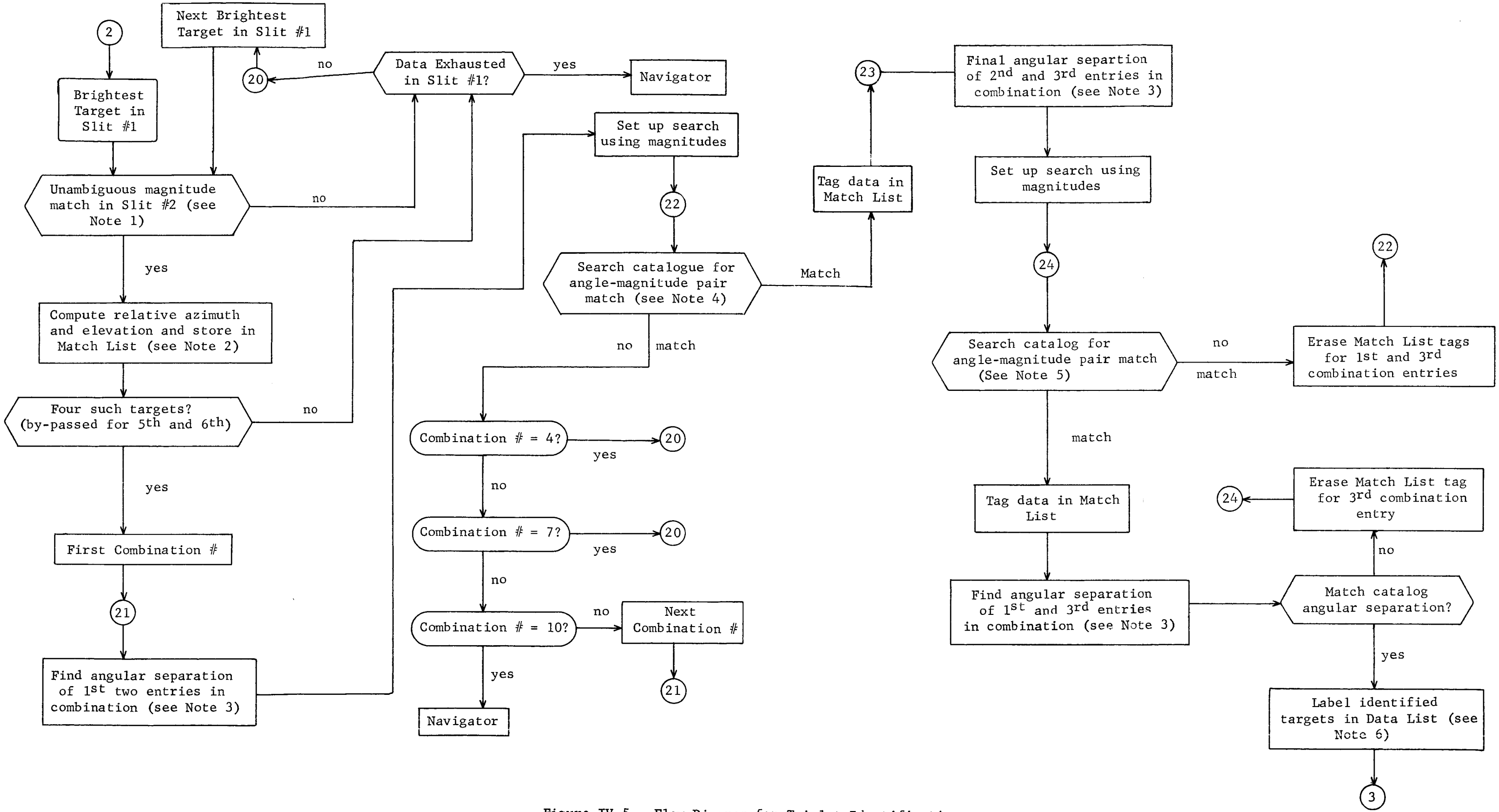

Figure IV-5. Flow Diagram for Triplet Identification

From a simulation of exactly the program shown in Figure IV-5, (see Section III-E and Appendix E), we estimate that it requires about 1450 locations and runs anywhere from 3×10^4 to 9×10^4 equivalent additions.

NOTES FOR FIGURE IV-5

Note 1

There will be a Data List as shown in Figure IV-2 for Slits #1 and #2 of the scanning camera. At the end of the measurement the magnitude codes in the first rows of these lists will be averaged over ten periods. The brightest (star-like) target in the Slit #1 Data List is chosen and a search conducted in the Slit #2 Data List for a target equally as bright. Actually, we require

$$m_1 - \Delta m < m_2 < m_1 + \Delta m \qquad (4\text{-}2)$$

where the subscripts denote the slit numbers and

$$\Delta m = 1\,\sigma \doteq .1 \text{ magnitude.}$$

That is, the magnitude range for the search is $\pm$ 0.1 magnitude. An individual measurement is expected to yield 10% accuracy on the intensity which is 0.1 magnitude. Therefore, a search should be $\pm 3\sigma \doteq 0.3$ magnitude, but ten measurements have been taken so that the RMS error is down by a factor of 3. Thus $\Delta m = 0.1$ magnitude should include 99.74% of the possi-

bilities.

Now fifty stars spread over about three magnitudes means that, on the average, within $\pm$ .1 magnitude of a particular brightness, 3-1/3 stars occur. But only about one-fourth of the fifty stars are seen during a scan of the camera, so about 0.8 star are expected to be detected in this range. Now "unambiguous match" means that one and only one Slit #2 target has the correct magnitude. If two or more Slit #2 targets agree with the Slit #1 magnitude, a check is made on the separation of the transit times in the two slits. Let t_1 be the transit time in Slit #1 and $t_2^{(1)}$, $t_2^{(2)}$, ... $t_2^{(k)}$ be the transit times of the compatible (in the sense of magnitude) Slit #2 targets. In order for t_1 and $t_2^{(i)}$ to belong to the same target, it must fall within the camera field of view which demands that

$$\left| \frac{\tan \pi \left(\frac{t_2^{(i)} - t_1}{T} \right)}{\sin 30^\circ} \right| \leq \tan 15^\circ \qquad (4\text{-}3)$$

where T is the spin period. (FOV = 30°, so maximum off-axis angle is 15°.) If only one $t_2^{(i)}$ survives this test, then t_1, $t_2^{(i)}$ are said to be matched. But if none or two or more are so paired, the match is void and the next brightest target is chosen from Slit #1. This is a highly reliable technique as is shown in Section III-E which presents the results of a computer simulation of the target identification.

If an unambiguous match cannot be found in Slit #2, the next Slit #1 target is taken until all such targets are surveyed. Not having found

four (at least three) suitable matches means that something must be wrong with the measurement, and control reverts to the navigator.

Note 2

Using the first period transit times of the matched pair, the elevation β of the target above the scanning plane (plane perpendicular to the spin axis) can be found using

$$\tan \beta = \frac{\sin \pi \left(\frac{t_2 - t_1}{T}\right)}{\tan 30^o} \qquad (4\text{-}4)$$

where t_1, t_2 are the transit times in Slits 1 and 2 respectively, T the spin period and 30^o the angle of inclination of the slits to the optical axis--spin axis plane.

The azimuth, λ, of the target relative to a zero azimuth at time t_o" (perhaps chosen as the transit time of the first target; quite arbitrary) is given by

$$\lambda = \left[\frac{t_2 + t_1}{2} - t_o''\right] \frac{2\pi}{T} \quad . \qquad (4\text{-}5)$$

(The assumption for both of these equations is that the capsule spins at a uniform rate without precessing. Such an approximation is sufficient for our present needs.)

This data is stored in a Match List whose structure is shown in the sketch. The first column contains the location of the target in the Data

List for Slit #1, the second column does a similar job for Slit #2. The next two columns are the relative elevations and azimuths of the targets as computed from the above equations. The final column is used for the identity number.

Since it is possible to examine six targets, the fifth target is to overwrite Target #1 in the Match List and the sixth overwrites Target #2.

MATCH LIST

Target #	Slit #1	Slit #2	Azimuth λ	Elevation β	Ident. Tag
1					
2					
3					
4					

Number of targets as given in Data Lists

Thus as each new target comes in, the brightest is rejected.

Note 3

Of the four targets present in the Match List, four combinations of three targets each are formed. The identification of one of these triplets is the subject of Notes 4 and 5. Which stars form the triplet are determined from the following matrix. The additional combinations (beyond 4)

are due to the ability to use two additional targets entered into the Match List if the original four are not identifiable. (See end of Note 2.)

To find the angular separation α_{ij} of any two entries in a particular combination, the spherical formula

$$\cos \alpha_{ij} = \sin \beta_i \sin \beta_j + \cos \beta_i \cos \beta_j \cos(\lambda_j - \lambda_i) \qquad (4\text{-}6)$$

is used where the notation is specified in Note 2.

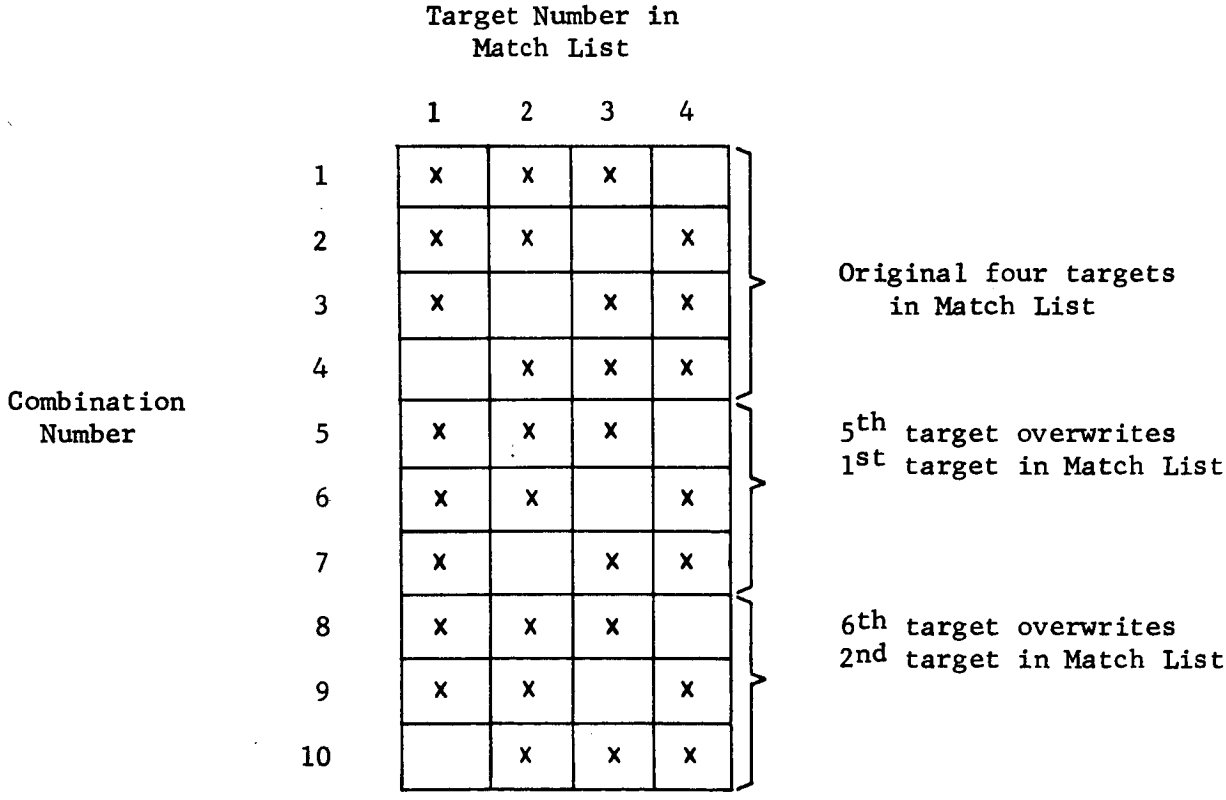

Note 4

Using the angular separation α_{12} of the first and second entries

in a particular combination (see Note 3) and their magnitudes m_1, m_2, the catalog of existing targets is searched for a pair having similar characteristics.

The method by which the search is made can be visualized using the following sketch. The entries in the boxes are the angular separations

Existing Target Magnitudes

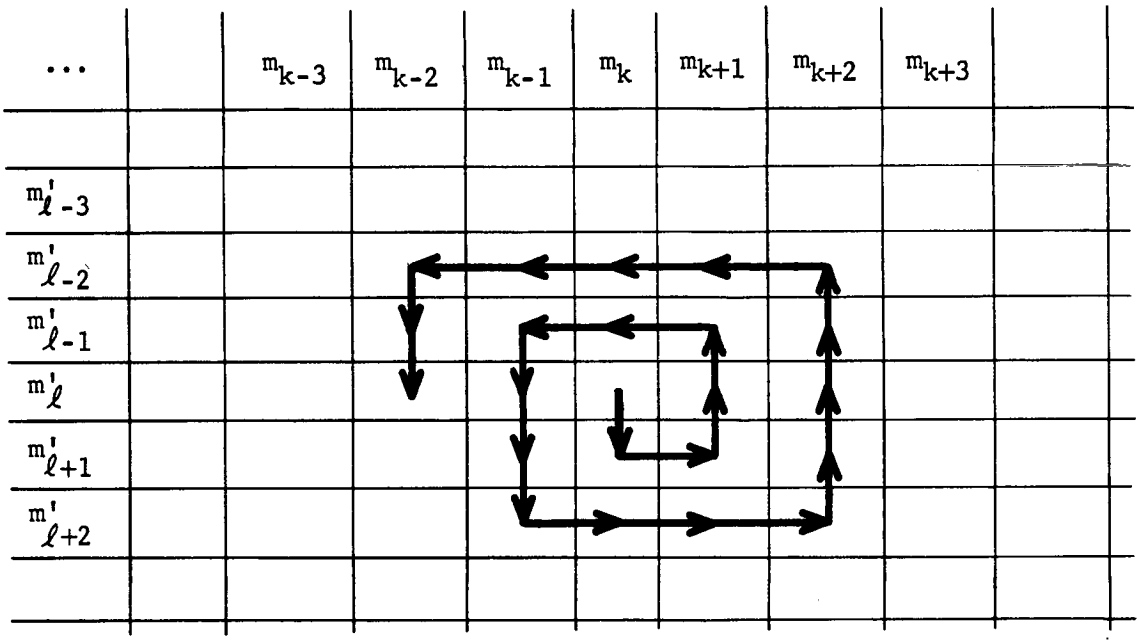

α'_{ij} of the particular pair. The "magnitude matrix" is used as follows:

(a) find the existing target magnitude m'_k for which

$$m'_k < m_1 < m'_{k+1},$$

(b) find the existing target magnitude m' for which

$$m'_\ell < m_2 < m'_{\ell+1},$$

(c) compare α'_k with α_{12},

(d) if no match, compare $\alpha_{k,\ell+1}$ with α_{12},

(e) if no match, continue the search of the "magnitude matrix" in a "circular" manner as shown in the above sketch.

How far to continue the search and what constitutes a match between angular separations are determined by the confidence placed in the magnitude measurement and the degree to which the capsule spins uniformly about a fixed axis during one period. (It is to be remembered that all of the angular data is taken from the first period while the magnitude data is averaged over ten periods. See Note 1.) The angular separations are probably good to one-tenth of a degree, but the magnitudes might be as bad as 0.1 magnitude. (Again see Note 1.) To allow for the phototubes being wrong in one direction, the search could probably proceed until a "square" which is 0.4 magnitude on a side is covered in the "magnitude matrix".

As soon as a match is achieved within the specified limits, the particular stars forming the target pair are labeled in the Match List with the corresponding Existing Target Numbers and the program continues through (23) and (24) to a similar type of search described in Note 5. Now a failure in this second search merely continues the first search from where it left off. And this first search, when it exhausts the "square", returns the program to the next combination of targets (see Note 3). Finally, running out of combinations and therefore out of six targets, the program throws in the towel and exits to the navigator.

Note 5

This search is very similar to the first search described in Note 4, but is much simpler in that the second entry in the combination has already been tentatively identified by the first search. Therefore, the sketch used to describe this second search is merely a line. Again m'_p is found such that $m'_p < m_3 < m'_{p+1}$ and the Catalog of Existing Targets (see Note 4) is searched within $\pm$ .2 magnitude of m'_p until an angular separation α'_{2p} is found near enough to α_{23}.

Again, the first match makes the program label the appropriate Match List target and then to compare (only once now) the angular separations of the first and third combination entries. These either match or don't and if not, the second search is merely continued. A match more definitely identifies the triplet and the program continues to (3) wherein the remaining targets are also identified but in a much more straightforward manner.

Note 6

When a triplet identification has been made, the data associated with these targets is labeled in the Data Lists shown in Figure IV-2. That is, for each slit, there will be three targets to which are attached the numbers of the Existing Targets with which they have become associated. The Data Lists are similarly labeled when the remaining targets become identified. Notation is also made in the Existing Target List so that these targets are not searched for by subsequent routines.

3. Identification of All Remaining Normal Targets

When a triplet of targets has been satisfactorily identified, the remaining targets are handled in a much simpler fashion as shown in Figure IV-6 and its accompanying notes.

Essentially, the attitude of the capsule (or rather the parameters of the attitude during one period since the capsule is spinning and slightly precessing) is computed from two of the identified stars, then the expected times of transit of the desirable bodies are found. If these match existing transit times and the intensities are also compatible, the target is assumed identified. An excessive number of (or a few key) failures would cause exit to the navigator or reversion to another triplet identification.

The computer requirements are estimated principally from Notes 1 and 2 and from part of the simulation program given in Appendix D (see also Section III-E):

	Storage Locations	Execution Time (equivalent adds)
Attitude	300 (?)	2×10^3
Verification	680	3.8×10^4

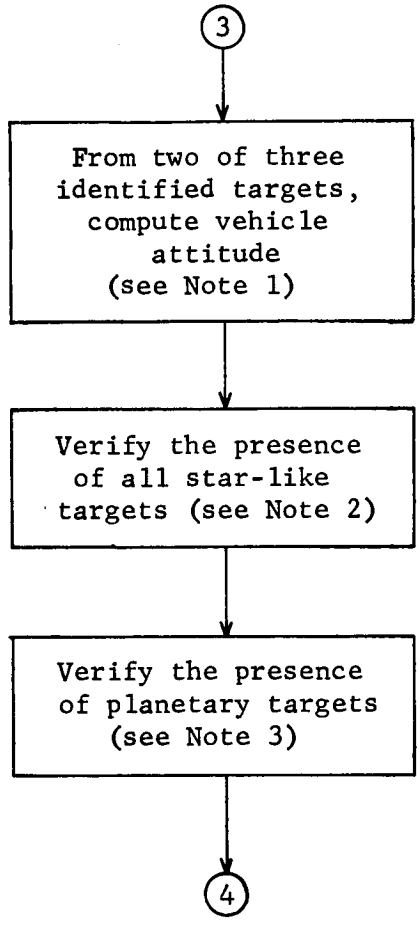

Figure IV-6. Flow Diagram for Verification of Remaining Targets

NOTES FOR FIGURE IV-6

Note 1

The attitude of the capsule is computed in two steps. The first involves approximating the scan plane by the plane of two of the three previously identified targets. Thus one chooses this pair to lie about 90° apart and as near to the scan plane as possible.* From the notation shown in the sketch, we see that the parameters describing the scan plane

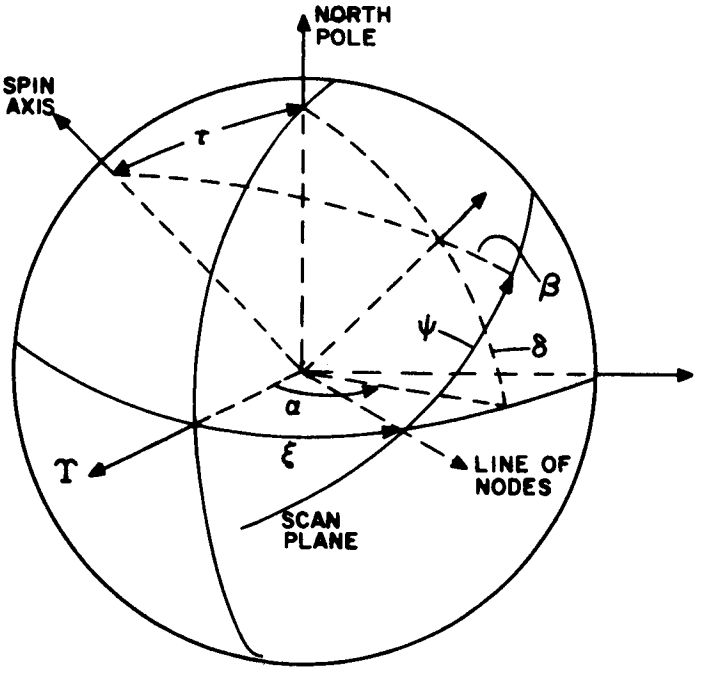

* The pair cannot be 0° or 180° apart since no attitude information can be derived from such a situation. Furthermore, target #2 must be ahead (later in time) of target #1 if the cross product is to give the correct sense to the normal vector.

are τ and ξ, the star is located in the astronomic frame by α, δ and in the instrument frame by ψ, β. Using subscripts 1 and 2 for the first and second targets scanned we can compute the approximate τ and ξ from the equations

$$\begin{pmatrix} \sin\tau \sin\xi \\ -\sin\tau\cos\xi \\ \cos\tau \end{pmatrix} = \frac{\hat{s}_1 \times \hat{s}_2}{|\hat{s}_1 \times \hat{s}_2|} \tag{4-7}$$

where

$$\hat{s}_1 = \begin{pmatrix} \cos\delta_1 \cos\alpha_1 \\ \cos\delta_1 \sin\alpha_1 \\ \sin\delta_1 \end{pmatrix} \tag{4-8}$$

and similarly for $\hat{s}_2$.

Using these approximate values, more accurate* ones can be obtained by solving the simultaneous equations

$$\begin{aligned} \sin\beta_1 &= \cos\tau \sin\delta_1 + \sin\tau\cos\delta_1 \sin(\xi - \alpha_1) \\ \sin\beta_2 &= \cos\tau \sin\delta_2 + \sin\tau\cos\delta_s \sin(\xi - \alpha_2) \end{aligned} \tag{4-9}$$

---

* Still not very accurate, however, due to the assumption that precession is zero. This will suffice, though, for target verification, if the precession is small.

The third attitude parameter t_o, in $\psi = \frac{2\pi}{T}(t - t_o)$ where T is the spin period and t the time at which the target lies in the plane defined by the optical and spin axes, can be found from

$$\sin(\Delta - \psi) = \frac{\cos \delta_k \cos \alpha_k}{\cos \beta_k} - \tan \beta_k \sin \tau \sin \xi \qquad (4\text{-}10)$$

where

$$\sin \Delta = \frac{\cos \xi}{\left[\cos^2 \xi + \cos^2 \tau \sin^2 \xi\right]^{\frac{1}{2}}}$$

$$\cos \Delta = \frac{\cos \tau \sin \xi}{\left[\cos^2 \xi + \cos^2 \tau \sin^2 \xi\right]^{\frac{1}{2}}} \qquad (4\text{-}11)$$

The quadrant of ψ is the first or fourth if $|3 - \alpha_k| \leq \pi/2$ and second or third if $|3 - \alpha_k| \geq \pi/2$.

Note 2

The remaining targets are identified in a very simple manner. This consists in verifying that those targets in the Existing Target List (see Note 4 of Figure IV-5) which should be detected do in fact have compatible transit times and magnitudes.

Let us use for an example, the k^{th} brightest target in the Existing Target List. Since its spherical coordinates α_k and δ_k are given, and the capsule attitude parameters τ, ξ, t_o are known (approximately), compute

$$D_k = \left[\cos \alpha_k \sin \tau \sin \xi - \sin \alpha_k \sin \tau \cos \xi\right] \cos \delta_k + \cos \tau \sin \delta_k \qquad (4\text{-}12)$$

If $|D_k| \leq \cos 15^o$, then the target will probably be detected. If $|D_k| > \cos 15^o$, then pass on to the k + 1st target. If detectable however, compute

$$A_k = - \cos(\xi - \alpha_k) \cos \delta_k \qquad (4\text{-}13)$$

and

$$B_k = - \sin(\xi - \alpha_k) \cos \delta_k \cos \tau + \sin \tau \sin \delta_k \qquad (4\text{-}14)$$

and Δ, where

$$\sin \Delta = \frac{B_k}{\sqrt{A_k^2 + B_k^2}}, \quad \cos \Delta = \frac{A_k}{\sqrt{A_k^2 + B_k^2}}. \qquad (4\text{-}15)$$

Then find, among the four values of

$$\psi = \sin^{-1} \left[\frac{\pm D_k \tan 30^o}{\sqrt{A_k^2 + B_k^2}}\right] - \Delta \qquad (4\text{-}16)$$

which pair (one for Slit #1 using the + sign: $\psi^{(+)}$, and one for Slit #2 using the - sign: $\psi^{(-)}$, satisfy the inequality

$$1 \geq - A_k \cos \psi_k + B_k \sin \psi_k \geq \cos 15^o \quad . \tag{4-17}$$

The expected transit times for each slit are then

$$t_k^{(\pm)} = t_o + \frac{T}{2\pi} \psi_k^{(\pm)} \quad . \tag{4-18}$$

If these times are matched by data in the first period of the Data List (or are perhaps found in the Odd Target List) and the corresponding magnitudes also match, then the data is taken as identified.

Several possibilities can occur:

(a) The existing target is uniquely verified--no problem then arises.

(b) The data matches several targets in the Existing Target Catalog. Since this data has been unambiguously gathered over several periods, one could say that the predicted order (in time) of appearance is the same as the measured order of appearance. That is, if three targets of similar magnitude appear adjacent in time and three existing targets predict a similar occurance, the first (in time) measured target is the first (in time) existing target and so forth, even though the time slot overlaps two or more of these targets. This is obviously of poorer quality than the other identifications, but could be retained if necessary.

(c) No data can be found for an existing target--a notation is made and if this happens too many times, it becomes possible that the original triplet was identified incorrectly.

In any case the Odd Target List should also be searched since it will happen that perfectly legitimate and easily identifiable targets can find their way into it. One must remember, however, that only second and subsequent periods can enter the Odd Target List while the verified transit times refer to the first period. Furthermore, the Odd Target magnitudes have only been measured once, and so have a higher probable error associated with them.

Note 3

The planets (or for that matter any known stationary targets) fall into three categories as far as identification goes. They may be:

(a) separable - that is, their sizes are widely separated from any other such targets,

(b) similar - that is, two or more might have nearly the same angular size,

(c) borderline small - that is, they may be so small as to sometimes appear as planets, sometimes as star-like targets.

For Case (a), the identification is unique on the basis of pulse length alone. To be sure, however, that another (unknown) target hasn't appeared, a check should be taken on the attitude. In Case (b) the

identification should rather easily be effected by attitude comparisons as done for star-like targets. To locate data referring to targets in Case (c), one can use attitude and magnitude in searching the Data Lists or Odd Target List, and attitude and size in searching the Planet Data Lists. From these two or three sources, a collection of data belonging to the target may be accomplished.

Planets remaining in the Planet Data Lists are classified as odd.

4. Processing Odd or Ambiguous Data

We assume that nearly all the data belonging to stars, planets, and other known objects has been extracted from the Odd Target List and that, except for a few such entries in the later periods, the list contains either (a) fast target data, (b) erratic appearances which can be neglected, or (c) data too similar for simple separation. Without spending a great deal of time analyzing these types of problems, it is suggested that fast moving targets be detected by a combination of magnitude and variable period searching. That is, the magnitude of such a target can be expected to change rather smoothly with time. Also, motion will show up as a change in the detection period. Therefore, choosing a particular entry in the Odd Target List, one can look forward (or backward) to a time slightly different from the spin period and search for an entry of near magnitude. If this is successful, further extrapolation in the same direction should yield other data. If several such matches can be established, one can say that these all belong to the same object. After solving the navigation equations, then, the path of this object can be computed and displayed to

the navigator.

The last type of odd target is the multiple correlation of star-like data and existing targets. This occurs in a particular slit when several targets of similar magnitude transit the slit at close times. (It is not necessarily true that the existence of this in one slit implies its existence in the other slit.)

It will be quite difficult, generally, to determine at the present level of accuracy, just which targets belong to which data. On the other hand, such information will usually not be needed because enough "good" targets will have been identified. If desired, though, a more accurate attitude could be computed from the already secure targets, then the expected transit times of the ambiguous targets will be highly accurate and perhaps sufficient to resolve the ambiguities. This would, of course, be required if it was felt that one of the ambiguous targets was on a collision course with the vehicle.

It is extremely difficult to estimate the computer requirements for this task as it depends entirely on the degree of sophistication required. A (rather uneducated) guess might put the storage requirements in the range 200 to 600 instructions.

C. Solution of Navigation Equations

The computer requirements for the solution of the navigation equations can be quite easily estimated since the explicit forms of the equations are given in Section III-A and in Appendices B and C. In those parts and here too the assumed motion is one of a freely-spinning symmetric body. (See, however, the introduction to this Section IV and Appendix A.)

Figure IV-7 shows the flow chart for the computation of the navigational unknowns. The six parameters describing attitude are found first by an iterative procedure starting from assumed values. (The approximate attitude found during target identification plus the assumptions that rotation takes place very nearly about the axis of symmetry will provide the necessary starting values.) The calculation involves the inversion of a six by six matrix, the use of up to 220 "targets" (11 stars, 2 slits, 10 periods), and perhaps two or three times through the iteration procedure.

When attitude has converged, position is computed using the planets. Here only a three by three matrix need be inverted and it is very possible that no iterations are needed due to the linearity of the function.

Along side of each enclosure in Figure IV-7 are notations which depict the computer requirements for that particular task. The first gives the number of locations in the computer memory taken up by that part of the program. The remainder permits a computation of the execution time. These are: additions (including such equivalent instructions as load, store, jump, decrement, etc.), multiplications, divisions, and functions (subroutines such as sine, cosine, and tangent).

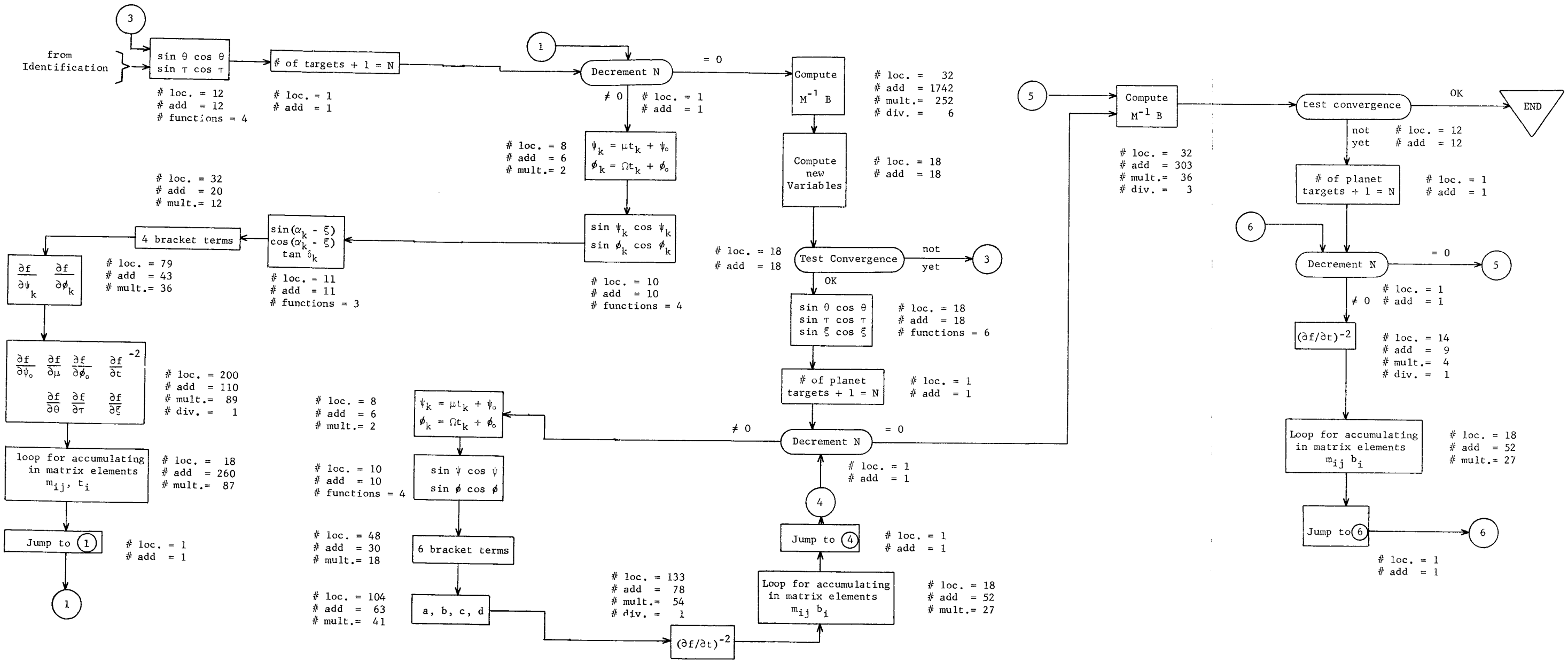

Figure IV-7. Flow Diagram and Computer Requirements for Solution of the Navigation Equations

The flow diagram can be divided into a few specific sequences and the requirements also so collected. The result is Table IV-4. We see that the number of memory locations needed for the program is 862 while an additional 73 are used in temporarily storing intermediate quantities. Thus in the neighborhood of 935 locations are required for the solution of the navigational equations.

To compute the running time of the program is not so easy due to the iterative nature of the solution and to the variability in the number of detected targets. However, empirical equations can be devised as is done in Table IV-5. There, each of the parameters is represented by a symbol and a conversion is made from multiplications, divisions, and functions into the equivalent number of additions. (See introduction to Section IV.) The coefficients of these parameters in the first series of equations are extracted from Table IV-5. (It must be remembered that with two slits, N_s targets, and P periods, that targets will be detected $2N_sP$ times. This is what is meant in Table IV-5 by "each target".)

The second series of equations shows the relative importance of the various arithmetic operations. While comparatively few functions are entered, they represent a significant amount of the total time. Multiplications become of primary importance, even though most of the program instructions consist of the addition-type (time-wise).

Table IV-6 gives some representative values for the total number of additions needed in computing attitude or position. (N_s is about 10, P between 1 and 10, and N_p between 4 and 6.) For the range of

TABLE IV-4

COMPUTER REQUIREMENTS DERIVED FROM FIGURE IV-7

Task Title	Symbol contained in Sequence in Figure IV-7	# loc.	# add	# mult.	# div.	# funct.
Attitude Set up	---	13	13	---	---	4
Each Star Target	(1)	360	462	226	1	7
Each Attitude Iteration (not including set up or star targets)	(3)	68	1778	252	---	6
Position Set up	---	19	19	---	---	6
Each Planet Target (1^{st} time)	(4)	323	241	142	1	4
Each Planet Iteration (not including planet targets)	(5)	45	316	36	3	---
Each Planet Target (subsequent times)	(6)	34	63	31	1	---

Total Program Locations	862
Temporary Storage	73
Total Overall Locations	935

TABLE IV-5

METHOD FOR COMPUTING TOTAL REQUIREMENTS

Define:

I_A = # of iterations in attitude computation

I_p = # of iterations in position computation

N_s = # of stars

N_p = # of planets

P = # of periods over which data accumulated

From Table IV-4 we have:

$$\text{Total adds} = I_A (1791 + 924 N_s P) + 333 + 482 N_p P + I_p (316 + 126 N_p P)$$

$$\text{Total mult.} = I_A (252 + 452 N_s P) + 36 + 284 N_p P + I_p (36 + 62 N_p P)$$

$$\text{Total div.} = I_A (2 N_s P) + 3 + 2 N_p P + I_p (3 + 2 N_p P)$$

$$\text{Total functions} = I_A (10 + 14 N_s P) + 6 + 8 N_p P$$

The equivalent number of additions using mult = 4.25 adds, division = 7 adds, functions = 55 adds is:

$$\text{Adds} = I_A (1791 + 924 N_s P) + 333 + 482 N_p P + I_p (316 + 126 N_p P)$$

$$\text{Mult} = I_A (1071 + 1921 N_s P) + 153 + 1208 N_p P + I_p (153 + 263 N_p P)$$

$$\text{Div} = I_A (0 + 14 N_B P) + 21 + 14 N_p P + I_p (21 + 14 N_p P)$$

$$\text{Func} = I_A (550 + 770 N_s P) + 330 + 440 N_p P$$

Thus, total equivalent additions for solving the equation are given by:

$$\text{Adds} = I_A (3412 + 3629 N_s P) + 837 + 2144 N_p P + I_p (490 + 403 N_p P)$$

TABLE IV-6

TOTAL NUMBER OF EQUIVALENT ADDITIONS FOR SOLUTION OF NAVIGATION EQUATIONS

Computation of Attitude From Stellar Measurements (units: 10^3)

$N_s P$ \ I_A	1	2	3
10	40	79	119
20	76	152	228
40	149	297	446
60	221	442	664
100	366	733	1099

Computation of Position From Planetary Measurements (units: 10^3)

$N_p P$ \ I_p	0	1	2
4	9	12	14
10	22	27	31
20	44	52	61
40	87	103	120
60	129	154	179

parameters shown, the solution of the navigation equations will require anywhere from 49 x 10^3 to 1.3 x 10^6 equivalent additions. A computer with a five microsecond add time can therefore handle this problem in from 0.25 to 6.5 seconds, a small time compared to the time of measurement ($\sim 1\frac{1}{2}$ minutes).

D. Space Computer Characteristics

While no attempt will be made here to design a space computer, the requirements examined in the previous section do form a basis for some general comments. Data input, instruction repertoire, word length, speed, and storage are discussed here in that order and as relates to the processing of the data from the scanning camera.

1. Buffered I/O and Interrupt Features

Information will be entering and leaving a space computer in a variety of modes and rates. Furthermore, some of the data will be arriving at unpredictable times. To accomodate these requirements, two features of a space computer which are highly desirable are: (1) at least one buffered input/output channel, and (2) an interrupt capability.

The interrupt feature is, of course, almost a necessity when the computer is dealing with a wide range of problems each having a different priority level. For example, if the computer is currently engaged in transmitting scientific data to Earth when other data suddenly arrives from a higher priority source, one would desire that the computer immediately devote its attention to this latter problem, but at the same time not destroy information being readied for transmission to Earth. This can be accomplished with "interrupt" in the following manner.

Upon receiving an interrupt signal, the computer automatically (i.e., by means of hardware) jumps to a pre-assigned location from which it extracts the next instruction. This instruction and the ensuing sequence

of instructions perform the tasks of (a) storing any data which is pertinent to the original program and which might be destroyed in the present routine, (b) sensing which device caused the interrupt, (c) carrying out the necessary program to remove the cause of the interrupt (this may merely be data input or may be serious enough to scrap the present program for some "emergency" function), and finally (d) restoring the original program data and returning to it. Using this capability, a number of functions can be monitored and updated "simultaneously". Each of these tasks is performed by the interrupt program shown in Appendix F which was constructed for the input and preliminary processing of measurements made by the scanning camera.

The buffered input/output feature is most useful when blocks of information need to be transferred rather than one word at a time. Also, on input, data may arrive in a random fashion as it does from the scanning camera, and, if two words should arrive in close succession, the second may be lost due to the computer being busy preprocessing the first. To avoid this, a buffer is added which retains information until the computer can accept it. In a sense, each input channel which contains a holding register is a buffer since the information is retained until the computer has available time to receive it. The word "buffer", however, is generally reserved for a set of holding registers. This device can accept data from a certain sensor at an extremely high rate of speed (the "instructions" are all performed with hardware) and also operates independently of the computer.

A typical sequence might be as follows. While the computer is executing

a given program, data arrives at the buffer in the form of single words, spaced randomly in time. When the first word arrives, an interrupt is sent to the computer. Before the computer can begin to empty the buffer, however, several more data words may enter it, being stored sequentially. The computer, during the interrupt routine, then empties the buffer of all its words and any that might enter even during this operation. Finally, the computer returns to its original sequence until the buffer, on receiving another word of data, interrupts again.

Because such a buffer stores incoming data sequentially, two index registers will be used. One will always contain the address of the next buffer location to be filled by incoming data. This is then stepped each time the data enters. The other index, or counter, contains the address of the next buffer location to be emptied by the computer, and this is also stepped each time a data word is transferred from the buffer to the computer. When the two indices are equal, no data is in the buffer, while their difference denotes the number of words ready to enter the computer.

It is interesting to investigate the improvement which a buffer provides in reducing lost target probability. If the buffer can contain B targets, and the computer can extract the first target in essentially zero time, a target becomes lost if B + 2 targets enter the buffer before the computer is finished processing the first. Let t_I be the time it takes to process one target, and T be the camera spin period. Then the probability that B + 2 or more targets will enter the buffer in the time t_I (i.e., before the computer can extract the second target), is given

by a Poisson distribution:*

$$P = \sum_{x=B+2}^{\infty} e^{-m} m^x/x! \qquad (4\text{-}19)$$

where

$$m = 2N_T \frac{t_I}{T} \qquad (4\text{-}20)$$

and N_T is the number of targets. (The factor 2 comes from seeing the target in each of two slits.) The quantity m is actually the expected number of targets in the time t_I and $2N_T/T$ is the average rate of arrival of targets. P is the probability of target loss per target, so one can expect to review 1/P targets before one is lost. Figure IV-8 is a plot of this reciprocal as a function of the ratio t_I/T and using $N_T = 15$ as the number of targets. It is immediately evident that even for a small buffer, a fantastic number of targets can be processed without a loss. This is mainly due to the rather low density of targets per scan ($N_T = 15$) and to the speed of processing relative to the spin period ($t_I/T < 10^{-2}$).

2. Instruction Repertoire

From the standpoint of capability, the two most important things are speed and the power of the elementary operations. Quite obviously, weak instructions will require excessive storage and long computation

* Burington and May, Handbook of Probability and Statistics with Tables, Handbook Publishers Inc., Sandusky, Ohio, 1958.

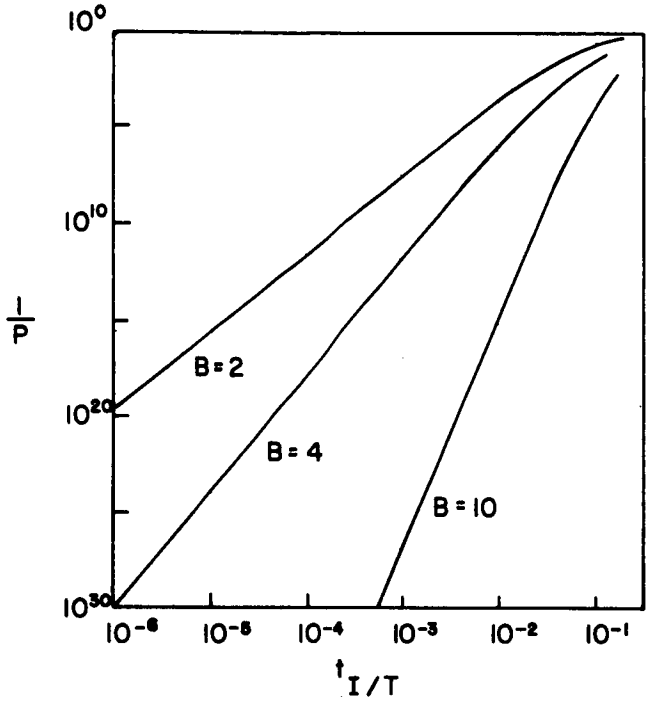

P = probability that target gets lost

T = scan period

t_I = time to process one target

B = buffer size (# of targets)

Figure IV-8. Expected Number of Targets Reviewed Before One Lost

times. On the other hand, powerful instructions make the computer itself larger, heavier, and more susceptible to failure because of increased complexity. It does seem that a satisfactory compromise can be reached by incorporating instructions such as add, subtract, multiply, divide, shift, scale, and conditional branching. These are certainly quite powerful, but do not require extreme complexity of design.

It is recommended that the arithmetic operations be performed in fixed point. Floating point instructions considerably increase basic hardware complexity, but will not provide the offsetting advantage of reduced overall computation time. This is because the major load during space missions consists of data handling, I/O, and monitoring functions. The only really mathematical problem (and therefore the only one requiring precise values having possibly large ranges) is that of navigation. Those intricate and accurate computations which require floating point (matrix inversion, e.g.) can be constructed by programming techniques which incorporate scaling instructions to great advantage. Thus, a floating point multiply could be a subroutine which the main program jumps to each time such an operation is called for. This does not excessively increase storage requirements, but may increase running time somewhat. It appears that a floating point operation on a fixed point machine takes on the order of six times as long to execute. This delay can to some extent be offset by increasing the basic speed.

Conditional branching (jump on zero, jump on negative, decrement and jump on zero, etc.) instructions are essential in complex logical processes

such as the target identification routine.

3. Word Length

The word length used is especially important since it is directly related to the size and weight of the computer and also to accuracy. If one is to resolve a second of arc relative to a full circle, between 20 and 21 bits are required. Similarly for an accuracy of 10^3 km in 10 astronomical units. During involved mathematical calculations such as occur in the solution of navigational equations, some round-off error will accumulate. An axample of this is the inversion of a matrix. Figure IV-9 and IV-10 show the effect of word length introduced by errors via the rounding operation. Two matrices whose exact inverses were known were inverted using various word lengths. One of the matrices, matrix B, was an ill-conditioned matrix; that is, its determinant is small in comparison to the value of its cofactors. This matrix is:

$$B = \begin{pmatrix} 1 & 1/2 & 1/3 & 1/4 & 1/5 & 1/6 \\ 1/2 & 1/3 & 1/4 & 1/5 & 1/6 & 1/7 \\ 1/3 & 1/4 & 1/5 & 1/6 & 1/7 & 1/8 \\ 1/4 & 1/5 & 1/6 & 1/7 & 1/8 & 1/9 \\ 1/5 & 1/6 & 1/7 & 1/8 & 1/9 & 1/10 \\ 1/6 & 1/7 & 1/8 & 1/9 & 1/10 & 1/11 \end{pmatrix}$$

and its exact inverse is

$$B^{-1} = \begin{pmatrix} 36 & -630 & 3360 & -7560 & 7560 & -2772 \\ -630 & 14700 & -88200 & 211680 & -220500 & 83160 \\ 3360 & -88200 & 564480 & -1411200 & 1512000 & -582120 \\ -7560 & 211680 & -1411200 & 3628800 & -396900 & 1552320 \\ 7560 & -220500 & 151200 & -3969000 & 4410000 & -1746360 \\ -2772 & 83160 & -582120 & 1552320 & -1746360 & 698544 \end{pmatrix}$$

The value of the determinant of B is 5.4×10^{-18} which is very small in comparison to the cofactors of matrix B. (Any element b_{ij}^{-1} in the inverse of B is the ratio of the cofactor of b_{ji} to the determinant of B.)

The other matrix, matrix A, was a well-conditioned matrix (its determenant is of the same order of magnitude as its cofactors) which is more likely to occur in the average computational process. This matrix was chosen to be:

$$A = \begin{pmatrix} 1 & 0 & 0 & 0 & 0 & 0 \\ 1 & 1 & 0 & 0 & 0 & 0 \\ 1 & 2 & 1 & 0 & 0 & 0 \\ 1 & 3 & 3 & 1 & 0 & 0 \\ 1 & 4 & 6 & 4 & 1 & 0 \\ 1 & 5 & 10 & 10 & 5 & 1 \end{pmatrix}$$

and its exact inverse is

$$A^{-1} = \begin{pmatrix} 1 & 0 & 0 & 0 & 0 & 0 \\ -1 & 1 & 0 & 0 & 0 & 0 \\ 1 & -2 & 1 & 0 & 0 & 0 \\ -1 & 3 & -3 & 1 & 0 & 0 \\ 1 & -4 & 6 & -4 & 1 & 0 \\ -1 & 5 & 10 & 10 & -5 & 1 \end{pmatrix}$$

Note that the determinant of matrix A is 1 which is of the same order of magnitude as its cofactors of 10, 5, 4, 3, 2 and 1.

Both of these matrices were inverted in a simulated satellite computer using various coefficient wordlengths of from 10 to 36 bits (a floating point computer word can be thought of as having an exponent length plus a coefficient length). By subtracting the exact inverse from the inverse obtained using a given coefficient length, a matrix called the error matrix for that coefficient length is obtained. Then by taking the root-mean-square (RMS) of all the elements in the error matrix, a measure of the error due to computer wordlength for inverting a six-by-six matrix can be obtained.

The graph of the RMS of the error matrix as a function of coefficient length for the well-conditioned matrix (matrix A) is given in Figure IV-9. Note that the graph in Figure IV-9 is roughly a straight line on semi-logarithmic graph paper which implies that the RMS error is a decreasing exponential function of the coefficient length. It can also be noted from Figure IV-9 that the RMS of the error matrix is decreased in magnitude by roughly a factor of ten for every increase of four bits in the coefficient

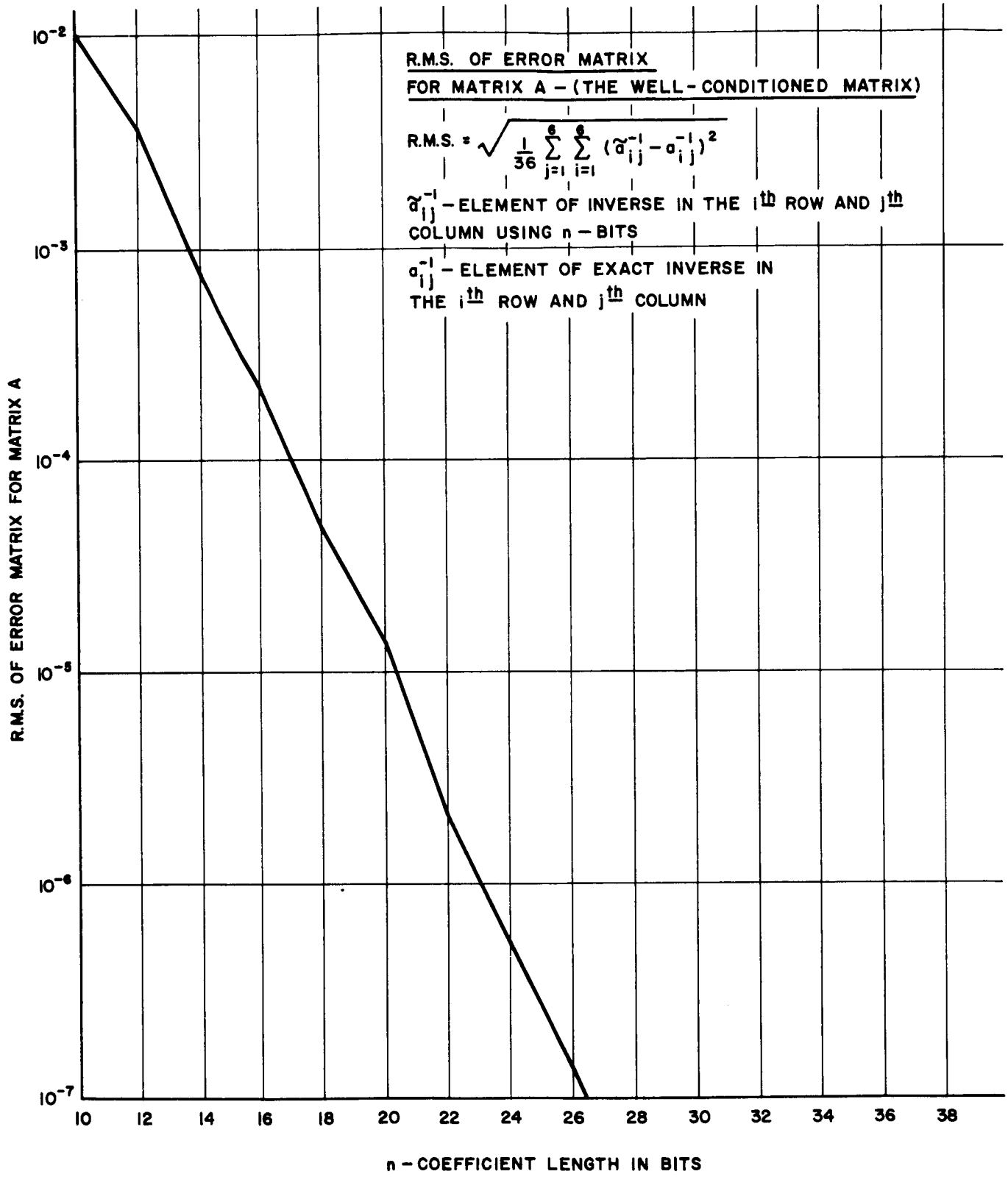

Figure IV-9. RMS of Error Matrix A

length.

The graph of the RMS of the error matrix as a function of coefficient length for an extremely ill-conditioned matrix (matrix B) is given in Figure IV-10. Note that the magnitudes of the RMS errors in Figure IV-10 are much greater (about 10^{10}) than the magnitudes of the errors in Figure IV-9. This is due mainly to the conditionality of the matrices chosen. Matrix B is an extremely ill-conditioned matrix, and it is one of the poorest matrices that would occur in a computational process. The curve in Figure IV-10 is also more erratic than the curve in Figure IV-9, but this again is due to the conditionality of matrix B.

Two general comments are immediately evident: (a) the errors introduced into the inverse by the finite wordlength are rather smooth functions of the wordlength itself. There is no "threshold" below which the inverse become completely meaningless and above which the errors are negligible. (b) For the ill-conditioned example, it appears that reducing the word-length below 18 bits does not cause a further increase in the error. The reason for this is that the errors had by that time completely dominated the value of the inverse. That is, the computed inverse was entirely meaningless and was representative only of the "noise" in the computation process itself.

The choice of wordlength, then, for a process such as this depends heavily upon the conditionality of the problem. It is probably safe to assume, however, that the navigation matrices encountered (especially those arising from least square equations) are well-conditioned. Hence an

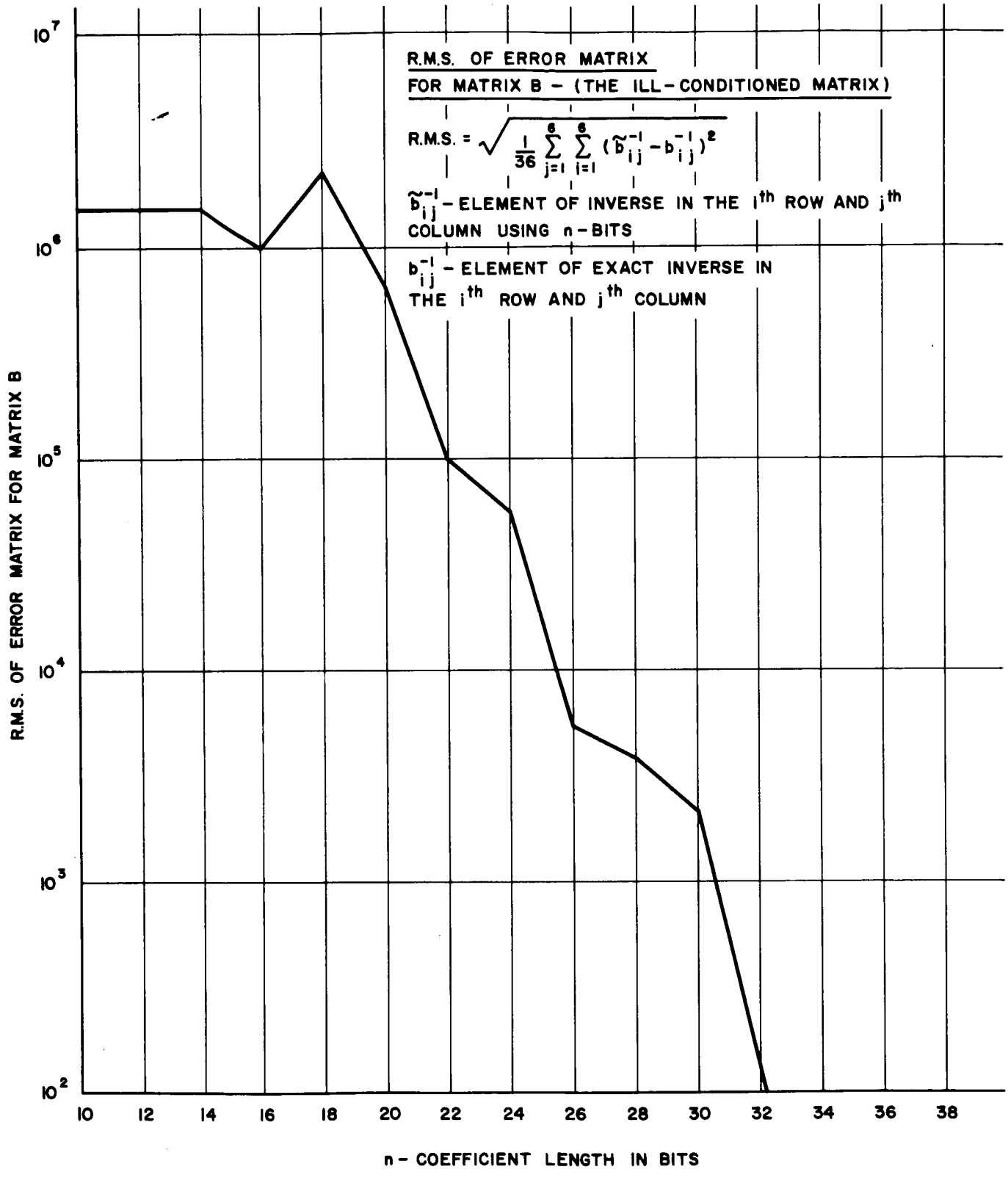

Figure IV-10. RMS of Error Matrix B

addition of, say, four bits to the basic 20 or 21 bits already present will keep round-off contributions a factor of 10 to 100 below the measurement errors. Thus a fixed point computer would probably have at least a 24 bit wordlength. If floating point instructions exist, another six bits for the exponent will permit the handling of numbers as small as 10^{-32} or as large as 10^{+32}.

As mentioned above, however, most tasks will be of the "housekeeping" type which require short instructions and handle only a few bits each time. Thus, not so much accuracy as speed and memory are the overall goals. Speed will depend mainly on the hardware while memory can be considerably reduced by incorporating two of the short instructions (say 12 bits a piece) in one word (24 bits). Or, one could have as a basis the 12-bit word, using double precision for those operations requiring higher accuracy. This would increase the memory requirements for these latter operations, but may result in a reduction of the total storage.

4. Speed

While it is not possible to firmly establish a computer speed without a more detailed study, it is felt that a moderately high speed addition (3 to 5 microseconds) is required, not so much because of high solution rates, but chiefly because of the enormous amount of data processing required. Again it is pointed out that the major portion of the computer time will not be spent in performing arithmetic computations but rather in data processing, searching, and testing.

To speed up such sub-routines as function evaluation or matrix inver-

sion, a high speed multiply (30 to 50 microseconds) would be very desirable.

5. Memory Requirements

We have seen that some 5400 locations (instructions) would be occupied by the programs required for the processing of the scanning camera data. This is probably of the same order of magnitude as is presently planned for random access storage in a space computer. Furthermore, the navigation task is not the only one in which a space computer would engage. Trajectory extrapolation, processing scientific measurements, coding for telemetry, monitoring and controlling the vehicle's functions, and many other applications would find a digital computer useful. The question immediately rises as to where the programs for each of these tasks is to be stored and in what manner.

We can distinguish three types of memory based largely on the applications in which they are used:*

a) memory units immediately accessible to the logic section for high-speed operations,

b) sufficient permanent memory for all of the programs likely to be executed during the mission, and

c) storage for large masses of data acquired during the mission.

These may physically be the same memory, but because of considerations of

---

* Aronson, Milton H., (editor), Data Storage Handbook, Instruments Publishing Co., Inc., (1962).

size, weight, power, cost and reliability they are, in general, different. At present, the types of memory shown in Figure IV-11 meet all of these requirements fairly well.

Both the core and diode matrix type of memories fulfill condition (a) while still being relatively cheap and quite reliable. However, they serve different purposes. Both are random access, that is, any particular entry can be chosen without sequencing through the previous entries. But the diode matrix is a permanent type* while the core memory can be changed at the will of the programs being executed by the computer.

The core memory is used mostly for the current program being executed and for the scratch pad (temporary results). The diode matrix section, being permanent, is used to store the basic subroutines (such as sine-cosine, arctangent, square root, etc.) which are most often used. This permits extremely high speed execution of these subroutines and helps immeasureably in increasing the speeds of the sophisticated calculations involved in orbit determination and trajectory generation. Since the diode matrix is also random access, it can contain the control error detection and error correction programs thus providing immediate access to these programs in an emergency.

The cost of incorporating all of the programs likely to be needed during a space mission in core or diode matrix memories would in some cases be prohibitive. For the more complex missions, it seems far more reasonable

---

* Those unwanted diodes in a particular matrix are merely burned out thereby creating the desired program.

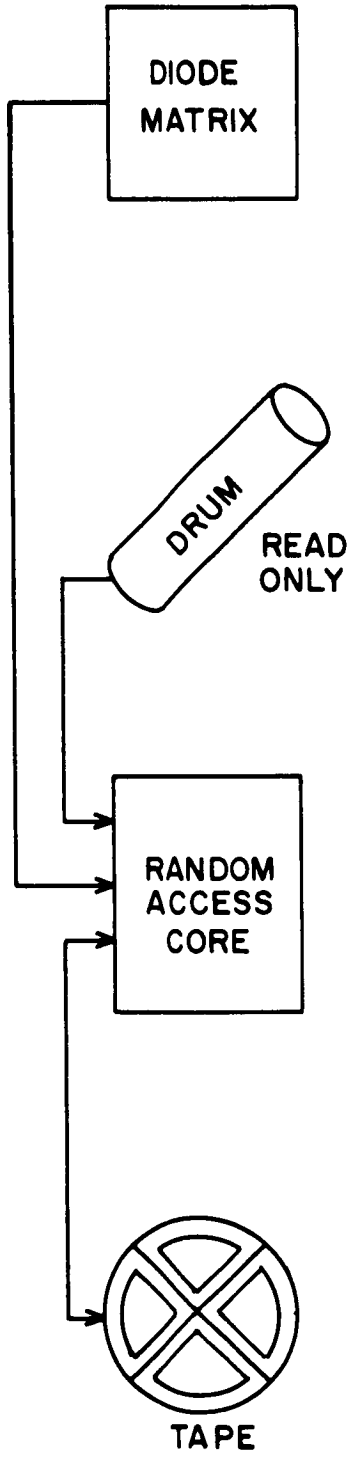

- MONITOR & CONTROL
- I/O PROGRAMS
- ERROR DETECT
- SUB ROUTINES

- STANDARD PROGRAMS
  - SENSOR SCAN
  - NAVIGATION
  - GUIDANCE
  - DATA PROCESS
- MAP OF DIODE STORAGE

- CURRENT PROGRAM
- SCRATCH PAD
- TEMPORARY DATA STORAGE

- BULK DATA STORAGE
- PRE- & POST- TELEMETRY STORAGE

Figure IV-11. Memory Units

to have the needed programs available in a cheaper form of memory and then to transfer each one as needed to the random-access core for execution. Such a memory unit would be the magnetic drum. It is a non-destructive read-out device which could be a read-only memory thereby prohibiting a program malfunction from erasing parts of vital routines. All programs, including those already in the diode matrix (for reliability purposes), would be inscribed on the drum prior to launch and read from the drum into the core as required to complete the mission functions.

A magnetic tape unit* can be used for the storage of bulk data such a television pictures and information transmitted via telemetry from the earth. For instance, data from a TV surveillance of a planet could be transcribed directly onto the tape and then at the computer's leisure processed prior to telemetry back to the earth. Similarly, messages received from the earth would have to be decoded after being put onto tape, in order to determine what instructions have been sent.

It will be noted that no mention has been made either of thin film memories or of the use of tunnel diodes for memories. The reason in the first case is the need for excessively high drive currents to switch the film spots. If this can be alleviated in the future (and it undoubtedly will be) then the size and time saving which will result will be significant, and thin films will become quite attractive. The tunnel diodes, used in a volatile memory, will, of course, not retain their bit

---

* "Magnetic Tapes", Space/Aeronautics, 37, January 1962, pp. 64-72.

if the power fails. Moreover, consistent fabrication has been a problem which makes it difficult to design circuits for these devices. Hence, the tunnel diode is at present unacceptable, but could in the future offer substantial savings in volume and in logic speed.

On a space mission, a control program in the computer will at all times have cognizance of the execution of the various subprograms (such as navigation, trajectory generation, error correction, etc) and will determine in which sequence and to what extent they shall operate. This is done, of course, mainly to detect errors so that they may be dealt with (corrected, programmed around, or forgotten) as swiftly as possible. An error, once detected will put in operation an error correction routine which will then attempt to rectify the fault. The subprograms in their turn govern the operation of the various sub-routines (sine-cosine, square root, etc.) and input-output equipment so that the details of the mission may be carried out along the lines laid down by the control program.

The memory allocation for the control program in the computer is obviously of prime importance. It is absolutely necessary that this part of the program never fail, because in its failure it will be unable to control the remaining program and in fact unable to reprogram itself. Possible storage in three mediums is desired: diode matrix, random access core, and the drum. The core used for this program might be multiple aperture. This would allow for a slight reprogramming bit by bit upon command from the control panel even though such requires rather high currents. The diode matrix section must be extremely reliable

for this part of the program ensuring failure rates of less than 10^{-10} for the entire mission. For error checking, the control program on the drum can be used as a match against the program in the diode matrix or in the multiple aperture core. To check whether these agree with each other, any error detecting and reprogramming sections would also have to be included in the memory in a similar type of hardware configuration.

The general operation of this memory groups is as follows: the control program (stored in the diode matrix for reasons of swift execution and immediate accessibility) commands subprograms to be read from the drum (which contains all programs) into a small but adequate random-access core memory. From here the subprogram can be executed swiftly using the subroutine in the diode store. Any errors bring about an immediate jump into the error detection and correction routine (part of the control program also in the diode store). If the program is in error, it will be read in again or other actions may be taken. (Just which depends upon the sophistication of this routine and the available technology.)

V. CONCLUSIONS AND RECOMMENDATIONS

In general it is felt that the studies presented in this final report show the feasibility of implementing the scanning camera concept for interplanetary, satellite, and surface navigation, attitude sensing, and multibody monitoring. The errors in the system are theoretically small (position accuracies of the order of 8000 kilometers in interplanetary space, and attitude determination accuracies of the order of ten seconds of arc), the mechanical and electronic design do not represent a significant advance in the state-of-the-art, and the on-board computer requirements are modest (about 5000 instructions including star and planet tables, and of the order of five seconds of time are needed to process the scanning camera data).

Specifically, it appears that an f/1.0 Schmidt corrected optical system of the Baker-Nunn type, with a 4 inch aperture, 30^{o} FOV, and 20 second of arc blur circle forms the basic instrument. Accurately positioned (within $.05 \times 10^{-3}$ inches) slits in the focal surface define the navigational capability while one or more miniature low noise photomultipliers serve as detectors. The entire instrument is scanned so that the optical axis traces a great circle arc on the celestial sphere in a period of one to ten seconds. Star and planet transit times (across the slits) and magnitudes are recorded and processed by the on-board digital computer. Target recognition is accomplished through a nearly foolproof magnitude, angular separation scheme which checks itself at many points. The navigation equations permit the computation of the motion of a nearly symmetric rigid body (the camera itself or a spinning vehicle to which the camera is

held fast) and the determination of position in a least squares sense from an overdetermination in the measurement set.

Several possibilities exist for further efforts related to the scanning camera concept. These are:

1. The construction and testing in the laboratory of an experimental model and its further evaluation by night-time scanning or by inclusion into a sounding rocket or Earth satellite,
2. A more extensive analysis of the sources and propagation of errors in the navigation system,
3. The introduction of more sophistication into the target identification routine,
4. Study of various slit designs and optical techniques to achieve optimum use of incoming photons,
5. Extension of scanning camera applications to: panoramic optical systems, navigation through the asteroid belts, attitude control and guidance implications, surface navigation, and
6. Development of the characteristics and logical design of a computer for the processing of camera data.

It is definitely felt that the system has great advantages in many respects over other celestial sensors and will certainly form, in some manner, an integral part of future navigation systems.

APPENDIXES

A. Torque-Free Motion of a Nearly Symmetric Body

B. Explicit Functions for Computation of Attitude

C. Explicit Functions for Computation of Position

D. Target Identification Program - BAKER

E. Camera-Computer Simulation Program - ABLE

F. Interrupt Program for Data Input

G. Analysis of a Torque-Free Body Containing a Swiftly Rotating Wheel

APPENDIX A

TORQUE-FREE MOTION OF A NEARLY SYMMETRIC BODY

The general problem of describing the orientation as a function of time of a torque-free rigid body with one point fixed is a classical problem of analytical dynamics. The solution may be written in terms of elliptic functions, and hence may be considered solved. However, the general solution is inconvenient for numerical computations and physical interpretation.

If the body has two equal moments of inertia the modulus of the elliptic functions, k, becomes zero and hence these functions degenerate into circular functions. If two moments are nearly equal, k is generally small in comparison to unity; and thus the elliptic functions may be written as a series of circular functions. (Reference 2) Our purpose here is to develop such a series. We will rely on the general solution as presented by Whittaker (Reference 1, pages 144-152) and will retain his notation.

The orientation of the principle axes of the body with respect to a preferred inertial system can be specified by the three Euler angles θ, ϕ, ψ. Utilizing Whittaker's results we may write

$$\cos\theta = \frac{(\sinh\gamma - q^2 \sinh 3\gamma + q^6 \sinh 5\gamma + \ldots)}{(\cosh\gamma + q^2 \cosh 3\gamma + q^6 \cosh 5\gamma + \ldots)}$$

$$\times \frac{(1 + 2q\cos 2\mu t + 2q^4 \cos 4\mu t + \ldots)}{(1 - 2q\cos 2\mu t + 2q^4 \cos 4\mu t + \ldots)}$$

$$\tan \psi = \frac{(1 + 2q \cosh 2\gamma + 2q^4 \cosh 4\gamma + \ldots)}{(1 - 2q \cosh 2\gamma + 2q^4 \cosh 4\gamma + \ldots)}$$

$$\times \frac{(\sin \mu t - q^2 \sin 3\mu t + q^6 \sin 5\mu t \ldots\ldots)}{(\cos \mu t + q^2 \cos 3\mu t + q^6 \cos 5\mu t \ldots\ldots)}$$

$$\phi = \phi_o + \left(\frac{d}{A} + 4\mu \frac{q \sinh 2\gamma - 2q^4 \sinh 4\gamma + \ldots}{1 - 2q \cosh 2\gamma + 2q^4 \cosh 4\gamma - \ldots} \right) \cdot t$$

$$- \tan^{-1} \left(\frac{2q \sin 2\mu t \sinh 2\gamma - 2q^4 \sin 4\mu t \sinh 4\gamma + \ldots}{1 - 2q \cos 2\mu t \cosh 2\gamma + 2q^4 \cos 4\mu t \cosh 4\gamma + \ldots} \right) \quad (1)$$

where either $A \geq B > C$, $Bc - d^2 > 0$ or $A \leq B < C$, $Bc - d^2 < 0$ and q is the parameter of the theta-functions (related to the original elliptic functions) and is small if the modulus k is small.

In order that approximations can be made in (1), we must attribute an order of smallness to the various terms. Let the three moments of inertia be given by

$$A = I_1 (1 - \epsilon)$$
$$B = I_1 (1 + \epsilon)$$
$$C = I_3 \qquad , A \geq B > C \text{ or } A \leq B < C \quad (2)$$

where $-1 \ll \epsilon \ll 1$, $\epsilon \geq 0$ if $I_3 > B$, $\epsilon \leq 0$ if $I_3 < B$. From page 146 of Reference [1],

$$k^2 = - \frac{2\epsilon (r + s)}{(1 - r\epsilon)(1 - s\epsilon)} \quad (3)$$

where

$$r = \frac{I_1}{I_3 - I_1}$$

$$s = \frac{I_1 c}{I_1 c - d'^2} \quad , \quad \frac{1}{s} + \epsilon > 0 \quad \text{if } \epsilon < 0$$

$$\frac{1}{s} + \epsilon < 0 \quad \text{if } \epsilon > 0 \quad .$$

In order to make further approximations in Equation (3) we must be assured that $r\epsilon$ and $s\epsilon$ are both between -1 and 1.

This smallness can be expressed as

$$\epsilon r = 0(n)$$

$$\epsilon s = 0(n)$$

where terms of order n are between -1 and 1. Approximations may now be made in Equation (3) with the result that

$$k^2 = -2\epsilon(r + s)(1 + \epsilon(r + s) + \epsilon^2(r^2 + s^2 + rs)) + 0(n^4) \quad . \qquad (4)$$

From page 147 of Reference [1] we have

$$q = \frac{k^2}{16} + \frac{k^4}{32} + \frac{21\ k^6}{1024} + 0(k^8) \quad .$$

So,

$$q = -\frac{\epsilon}{8}(r + s)\left[1 + \frac{\epsilon^2}{16}(7r^2 + 7s^2 - 2rs)\right] + 0(n^4) \quad . \qquad (5)$$

Now the parameter γ must be determined. Again Reference [1] gives the result

$$\frac{1 + 2q \cosh 2\gamma + 2q^4 \cosh 4\gamma + \ldots}{1 - 2q \cosh 2\gamma + 2q^4 \cosh 4\gamma - \ldots} = \left(\frac{B^2}{A^2} \cdot \frac{d^2 - cA}{d^2 - cB} \cdot \frac{A - C}{B - C}\right)^{\frac{1}{4}}$$

$$= \left[\left(\frac{1 + \epsilon}{1 - \epsilon}\right)^2 \cdot \frac{1 - \epsilon s}{1 + \epsilon s} \cdot \frac{1 + \epsilon r}{1 - \epsilon r}\right]^{\frac{1}{4}}$$

$$= 1 + \frac{\epsilon}{2}(r - s + 2) + \frac{\epsilon^2}{8}(r - s + 2)^2 + O(n^3) .$$

Hence $2q \cosh 2\gamma = O(n)$, and

$$q \cosh 2\gamma = \frac{\epsilon}{8}(r - s + 2) + O(n^3) . \tag{6}$$

Since $q \cosh 2\gamma = O(n)$, approximations can now be made in Equation (1) with the result

$$\cos \theta = \tanh \gamma[1 + 4q \cos 2\mu t + 4q^2(2 \cos^2 2\mu t - \cosh 2\gamma) - 4q^3 \cos 2\mu t \cosh 3\gamma] + O(n^4) \tag{7}$$

$$\tan \psi = \tan \mu t[1 + \frac{\epsilon}{2}(r - s + 2) + \frac{\epsilon^2}{8}((r - s + 2)^2 - \tfrac{1}{2}(r + s)^2) + O(n^3)] \tag{8}$$

$$\phi = \phi_o \left[\frac{d}{A} + 4\mu q \sinh 2\gamma(1 + 2q \cosh 2\gamma + 4q^2 \cosh^2 2\gamma) + o(n^4) \right] t$$

$$- 2q \sin 2\mu t \sinh 2\gamma(1 + 2q \cosh 2\gamma \cos 2\mu t$$

$$+ 4q^2 \cosh^2 2\gamma \cos^2 2\mu t + \frac{4q^3}{3} \sinh 2\gamma \sin 2\mu t) + 0(n^5) \quad . \quad (9)$$

In Equation (8) we may take the arctangent of each side, and in Equation (7) we may set

$$\tanh \gamma \equiv \cos \theta_o$$

and then take the arc cosine of each side. Hence,

$$\theta = \theta_o - 4q \cot \theta_o [\cos 2\mu t + q(2 \csc^2 \theta_o \cos^2 2\mu t - \cosh 2\gamma)]$$

$$+ 0(n^3) \qquad (10)$$

$$\psi = \mu t + \frac{\epsilon \sin 2\mu t}{4} \left[(r - s + 2) + \frac{\epsilon}{4} ((r - s + 2)^2 \cos 2\mu t \right.$$

$$\left. - \frac{(r + s)^2}{2}) \right] + 0(n^3) \quad . \qquad (11)$$

Now, Equations (9), (10), and (11) are not useful as given since they involve the dependent parameters, θ_o, r, and s. We choose to eliminate s from the system in favor of the more physically meaningful parameters r and θ_o. From Equations (5) and (6),

$$s = \frac{2 + r(1 + \cosh 2\gamma)}{1 - \cosh 2\gamma} + \frac{0(n^3)}{\epsilon} .$$

But,

$$\cosh 2\gamma \equiv \frac{1 + \tanh^2 \gamma}{1 - \tanh^2 \gamma} \equiv \frac{1 + \cos^2 \theta_o}{\sin^2 \theta_o} .$$

Thus,

$$s = - \frac{\sin^2 \theta_o + r}{\cos^2 \theta_o} + \frac{0(n^3)}{\epsilon} ,$$

$$q = \frac{\epsilon}{8} \tan^2 \theta_o (1 + r) + 0(n^3).$$

Hence, (9), (10), and (11) become

$$\theta = \theta_o - \frac{\epsilon}{2} \tan \theta_o (1 + r)[\cos 2\mu t + \frac{\epsilon}{8} \sec^2 \theta_o (1 + r)(\cos 4\mu t - \cos^2 \theta_o)] + 0(n^3) \qquad (12)$$

$$\psi = \mu t + \frac{\epsilon(1 + r)(1 + \cos^2 \theta_o) \sin 2\mu t}{4 \cos^2 \theta_o} \left[1 + \frac{\epsilon(1 + r)(1 + \cos^2 \theta_o)}{8 \cos^2 \theta_o} \times \left(2 \cos 2 \mu t - \left(\frac{\sin \theta_o}{1 + \cos^2 \theta_o} \right)^2 \right) \right] + 0(n^3) \qquad (13)$$

$$\phi = \phi_o + \left[\frac{d}{A} + \frac{\mu\epsilon(1 + r)}{\cos \theta_o} \left(1 + \frac{\epsilon}{4} \frac{(1 + \cos^2 \theta_o)(1 + r)}{\cos^2 \theta_o}\right) + O(n^3)\right] t - \frac{\epsilon(1 + r)}{2 \cos \theta_o} \sin 2\mu t \left(1 + \frac{\epsilon}{4} \frac{(1 + \cos^2 \theta_o)(1 + r)}{\cos^2 \theta_o} \cos 2\mu t\right) + O(n^3) \quad (14)$$

where

$$1 + r = \frac{I_3}{I_3 - I_1}$$

$$\epsilon \leq 0 \quad \text{if } I_3 > I_1$$

$$\epsilon \geq 0 \quad \text{if } I_3 < I_1$$

$$\theta_o \neq \frac{\pi}{2} .$$

The only problem now remaining is to find the angular rate μ in terms of α, θ_o, and r. Again from Whittaker,

$$\mu^2 = \frac{(B - C)(Ac - d^2)}{ABC(1 + 2q + O(q^4))} = \frac{d^2(1 - \epsilon r)(1 - \epsilon s) \cos^2 \theta_o}{I_1^2(1 + r)^2(1 - \epsilon^2)(1 + 2q + O(q^4))} .$$

So,

$$\mu = - \frac{d}{(r + 1) I_1} \cos \theta_o \left(1 + \frac{3\epsilon}{4} \tan^2 \theta_o (1 + r)\right) + O(n^2) . \quad (15)$$

Hence, the coefficient of t in Equation (14) becomes

$$\frac{d}{I_1}\left[1 + \epsilon^2\left(1 - \frac{(1 + \cos^2\theta_o)(1 + r)}{4\cos^2\theta_o}\right)\right] + O(n^3) \quad .$$

References

[1] Whittaker, E. T., Analytical Dynamics of Particles and Rigid Bodies, Cambridge University Press, 1959, pp. 144-152.

[2] Bateman, H., Higher Transcendental Functions, Volume II, McGraw-Hill, New York, 1953, p. 345.

APPENDIX B

EXPLICIT FUNCTIONS FOR COMPUTATION OF ATTITUDE

The instantaneous attitude of the scanning camera, as described in Section III-A of the body of this final report, is specified by the direction of the angular momentum vector given by the (constant) angles τ and ξ and by the three Euler angles θ, ψ, ϕ relative to this direction. (See especially Figure III-1 for an explanation of the angles.) We assume the motion to be no worse than uniform spin about the axis of symmetry of the camera capsule (instrument axis) coupled with uniform precession of this axis about the angular momentum direction. Thus θ = constant, $\psi = \mu t + \psi_o$, and $\phi = \Omega t + \phi_o$ where μ, ψ_o, Ω, and ϕ_o are constants with a final relation $\Omega = K\mu$ where K is a further (known) constant dependent upon the moments of inertial of the spinning body. Thus there are six unknowns to be computed by an iterative technique as discussed in Section III-A2. Here we merely give the explicit forms of the functions and derivatives appearing in that section which are relavant to the attitude determination.

Time will be denoted by t and a subscript k will be used to specify the k^{th} target whose celestial position is given by α_k, δ_h, right ascension and declination. Subscripts on ψ and ϕ will mean that their t is to be subscripted. The basic function f_k and its derivatives follow.

$$f_k = \cos(\alpha_k - \xi)\left[-\sin\psi_k \cos\phi_k - \cos\theta \sin\phi_k \cos\psi_k\right]$$

$$+ \cos\tau \sin(\alpha_k - \xi)\left[-\sin\psi_k \sin\phi_k + \cos\theta \cos\phi_k \cos\psi_k\right]$$

$$- \sin\tau \cos\psi_k \sin\theta \sin(\alpha_k - \xi) - \tan\Gamma\left\{\cos(\alpha_k - \xi) \sin\theta \sin\phi_k\right.$$

$$\left. - \sin(\alpha_k - \xi) \cos\tau \sin\theta \cos\phi_k - \sin\tau \cos\theta \sin(\alpha_k - \xi)\right\}$$

$$+ \tan\delta_k\left\{\sin\tau\left[-\sin\psi_k \sin\phi_k + \cos\theta \cos\phi_k \cos\psi_k\right]\right.$$

$$+ \cos\tau \cos\psi_k \sin\theta - \tan\Gamma\left[-\sin\tau \sin\theta \cos\phi_k\right.$$

$$\left.\left. + \cos\tau \cos\theta\right]\right\}$$

$$\frac{\partial f_k}{\partial\theta} = \cos(\alpha_k - \xi) \sin\theta \sin\phi_k \cos\psi_k - \cos\tau \sin(\alpha_k - \xi) \sin\theta \cos\phi_k \cos\psi_k$$

$$- \sin\tau \cos\psi_k \cos\theta \sin(\alpha_k - \xi) - \tan\Gamma\left\{\cos(\alpha_k - \xi) \cos\theta \sin\phi_k\right.$$

$$\left. - \sin(\alpha_k - \xi) \cos\tau \cos\theta \cos\phi_k + \sin\tau \sin\theta \sin(\alpha_k - \xi)\right\}$$

$$+ \tan\delta_k\left\{-\sin\tau \sin\theta \cos\phi_k \cos\psi_k + \cos\tau \cos\psi_k \cos\theta\right.$$

$$\left. - \tan\Gamma\left[-\sin\tau \cos\theta \cos\phi_k - \cos\tau \sin\theta\right]\right\}$$

$$\frac{\partial f_k}{\partial \tau} = - \sin\tau \sin(\alpha_k - \xi) \left[- \sin\psi_k \sin\phi_k + \cos\theta \cos\phi_k \cos\psi_k \right]$$

$$- \cos\tau \cos\psi_k \sin\theta \sin(\alpha_k - \xi)$$

$$- \tan\Gamma \left\{ \sin(\alpha_k - \xi) \sin\tau \sin\theta \cos\phi_k - \sin\tau \cos\theta \sin(\alpha_k - \xi) \right\}$$

$$+ \tan\delta_k \left\{ \cos\tau \left[- \sin\psi_k \sin\phi_k + \cos\theta \cos\phi_k \cos\psi_k \right] \right.$$

$$\left. - \sin\tau \cos\psi_k \sin\theta - \tan\Gamma \left[- \cos\tau \sin\theta \cos\phi_k - \sin\tau \cos\theta \right] \right\}$$

$$\frac{\partial f_k}{\partial \xi} = + \sin(\alpha_k - \xi) \left[- \sin\psi_k \cos\phi_k - \cos\theta \sin\phi_k \cos\psi_k \right]$$

$$- \cos\tau \cos(\alpha_k - \xi) \left[- \sin\psi_k \sin\phi_k + \cos\theta \cos\phi_k \cos\psi_k \right]$$

$$+ \sin\tau \cos\psi_k \sin\theta \cos(\alpha_k - \xi)$$

$$- \tan\Gamma \left\{ \cos(\alpha_k - \xi) \cos\tau \sin\theta \cos\phi_k \right.$$

$$\left. + \sin(\alpha_k - \xi) \sin\theta \sin\phi_k + \sin\tau \cos\theta \cos(\alpha_k - \xi) \right\}$$

$$\frac{\partial f_k}{\partial \mu} = \frac{\partial f_k}{\partial \psi_k} \cdot t_k + \frac{\partial f_k}{\partial \phi_o} \cdot K\, t_k$$

$$\frac{\partial f_k}{\partial \psi_o} = \frac{\partial f_k}{\partial \psi_k}$$

$$\begin{aligned}\frac{\partial f_k}{\partial \psi_k} &= \cos(\alpha_k - \xi)\left[-\cos\psi_k \cos\phi_k + \cos\theta \sin\phi_k \sin\psi_k\right] \\ &+ \cos\tau \sin(\alpha_k - \xi)\left[-\cos\psi_k \sin\phi_k - \cos\theta \cos\phi_k \sin\psi_k\right] \\ &+ \sin\tau \sin\psi_k \sin\theta \sin(\alpha_k - \xi) \\ &+ \tan\delta_k \left\{\sin\tau\left[-\cos\psi_k \sin\phi_k - \cos\theta \cos\phi_k \sin\psi_k\right]\right. \\ &\left. - \cos\tau \sin\psi_k \sin\theta\right\}\end{aligned}$$

$$\frac{\partial f_k}{\partial \phi_o} = \cos(\alpha_k - \xi)\left[\sin\psi_k \sin\phi_k - \cos\theta \cos\phi_k \cos\psi_k\right]$$

$$+ \cos\tau \sin(\alpha_k - \xi)\left[-\sin\psi_k \cos\phi_k - \cos\theta \sin\phi_k \cos\psi_k\right]$$

$$- \tan\Gamma \left\{\cos(\alpha_k - \xi) \sin\theta \cos\phi_k\right.$$

$$\left. + \sin(\alpha_k - \xi) \cos\tau \sin\theta \sin\phi_k \right\}$$

$$+ \tan\delta_k \left\{\sin\tau \left[-\sin\psi_k \cos\phi_k - \cos\theta \sin\phi_k \cos\psi_k\right]\right.$$

$$\left. - \tan\Gamma \sin\tau \sin\theta \sin\phi_k \right\}$$

$$\frac{\partial f_k}{\partial t_k} = \mu \frac{\partial f_k}{\partial \psi_k} + \Omega \frac{\partial f_k}{\partial \phi_o}$$

APPENDIX C

EXPLICIT FUNCTIONS FOR COMPUTATION OF POSITION

The interplanetary position of the scanning camera, as described in Section III-A of the body of this final report, is specified by r_x, r_y, and r_z--three components of the position vector relative to the ecliptic coordinate system with the sun as center. We give here the explicit forms of the functions and derivatives used in Section III-A2 for the computation of these position components. For the definition of most quantities, see Section III and Appendix B. The only remaining notations needing explanation are $p_x^{(k)}$, $p_y^{(k)}$, and $p_z^{(k)}$ which are the three position components of the k^{th} planet. There are only three unknowns in this problem since attitude is assumed known and the transit time t_k is measured.

The method of solution is given in Section III-A2 and the functions and derivative used there are as follows.

$$a_k = \tan\Gamma \left\{\cos\xi \sin\theta \sin\phi_k + \sin\theta \cos\phi_k \cos\tau \sin\xi \right.$$

$$\left. + \sin\tau \sin\xi \cos\theta\right\} - \cos\xi \left[- \sin\psi_k \cos\phi_k - \cos\theta \sin\phi_k \cos\psi_k \right]$$

$$+ \cos\tau \sin\xi \left[- \sin\psi_k \sin\phi_k + \cos\theta \cos\phi_k \cos\psi_k \right]$$

$$- \sin\tau \sin\xi \cos\psi_k \sin\theta$$

$$b_k = - y_1 \cos\epsilon - y_2 \sin\epsilon$$

$$c_k = y_1 \sin\epsilon - y_2 \cos\epsilon$$

$$y_1 = \sin\xi \left[- \sin\psi_k \cos\phi_k - \cos\theta \sin\phi_k \cos\psi_k \right]$$

$$+ \cos\tau \cos\xi \left[- \sin\psi_k \sin\phi_k + \cos\theta \cos\phi_k \cos\psi_k \right]$$

$$- \sin\tau \cos\xi \cos\psi_k \sin\theta - \tan\Gamma \left[\sin\xi \sin\theta \sin\phi_k \right.$$

$$\left. - \cos\tau \cos\xi \sin\theta \cos\phi_k - \sin\tau \cos\xi \cos\theta \right]$$

$$y_2 = \sin\tau \left[- \sin\psi_k \sin\phi_k + \cos\theta \cos\phi_k \cos\psi_k \right] + \cos\tau \cos\psi_k \sin\theta$$

$$- \tan\Gamma \left[- \sin\tau \sin\theta \cos\phi_k + \cos\tau \cos\theta \right]$$

$$d_k = - p_x^{(k)} a_k - p_y^{(k)} b_k - p_z^{(k)} c_k$$

$$\frac{\partial f_k}{\partial t_k} = r_x \frac{\partial a_k}{\partial t_k} + r_y \frac{\partial b_k}{\partial t_k} + r_z \frac{\partial c_k}{\partial t_k} + \frac{\partial d_k}{\partial t_k}$$

$$\frac{\partial d_k}{\partial t_k} = - p_x \frac{\partial a_k}{\partial t_k} - p_y \frac{\partial b_k}{\partial t_k} - p_z \frac{\partial c_k}{\partial t_k}$$

$$\begin{aligned}\frac{\partial a_k}{\partial t_k} = \Omega \Big\{ & \tan \Gamma \Big[\cos \xi \sin \theta \cos \phi_k - \sin \theta \sin \phi_k \cos \tau \sin \xi \Big] \\ & - \cos \xi \Big[\sin \psi_k \sin \phi_k - \cos \theta \cos \phi_k \cos \psi_k \Big] \\ & + \cos \tau \sin \xi \Big[- \sin \psi_k \cos \phi_k - \cos \theta \sin \phi_k \cos \psi_k \Big] \Big\} \\ & + \mu \Big\{ - \cos \xi \Big[- \cos \psi_k \cos \phi_k + \cos \theta \sin \phi_k \sin \psi_k \Big] \\ & + \cos \tau \sin \xi \Big[- \cos \psi_k \sin \phi_k - \cos \theta \cos \phi_k \sin \psi_k \Big] \\ & + \sin \tau \sin \xi \sin \psi_k \sin \theta \Big\}\end{aligned}$$

$$\frac{\partial b_k}{\partial t_k} = - \frac{\partial y_1}{\partial t_k} \cos \epsilon - \frac{\partial y_2}{\partial t_k} \sin \epsilon$$

$$\frac{\partial c_k}{\partial t_k} = \frac{\partial y_1}{\partial t_k} \sin \epsilon - \frac{\partial y_2}{\partial t_k} \cos \epsilon$$

$$\frac{\partial y_1}{\partial t_k} = \Omega \Big\{ \sin \xi \Big[\sin \psi_k \sin \phi_k - \cos \theta \cos \phi_k \cos \psi_k \Big]$$

$$+ \cos \tau \cos \xi \Big[- \sin \psi_k \cos \phi_k - \cos \theta \sin \phi_k \cos \psi_k \Big]$$

$$- \tan \Gamma \Big[\sin \xi \sin \theta \cos \phi_k + \cos \tau \cos \xi \sin \theta \sin \phi_k \Big] \Big\}$$

$$+ \mu \Big\{ \sin \xi \Big[- \cos \psi_k \cos \phi_k + \cos \theta \sin \phi_k \sin \psi_k \Big]$$

$$+ \cos \tau \cos \xi \Big[- \cos \psi_k \sin \phi_k - \cos \theta \cos \phi_k \sin \psi_k \Big]$$

$$+ \sin \tau \cos \xi \sin \psi_k \sin \theta \Big\}$$

$$\frac{\partial y_2}{\partial t_k} = \Omega \Big\{ \sin \tau \Big[- \sin \psi_k \cos \phi_k - \cos \theta \sin \phi_k \cos \psi_k \Big]$$

$$- \tan \Gamma \Big[\sin \tau \sin \theta \sin \phi_k \Big] \Big\}$$

$$+ \mu \Big\{ \sin \tau \Big[- \cos \psi_k \sin \phi_k - \cos \theta \cos \phi_k \sin \psi_k \Big]$$

$$- \cos \tau \sin \psi_k \sin \theta \Big\}$$

APPENDIX D

TARGET IDENTIFICATION PROGRAM - BAKER

BAKER simulates the computer program which collects camera data from star-like objects as they pass through the field of view, stores their transit times and magnitudes, and finally after having collected this data, attempts to identify three of the targets. The transit time calculations are done in the same fashion as is done in ABLE (see Appendix E). Only minor changes are apparent and will be pointed out. The identification process itself is contained in a subroutine (CHARLIE) and will be explained to some extent here. Many details are left out for clearness, but can be found by anyone familiar with FORTRAN programming by checking the program listing contained at the end of this appendix.

A. Main Program Description

A general understanding can be obtained by following the schematic diagram of Figure 1 along with this explanation. All initial data and tables are read in and stored. Star right ascension and declination are read in along with the orbital radius, longitudinal position, and phase data of the six innermost planets. Planet positions are converted to right ascension and declination; magnitudes are found and the planet is made to appear as a star to the camera.

A target list is formed by arranging the star-like objects in order according to brightness from brightest to dimmest. This list is scanned for those targets that fall within the camera field of view. Those that do are stored in two lists (one for each slit) along with a computed

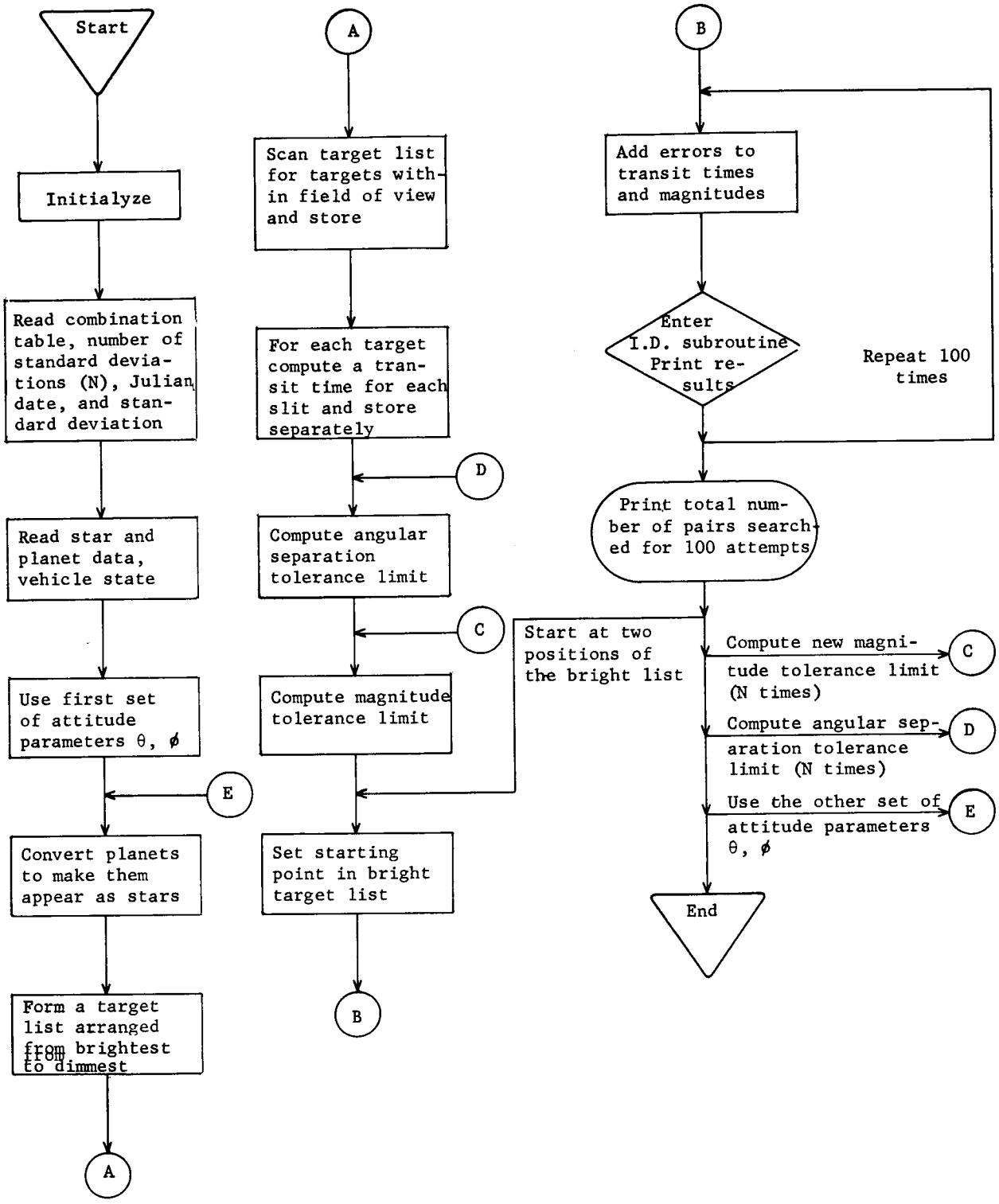

Figure 1. Schematic Flow Diagram of BAKER

transit time. Next, each list is sorted internally by time (from earliest to latest) to form a chronological ordering.

Angular separation and magnitude tolerance limits are computed from their respective standard deviations. The angular limit dictates how closely a target pair measured angular separation must agree with the catalog separation before a pair is accepted as tentatively identified. Similarly, the magnitude limit is used in developing the extremeties of the target catalog search area. These tolerances are functions of program parameters (1σ in angle and magnitude) which are read in at the beginning of BAKER. Any number of cases can be considered (this too is a program parameter).

A starting position is next defined as being either the brightest target in the first slit or the sixth brightest (only slit one targets are sorted by brightness). Each starting position is used for a range of pairs of angle and magnitude tolerances. For each starting point in the bright list, a set of transit time and magnitude errors is added to the true time and magnitude to simulate noisy data, and an identification is attempted. This is done 100 times before moving to the next starting point.

The identification process is started by branching to the sub-routine CHARLIE. A count of all pairs of targets searched in the target catalog is kept (for each of the 100 attempted identifications) and is returned to the main program. This number is added to the current total until 100 identifications have been attempted after which the final total is

printed. Details of the identification process are found in the next section.

In summary, BAKER will make an attempt at identification (defined to mean recognizing some three targets) from a given list of target data (transit time and magnitude) 100 times for a given angular separation and magnitude tolerance limit and for each of two starting points of the bright list, for a given vehicle orientation. Therefore the total number of possible identifications for one vehicle state is given by

$$N^2 \cdot 2 \cdot 100 = 200\, N^2$$

where N denotes the number of tolerance limits of interest. Each identification takes from about one-half to one second for all searching, counting, and pointing.

B. CHARLIE

The identification subroutine is supplied with a chronological list of target transit times and magnitudes for each slit and attempts to pick out three targets and positively identify them from a target catalog (consisting of the 100 brightest stars and the six inner-most planets made to resemble stars). Four possibilities as to the outcome of an attempted identification are possible:

1) a correct identification will be made,
2) an incorrect identification will be made,
3) four targets from slit one will not match (in magnitude) four targets from slit two, and

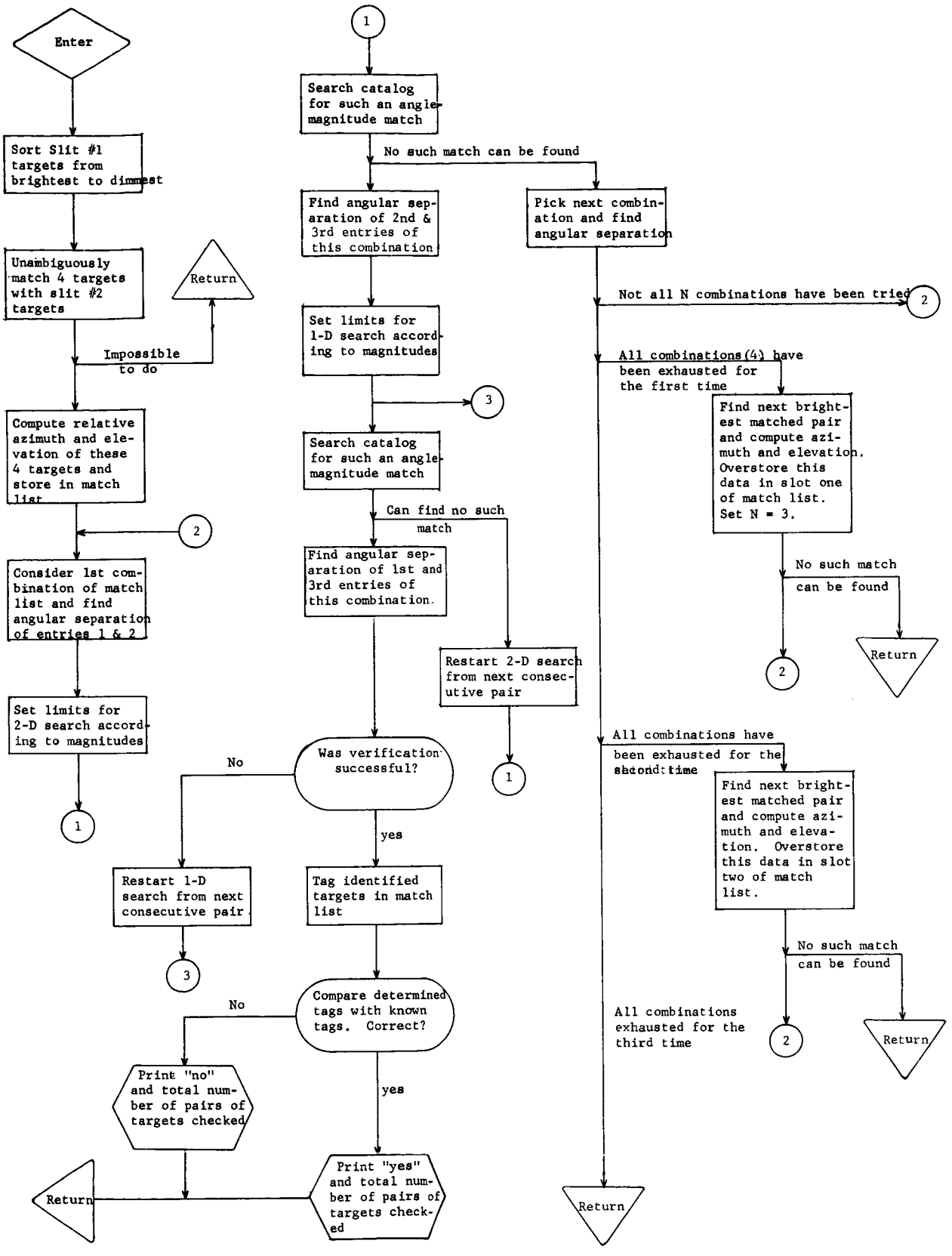

Figure 2. Schematic Flow Diagram of the Identification Subroutine (CHARLIE)

4) all combinations of the matched targets will be investigated but no identification will be made.

Reference to Figure 2 will aid in following the subroutine description.

Data in the list for slit one is sorted according to magnitude from the brightest target to the dimmest. Starting at either the first position in this list or the sixth (depending on which case is being considered) list two is scanned for one and only one target with similar brightness. Finding a match, this target is stored in a match list with an identifying tag, relative azimuth, and elevation. Failing to find a match (exhausting list two), the next slit one target is used until either four matches have been made, or fewer than four in which case a "failure to identify" message (see 3) above) is sent to the navigator (printed) and control reverts to the main program.

Once matching and sorting of four targets has been accomplished, first and second entries (out of 3) of the first combination (out of a possible 10) are considered. First their angular separation is computed from a knowledge of their transit times. Then by using the magnitude tolerance limit, a two-dimensional search area is defined (see Section IV-B for all mathematical details).

Searching is initiated at the most probable position in the target catalog and proceeds in a counter-clockwise "circular" fashion (see Note 4, Figure IV-5). Angular separation of a pair of prospective targets is computed and compared with the measured separation. If the angles compare favorably (catalog separation falls within measured separation

plus or minus angular tolerance limit), the search is halted and the identification process continues with the second and third entries. If the angles do not compare, searching continues until either a favorable comparison is made or the search limits are exceeded. In the latter case, a new combination of the original four targets is considered. Four failures of this nature will exhaust the match list requiring that a new target be added (failure to be able to find such a target causes an error output (of the type in 3) and control reverts to the main program). The new target is stored on top of the first target in the match list. A second new target (if needed later) will replace the second match list target, but the replacing process stops after two such overwritings. That is, four combinations may be tried with the original four match list targets. Failing to identify, a new target is written in slot one of the list and three combinations of these four targets are considered (one of of the four possible combinations has already been tested, hence only three). Finally, failing to identify, a second new target is written in slit two of the match list and three more combinations of these four (two old and two new) are considered. This failing, a message (of the type in 4) is sent to the navigator and control is returned to the main program (again see Section IV-B for details).

Having successfully found a matching pair of targets for entires one and two of any combination, the identification process proceeds to find a pair which agrees in magnitude and angular separation with entries two and three of this combination. Again by using the magnitude tolerance

limit, a one-dimensional search area (since entry two has tentatively been identified) is defined. Searching commences at the most probable point and considers pairs on either side of this point as indicated in Figure 3. If the search area is exhausted, a return is made to the two-

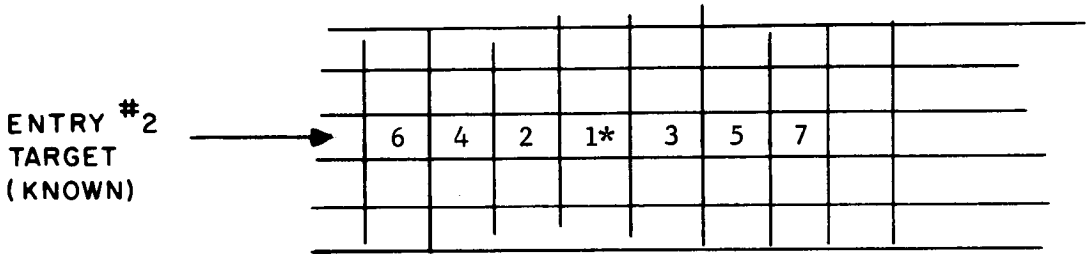

* Most Probable Point

Figure 3. Method of One-Dimensional Searching

dimensional search portion of the subroutine and searching continues from the last point.

Finding a match for the second and third entries of any combination, the identification process attempts now to verify that entries one and three agree (since they were identified independently). Angular separation is computed and compared with the measured. If this difference is less than the angular tolerance limit, identification has taken place; if not, a return is made to the one-dimensional search portion of the subroutine and continues from there.

Verification that the identification is correct is accomplished by comparing the determined star's or planet's identifying tags with the known tags. If correct, a "yes" message (of the type in 1) is printed along with the total number of pairs of targets searched in order to make

this identification and a normal return to the main program is taken. If not correct, a "no" message (of the type in 2) is printed along with this number (a minimum of three pairs for the most direct identification, one for the two-dimensional search, one for the one-dimensional search, and a third one for verification), and the normal return to the main program is taken.

C. Method of Operation

BAKER requires a running deck of 61 data cards for operation. These cards and the order in which they are expected to be found is described in detail.

1) Combination table card (1 card)

This card simply indicates the order in which the entries of a given combination should be considered (see Note 3, Figure IV-5) and is only used internally.

Current settings: 123124134234123124134123124134

Format (30I2)

2) Standard deviation and Julian date card (1 card)

Indicates the number of angle and magnitude standard deviations to be considered for a particular run (four will consume from 70 to 80 minutes of running time and seems to be a practical limit). Also, the Julian date (in days) is read and printed to indicate the date of the star and planet information.

Current values: 4 and 2440600.5

Format (I5, F10.1)

3) Angle and magnitude standard deviation card (1 card)

Standard deviation pairs to control the size of the errors added to the actual transit time and magnitude for the identification process.

Typical values for angle: 10, 20, 50, 100 seconds of arc,

" " " magnitude: .07, .14, .21, .28

Format (10F8.4)

4) Star card (50 cards)

Contains star identification number, right ascension, declination, and magnitude of the fifty brightest stars.

Format (F6.0, F14.10, F20.10, F12.2)

5) Planet card (6 cards)

Contains planet orbital radius, longitude (as of 2440600.5 J.D.), phase constant and equatorial radius of the six innermost planets.

Format (5X, F15.10, F16.6, E12.4, 8X, F8.3)

6) Vehicle data card (2 cards)

Vehicle position, attitude, period, etc., are contained on two cards. This positions and orients the vehicle in the coordinate system (with the sun at (0,0), +X axis in the direction of the first point of Aries, +Z in the direction of Polaris).

Typical values:

Vehicle position (X, Y, Z coordinates) 1.0, 0.8, 0.0 (A.U.)

Vehicle attitude (θ, ϕ, t_o) .1745, .5236, .0 (radians)

Precession rate .0 (radians/second)

Moment of inertia ratio 1.2

Precession angle .0175 (radians)

BAKER has been programmed to operate with two sets of vehicle attitude parameters θ and ϕ. The pairs $\theta = 0^{o}$, $\phi = 135^{o}$ and $\theta = 45^{o}$, $\phi = 90^{o}$ are both used for a given run (to alter the list of "seen" targets), so two sets of data will be available unless the program is altered slightly.

To estimate program running time (T) in minutes, use

$$T = 5\ N^{2}$$

where N is the number of standard deviation sets used. To this must be added about five minutes of compile and set-up times and the time required to list the output tape (if this is done on-line). Output is assumed to be to a magnetic tape unit to conserve time since from one-fourth to one-half of the total time for one identification is the printing time. A listing of the program with a few pages of sample output follows.

```
      PROGRAM BAKER
      DIMENSION NCOMB(10,3),VEH(10),PLANET(6,4),STAR(50,4),RP(2),RR(3),
     1PLANT(7,4),TARG(56,4),SSI(2),TT(2),SAVE(2,30,3),SEEN(2,31,4),
     2BRIGHT(31,2),CORE(4,5),WEE(2),FN(69),SAM(5,2)
      COMMON NCOMB,VEH,PLANET,STAR,RP,RR,PLANT,TARG,SSI,TT,SAVE,SEEN,
     1BRIGHT,CORE,PIT,SINGAM,TCH,TTCC,NSEE,NTARG,TANGAM,FN,TTC,DSEP,DMAG
C
      PI=3.1415926536
      ECLIP=.40916094
      SECLIP=SINF(ECLIP)
      CECLIP=COSF(ECLIP)
      CH=.2617993878
      CCH=COSF(CH)
      TCH=TANF(CH)
      GAMMA=.5235987756
      TANGAM=TANF(GAMMA)
      SINGAM=SINF(GAMMA)
      CGSCH=COSF(GAMMA)*SINF(CH)
      SEC20=20.*4.8481E-06
      FN(1) =.0003
      FN(2) =.0005
      FN(3) =.0007
      FN(4) =.0010
      FN(5) =.0013
      FN(6) =.0019
      FN(7) =.0026
      FN(8) =.0035
      FN(9) =.0047
      FN(10)=.0062
      FN(11)=.0082
      FN(12)=.0107
      FN(13)=.0139
      FN(14)=.0179
      FN(15)=.0228
      FN(16)=.0287
      FN(17)=.0359
      FN(18)=.0446
      FN(19)=.0548
      FN(20)=.0668
      FN(21)=.0808
      FN(22)=.0968
      FN(23)=.1151
      FN(24)=.1357
      FN(25)=.1587
      FN(26)=.1841
      FN(27)=.2119
      FN(28)=.2420
      FN(29)=.2743
      FN(30)=.3085
      FN(31)=.3446
      FN(32)=.3821
      FN(33)=.4207
      FN(34)=.4602
      FN(35)=.5000
      FN(36)=.5398
      FN(37)=.5793
```

```
      FN(38)=.6179
      FN(39)=.6554
      FN(40)=.6915
      FN(41)=.7257
      FN(42)=.7580
      FN(43)=.7881
      FN(44)=.8159
      FN(45)=.8413
      FN(46)=.8643
      FN(47)=.8849
      FN(48)=.9032
      FN(49)=.9192
      FN(50)=.9332
      FN(51)=.9452
      FN(52)=.9554
      FN(53)=.9641
      FN(54)=.9713
      FN(55)=.9772
      FN(56)=.9821
      FN(57)=.9861
      FN(58)=.9893
      FN(59)=.9918
      FN(60)=.9938
      FN(61)=.9953
      FN(62)=.9965
      FN(63)=.9974
      FN(64)=.9981
      FN(65)=.9987
      FN(66)=.9990
      FN(67)=.9993
      FN(68)=.9995
      FN(69)=.9997
C
      READ 101,((NCOMB(I,J),J=1,3),I=1,10)
  101 FORMAT (30I2)
C
      READ 103,ISAM,DATE
  103 FORMAT (I5,F10.1)
C
      READ 102,((SAM(I,J),J=1,2),I=1,ISAM)
  102 FORMAT (10F8.4)
C
      READ 117,(STAR(I,4),STAR(I,1),STAR(I,2),STAR(I,3),I=1,50)
  117 FORMAT (F6.0 ,F14.10,F20.10,F12.2)
C
      READ 125,((PLANET(I,J),J=1,4),I=1,6)
  125 FORMAT (5X,F15.10,F16.6,E12.4,8X,F8.3)
C
      PRINT 119,DATE
  119 FORMAT (1H1,/,8X,24HBAKER --- JULIAN DATE IS,F10.1)
C
      PRINT 127,((PLANET(I,J),J=1,4),I=1,6)
  127 FORMAT (/,8X,11HPLANET DATA,/,(8X,F15.6,F12.6,E15.4,F13.3))
C
      READ 105,VEH
  105 FORMAT (6F12.5)
```

```
C
      PRINT 111,VEH
  111 FORMAT (/,8X,12HVEHICLE DATA,/,8X,10F8.4)
C
      RPD=PI/180.
      STH=SINF(VEH(10))
      CTH=COSF(VEH(10))
      PIT=PI/VEH(8)
      OMEGA=2.*PI/(VEH(8)*(2.-VEH(9)))
      OMH=OMEGA*(1.-VEH(9))
      SIG10=.05*VEH(8)/PI*4.8481E-06*SAM(1,1)
      DO 500 ITZ=1,2
      GO TO (112,114),ITZ
  112 VEH4=0.
      VEH(4)=0.
      VEH5=135.
      VEH(5)=VEH5*RPD
      GO TO 116
  114 VEH4=45.
      VEH(4)=VEH4*RPD
      VEH5=90.
      VEH(5)=VEH5*RPD
C
  116 PRINT 113,VEH4,VEH5
  113 FORMAT (/,8X,27HVEHICLE ATTITUDE IN DEGREES,2F10.1)
C
      SZ=SINF(VEH(5))
      CZ=COSF(VEH(5))
      STAU=SINF(VEH(4))
      CTAU=COSF(VEH(4))
  118 NPT=0
      DO 130 I=1,6
      RP(1)=PLANET(I,2)*COSF(PLANET(I,1))
      RP(2)=PLANET(I,2)*SINF(PLANET(I,1))
      RR(1)=RP(1)-VEH(1)
      RR(2)=RP(2)-VEH(2)
      RR(3)=-VEH(3)
      R=SQRTF(RR(1)**2+RR(2)**2+RR(3)**2)
      IF(PLANET(I,3)/R-SEC20)126,126,130
  126 NPT=NPT+1
      TL=ALPH(RR(2),RR(1))
      SL=SINF(TL)
      CL=COSF(TL)
      SB=RR(3)/R
      CB=COSF(ASINF(SB))
      A=CB*CL
      B=CECLIP*CB*SL-SECLIP*SB
      C=SECLIP*CB*SL+CECLIP*SB
      PLANT(NPT,1)=ALPH(B,A)
      PLANT(NPT,2)=ASINF(C)
      COSA=(RP(1)*RR(1)+RP(2)*RR(2))/(R*SQRTF(RP(1)**2+RP(2)**2))
      PLANT(NPT,3)=-2.5*LOG10F(PLANET(I,4)*(1.+COSA)*(1.+COSA**2)/R**2)
      PLANT(NPT,4)=100+I
  130 CONTINUE
      IF(NPT)162,162,132
  132 NPU=NPT-1
```

```
      DO 140 I=1,NPU
      JNPT=I+1
      DO 140 J=JNPT,NPT
      IF(PLANT(I,3)-PLANT(J,3))140,140,136
  136 DO 138 K=1,4
      PLANT(7,K)=PLANT(I,K)
      PLANT(I,K)=PLANT(J,K)
  138 PLANT(J,K)=PLANT(7,K)
  140 CONTINUE
      NTAR=50+NPT
      MT=1
      DO 152 I=1,NPT
      PLT=PLANT(I,3)
      DO 150 J=MT,50
      L=I+J-1
      IF(PLT-STAR(J,3))142,142,146
  142 DO 144 K=1,4
  144 TARG(L,K)=PLANT(I,K)
      MT=J
      GO TO 152
  146 DO 148 K=1,4
  148 TARG(L,K)=STAR(J,K)
  150 CONTINUE
      GO TO 158
  152 CONTINUE
  154 KS=J
      DO 156 I=KS,50
      L=NPT+I
      DO 156 J=1,4
  156 TARG(L,J)=STAR(I,J)
      GO TO 170
  158 KP=I
      DO 160 I=KP,NPT
      L=50+I
      DO 160 J=1,4
  160 TARG(L,J)=PLANT(I,J)
      GO TO 170
  162 DO 164 I=1,50
      DO 164 J=1,4
  164 TARG(I,J)=STAR(I,J)
      NTAR=50
  170 NSEE=0
      NTARG=NTAR
C
      PRINT 165,((TARG(I,J),J=1,4),I=1,NTAR)
  165 FORMAT (/,10X,3F15.7,F8.0)
C
      DO 300 I=1,NTAR
      SRA=SINF(TARG(I,1))
      CRA=COSF(TARG(I,1))
      SDEC=SINF(TARG(I,2))
      CDEC=COSF(TARG(I,2))
      ZRA=VEH(5)-TARG(I,1)
      SZRA=SINF(ZRA)
      CZRA=COSF(ZRA)
      D=STAU*SZRA*CDEC+SDEC*CTAU
```

```
      IF(ABSF(D)-CGSCH)210,210,300
  210 NSEE=NSEE+1
      A=-CZRA*CDEC
      B=-CTAU*SZRA*CDEC+STAU*SDEC
      DEL=ALPH(B,A)
      DO 230 J=1,2
      TEMP=(-1.)**(J+1)*D*TANGAM/SQRTF(A*A+B*B)
      SSI(1)=ASINF(TEMP)-DEL
      SSI(2)=PI-SSI(1)-2.*DEL
      DO 216 K=1,2
      CADA=-A*COSF(SSI(K))+B*SINF(SSI(K))
      IF(ABSF(CADA)-1.00000001)212,212,226
  212 IF(CCH-CADA)214,214,216
  214 TT(J)=(SSI(K)+OMEGA*VEH(6)+OMH*VEH(7))/(OMEGA+OMH)
      GO TO 230
  216 CONTINUE
C
  218 PRINT 225,SSI,I
  225 FORMAT (//,10X,2E20.6,I10,E20.10)
C
      GO TO 300
  226 PRINT 225,SSI,I,CADA
      GO TO 300
  230 CONTINUE
      DO 258 J=1,2
  240 WEE(J)=OMH*(TT(J)-VEH(7))
      SFEE=SINF(WEE(J))
      CFEE=COSF(WEE(J))
      A=(-CFEE*CZRA+SFEE*CTAU*SZRA)*CDEC-SFEE*STAU*SDEC
      B=(-CTH*SFEE*CZRA-CTH*CFEE*CTAU*SZRA+STH*STAU*SZRA)*CDEC+SDEC*(CTH
     1*CFEE*STAU+STH*CTAU)
      D=(STH*SFEE*CZRA+STH*CFEE*CTAU*SZRA+CTH*STAU*SZRA)*CDEC+SDEC*(CTH*
     1CTAU-STH*CFEE*STAU)
      DEL=ALPH(B,A)
      TEMP=(-1.)**(J+1)*D*TANGAM/SQRTF(A*A+B*B)
      SSI(1)=ASINF(TEMP)-DEL
      SSI(2)=PI-SSI(1)-2.*DEL
      DO 254 K=1,2
      SY=SINF(SSI(K))
      CY=COSF(SSI(K))
      CADA=-A*CY+B*SY
      IF(ABSF(CADA)-1.00000001)242,242,241
C
  241 PRINT 243,SSI,I,J,CADA
  243 FORMAT (//,20X,2E20.6,2I10,E20.10)
C
      GO TO 300
  242 IF(CCH-CADA)244,244,254
  244 F=(-1.)**(J+1)*D*TANGAM-A*SY-B*CY
      PD=OMH*STH*(CDEC*(CFEE*CZRA-SFEE*CTAU*SZRA)+SFEE*STAU*SDEC)
      PA=OMH*(CDEC*(SFEE*CZRA+CFEE*CTAU*SZRA)-CFEE*STAU*SDEC)
      PB=OMH*CTH*(CDEC*(SFEE*CTAU*SZRA-CFEE*CZRA)-SFEE*STAU*SDEC)
      PF=(-1.)**(J+1)*PD*TANGAM-CY*(PB+OMEGA*A)-SY*(PA-OMEGA*B)
      QUO=F/PF
      IF(ABSF(QUO)-SIG10)256,256,248
  248 TT(J)=TT(J)-QUO
```

```
      GO TO 240
  254 CONTINUE
C
      PRINT 243,SSI,I,J
C
      GO TO 300
  256 TT(J)=TT(J)-QUO
  258 CONTINUE
  260 SAVE(1,NSEE,1)=TT(1)
      SAVE(2,NSEE,1)=TT(2)
      SAVE(1,NSEE,2)=TARG(I,3)
      SAVE(2,NSEE,2)=TARG(I,3)
      SAVE(1,NSEE,3)=TARG(I,4)
      SAVE(2,NSEE,3)=TARG(I,4)
  300 CONTINUE
      NS=NSEE-1
      DO 320 I=1,2
      DO 320 J=1,NS
      NK=J+1
      DO 320 K=NK,NSEE
      IF(SAVE(I,J,1)-SAVE(I,K,1))320,320,316
  316 DO 318 L=1,3
      SEEN(I,31,L)=SAVE(I,J,L)
      SAVE(I,J,L)=SAVE(I,K,L)
  318 SAVE(I,K,L)=SEEN(I,31,L)
  320 CONTINUE
      NPLANS=0
      DO 324 I=1,NSEE
      IF(SAVE(1,I,3)-100.)324,322,322
  322 NPLANS=NPLANS+1
  324 CONTINUE
      NSTARS=NSEE-NPLANS
C
      PRINT 321,NSTARS,NPLANS
  321 FORMAT (/,8X,32HNUMBER OF STARS AND PLANETS SEEN,2I6)
C
      DO 500 KQ=1,ISAM
      TTC=.5*VEH(8)/PI*4.8481E-06*SAM(KQ,1)
      DSEP=3.*4.8481E-06*SAM(KQ,1)+ABSF(1.-VEH(9))*VEH(10)
      DO 500 KR=1,ISAM
      DMAG=3.*SAM(KR,2)
C
      PRINT 327,SAM(KQ,1),SAM(KR,2)
  327 FORMAT(1H18X,28HSIGMA IN ANGLE AND INTENSITY,2F9.2,/)
C
      DO 500 IRMA=1,6,5
      IRA=IRMA-1
C
      PRINT 419,IRA
  419 FORMAT (/ ,4X,17HSTARTING POINT IS,I2,31H DOWN FROM THE BRIGHTEST
     1TARGET,///)
C
      MTCT=0
      DO 400 JMC=1,100
      DO 408 I=1,2
      DO 408 J=1,NSEE
```

```
      SEEN(I,J,3)=SAVE(I,J,3)
      QQ=XNORMAL(ZQZ)
  404 SEEN(I,J,1)=SAVE(I,J,1)+TTC*QQ*10.**(.133*SAVE(I,J,2))
      QQ=XNORMAL(ZQZ)
  408 SEEN(I,J,2)=SAVE(I,J,2)-2.5*LOG10F(QQ*SAM(KR,2)+1.)
      CALL CHARLIE (IRMA,MCONT)
      MTCT=MTCT+MCONT
  400 CONTINUE
C
      PRINT 405,MTCT
  405 FORMAT (/,8X,18HTOTAL NO. OF BOXES,I8,//)
C
  500 CONTINUE
      END



      SUBROUTINE CHARLIE (IRMA,MCONT)
      DIMENSION NCOMB(10,3),VEH(10),PLANET(6,4),STAR(50,4),RP(2),RR(3),
     1PLANT(7,4),TARG(56,4),SSI(2),TT(2),SAVE(2,30,3),SEEN(2,31,4),
     2BRIGHT(31,2),CORE(4,5),WEE(2),FN(69),SAM(5,2)
      COMMON NCOMB,VEH,PLANET,STAR,RP,RR,PLANT,TARG,SSI,TT,SAVE,SEEN,
     1BRIGHT,CORE,PIT,SINGAM,TCH,TTCC,NSEE,NTARG,TANGAM,FN,TTC,DSEP,DMAG
C
      MCONT=0
      KKK=1
      DO 410 I=1,NSEE
      BRIGHT(I,1)=SEEN(1,I,2)
  410 BRIGHT(I,2)=I
      DO 414 I=1,4
      DO 414 J=1,5
  414 CORE(I,J)=0.
      NB=NSEE-1
      DO 420 I=1,NB
      IJ=I+1
      DO 420 J=IJ,NSEE
      IF(BRIGHT(I,1)-BRIGHT(J,1))420,420,416
  416 DO 418 K=1,2
      BRIGHT(31,K)=BRIGHT(I,K)
      BRIGHT(I,K)=BRIGHT(J,K)
  418 BRIGHT(J,K)=BRIGHT(31,K)
  420 CONTINUE
      I=IRMA
      IREJ=0
      NUMB=4
      NCORE=0
  421 IM=BRIGHT(I,2)
      ITWO=0
      J=1
  423 IF(ABSF(SEEN(1,IM,2)-SEEN(2,J,2))-DMAG)422,422,430
  422 DIF=SEEN(2,J,1)-SEEN(1,IM,1)
      IF(ABSF(TANF(PIT*DIF)/SINGAM)-TCH)424,424,430
  424 ITWO=ITWO+1
      IF(ITWO-1)426,426,438
  426 NCORE=NCORE+1
      CORE(NCORE,1)=IM
```

```
      CORE(NCORE,2)=J
      CORE(NCORE,3)=PIT*(SEEN(2,J,1)+SEEN(1,IM,1))
      CORE(NCORE,4)=ATANF(SINF(PIT*DIF)/TANGAM)
  430 J=J+1
      IF(J-NSEE)423,423,436
  436 IF(NCORE-NUMB)440,448,448
  438 NCORE=NCORE-1
      IREJ=IREJ+1
  440 I=I+1
      IF(I-NSEE)421,421,442
C
  442 PRINT 445,NCORE
  445 FORMAT (  8X, 31HSEARCHED LIST BUT CAN FIND ONLY,I4,20H MATCHED IN
     1TENSITIES)
C
      GO TO 600
  448 KEEPI=I
  446 N1=NCOMB(KKK,1)
      N2=NCOMB(KKK,2)
      AN1N2=       SINF(CORE(N1,4))*SINF(CORE(N2,4))+COSF(CORE(N1,4))*
     1COSF(CORE(N2,4))*COSF(CORE(N2,3)-CORE(N1,3))
      IF(ABSF(AN1N2)-1.)441,441,443
  443 IN1=100+N1
      IN2=100+N2
      COANG=AN1N2
      GO TO 618
  441 AN1N2=ACOSF(AN1N2)
      NN=N1
  450 MI=CORE(NN,1)
      XMAG=SEEN(1,MI,2)-DMAG
      DO 454 L=1,NTARG
      IF(XMAG-TARG(L,3))452,452,454
  452 L1=MAXO (1,L-1)
      GO TO 456
  454 CONTINUE
      L1=NTARG
      L2=L1
      L3=L1
      GO TO 474
  456 XMAG=XMAG+DMAG
      DO 464 L=L1,NTARG
      ADIF=XMAG-TARG(L,3)
      IF(ADIF)458,458,464
  458 IF(L-1)460,460,459
  459 BDIF=TARG(L-1,3)-XMAG
      IF(ADIF-BDIF)462,462,460
  460 L2=L
      GO TO 466
  462 L2=L-1
      GO TO 466
  464 CONTINUE
      L2=NTARG
      L3=L2
      GO TO 474
  466 XMAG=XMAG+DMAG
      DO 470 L=L2,NTARG
```

```
      IF(XMAG-TARG(L,3))468,468,470
  468 L3=L
      GO TO 474
  470 CONTINUE
      L3=NTARG
  474 IF(NN-N2)476,478,476
  476 LV1=L1
      LV2=L2
      LV3=L3
      NN=N2
      GO TO 450
  478 LH1=L1
      LH2=L2
      LH3=L3
  484 LIMIT=(LV3-LV1+1)*(LH3-LH1+1)
      LIM=1
      KEY=0
      KIK=0
      JIJ=0
      IV=LV2
      JH=LH2
  485 IF(IV-JH) 486,492,486
  486 ANGSEP=       SINF(TARG(IV,2))*SINF(TARG(JH,2))+COSF(TARG(IV,2))*
     1COSF(TARG(JH,2))*COSF(TARG(JH,1)-TARG(IV,1))
      IF(ABSF(ANGSEP)-1.)487,487,489
  489 IN1=IV
      IN2=JH
      COANG=ANGSEP
      GO TO 618
  487 ANGSEP=ACOSF(ANGSEP)
      DELT=ABSF(ANGSEP-AN1N2)
      MCONT=MCONT+1
      IF(DELT-DSEP)488,488,492
  488 CORE(N1,5)=TARG(IV,4)
      CORE(N2,5)=TARG(JH,4)
      GO TO 526
  492 IF(LIM-LIMIT)496,519,519
  496 IF(KIK-KEY)500,508,508
  500 KIK=KIK+1
      IV=IV+(-1)**(KEY+1)
      IF(IV-LV3)504,504,496
  504 IF(LV1-IV)518,518,496
  508 IF(JIJ-KEY)512,520,520
  512 JIJ=JIJ+1
      JH=JH+(-1)**(KEY+1)
      IF(JH-LH3)516,516,496
  516 IF(LH1-JH)518,518,496
  518 LIM=LIM+1
      GO TO 485
  520 KIK=0
      JIJ=0
      KEY=KEY+1
      GO TO 496
  519 KKK=KKK+1
      KMONE=KKK-1
      IF(KKK-5)446,521,522
```

```
  521 I=KEEPI
      NUMB=1
      NCORE=0
      GO TO 430
  522 IF(KKK-8)446,2522,523
 2522 NUMB=2
      NCORE=1
      GO TO 430
  523 IF(KKK-10)446,446,524
C
  524 PRINT 525
  525 FORMAT (/,8X,36HALL COMBINATIONS HAVE BEEN EXHAUSTED,/)
C
      GO TO 600
  526 N3=NCOMB(KKK,3)
      AN2N3=       SINF(CORE(N2,4))*SINF(CORE(N3,4))+COSF(CORE(N2,4))*
     1COSF(CORE(N3,4))*COSF(CORE(N3,3)-CORE(N2,3))
      IF(ABSF(AN2N3)-1.)533,533,537
  537 IN1=100+N2
      IN2=100+N3
      COANG=AN2N3
      GO TO 618
  533 AN2N3=ACOSF(AN2N3)
      MI=CORE(N3,1)
      XMAG=SEEN(1,MI,2)-DMAG
      DO 528 L=1,NTARG
      IF(XMAG-TARG(L,3))527,527,528
  527 M1=MAXO (1,L-1)
      GO TO 529
  528 CONTINUE
      M1=NTARG
      M2=M1
      M3=M1
      GO TO 541
  529 XMAG=XMAG+DMAG
      DO 534 L=M1,NTARG
      ADIF=XMAG-TARG(L,3)
      IF(ADIF)530,530,534
  530 BDIF=TARG(L-1,3)-XMAG
      IF(ADIF-BDIF)532,532,531
  531 M2=L
      GO TO 536
  532 M2=L-1
      GO TO 536
  534 CONTINUE
      M2=NTARG
      M3=M2
      GO TO 541
  536 XMAG=XMAG+DMAG
      DO 540 L=M2,NTARG
      IF(XMAG-TARG(L,3))538,538,540
  538 M3=L
      GO TO 541
  540 CONTINUE
      M3=NTARG
  541 LIMIT2=M3-M1+1
```

```
      KEY2=0
      LIM2=1
      MV=M2
      STH2=SINF(TARG(JH,2))
      CTH2=COSF(TARG(JH,2))
  539 IF(MV-JH) 542,544,542
  542 ANGSEP=       SINF(TARG(MV,2))*STH2+COSF(TARG(MV,2))*CTH2*COSF
     1(TARG(JH,1)-TARG(MV,1))
      IF(ABSF(ANGSEP)-1.)543,543,551
  551 IN1=MV
      IN2=JH
      COANG=ANGSEP
      GO TO 618
  543 ANGSEP=ACOSF(ANGSEP)
      DELT=ABSF(ANGSEP-AN2N3)
      MCONT=MCONT+1
      IF(DELT-DSEP)549,549,544
  544 IF(LIM2-LIMIT2)546,545,545
  545 CORE(N1,5)=0.
      CORE(N2,5)=0.
      GO TO 492
  546 KEY2=KEY2+1
      MV=MV+KEY2*(-1)**KEY2
      IF(MV-M3)547,547,546
  547 IF(M1-MV)548,548,546
  548 LIM2=LIM2+1
      GO TO 539
  549 CORE(N3,5)=TARG(MV,4)
  550 AN1N3=       SINF(CORE(N1,4))*SINF(CORE(N3,4))+COSF(CORE(N1,4))*
     1COSF(CORE(N3,4))*COSF(CORE(N3,3)-CORE(N1,3))
      IF(ABSF(AN1N3)-1.)553,553,557
  557 IN1=100+N1
      IN2=100+N3
      COANG=AN1N3
      GO TO 618
  553 AN1N3=ACOSF(AN1N3)
      IF(IV-MV) 556,544,556
  556 ANGSEP=       SINF(TARG(IV,2))*SINF(TARG(MV,2))+COSF(TARG(IV,2))*
     1COSF(TARG(MV,2))*COSF(TARG(MV,1)-TARG(IV,1))
      IF(ABSF(ANGSEP)-1.)561,561,563
  563 IN1=IV
      IN2=MV
      COANG=ANGSEP
      GO TO 618
  561 ANGSEP=ACOSF(ANGSEP)
      DELT=ABSF(ANGSEP-AN1N3)
      MCONT=MCONT+1
      IF(DELT-DSEP)554,554,552
  552 CORE(N3,5)=0.
      GO TO 544
  554 IS1=CORE(N1,1)
      IS2=CORE(N1,2)
      ID1=SEEN(1,IS1,3)
      ID2=SEEN(2,IS2,3)
      ID3=CORE(N1,5)
      IF(ID1-ID3)620,602,620
```

```
  602 IF(ID2-ID3)620,604,620
  604 IS1=CORE(N2,1)
      IS2=CORE(N2,2)
      ID1=SEEN(1,IS1,3)
      ID2=SEEN(2,IS2,3)
      ID3=CORE(N2,5)
      IF(ID1-ID3)620,606,620
  606 IF(ID2-ID3)620,608,620
  608 IS1=CORE(N3,1)
      IS2=CORE(N3,2)
      ID1=SEEN(1,IS1,3)
      ID2=SEEN(2,IS2,3)
      ID3=CORE(N3,5)
      IF(ID1-ID3)620,610,620
  610 IF(ID2-ID3)620,612,620
C
  618 PRINT 619,IN1,IN2,COANG
  619 FORMAT (/,50X,2I5,F20.15)
C
      GO TO 600
C
  620 PRINT 625,MCONT
  625 FORMAT (/,2X,2HNO,11X,20HTOTAL BOXES SEARCHED,I5,/)
C
      GO TO 600
C
  612 PRINT 615,MCONT
  615 FORMAT ( ,8X,3HYES,10X,5HBOXES,I6)
C
  600 CONTINUE
      END



      FUNCTION MAXO (L,M)
      IF(L-M)10,20,20
   10 MAXO =M
      RETURN
   20 MAXO =L
      END



      FUNCTION ALPH(X,Y)
C     ALPH COMPUTES THE ARC TANGENT OF THE QUOTIENT OF TWO NUMBERS AND
C     RESOLVES THE ANGLE TO THE PROPER QUADRANT BY EXAMINING THE
C     NUMERATOR AND DENOMINATOR SIGNS.
      PI=3.1415926536
      IF(Y)10,30,20
   10 IF(X)11,12,11
   11 ALPH=PI+ATANF(X/Y)
      RETURN
   12 ALPH=PI
      RETURN
   20 IF(X)21,23,22
   21 ALPH=2.*PI+ATANF(X/Y)
```

```
      RETURN
   22 ALPH=ATANF(X/Y)
      RETURN
   23 ALPH=0.0
      RETURN
   30 IF(X)31,33,32
   31 ALPH=1.5*PI
      RETURN
   32 ALPH=.5*PI
      RETURN
   33 ALPH=2.*PI
      END



      FUNCTION XNORMAL (R)
      DIMENSION NCOMB(10,3),VEH(10),PLANET(6,4),STAR(50,4),RP(2),RR(3),
     1PLANT(7,4),TARG(56,4),SSI(2),TT(2),SAVE(2,30,3),SEEN(2,31,4),
     2BRIGHT(31,2),CORE(4,5),WEE(2),FN(69),SAM(5,2)
      COMMON NCOMB,VEH,PLANET,STAR,RP,RR,PLANT,TARG,SSI,TT,SAVE,SEEN,
     1BRIGHT,CORE,PIT,SINGAM,TCH,TTCC,NSEE,NTARG,TANGAM,FN,TTC,DSEP,DMAG
      IF(M)2,1,2
    1 M=2
B     X=3625176463724015
B     Y=3625176463724015
B     Z=200000000000000
    2 LDA (X)         MUI (Y)
      STA (X)         ARS (12)
      ADD (Z)         FAD (Z)
      STA (R)
      IF(R-.0003)3,6,4
    3 R=.0003
      GO TO 6
    4 IF(.9997-R)5,6,6
    5 R=.9997
    6 DO 7 I=1,69
      IF(R-FN(I))8,9,7
    7 CONTINUE
    8 I=I-1
      UNIFORM=.1*(FLOATF(I-35)+(R-FN(I))/(FN(I+1)-FN(I)))
      RETURN
    9 UNIFORM=.1*FLOATF(I-35)
      END
      END
```

```
STARTING POINT IS 5 DOWN FROM THE BRIGHTEST TARGET

MATCHING WAS SUCCESSFUL, 4 TARGET(S) WERE REJECTED

FIRST AND SECOND ENTRIES IDENTIFIED IN BOX 25

ONE DIMENSIONAL SEARCH EXHAUSTED FOR COMBINATION  1

FIRST AND SECOND ENTRIES IDENTIFIED IN BOX 30

SECOND AND THIRD ENTRIES IDENTIFIED IN BOX  3

IDENTIFICATION HAS BEEN MADE.    SLIT ONE   SLIT TWO    TAG

                                    12.        12.       12.

                                    16.        16.       16.

                                    21.        21.       21.

0 MINUTES ---  36 SECONDS
```

Figure 4. Example of Output from Program BAKER

APPENDIX E

CAMERA - COMPUTER SIMULATOR PROGRAM - ABLE

ABLE simulates in part the operation of the Scanning Celestial Camera and the associated space computer, in addition to doing an error analysis on position and attitude. This program is not designed to duplicate exactly the functions of the camera and computer but will accomplish the same objectives perhaps in a less sophisticated but more easily implemented fashion.

Description

Basically, ABLE performs four operations:

1. It places the space vehicle at a given position relative to the planets and the celestial sphere. This is done for a specified Julian Date, of course.
2. It spins the scanning camera about the specified spin axis and determines which stars and planets pass by the crossed-slit configuration.
3. It computes the exact (relative to the given position and attitude parameters) transit times of all the targets and adds to them a randomized set of errors.
4. From the "errored" times, it then computes, using the equations of Section III-A, the position and attitude of the vehicle.

In this way and by the repeated application of random errors to the "true"

transit times, error patterns are established for position and attitude.

The positions of the space vehicle are consecutive intersections of a planar grid (usually lying in the ecliptic plane). To better understand the ABLE sequence, consult Figure 1. A grid center and a grid unit size (with coordinate system centered at the sun) are read in and an initial grid point is found. Since the grid is to contain eighty-one points, a square eight units on a side is used and the coordinates of the initial point (x_s, y_s) are given by

$$x_s = x_{center} - 4 \cdot \Delta x,$$

$$y_s = y_{center} - 4 \cdot \Delta y .$$

This places the starting position at the lower left hand corner of the grid. Successive points are found by incrementing y by Δy until the upper edge of the grid has been reached, adding Δx to x and starting over at $y = y_s$ again until the right hand column has been completed (see Figure 2).

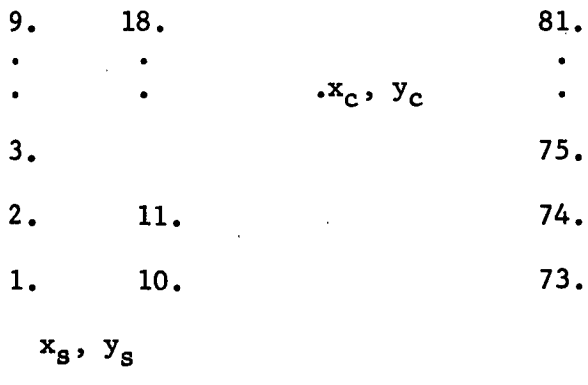

Figure 2. Ordered Grid Points

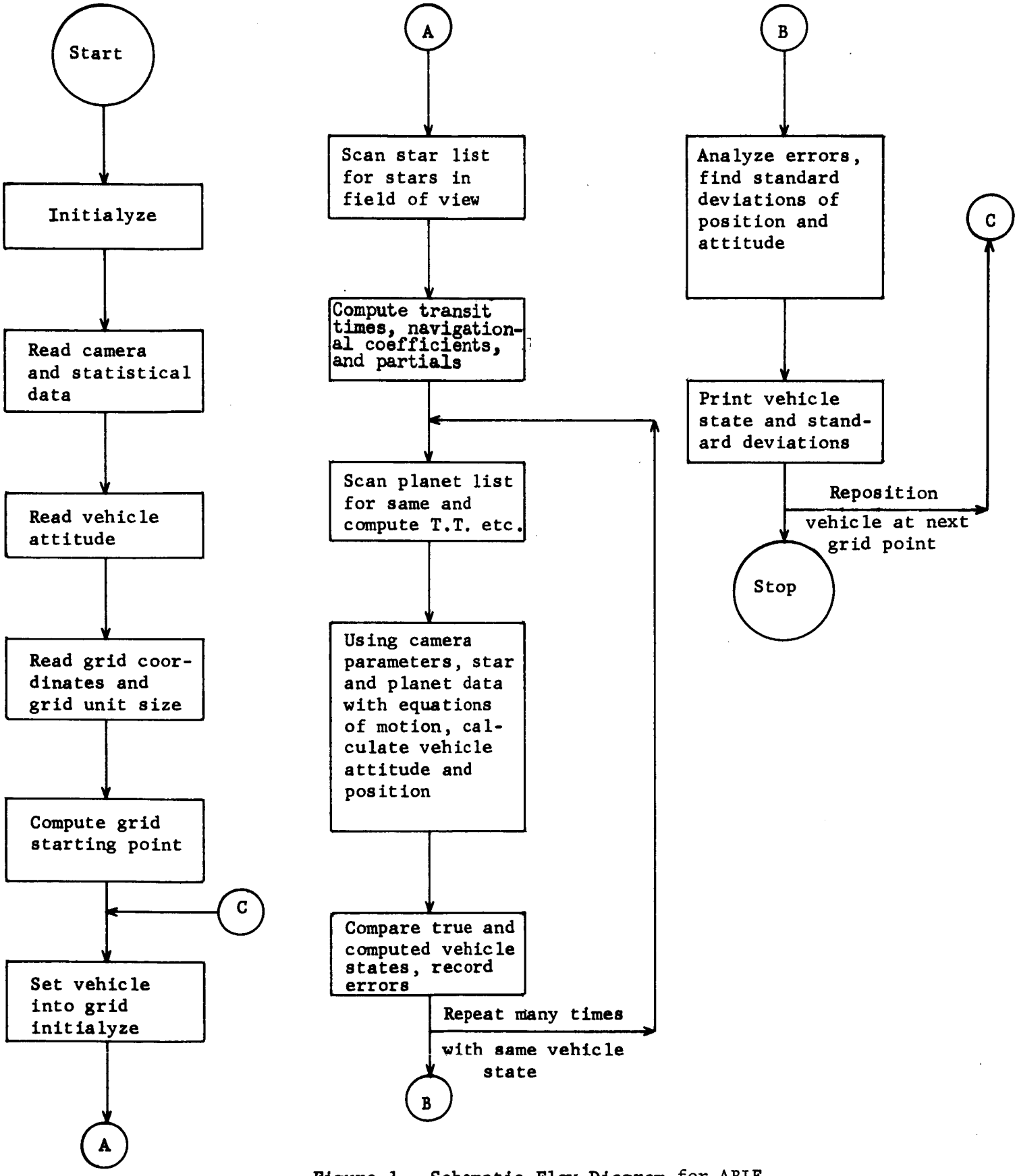

Figure 1. Schematic Flow Diagram for ABLE

A given number of stars and planets (no more than 100 and 9 respectively, each of these numbers being a program parameter) are checked sequentially to determine if they can be seen by the camera. These that are not seen are discarded; transit times are computed for the others, along with the necessary partial derivative coefficients. This process is repeated until all targets are checked.

Normally distributed errors with mean zero and assigned standard deviation (this is a program parameter) are added to each transit time. These times plus the partial derivatives are then used in the navigation equations to determine the least squares best vehicle attitude and position. The differences between these values and the true vehicle state are found and saved until a sufficient number (usually fifty, also a program parameter) of them exist.

Next the standard deviations of each component of position and attitude are computed and printed along with the resulting error vector for position and attitude. The vehicle is then repositioned to the next grid point and the process repeated until the grid is complete. In this way, equal error contours can be constructed and two of them are shown in Figures III-25 and III-26 in the body of this report.

Method of Operation

To operate ABLE, two cards containing camera and vehicle data must be read in followed by one card designating the grid center and unit size. These cards and their formats are as follows:

1) Initialyzing Camera Data

a) Zero Julian date (in days)

b) Vehicle spin period (in seconds)

c) Present Julian date (in days)

d) Camera angle between slits (Γ, in radians)

e) Camera slit length (H, in radians)

f) Number of stars to be considered (less than 101)

g) Number of planets to be considered (less than 10)

h) One standard deviation of angular error (in seconds of arc)

i) Number of Monte Carlo sets per vehicle state (less that 101).

Format (F15.2, F4.0, F16.2, 2F10.8, 4I6)

2) Vehicle Data Card

a) Vehicle attitude (θ, in radians)

b) " " (ϕ, in radians)

c) " " (t_o, in seconds)

d) Vehicle position (x, in A.U.)

e) " " (y, in A.U.)

f) " " (z, in A.U.)

Format (6F10.6)

3) Grid Data Card

a) Grid center (x, in A.U.)

b) " " (y, in A.U.)

c) " " (z, in A.U.)

d) Grid unit size (Δx, in A.U.)

e) Grid unit size (Δy, in A.U.)

Format (10F5.1)

A good estimate of running time for ABLE is about 15 seconds per grid point, or 20 minutes per grid. A listing of the program with a few pages of sample output follows.

```
      PROGRAM ABLE
      DIMENSION DELT(6),R(3),P(3),TARLIST(110,2),PSI(4),SAVEP(9,2),
     1SAVES(100,2)
      DIMENSION VEH(6),PAREF(100,7,4),PLANCO(9,5,4),ERR(6),SEENS(100,3),
     1SEENP(9,3),PMAG(9),FN(69),STARPOS(100,2),PLANPOS(9,2),DELTA(100,6)
      COMMON PI,K1,K2,K3,NTAPE,ISHIFT,VEH,ISIG,NR,PAREF,PLANCO,T,ERR,FN,
     1SEENS,SEENP,PMAG,STARPOS,PLANPOS,DELTA
C
      PI=3.1415926536
      G=1.996E-47
      ECLIP=.40916094
      SM=1.99E+33
      CALL FILLTAB
      ISHIFT=0
C
      READ 45,TZ,T,TAU,GAMMA,CH,K1,K2,ISIG,NR
   45 FORMAT (F15.2,F4.0,F16.2,2F10.8,4I6)
C
      READ 55,VEH
   55 FORMAT (6F10.6)
C
      READ 65,XGRID,YGRID,ZGRID,DXQ,DYQ
   65 FORMAT (10F5.1)
C
      PRINT 75,TZ,TAU,T,GAMMA,CH,ISIG,NR,K1,K2
   75 FORMAT (1H1,/, 5X,9HZERO TIME,8X,4HTIME, 5X,6HPERIOD,5X,5HGAMMA,8X
     1,3HETA,8X,5HSIGMA,5X,8HNO. RUNS,5X,9HNO. STARS,5X,11HNO. PLANETS,/
     2/,F14.2,F15.2,F7.1,F11.4,F12.4,7X,I4,7X,I4,10X,I4,10X,I4,///)
C
      TTCONST=.5*T/PI*4.8481E-06*FLOATF(ISIG)
      TANGAM=TANF(GAMMA)
      TANG=F(TANF(F(GAMMA)))
      PI2T=F(F(2.*F(PI))/F(T))
      FAC=86400.*SQRTF(SM*G)
      MXM=0
      STHETA=SINF(VEH(1))
      CTHETA=COSF(VEH(1))
      SPHI=SINF(VEH(2))
      CPHI=COSF(VEH(2))
      SECLIP=SINF(ECLIP)
      CECLIP=COSF(ECLIP)
      CP=F(COSF(VEH(2)))
      SP=F(SINF(VEH(2)))
      CT=F(COSF(VEH(1)))
      ST=F(SINF(VEH(1)))
      VEH(6)=ZGRID
      XSTART=XGRID-4.*DXQ
      YSTART=YGRID-4.*DYQ
      DO 6200 IXY=1,9
      VEH(4)=XSTART+DXQ*FLOATF(IXY-1)
      DO 6200 IYX=1,9
      VEH(5)=YSTART+DYQ*FLOATF(IYX-1)
      NP=0
      NS=0
      IF(K1)1302,1302,76
   76 NNN=1
```

```
      MMM=K1
  990 DO 1300 J=NNN,MMM
      IF(J-100)1000,1000,1010
 1000 SRA=SINF(STARPOS(J,1))
      CRA=COSF(STARPOS(J,1))
      SDEC=SINF(STARPOS(J,2))
      CDEC=COSF(STARPOS(J,2))
      P(1)=CRA*CDEC
      P(2)=CECLIP*CDEC*SRA+SECLIP*SDEC
      P(3)=-SECLIP*CDEC*SRA+CECLIP*SDEC
      RP=1.
      GO TO 1020
 1010 MM=J-100
      XLAMB=PLANPOS(MM,1)+FAC*(TAU-TZ)/PLANPOS(MM,2)**1.5
      R(1)=PLANPOS(MM,2)*COSF(XLAMB)
      R(2)=PLANPOS(MM,2)*SINF(XLAMB)
      R(3)=0.
      DO 1018 K=1,3
 1018 P(K)=R(K)-VEH(K+3)
      RP=SQRTF(R(1)**2+R(2)**2+R(3)**2+VEH(4)**2+VEH(5)**2+VEH(6)**2-
     12.*(R(1)*VEH(4)+R(2)*VEH(5)+R(3)*VEH(6)))
 1020 D=P(1)*STHETA*SPHI-P(2)*STHETA*CPHI+P(3)*CTHETA
      IF(ABSF(D)/RP-COSF(GAMMA)*SINF(CH))1030,1030,1300
 1030 A=-P(1)*CPHI-P(2)*SPHI
      B=-P(1)*CTHETA*SPHI+P(2)*CTHETA*CPHI+P(3)*STHETA
      DEL=ALPH(B,A)
      TEMP=D*TANGAM/SQRTF(A*A+B*B)
C     COMPUTE THE FOUR VALUES OF PSI
      PSI(1)=ASINF(TEMP)-DEL
      PSI(2)=ASINF(-TEMP)-DEL
      PSI(3)=PI-PSI(1)-2.*DEL
      PSI(4)=PI-PSI(2)-2.*DEL
      K=1
      ILAG=0
      IDICAT1=0
      IDICAT2=0
      IF(J-100)1034,1034,1036
 1034 NS=NS+1
      GO TO 1038
 1036 NP=NP+1
 1038 CADA=(-A*COSF(PSI(K))+B*SINF(PSI(K)))/RP
      IF(ABSF(CADA)-1.00000001)1040,1040,1042
C
 1042 PRINT 1045
 1045 FORMAT (/,6HSTOP 4,/)
C
      GO TO 6200
 1040 IF(COSF(CH)-CADA)1050,1050,1082
 1050 TT=VEH(3)+T*PSI(K)/(2.*PI)
      IF(J-100)1054,1054,1056
 1054 SEENS(NS,1)=J
      GO TO 1058
 1056 SEENP(NP,1)=J
 1058 IF(XABSF(K-2)-1)1070,1060,1070
 1060 IF(IDICAT1)1064,1062,1064
 1062 IF(J-100)1063,1063,1066
```

```
 1063 SEENS(NS,2)=TT
      GO TO 1068
 1066 SEENP(NP,2)=TT
 1068 IDICAT1=1
      GO TO 1080
 1070 IF(IDICAT2)1064,1072,1064
 1072 IF(J-100)1074,1074,1076
 1074 SEENS(NS,3)=TT
      GO TO 1078
 1076 SEENP(NP,3)=TT
 1078 IDICAT2=1
 1080 ILAG=ILAG+1
      IF(ILAG-2)1082,1090,1090
C
 1064 PRINT 1065,(PSI(M),M=1,4)
 1065 FORMAT (///,3X,14HPSI(J),J=1,4   ,4E20.8,/)
C
      GO TO 6200
 1082 IF(K-4)1084,1086,1086
 1084 K=K+1
      GO TO 1038
C
 1086 PRINT 1085
 1085 FORMAT (/,6HSTOP 3,/)
C
      GO TO 6200
 1090 IF(J-100)1094,1094,1200
 1094 K=NS
      SRA=F(SINF(F(STARPOS(J,1))))
      CRA=F(COSF(F(STARPOS(J,1))))
      SDEC=F(SINF(F(STARPOS(J,2))))
      CDEC=F(COSF(F(STARPOS(J,2))))
      P(1)=F(CRA*CDEC)
      P(2)=F(F(F(F(CECLIP)*CDEC)*SRA)+F(F(SECLIP)*SDEC))
      P(3)=F(F(F(F(-SECLIP)*CDEC)*SRA)+F(F(CECLIP)*SDEC))
      PAREF(K,1,1)=F(F(P(1)*F(CT*SP))-F(P(2)*F(CT*CP))-F(P(3)*ST))
      PAREF(K,1,2)=F(F(P(1)*CP)+F(P(2)*SP))
      PAREF(K,1,3)=F(F(F(P(1)*F(ST*SP))-F(P(2)*F(ST*CP))+F(P(3)*CT))
     1*TANG)
      PAREF(K,1,4)=F(-PAREF(K,1,3))
      PAREF(K,2,1)=F(F(-P(1)*F(ST*SP))+F(P(2)*F(ST*CP))-F(P(3)*CT))
      PAREF(K,2,2)=0.
      PAREF(K,2,3)=F(F(F(P(1)*F(CT*SP))-F(P(2)*F(CT*CP))-F(P(3)*ST))
     1*TANG)
      PAREF(K,2,4)=F(-PAREF(K,2,3))
      PAREF(K,3,1)=F(F(P(1)*F(CT*CP))+F(P(2)*F(CT*SP)))
      PAREF(K,3,2)=F(F(-P(1)*SP)+F(P(2)*CP))
      PAREF(K,3,3)=F(F(F(P(1)*F(ST*CP))+F(P(2)*F(ST*SP)))*TANG)
      PAREF(K,3,4)=F(-PAREF(K,3,3))
      PAREF(K,4,1)=F(-PAREF(K,1,2)*PI2T)
      PAREF(K,4,2)=F(PAREF(K,1,1)*PI2T)
      PAREF(K,4,3)=0.
      PAREF(K,4,4)=0.
      GO TO 1300
 1200 L=NP
      MM=J-100
```

```
      XLAMB=F(F(PLANPOS(MM,1))+F(F(F(FAC)*F(TAU-TZ))/F(PLANPOS(MM,2)
     1**1.5)))
      R(1)=F(F(PLANPOS(MM,2))*F(COSF(XLAMB)))
      R(2)=F(F(PLANPOS(MM,2))*F(SINF(XLAMB)))
      R(3)=0.0
      DO 1204 K=1,3
 1204 P(K)=F(R(K)-F(VEH(K+3)))
      A=F(F(-P(1)*F(COSF(F(VEH(2)))))-F(P(2)*F(SINF(F(VEH(2))))))
      B=F(F(-P(1)*F(F(COSF(F(VEH(1))))*F(SINF(F(VEH(2)))))+F(P(2)*F(
     1F(COSF(F(VEH(1))))*F(COSF(F(VEH(2)))))+F(P(3)*F(SINF(F(VEH(1))))
     2))
      PLANCO(L,1,1)=F(-CT*SP)
      PLANCO(L,1,2)=F(-CP)
      PLANCO(L,1,3)=F(F(-ST*SP)*TANG)
      PLANCO(L,1,4)=F(-PLANCO(L,1,3))
      PLANCO(L,2,1)=F(CT*CP)
      PLANCO(L,2,2)=F(-SP)
      PLANCO(L,2,3)=F(F(ST*CP)*TANG)
      PLANCO(L,2,4)=F(-PLANCO(L,2,3))
      PLANCO(L,3,1)=F(ST)
      PLANCO(L,3,2)=0.
      PLANCO(L,3,3)=F(-CT*TANG)
      PLANCO(L,3,4)=F(-PLANCO(L,3,3))
      PLANCO(L,4,1)=F(F(-R(1)*F(CT*SP))+F(R(2)*F(CT*CP))+F(R(3)*ST))
      PLANCO(L,4,2)=F(F(-R(1)*CP)+F(-R(2)*SP))
      PLANCO(L,4,3)=F(F(F(-R(1)*F(ST*SP))+F(R(2)*F(ST*CP))-F(R(3)*CT))
     1*TANG)
      PLANCO(L,4,4)=F(-PLANCO(L,4,3))
      PLANCO(L,5,1)=F(PI2T*A)
      PLANCO(L,5,2)=F(-PI2T*B)
 1300 CONTINUE
      IF(NNN-1)1310,1302,1310
 1302 NNN=101
      MMM=K2+100
      GO TO 990
 1310 IF(MXM)1314,1312,1314
 1312 MXM=4
      IF(NS)1270,1270,1280
C
 1280 PRINT 1285
 1285 FORMAT (////////,5X,31HTABLE OF STARS THAT CAN BE SEEN,//,3X,6HNUMB
     1ER,9X,10HT.T. NO. 1,10X,10HT.T. NO. 2,/)
C
      PRINT 1295,((SEENS(J,K),K=1,3),J=1,NS)
C
 1270 PRINT 1275
 1275 FORMAT (////////,5X,33HTABLE OF PLANETS THAT CAN BE SEEN,//,3X,6HNU
     1MBER,9X,10HT.T. NO. 1,10X,10HT.T. NO. 2,/)
C
      PRINT 1295,((SEENP(J,K),K=1,3),J=1,NP)
 1295 FORMAT(///,(3X,F5.0,2X,2E20.8))
C
      PRINT 6005,VEH
 6005 FORMAT (//,13HVEHICLE STATE,/,6E15.7)
C
 1314 DO 1410 J=1,2
```

```
      L=J+1
      DO 1400 I=1,NS
 1400 SAVES(I,J)=SEENS(I,L)
      DO 1410 I=1,NP
 1410 SAVEP(I,J)=SEENP(I,L)
      DO 1450 K=1,NR
      DO 1440 N=2,3
      DO 1430 I=1,NS
      QQ=XNORMAL(ZQZ)
 1430 SEENS(I,N)=SAVES(I,N-1)+TTCONST*QQ
      DO 1440 I=1,NP
      QQ=XNORMAL(ZQZ)
 1440 SEENP(I,N)=SAVEP(I,N-1)+TTCONST*QQ
      CALL NAVIG (NP,NS)
      DO 1450 M=1,6
 1450 DELTA(K,M)=ERR(M)
      CALL STATIS (VEH(1))
 6200 CONTINUE
      STOP
      END


      SUBROUTINE STATIS (V)
      DIMENSION X(100),BELTA(6)
      DIMENSION VEH(6),PAREF(100,7,4),PLANCO(9,5,4),ERR(6),SEENS(100,3),
     1SEENP(9,3),PMAG(9),FN(69),STARPOS(100,2),PLANPOS(9,2),DELTA(100,6)
      COMMON PI,K1,K2,K3,NTAPE,ISHIFT,VEH,ISIG,NR,PAREF,PLANCO,T,ERR,FN,
     1SEENS,SEENP,PMAG,STARPOS,PLANPOS,DELTA
C
      TOT=NR
      DO 140 I=1,6
      DO 40 J=1,NR
   40 X(J)=DELTA(J,I)
      XMEAN=0.
      XSIG2=0.
      XSIG3=0.
      XSIG4=0.
      DO 70 J=1,NR
      XMEAN=XMEAN+X(J)
      ZQ=X(J)*X(J)
      ZR=ZQ*X(J)
      XSIG2=XSIG2+ZQ
      XSIG3=XSIG3+ZR
   70 XSIG4=XSIG4+ZR*X(J)
      XMEAN=XMEAN/TOT
      XSIG2=XSIG2/TOT
      XSIG3=XSIG3/TOT
      XSIG4=XSIG4/TOT
      XMEAN2=XMEAN**2
      U2=XSIG2-XMEAN2
      U3=XSIG3-3.*XSIG2*XMEAN+2.*XMEAN2*XMEAN
      U4=XSIG4-4.*XSIG3*XMEAN+6.*XSIG2*XMEAN2-3.*XMEAN2**2
      SIGMA=SQRTF(U2)
      G1=U3/(SIGMA*U2)
      G2=U4/(U2*U2)-3.
```

```
      BELTA(I)=SIGMA
  140 CONTINUE
      SIGMAA=SQRTF(BELTA(1)**2+BELTA(2)**2+BELTA(3)**2)
      SIGMAP=SQRTF(BELTA(4)**2+BELTA(5)**2+BELTA(6)**2)
C
      PRINT 155,(BELTA(I),I=1,3),SIGMAA
  155 FORMAT (/,19HSTANDARD DEVIATIONS,1P,3E15.4,5X,14HSIGMA ATTITUDE,
     1E15.4,/)
C
      PRINT 145, (BELTA(I),I=4,6),SIGMAP
  145 FORMAT (/,19HSTANDARD DEVIATIONS,1P,3E15.4,5X,14HSIGMA POSITION,E1
     15.4,///)
C
      END


      SUBROUTINE NAVIG  (NP,NS)
      DIMENSION A(20),B(20),C(20),D(20),XM(3,4),SOL(3),PSI(100,2),
     1FF(4,200)
      DIMENSION VEH(6),PAREF(100,7,4),PLANCO(9,5,4),ERR(6),SEENS(100,3),
     1SEENP(9,3),PMAG(9),FN(69),STARPOS(100,2),PLANPOS(9,2),DELTA(100,6)
      COMMON PI,K1,K2,K3,NTAPE,ISHIFT,VEH,ISIG,NR,PAREF,PLANCO,T,ERR,FN,
     1SEENS,SEENP,PMAG,STARPOS,PLANPOS,DELTA
C
      IF(NP-2)10,20,20
C
   10 PRINT 15,NP
   15 FORMAT(///,3X,31HHALT IN NAVIG,  WE CAN ONLY SEE,I3,9H PLANETS.)
C
      GO TO 192
   20 Q=F(F(2.*PI)/T)
      DO 30 I=1,NP
      DO 30 J=1,2
   30 PSI(I,J)=F(Q*F(SEENP(I,J+1)-VEH(3)))
      DO 40 I=1,NP
      DO 40 J=1,2
      K=2*I+J-2
      CPSI=F(COSF(PSI(I,J)))
      SPSI=F(SINF(PSI(I,J)))
      DENOM=F(F(PLANCO(I,5,1)*CPSI)+F(PLANCO(I,5,2)*SPSI))
      A(K)=F(F(F(PLANCO(I,1,1)*CPSI)+F(PLANCO(I,1,2)*SPSI)
     1+PLANCO(I,1,J+2))/DENOM)
      B(K)=F(F(F(PLANCO(I,2,1)*CPSI)+F(PLANCO(I,2,2)*SPSI)
     1+PLANCO(I,2,J+2))/DENOM)
      C(K)=F(F(F(PLANCO(I,3,1)*CPSI)+PLANCO(I,3,J+2))/DENOM)
   40 D(K)=F(F(F(PLANCO(I,4,1)*CPSI)+F(PLANCO(I,4,2)*SPSI)
     1+PLANCO(I,4,J+2))/DENOM)
C     FORM THE MATRIX ELEMENTS XM
      NPTT=2*NP
      DO 50 I=1,3
      DO 50 J=1,4
   50 XM(I,J)=0.
      DO 60 I=1,NPTT
      XM(1,1)=F(XM(1,1)+F(A(I)*A(I)))
      XM(1,2)=F(XM(1,2)+F(A(I)*B(I)))
```

```
      XM(1,3)=F(XM(1,3)+F(A(I)*C(I)))
      XM(2,2)=F(XM(2,2)+F(B(I)*B(I)))
      XM(2,3)=F(XM(2,3)+F(B(I)*C(I)))
      XM(3,3)=F(XM(3,3)+F(C(I)*C(I)))
      XM(1,4)=F(XM(1,4)+F(A(I)*D(I)))
      XM(2,4)=F(XM(2,4)+F(B(I)*D(I)))
   60 XM(3,4)=F(XM(3,4)+F(C(I)*D(I)))
      XM(2,1)=XM(1,2)
      XM(3,1)=XM(1,3)
      XM(3,2)=XM(2,3)
      CALL GAUSS2 (3,1,1,E-12,XM,SOL,IERR)
      IF(IERR-1)70,80,70
C
   70 PRINT 75
   75 FORMAT (/,7HSTOP 11,/)
C
      GO TO 192
   80 DO 90 I=1,3
   90 ERR(I+3)=F(F(SOL(I))-VEH(I+3))
      IF(NS)192,192,92
   92 IF(NS-2)110,120,120
C
  110 PRINT 115,NS
  115 FORMAT(///,3X,31HHALT IN NAVIG,  WE CAN ONLY SEE,I3,7H STARS.)
C
      STOP
  120 DO 130 I=1,NS
      DO 130 J=1,2
  130 PSI(I,J)=F(Q*F(SEENS(I,J+1)-VEH(3)))
      DO 140 I=1,NS
      DO 140 J=1,2
      CPSI=F(COSF(PSI(I,J)))
      SPSI=F(SINF(PSI(I,J)))
      K=2*I+J-2
      DO 140 L=1,4
  140 FF(L,K)=F(F(PAREF(I,L,1)*CPSI)+F(PAREF(I,L,2)*SPSI)
     1+PAREF(I,L,J+2))
C     FORM THE MATRIX ELEMENTS XM
      NSTT=2*NS
      DO 150 I=1,3
      DO 150 J=1,4
  150 XM(I,J)=0.
      DO 160 J=1,4
      IF(J-4)158,156,158
  156 L=1
      GO TO 159
  158 L=J+1
  159 DO 160 I=1,3
      DO 160 K=1,NSTT
  160 XM(I,J)=F(XM(I,J)+F(F(FF(I+1,K)*FF(L,K))/F(FF(4,K)**2)))
      DO 162 I=1,3
  162 XM(I,4)=F(-XM(I,4))
      CALL GAUSS2 (3,1,1,E-12,XM,SOL,IERR)
      IF(IERR-1)170,180,170
C
  170 PRINT 175
```

```
  175 FORMAT (/,7HSTOP 12,/)
C
      GO TO 192
  180 DO 190 I=1,3
  190 ERR(I)=F(SOL(I))
  192 END


      SUBROUTINE   GAUSS2(N,M,EP,A,X,KER)
      DIMENSION A(3,4),X(3)
      NPM=N+M
   10 DO 34 L=1,N
      KP=0
      Z=0.0
      DO 12 K=L,N
      IF(Z-ABSF(A(K,L)))11,12,12
   11 Z=ABSF(A(K,L))
      KP=K
   12 CONTINUE
      IF(L-KP)13,20,20
   13 DO 14 J=L,NPM
      Z=A(L,J)
      A(L,J)=A(KP,J)
   14 A(KP,J)=Z
   20 IF(ABSF(A(L,L))-EP)50,50,30
   30 IF(L-N)31,40,40
   31 LP1=L+1
      DO 34 K=LP1,N
      IF(A(K,L))32,34,32
   32 RATIO=A(K,L)/A(L,L)
      DO 33 J=LP1,NPM
   33 A(K,J)=A(K,J)-RATIO*A(L,J)
   34 CONTINUE
   40 DO 43 I=1,N
      II=N+1-I
      DO 43 J=1,M
      JPN=J+N
      S=0.0
      IF(II-N)41,43,43
   41 IIP1=II+1
      DO 42 K=IIP1,N
   42 S=S+A(II,K)*X(K,J)
   43 X(II,J)=(A(II,JPN)-S)/A(II,II)
      KER=1
      GO TO 75
   50 KER=2
   75 CONTINUE
      END


      FUNCTION XNORMAL (R)
      DIMENSION VEH(6),PAREF(100,7,4),PLANCO(9,5,4),ERR(6),SEENS(100,3),
     1SEENP(9,3),PMAG(9),FN(69),STARPOS(100,2),PLANPOS(9,2),DELTA(100,6)
      COMMON PI,K1,K2,K3,NTAPE,ISHIFT,VEH,ISIG,NR,PAREF,PLANCO,T,ERR,FN,
```

```
     1SEENS,SEENP,PMAG,STARPOS,PLANPOS,DELTA
C
      IF(M)2,1,2
    1 M=2
B     X=3625176463724015
B     Y=3625176463724015
B     Z=200000000000000
    2 LDA (X)        MUI (Y)
      STA (X)        ARS (12)
      ADD (Z)        FAD (Z)
      STA (R)
      IF(R-.0003)3,6,4
    3 R=.0003
      GO TO 6
    4 IF(.9997-R)5,6,6
    5 R=.9997
    6 DO 7 I=1,69
      IF(R-FN(I))8,9,7
    7 CONTINUE
    8 I=I-1
      XNORMAL=.1*(FLOATF(I-35)+(R-FN(I))/(FN(I+1)-FN(I)))
      RETURN
    9 XNORMAL=.1*FLOATF(I-35)
      END



      FUNCTION F(X)
C     F FUNCTION FIRST RIGHT SHIFTS A QUANTITY (TO DROP OFF RIGHT-HAND
C     BITS) ISHIFT PLACES AND THEN LEFT SHIFTS TO TRUNCATE.
      DIMENSION VEH(6),PAREF(100,7,4),PLANCO(9,5,4),ERR(6),SEENS(100,3),
     1SEENP(9,3),PMAG(9),FN(69),STARPOS(100,2),PLANPOS(9,2),DELTA(100,6)
      COMMON PI,K1,K2,K3,NTAPE,ISHIFT,VEH,ISIG,NR,PAREF,PLANCO,T,ERR,FN,
     1SEENS,SEENP,PMAG,STARPOS,PLANPOS,DELTA
C
      I=ISHIFT
      LDA (X)     ARS1(N)
      ALS1(N)     STA (F)
      F=F+0.0
      END



      SUBROUTINE FILLTAB
      DIMENSION VEH(6),PAREF(100,7,4),PLANCO(9,5,4),ERR(6),SEENS(100,3),
     1SEENP(9,3),PMAG(9),FN(69),STARPOS(100,2),PLANPOS(9,2),DELTA(100,6)
      COMMON PI,K1,K2,K3,NTAPE,ISHIFT,VEH,ISIG,NR,PAREF,PLANCO,T,ERR,FN,
     1SEENS,SEENP,PMAG,STARPOS,PLANPOS,DELTA
C
      FN(1) =.0003
      FN(2) =.0005
      FN(3) =.0007
      FN(4) =.0010
      FN(5) =.0013
      FN(6) =.0019
      FN(7) =.0026
```

```
FN(8) =.0035
FN(9) =.0047
FN(10)=.0062
FN(11)=.0082
FN(12)=.0107
FN(13)=.0139
FN(14)=.0179
FN(15)=.0228
FN(16)=.0287
FN(17)=.0359
FN(18)=.0446
FN(19)=.0548
FN(20)=.0668
FN(21)=.0808
FN(22)=.0968
FN(23)=.1151
FN(24)=.1357
FN(25)=.1587
FN(26)=.1841
FN(27)=.2119
FN(28)=.2420
FN(29)=.2743
FN(30)=.3085
FN(31)=.3446
FN(32)=.3821
FN(33)=.4207
FN(34)=.4602
FN(35)=.5000
FN(36)=.5398
FN(37)=.5793
FN(38)=.6179
FN(39)=.6554
FN(40)=.6915
FN(41)=.7257
FN(42)=.7580
FN(43)=.7881
FN(44)=.8159
FN(45)=.8413
FN(46)=.8643
FN(47)=.8849
FN(48)=.9032
FN(49)=.9192
FN(50)=.9332
FN(51)=.9452
FN(52)=.9554
FN(53)=.9641
FN(54)=.9713
FN(55)=.9772
FN(56)=.9821
FN(57)=.9861
FN(58)=.9893
FN(59)=.9918
FN(60)=.9938
FN(61)=.9953
FN(62)=.9965
FN(63)=.9974
```

```
FN(64)=.9981
FN(65)=.9987
FN(66)=.9990
FN(67)=.9993
FN(68)=.9995
FN(69)=.9997
STARPOS(  1,  1)=   1.7620189629
STARPOS(  1,  2)=   -.2910045640
STARPOS(  2,  1)=   1.6723963058
STARPOS(  2,  2)=   -.9194200574
STARPOS(  3,  1)=   3.8290196683
STARPOS(  3,  2)=  -1.0596427184
STARPOS(  4,  1)=   3.7275578611
STARPOS(  4,  2)=    .3375127404
STARPOS(  5,  1)=   4.8691268192
STARPOS(  5,  2)=    .6763975035
STARPOS(  6,  1)=   1.3721269524
STARPOS(  6,  2)=    .8023278571
STARPOS(  7,  1)=   1.3661273831
STARPOS(  7,  2)=   -.1437230158
STARPOS(  8,  1)=   1.9972311685
STARPOS(  8,  2)=    .0925606280
STARPOS(  9,  1)=    .4214824699
STARPOS(  9,  2)=  -1.0016202170
STARPOS( 10,  1)=   3.6725581731
STARPOS( 10,  2)=  -1.0512021122
STARPOS( 11,  1)=   1.5426383481
STARPOS( 11,  2)=    .1292125423
STARPOS( 12,  1)=   5.1893874649
STARPOS( 12,  2)=    .1533708080
STARPOS( 13,  1)=   1.1964013856
STARPOS( 13,  2)=    .2871115101
STARPOS( 14,  1)=   3.2502975773
STARPOS( 14,  2)=  -1.0983938759
STARPOS( 15,  1)=   4.3090579346
STARPOS( 15,  2)=   -.4601948424
STARPOS( 16,  1)=   3.5064028283
STARPOS( 16,  2)=   -.1920831805
STARPOS( 17,  1)=   6.0039108101
STARPOS( 17,  2)=   -.5197881401
STARPOS( 18,  1)=   2.0223275487
STARPOS( 18,  2)=    .4904423679
STARPOS( 19,  1)=   5.4122878271
STARPOS( 19,  2)=    .7884088563
STARPOS( 20,  1)=   3.3421091681
STARPOS( 20,  2)=  -1.0389120854
STARPOS( 21,  1)=   2.6475553922
STARPOS( 21,  2)=    .2114369426
STARPOS( 22,  1)=   1.8214546961
STARPOS( 22,  2)=   -.5049237526
STARPOS( 23,  1)=   1.9752254755
STARPOS( 23,  2)=    .5577296588
STARPOS( 24,  1)=   4.5883251592
STARPOS( 24,  2)=   -.6472359606
STARPOS( 25,  1)=   1.4116295712
STARPOS( 25,  2)=    .1103823789
```

```
STARPOS( 26, 1)=   1.4154329346
STARPOS( 26, 2)=    .4988829741
STARPOS( 27, 1)=   2.4124013643
STARPOS( 27, 2)=  -1.2146328041
STARPOS( 28, 1)=   3.2702597805
STARPOS( 28, 2)=   -.9938922870
STARPOS( 29, 1)=   1.4603533462
STARPOS( 29, 2)=   -.0212833206
STARPOS( 30, 1)=   5.7872936333
STARPOS( 30, 2)=   -.8221809774
STARPOS( 31, 1)=   3.3716052324
STARPOS( 31, 2)=    .9795224095
STARPOS( 32, 1)=   1.4802355552
STARPOS( 32, 2)=   -.0341551238
STARPOS( 33, 1)=    .8821330372
STARPOS( 33, 2)=    .8684079619
STARPOS( 34, 1)=   4.8091674873
STARPOS( 34, 2)=   -.6004078071
STARPOS( 35, 1)=   2.8880472187
STARPOS( 35, 2)=   1.0805963657
STARPOS( 36, 1)=   2.1319560424
STARPOS( 36, 2)=   -.8246195902
STARPOS( 37, 1)=   1.8638880136
STARPOS( 37, 2)=   -.4597924470
STARPOS( 38, 1)=   3.6056684294
STARPOS( 38, 2)=    .8632786331
STARPOS( 39, 1)=   4.6040040338
STARPOS( 39, 2)=   -.7501570569
STARPOS( 40, 1)=   1.5591317096
STARPOS( 40, 2)=    .7844721693
STARPOS( 41, 1)=   1.7277886930
STARPOS( 41, 2)=    .2866945703
STARPOS( 42, 1)=   2.2858431768
STARPOS( 42, 2)=   -.9529158346
STARPOS( 43, 1)=   4.3871905076
STARPOS( 43, 2)=  -1.2038505478
STARPOS( 44, 1)=   5.3375804627
STARPOS( 44, 2)=   -.9919287916
STARPOS( 45, 1)=   2.1899518789
STARPOS( 45, 2)=  -1.0369437418
STARPOS( 46, 1)=   1.6640696309
STARPOS( 46, 2)=   -.3131072197
STARPOS( 47, 1)=    .5474879697
STARPOS( 47, 2)=    .4070350222
STARPOS( 48, 1)=    .6013822826
STARPOS( 48, 2)=   -.0543330692
STARPOS( 49, 1)=    .4804818709
STARPOS( 49, 2)=   1.5555731772
STARPOS( 50, 1)=   2.6979372299
STARPOS( 50, 2)=    .3489640395
STARPOS( 51, 1)=    .1836231817
STARPOS( 51, 2)=   -.3167918037
STARPOS( 52, 1)=   3.8867246167
STARPOS( 52, 2)=   1.2963966314
STARPOS( 53, 1)=   2.4701354014
STARPOS( 53, 2)=   -.1488329520
```

```
STARPOS( 54, 1)=   1.5111642440
STARPOS( 54, 2)=   -.1689236309
STARPOS( 55, 1)=    .0298014970
STARPOS( 55, 2)=    .5048364862
STARPOS( 56, 1)=   4.5969281781
STARPOS( 56, 2)=    .2195721162
STARPOS( 57, 1)=   3.6866080735
STARPOS( 57, 2)=   -.6322164327
STARPOS( 58, 1)=    .2969023224
STARPOS( 58, 2)=    .6189325379
STARPOS( 59, 1)=   4.9454122521
STARPOS( 59, 2)=   -.4596470029
STARPOS( 60, 1)=   3.2503484826
STARPOS( 60, 2)= -1.0984035722
STARPOS( 61, 1)=    .8124944000
STARPOS( 61, 2)=    .7128215553
STARPOS( 62, 1)=   3.5025412873
STARPOS( 62, 2)=    .9613515927
STARPOS( 63, 1)=   3.0871820141
STARPOS( 63, 2)=    .2572615318
STARPOS( 64, 1)=    .2394519012
STARPOS( 64, 2)=   1.0568792804
STARPOS( 65, 1)=   3.3154783525
STARPOS( 65, 2)=   -.8516431048
STARPOS( 66, 1)=    .5325290436
STARPOS( 66, 2)=    .7363010819
STARPOS( 67, 1)=   5.9379737254
STARPOS( 67, 2)=   -.8210416652
STARPOS( 68, 1)=   1.4419619392
STARPOS( 68, 2)=    .0060989561
STARPOS( 69, 1)=    .1692605764
STARPOS( 69, 2)=    .9838954289
STARPOS( 70, 1)=   4.6945284442
STARPOS( 70, 2)=    .8986991207
STARPOS( 71, 1)=   4.0727985316
STARPOS( 71, 2)=    .4680003427
STARPOS( 72, 1)=   5.3282647679
STARPOS( 72, 2)=    .7009145313
STARPOS( 73, 1)=   2.1054343099
STARPOS( 73, 2)=   -.6966918042
STARPOS( 74, 1)=   2.3862650588
STARPOS( 74, 2)=   -.7559117953
STARPOS( 75, 1)=   2.4272657518
STARPOS( 75, 2)= -1.0323428600
STARPOS( 76, 1)=    .0330012673
STARPOS( 76, 2)=   1.0294776111
STARPOS( 77, 1)=   4.3991751018
STARPOS( 77, 2)=   -.5976104322
STARPOS( 78, 1)=   4.1824852028
STARPOS( 78, 2)=   -.3933584283
STARPOS( 79, 1)=   3.5690746929
STARPOS( 79, 2)=   -.9305174426
STARPOS( 80, 1)=   2.8799896152
STARPOS( 80, 2)=    .9868721849
STARPOS( 81, 1)=    .1082249580
STARPOS( 81, 2)=   -.7412267889
```

```
STARPOS( 82,  1)=   5.6841519471
STARPOS( 82,  2)=    .1699320434
STARPOS( 83,  1)=   4.6269042081
STARPOS( 83,  2)=   -.6809741446
STARPOS( 84,  1)=   3.8117627252
STARPOS( 84,  2)=   -.7335134032
STARPOS( 85,  1)=   3.8557668390
STARPOS( 85,  2)=    .4747198603
STARPOS( 86,  1)=   1.9325449030
STARPOS( 86,  2)=   -.5103924509
STARPOS( 87,  1)=   3.1078205325
STARPOS( 87,  2)=    .9400634240
STARPOS( 88,  1)=   5.5757306392
STARPOS( 88,  2)=   1.0901035620
STARPOS( 89,  1)=   4.4883541542
STARPOS( 89,  2)=   -.2738373115
STARPOS( 90,  1)=   2.4486314907
STARPOS( 90,  2)=   -.9578754786
STARPOS( 91,  1)=   5.4323227525
STARPOS( 91,  2)=    .5909151552
STARPOS( 92,  1)=   6.0356321694
STARPOS( 92,  2)=    .2625605453
STARPOS( 93,  1)=   3.8393825608
STARPOS( 93,  2)=   -.8248619971
STARPOS( 94,  1)=   6.0314942845
STARPOS( 94,  2)=    .4872862309
STARPOS( 95,  1)=   4.2048835949
STARPOS( 95,  2)=   -.3442710431
STARPOS( 96,  1)=    .7884961228
STARPOS( 96,  2)=    .0693429008
STARPOS( 97,  1)=   2.9344002547
STARPOS( 97,  2)=    .3610795334
STARPOS( 98,  1)=   4.3436954480
STARPOS( 98,  2)=   -.1834001674
STARPOS( 99,  1)=   4.9772645110
STARPOS( 99,  2)=   -.5222946268
STARPOS(100,  1)=   3.2038209136
STARPOS(100,  2)=   -.3032606538
PLANPOS(1,1)=2.032716
PLANPOS(1,2)=.387099
PLANPOS(2,1)=5.009707
PLANPOS(2,2)=.723332
PLANPOS(3,1)=1.974492
PLANPOS(3,2)=1.0
PLANPOS(4,1)=.481677
PLANPOS(4,2)=1.52369
PLANPOS(5,1)=3.550211
PLANPOS(5,2)=5.2028
PLANPOS(6,1)=.662074
PLANPOS(6,2)=9.540
PLANPOS(7,1)=3.238145
PLANPOS(7,2)=19.18
PLANPOS(8,1)=4.162384
PLANPOS(8,2)=30.07
PLANPOS(9,1)=3.222018
PLANPOS(9,2)=39.44
```

```
      END


      FUNCTION ALPH(X,Y)
C     ALPH COMPUTES THE ARC TANGENT OF THE QUOTIENT OF TWO NUMBERS AND
C     RESOLVES THE ANGLE TO THE PROPER QUADRANT BY EXAMINING THE
C     NUMERATOR AND DENOMINATOR SIGNS.
C
      PI=3.1415926536
      IF(Y)10,30,20
   10 IF(X)11,12,11
   11 ALPH=PI+ATANF(X/Y)
      RETURN
   12 ALPH=PI
      RETURN
   20 IF(X)21,23,22
   21 ALPH=2.*PI+ATANF(X/Y)
      RETURN
   22 ALPH=ATANF(X/Y)
      RETURN
   23 ALPH=0.0
      RETURN
   30 IF(X)31,33,32
   31 ALPH=1.5*PI
      RETURN
   32 ALPH=.5*PI
      RETURN
   33 ALPH=2.*PI
      END
      END
```

```
  T ZERO          K3     NTAPE   ISHIFT
  2440600.50       1       4       0

   THETA       PHI         TO           X           Y            Z        PERIOD     TIME
   .174500     .785400     .000000      .900000     1.000000     .000000   50.       2440600.50

  SIGMA   NR    GAMMA        H
   10     50    .52360000    .26180000

  NUMBER OF STARS AND PLANETS CONSIDERED
               0      6


VEHICLE STATE
  .1745000E+00   .7854000E+00   .0000000E+00   .5000000E+00   .5000000E+00   .0000000E+00


  TABLE OF STARS THAT CAN BE SEEN

  NUMBER         T.T. NO. 1        T.T. NO. 2

  TABLE OF PLANETS THAT CAN BE SEEN

  NUMBER         T.T. NO. 1        T.T. NO. 2


     101.         .21016498E+02      .20163623E+02
     102.        -.21109316E+02     -.20274133E+02
     103.         .16054574E+02      .14531063E+02
     104.        -.47231380E+01     -.38883937E+01
     105.         .22552818E+02      .22131287E+02
     106.        -.11497437E+01     -.93786311E+00
STANDARD DEVIATIONS     3.1713E-05     1.9184E-05     2.7113E-05     SIGMA POSITION     4.5922E-05


VEHICLE STATE
  .1745000E+00   .7854000E+00   .0000000E+00   .5000000E+00   .6250000E+00   .0000000E+00
STANDARD DEVIATIONS     2.9497E-05     1.3686E-05     2.5589E-05     SIGMA POSITION     4.1379E-05


VEHICLE STATE
  .1745000E+00   .7854000E+00   .0000000E+00   .5000000E+00   .7500000E+00   .0000000E+00
STANDARD DEVIATIONS     3.6387E-05     1.9791E-05     2.1517E-05     SIGMA POSITION     4.6677E-05


VEHICLE STATE
  .1745000E+00   .7854000E+00   .0000000E+00   .5000000E+00   .8750000E+00   .0000000E+00
STANDARD DEVIATIONS     4.1696E-05     1.6771E-05     2.3896E-05     SIGMA POSITION     5.1472E-05
```

Figure 3. Example of Output from Program ABLE

APPENDIX F

INTERRUPT PROGRAM FOR DATA INPUT

The program presented in the following pages is fairly self-explanatory. Some general comments may, however, be in order. The symbols A and Q refer to the usual arithmetic registers: accumulator, quotient. I is the one index register used in the routine. "Left" and "right" refer to left and right shifts by the indicated number of places. Four index registers I_1, I_2, I_3, and I_4 are used to count the number of targets of each kind detected by each slit. I_1 and I_2 count planets in Slits #1 and #2 respectively. I_3 and I_4 do the same for stars. When certain maximum values are reached in any one index, the measurement sequence is terminated and control switched to the target identification program.

The operations $Q \cdot T_1$ and $Q \cdot T_2$ appear twice each. These are logical products; i.e., 1's are inserted into A where 1's exist both in Q and T_1 (or T_2), otherwise 0's. Also L(I) appears several times which means that the contents of I modify (or maybe even specify) the operand for that particular instruction. Finally, two registers, BIE and BII are used to tell whether and where camera data is stored in the buffer. BIE is an externally controlled counter which always contains the buffer address of the next location to be filled by the camera electronics. BII is an internal location which contains the buffer address of the next location to be emptied by the program herein given. Thus BIE-BII is the number of data words waiting to be accepted by the computer. If BIE = BII, then the interrupt program is terminated and control reverts back to the sequence

in operation at the time of interrupt.

On the following page is a general flow diagram for this interrupt program. By far the bulk of the task is in Star Data Processing and the reader is therefore referred to a somewhat more detailed diagram in Section IV-A of the body of this report. The pages following the general diagram contain the details of the program.

GENERAL FLOW CHART

FOR

DATA INPUT INTERRUPT PROGRAM

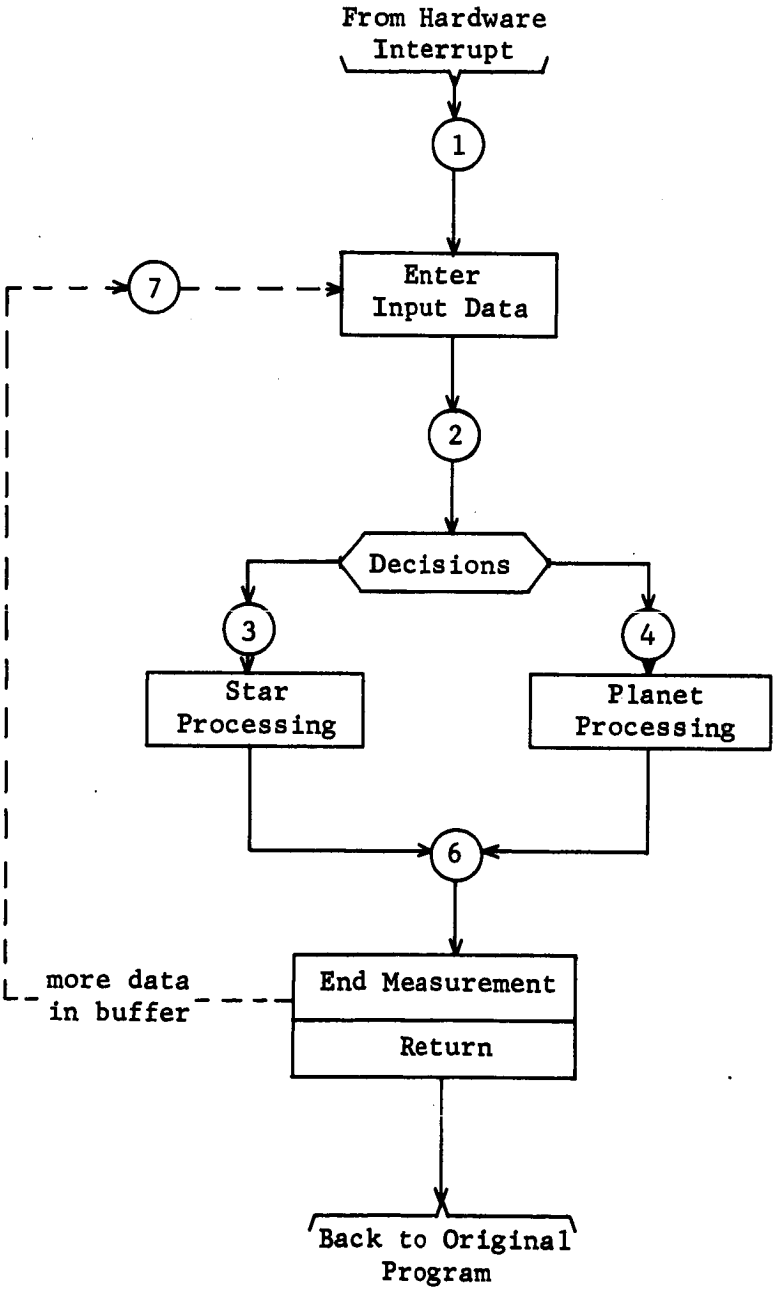

INPUT

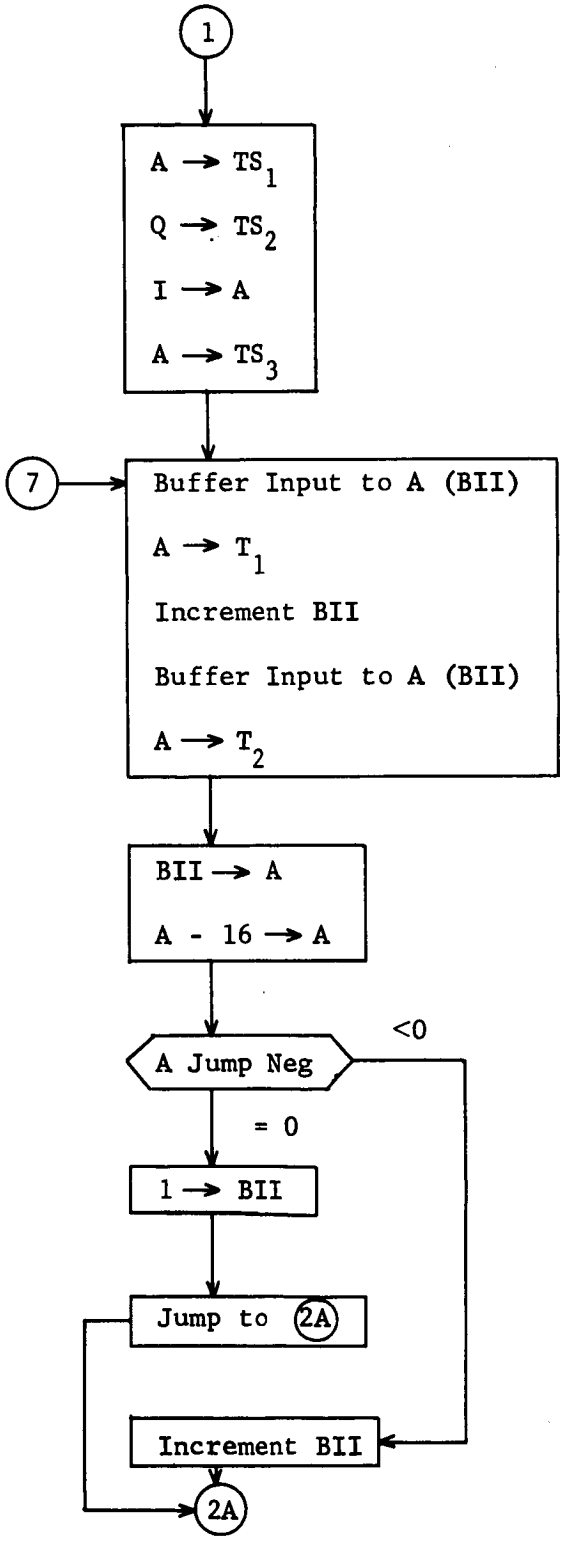

Computer Hardware exits from current program to 1. Store away constants of registers to be used.

Input two words from the buffer and store at T_1, T_2. Use BII index to hold the buffer address of the next word to come in.

Test the index register to see if it is about to exceed the buffer capacity. If it is, then reset to zero; otherwise increment.

DECISIONS

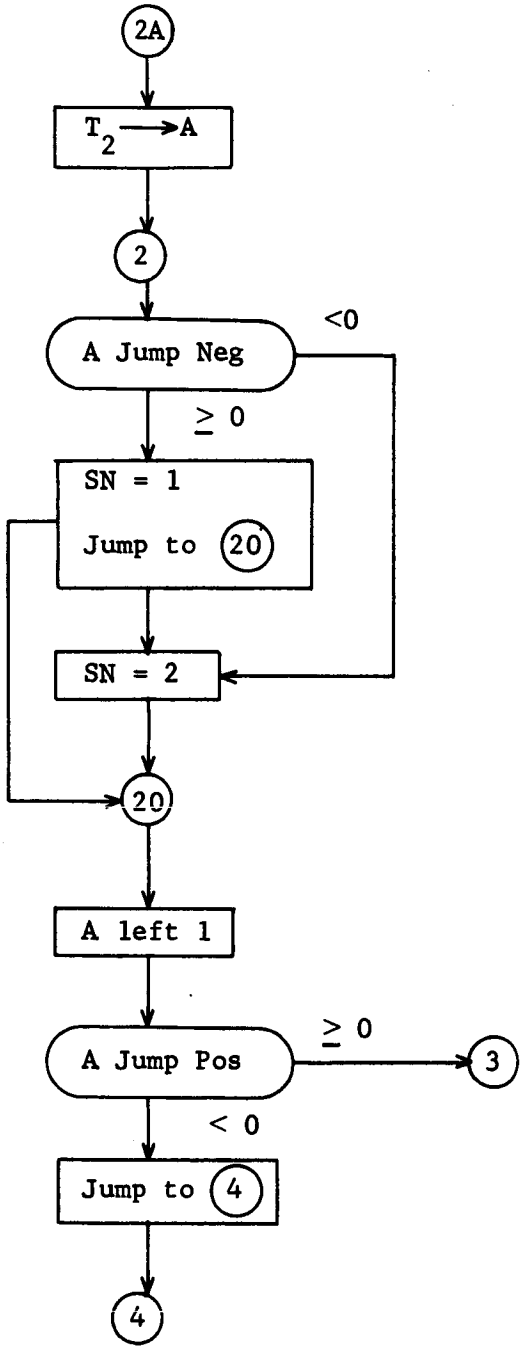

Restore second word to A

Test slit number; set SN accordingly.

Test target tag. Go to (3) for star, (4) for planet.

STAR DATA PROCESSING (1)

Separate Target Data

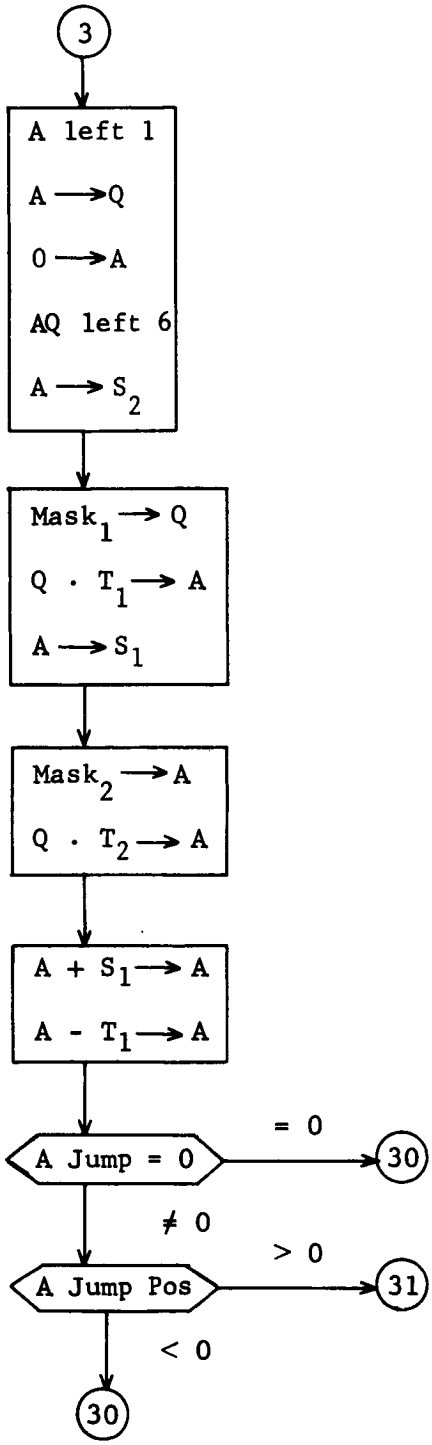

Separate out of the second word the 6-bit intensity code and store in the least significant bits of S_2.

Form from T_1 and T_2 a composite word whose lower 16 bits are identical to the lower 16 bits in T_2 and whose remaining upper bits are identical to the corresponding bits of T_1. This is the anode current fall time, except it may be deficient by 2^{16}.

If the difference between the composite word and T_1 is zero or negative, the composite needs 2^{16} added.

STAR DATA PROCESSING (2)

Closeness Testing

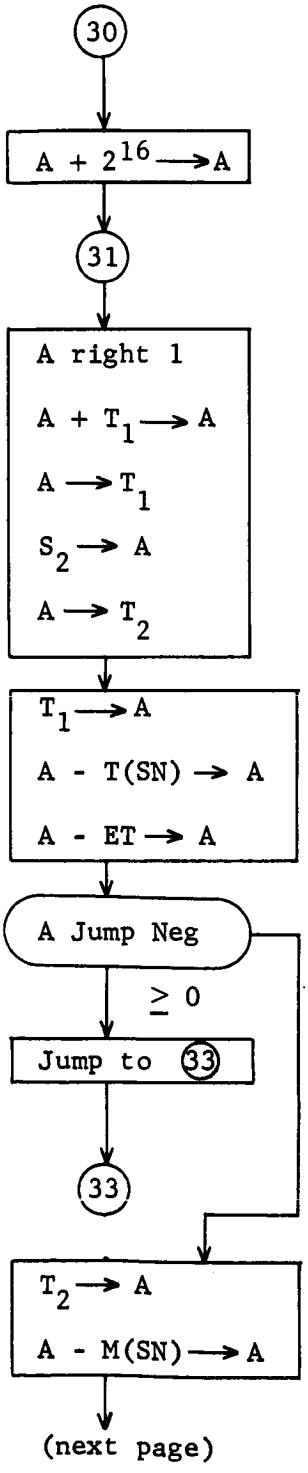

Correct composite word for 16-bit overflow.

Compute average transit time by:

$$\frac{\text{Fall - Rise}}{2} + \text{Rise} = \text{Average}$$

and store in T_1. Store magnitude in T_2.

Test that the present transit time and that of the previous target are not too close. If they are not ($A \geq 0$), go to (33).

If transit times are too close, test similarly for magnitudes. If close ($A < 0$), go to (34).

STAR DATA PROCESSING (3)

Closeness Testing

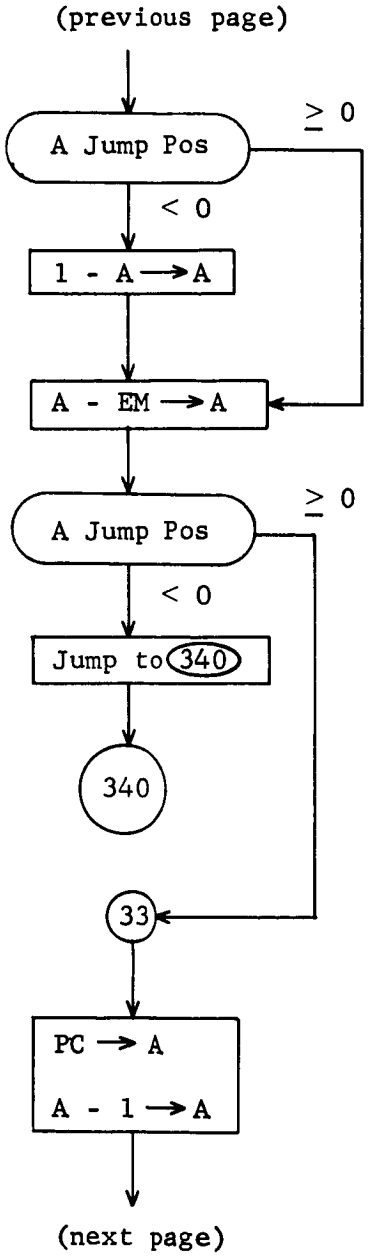

Set magnitude difference positive.

Test less than acceptable error.

Load period counter - 1 into A.

STAR DATA PROCESSING (4)

Period #1 Test, Test Slit #1 Data List Full

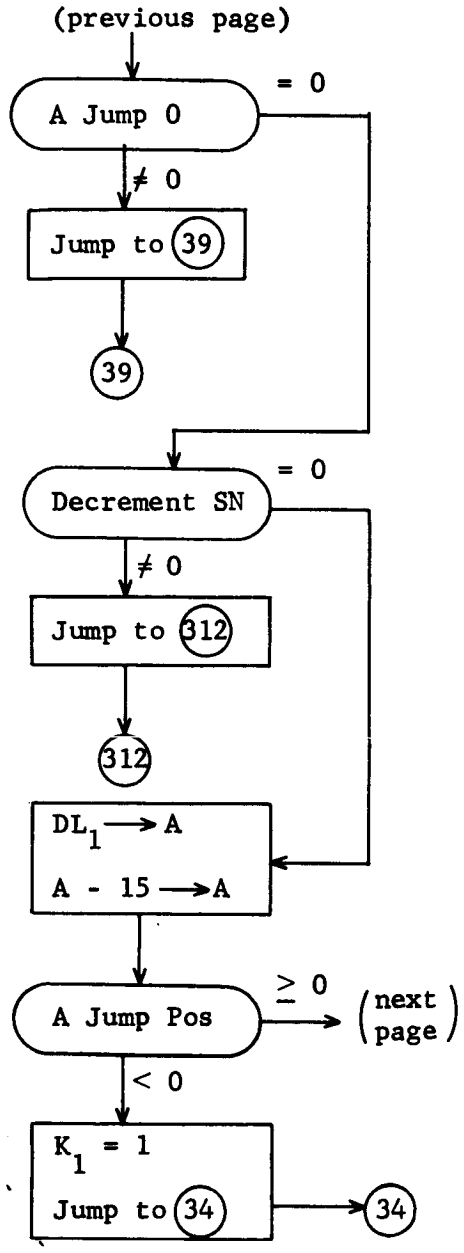

Test period counter for period #1. If not, got to (39).

For 1st period, test for slit. If #2, go to (312).

For slit #1, test whether fifteen targets have already been counted in the first period. If so, then all remaining 1st period targets go into the Odd Target List (set flag $K_1 = 1$ and go to (34)).

STAR DATA PROCESSING (5)

Test Slit #2 Data List Full

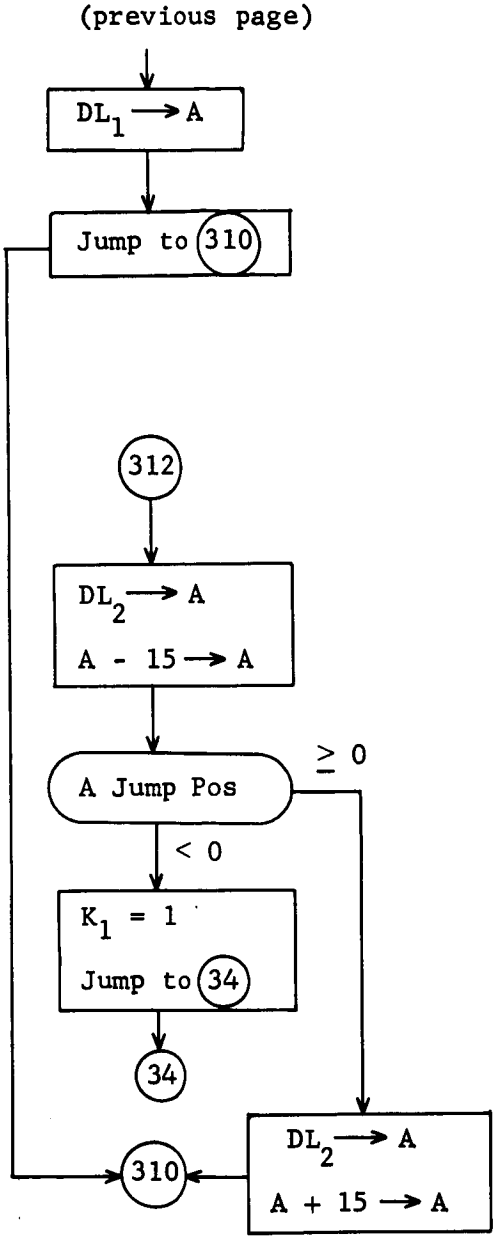

If 1st period of Data List not yet full, go to (310).

For slit #2, test whether fifteen targets have already been counted in the first period. If so, then all remaining 1st period targets go into the Odd Target List (set flag K_1 = 1 and to to (34)).

DL_2 is augmented by fifteen because the Data List is necessarily stored in a linear manner in the computer memory.

STAR DATA PROCESSING (6)

Store Previous Target in Data List (1st Period)

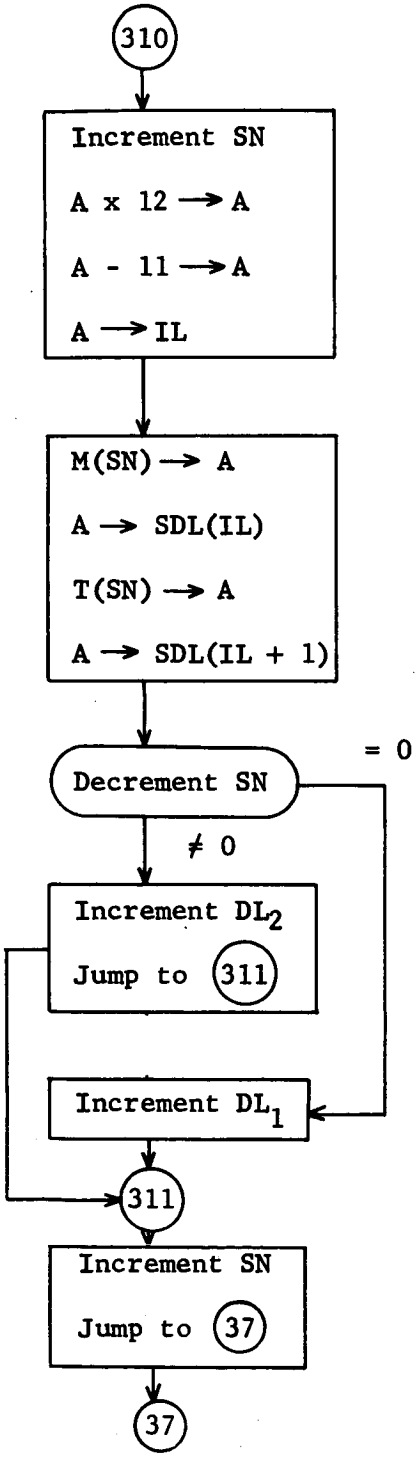

Reset the slit number tag. Set up index register IL for storage of data.

Store previous target magnitude and transit time in Star Data List.

Test slit number and increment appropriate DL counter.

Reset slit number tag.

STAR DATA PROCESSING (7)

Decisions, Store Odd Target List

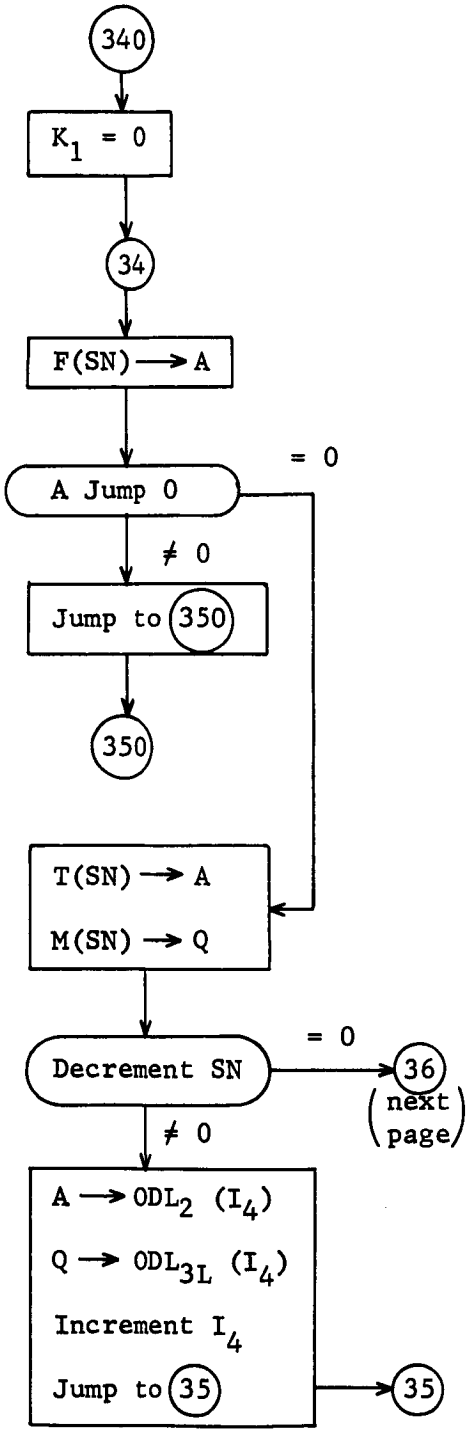

Flag $K_1 = 0$ specifies that sequence is coming from 'close' testing routine.

Test if previous target is already in the Odd Target List. If it is, to to 350.

If it is not, load present target data into A and Q registers.

Test slit number.

For slit #2, store previous target data in Odd Target Lists 2 and 3 (lower) according to index I_4.

STAR DATA PROCESSING (8)

Store Odd Target List

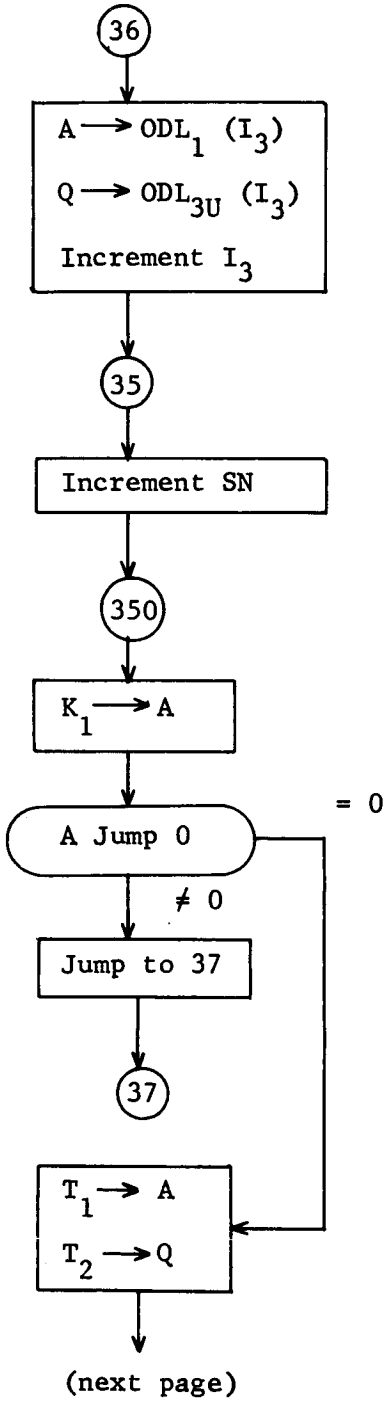

For slit #1, store previous target data in Odd Target Lists 1 and 3 (upper) according to index I_3.

Reset slit number tag.

Test whether sequence comes from 'close' routine. If from search routine, go to (37).

Load present data into A and Q registers.

STAR DATA PROCESSING (9)

Store Odd Target List

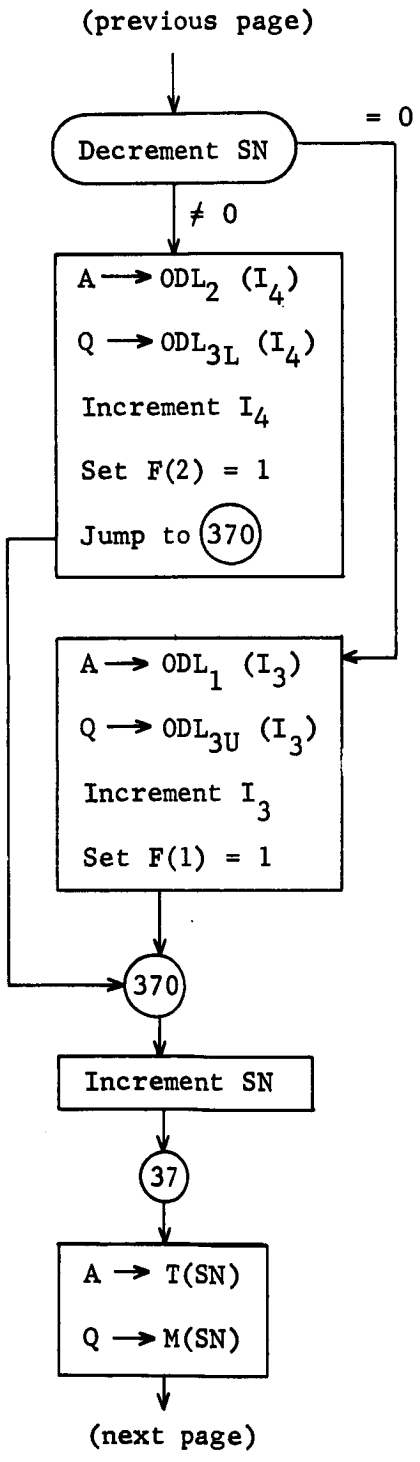

Test slit number.

For slit #2, store present target data in Odd Target Lists 2 and 3 (lower) according to index I_4.

For slit #1, store present target data in Odd Target Lists 1 and 3 (upper) according to index I_3.

Reset slit number tag.

Store present target data over previous target data.

STAR DATA PROCESSING (10)

Indexing

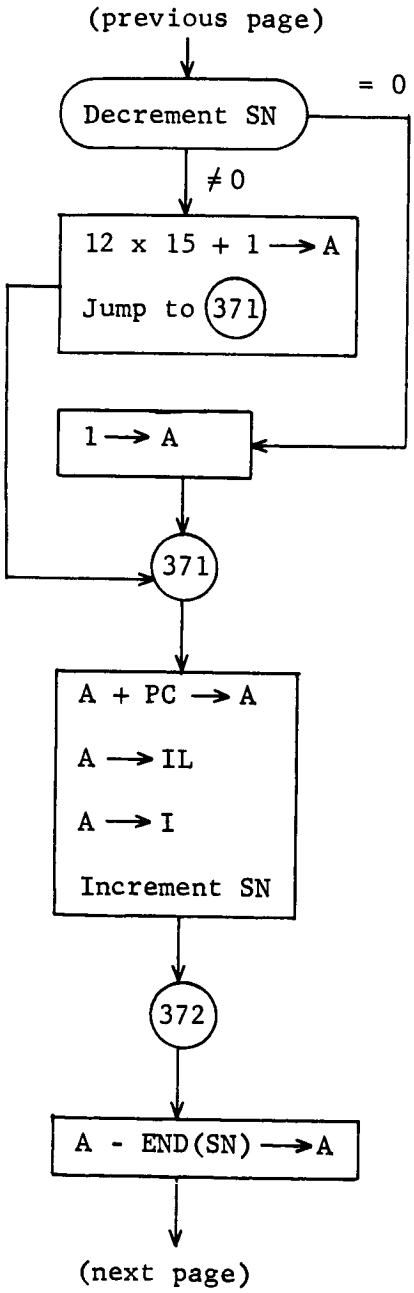

Test slit number.

Set up index I for location of data in Data List.

Reset slit number tag.

STAR DATA PROCESSING (11)

Period Change Testing

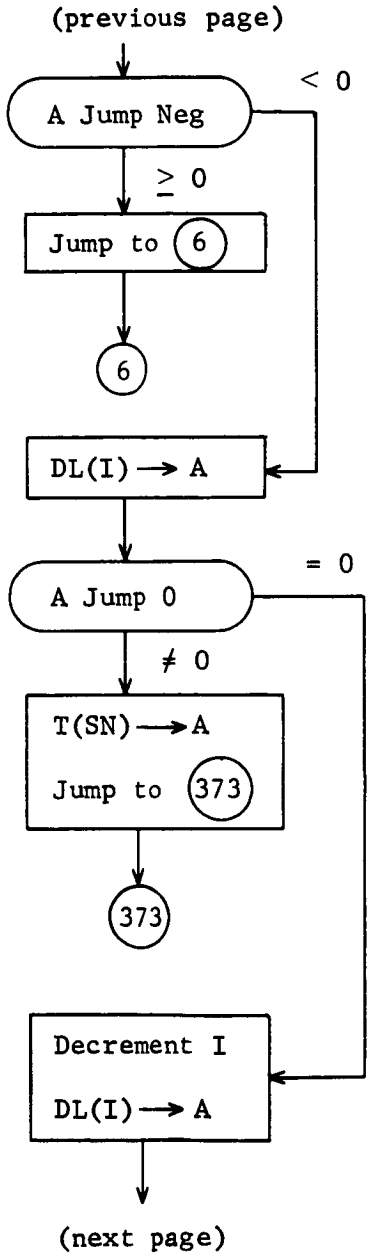

Test if the first three targets in the Data List have been tested for period change.

If no entry has been made for this period, (A = 0), try last period.

STAR DATA PROCESSING (12)

Period Change Testing

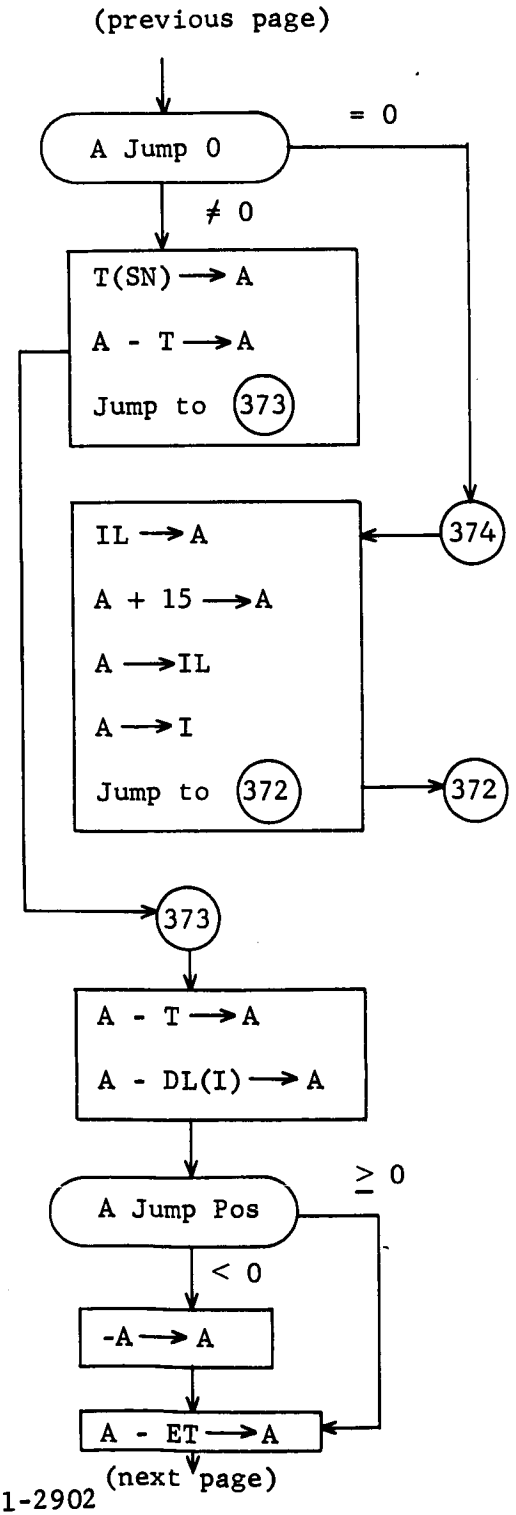

If also no entry, take next target.

Since two periods back, subtract one period here.

Set up index for next target in Data List.

Subtract period from present transit time.

Make contents of A positive.

Subtract acceptable error.

STAR DATA PROCESSING (13)

Period Change Testing

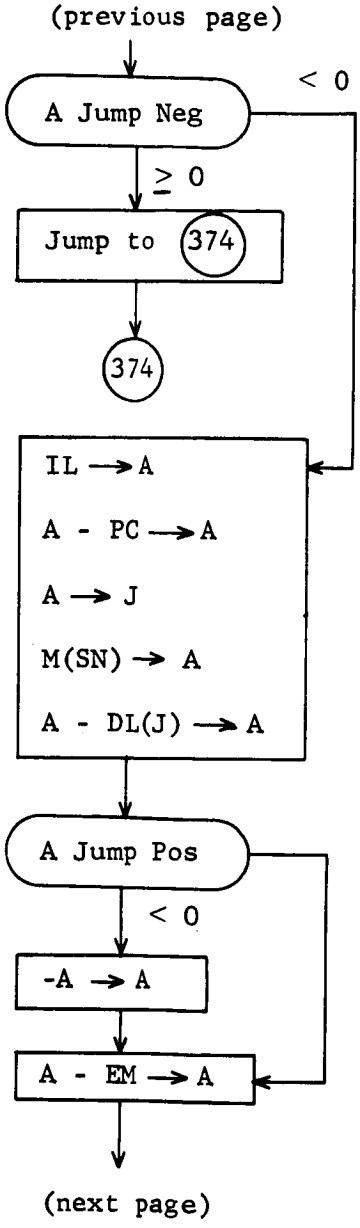

Test whether present transit time is one (or two) periods different from Data List entry. If not, return to 374.

If transit time acceptable, test whether magnitudes match.

Make contents of A positive.

Subtract acceptable error.

STAR DATA PROCESSIONG (14)

Period Change Testing

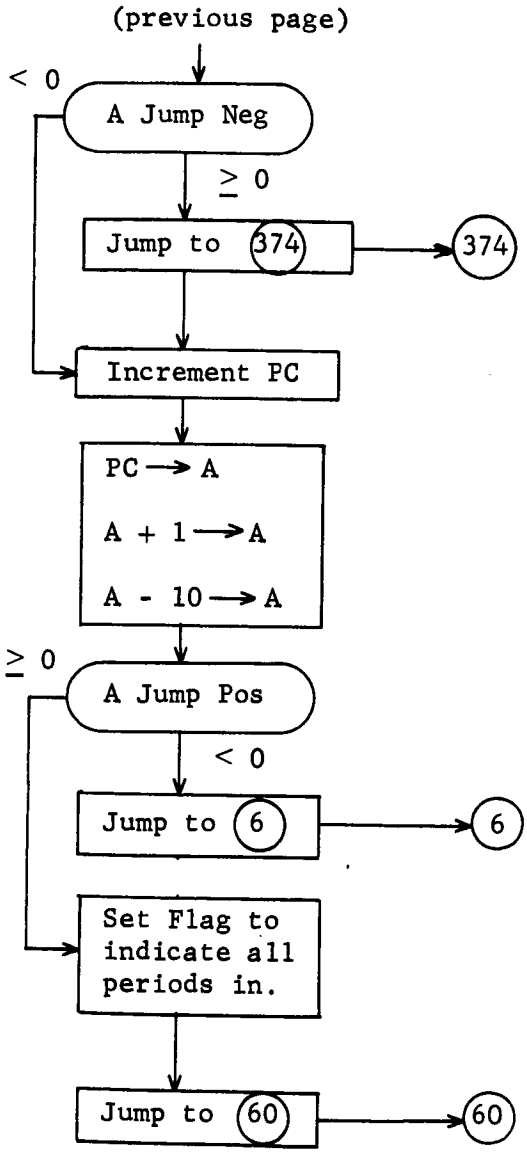

Test magnitude match. If not, return to 374.

If pass, increase period counter.

Test period number > 10.

If not, go to end of program.

If period > 10, stop measurement.

STAR DATA PROCESSING (15)

Data List Search

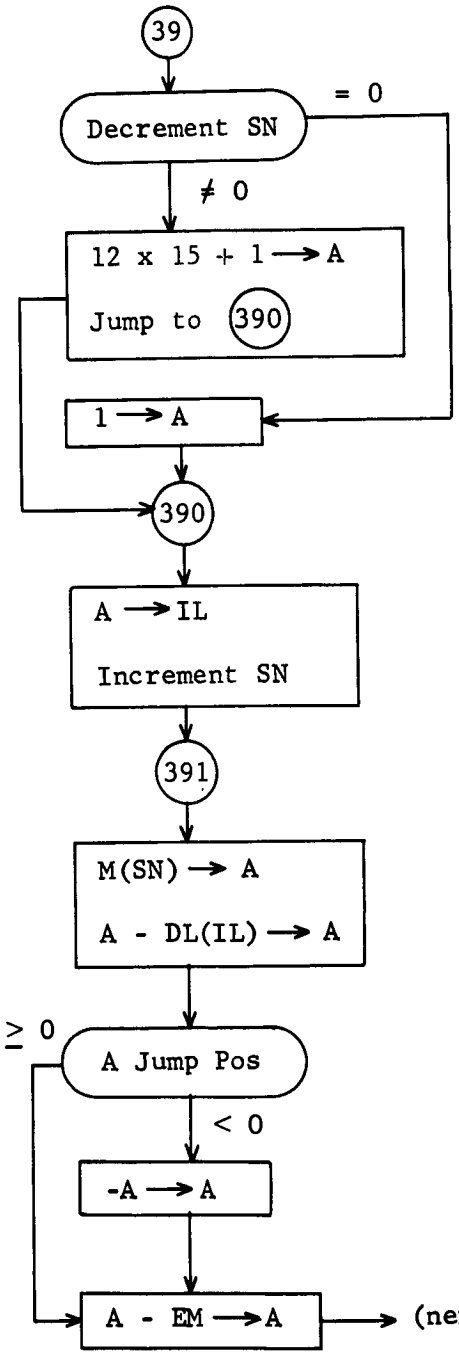

Set up index register according to slit #.

Load index register. Reset slit number.

Compare previous magnitude with Data List entry.

Make contents of A positive.

Subtract acceptable error.

STAR DATA PROCESSING (16)

Data List Search

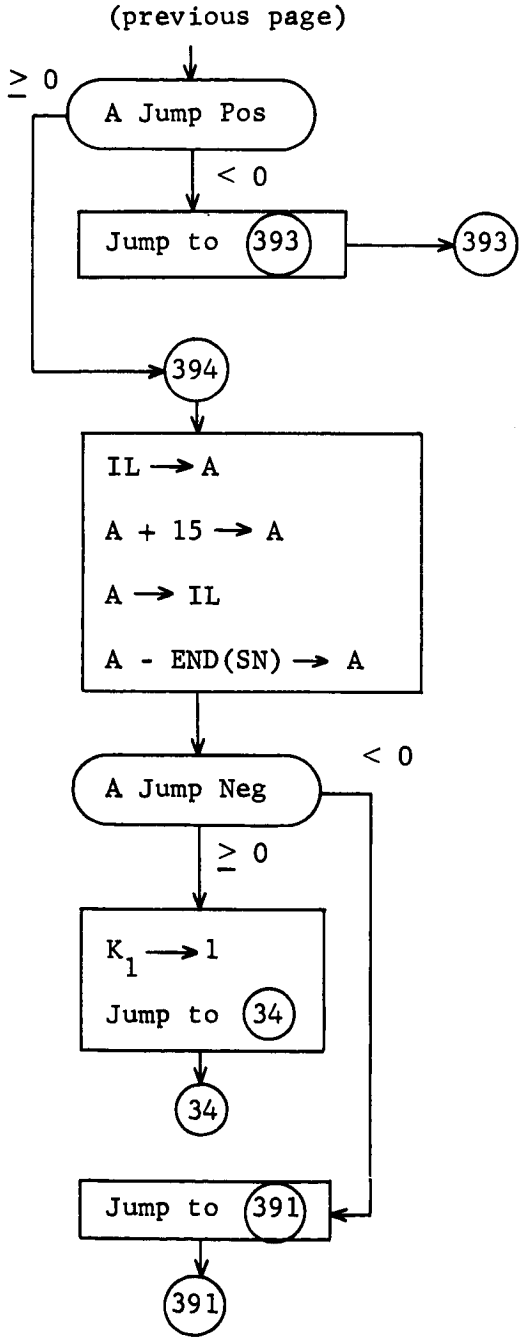

Test magnitude match.

If match, pass to (393).

If no match, increase index.

Test index exceeding maximum value.

If index high, stop search, go to 34 with flag $K_1 = 1$.

If index still OK, return to 391 for continuation of search.

STAR DATA PROCESSING (17)

Data List Search

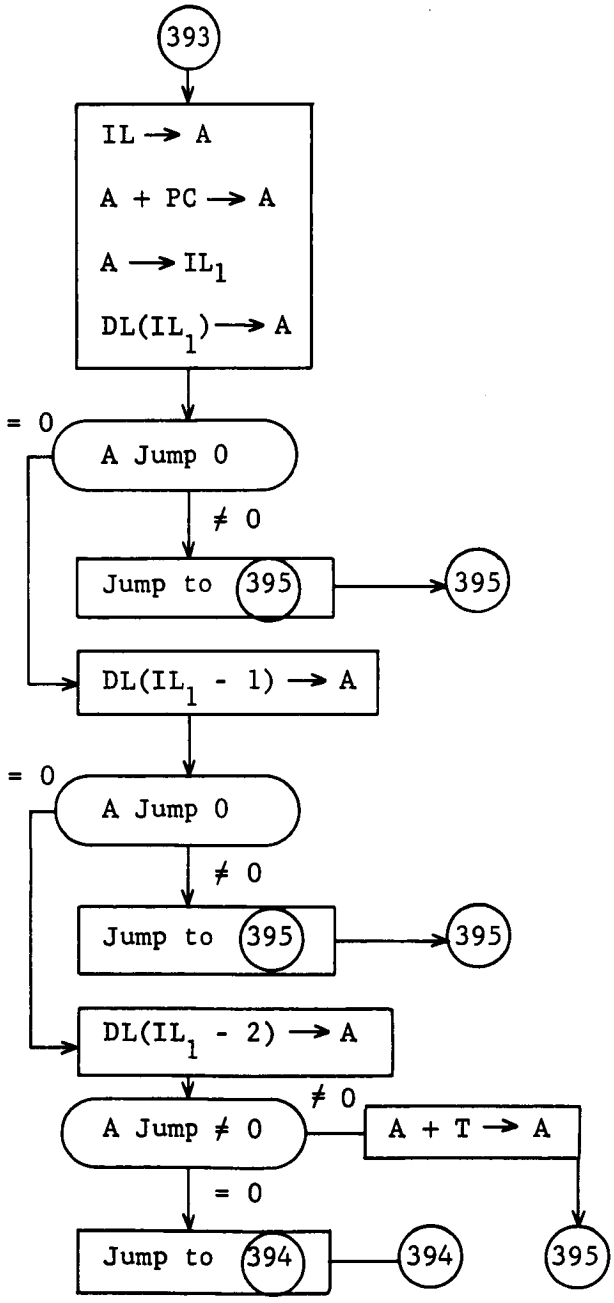

Set up index IL_1 using IL as standard.

Test Data List entry = 0.

If transit time entry made (A ≠ 0), go to 395.

If empty, try previous period entry.

If still empty, try period entry previous to that.

If all empty, return to 394.

STAR DATA PROCESSING (18)

Data List Search

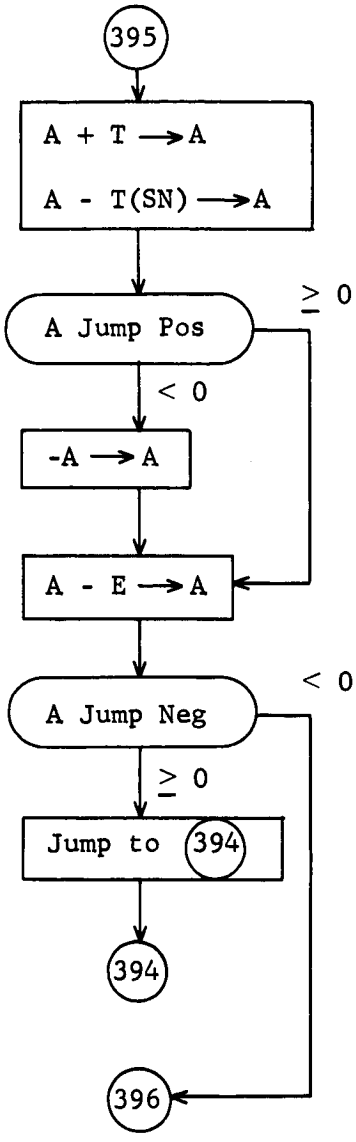

Add one period to Data List entry compare to previous target transit time.

Test period difference in transit times.

If not compatible, return to (394).

If within acceptable error, continue.

STAR DATA PROCESSING (19)

Data List Search

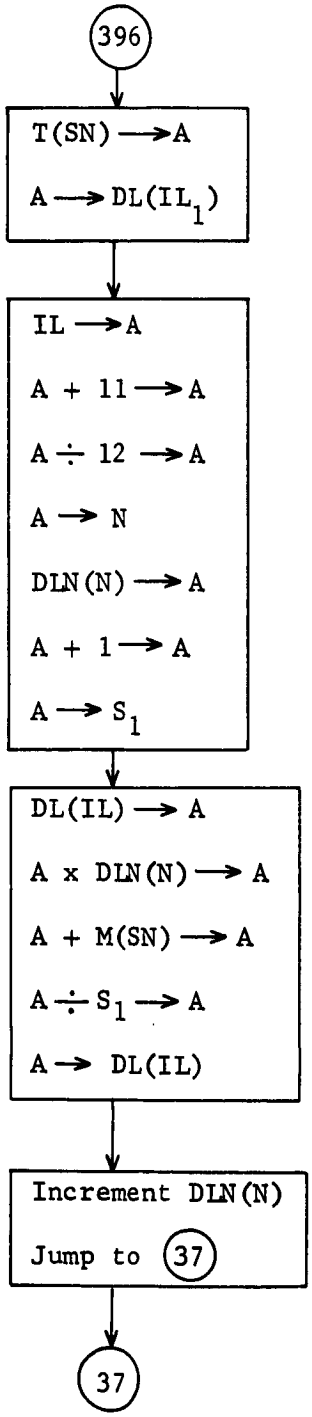

Store previous transit time into Data List.

Set up numbers for averaging magnitudes.

Average previous magnitude with Data List magnitude. (N = target number, DLN(N) = number of measurements entered so far under that target.)

Increase by 1 the number of measurements under N^{th} target. Return to (37).

PLANET DATA PROCESSING (1)

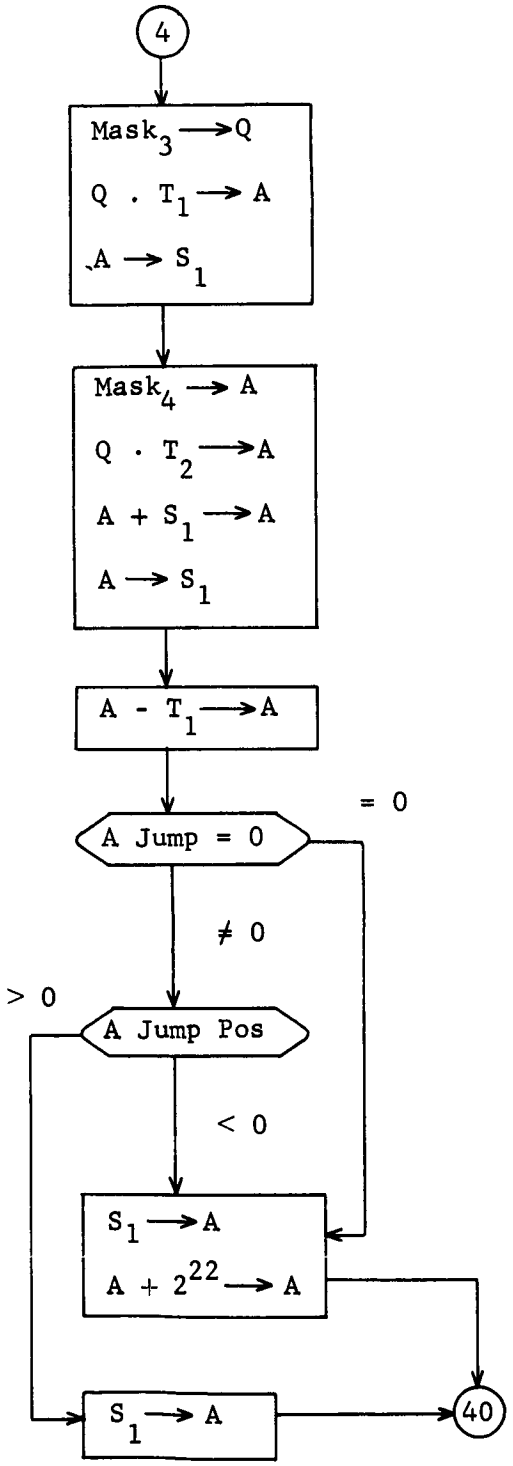

Form from T_1 and T_2 a composite word whose lower 22 bits are identical to the lower 22 bits in T_2 and whose remaining upper bits are identical to the corresponding bits of T_1. This is the anode current fall time, except it may be deficient by 2^{22}.

If the difference between the composite word and T_1 is zero or negative, the composite word needs 2^{22} added.

In either case, A now contains the correct fall time.

PLANET DATA PROCESSING (2)

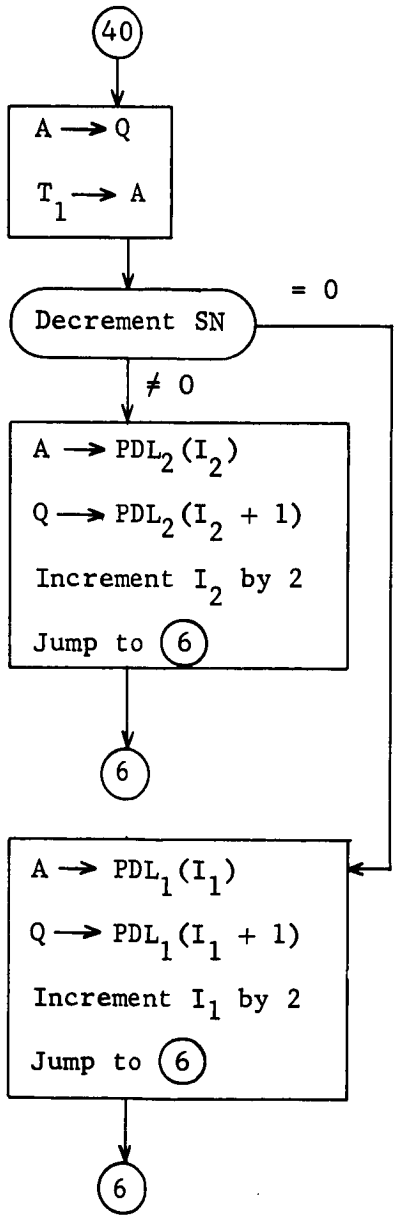

Load the rise and fall times into registers A and Q respectively.

Store data in Planet Data List according to slit and number of data words already there (I_1 or I_2).

RETURN

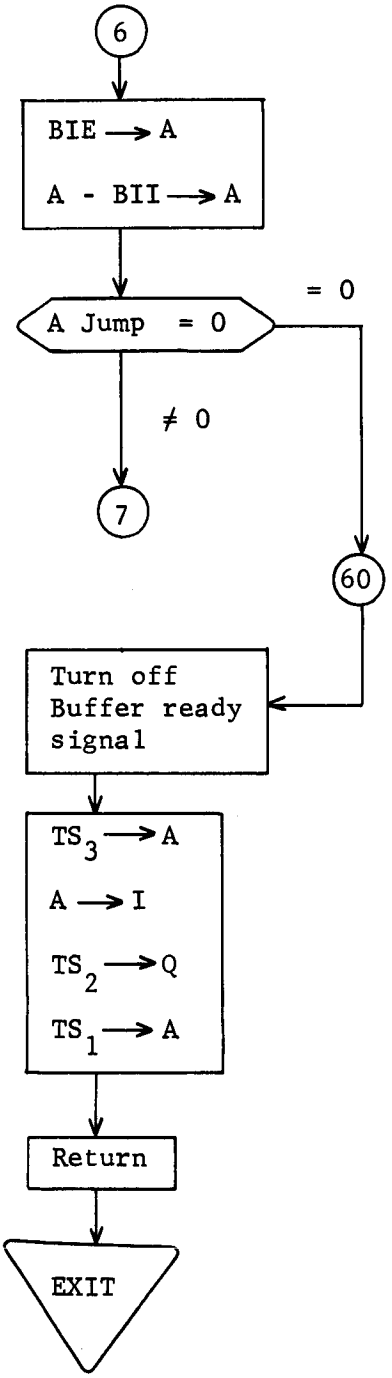

Test whether more information is storedin the buffer.

If there is, then repeat entire sequence from (1).

If no more data, turn off the interrupt signal.

Restore original data to used registers.

Return to original interrupted sequence.

APPENDIX G

ANALYSIS OF A TORQUE-FREE BODY CONTAINING A SWIFTLY ROTATING WHEEL

The body is defined by the $\hat{i}_4$, $\hat{j}_4$, $\hat{k}_4$ reference frame which is related to the inertia frame I, J, K by the angles γ, α, ϕ, θ, ψ. (See Figure 1.) This representation was chosen because of a certain inconvenience that occurs if the standard Euler representation is used. There is a wheel contained in the body which is caused to rotate about the $\hat{k}_4$ axis. This wheel is assumed to be perfect, i.e., two of the moments of inertia are equal. The body has two moments of inertia which are nearly equal, one product of inertia which is zero and two products of inertia which are small but non-zero. The centers of mass of the wheel and the body are assumed to nearly coincide (and are assumed to lie in the $\hat{i}_4$, $\hat{j}_4$ plane). It is also assumed that the angular velocity vector is nearly constant in direction. With these assumptions an approximate solution can be found.

The approximate solution indicates the motion shown in Figure 2. The motion consists of a slow conical motion described by γ, a fast conical motion described by θ_o (precession), and a swiftly oscillating motion (small amplitude) superimposed on the cone θ (nutation).

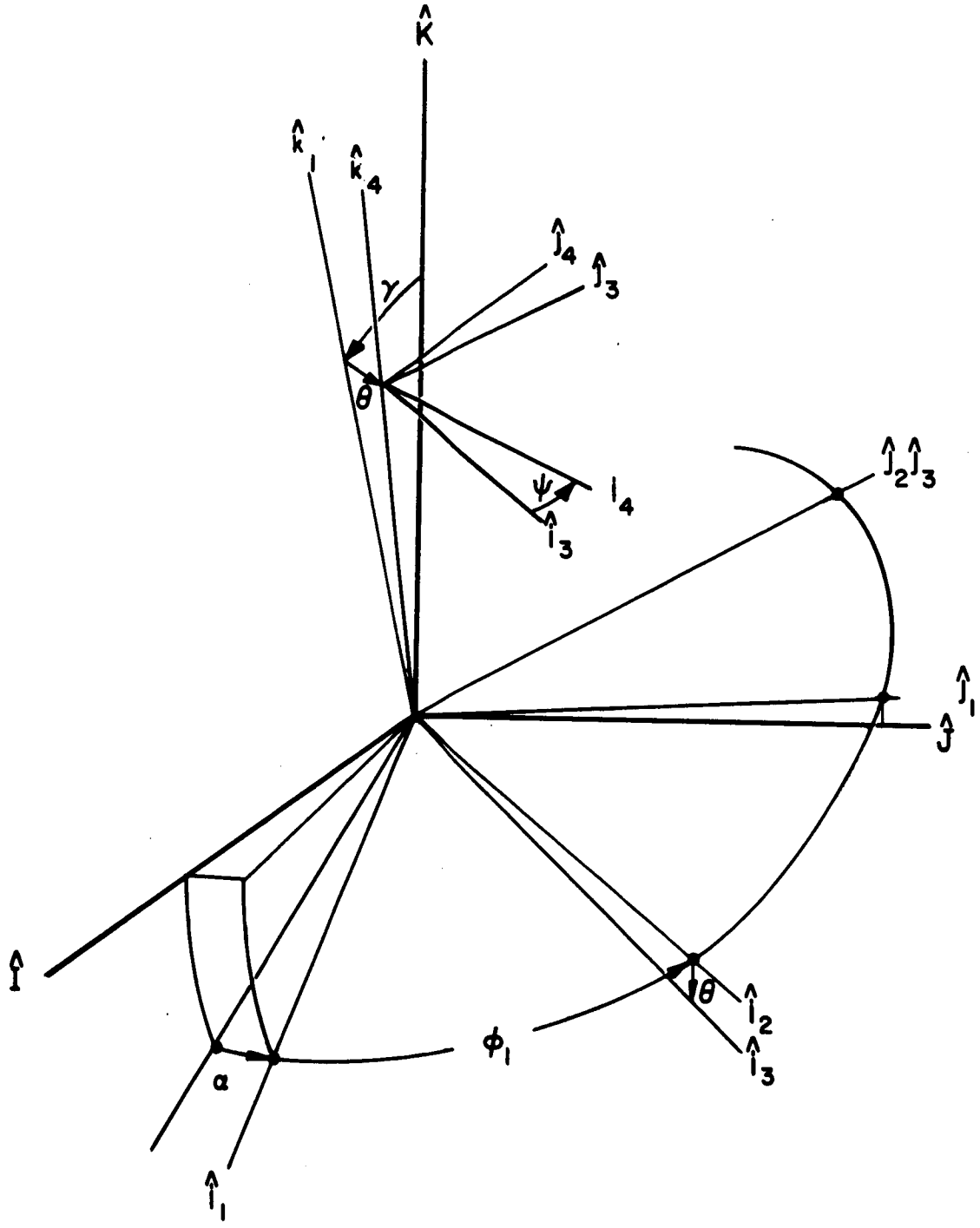

Figure 1. The Relationship Between the Inertial Frame $\hat{I}\hat{J}\hat{K}$ and the Body Frame $\hat{i}_4$, $\hat{j}_4$, $\hat{k}_4$

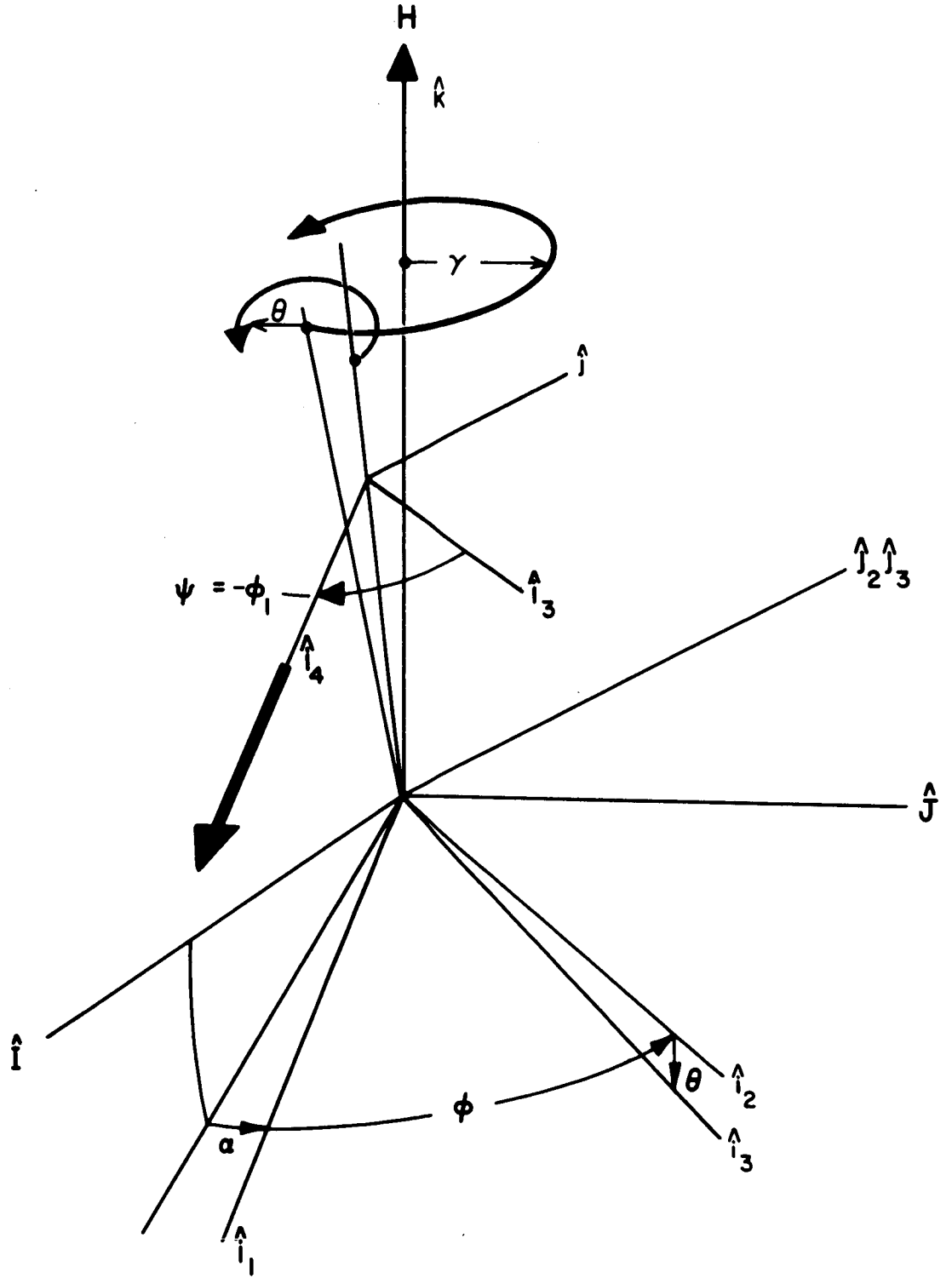

Figure 2. The Motion of the Camera (with Momentum Wheel)

Nomenclature:

I_1, I_2, I_3	Moments of inertia of the body
I_{xz}, I_{xy}	Products of inertia of the body
A_1	Moment of inertia of the wheel about $\hat{i}$ and $\hat{j}$ axes
C_1	Moment of inertia of wheel about $\hat{k}$ axis
$\theta, \phi_1, \psi, \gamma, \alpha$	angles which describe orientation of the body
$\bar{H}$	the total momentum
ν_s	scan rate
$\bar{\omega}$	angular rate vector of the body
ω_b	initial angular rate of the body perpendicular to axis $\hat{k}_4$
$\dot{\psi}_1$	angular rate of the wheel with respect to the body
μ	$\frac{I_2 - I_1}{2(I_1 + A_1)}$
ρ_y	$\frac{I_{xy}}{I_1 + A_1}$
ρ_z	$\frac{I_{xz}}{I_1 + A_1}$
$\dot{\phi}$	$\dot{\phi}_1 + \dot{\alpha}$

The Derivation

Consider the total angular momentum and the angular rate of the body*.

$$\bar{H} = [\, A\omega_1 - I_{xy}\,\omega_2 - I_{xz}\,\omega_3 + A_1\,\omega_1 \,]\,\hat{i}_4$$

$$+ [\, - I_{xy}\,\omega_1 + B\omega_2 + A_1\,\omega_2 \,]\,\hat{j}_4$$

$$+ [\, - I_{xz}\,\omega_1 + I_3\,\omega_3 + C_1(\omega_3 + \dot{\psi}_1) \,]\,\hat{k}_4$$

Letting $\phi_1 + \psi = 0$ and assuming γ and θ are small,

$$\bar{\omega} = [- (\dot{\phi}_1 + \dot{\alpha})\,\theta \cos\psi + \dot{\theta} \sin\psi - \dot{\alpha}\,\gamma \,]\,\hat{i}_4$$

$$+ [(\dot{\phi}_1 + \dot{\alpha})\,\theta \sin\psi + \dot{\theta} \cos\psi \,]\,\hat{j}_4$$

$$+ [\, \dot{\alpha} \,]\,\hat{k}_4$$

Using $\bar{H}$ and $\bar{\omega}$ and substituting the smallness relationships

$$\mu = \frac{I_2 - I_1}{2(I_1 + A_1)}$$

$$\rho_y = \frac{I_{xy}}{I_1 + A_1}$$

---

* Synge, J. L. and Griffith, B. A., Principles of Mechanics, McGraw-Hill, New York, 1949.

$$\rho_z = \frac{I_{xz}}{I_1 + A_1}$$

where μ, ρ_y, ρ_z are small, the following equations are obtained,

$$\dot{\theta} = \frac{H\gamma}{I_1 + A_1} \sin \phi_1 + \dot{\theta} (-\mu \cos 2\psi + \rho_y \sin 2\psi)$$

$$- \dot{\phi} (\mu \theta \sin 2\psi + \rho_y \theta \cos 2\psi)$$

$$+ \dot{\alpha}(\gamma \sin \psi + \rho_z \sin \psi - \rho_y \gamma \cos \psi - \mu \gamma \sin \psi) \quad (1)$$

$$\dot{\phi}\theta = \frac{H \theta}{I_1 + A_1} + \frac{H \gamma}{I_1 + A_1} \cos \phi_1 - \rho_z(\dot{\psi} + \dot{\phi}) \cos \psi$$

$$- \rho_y(\dot{\phi} \theta \sin 2\psi + \dot{\theta} \cos 2\psi + \dot{\alpha} \gamma \sin \psi)$$

$$- \mu(\dot{\theta} \sin 2\psi - \dot{\phi} \theta \cos 2\psi - \dot{\alpha} \gamma \cos \psi)$$

$$- \dot{\alpha} \sin \gamma \cos \psi \quad (2)$$

$$\dot{\psi} + \dot{\phi} = \frac{H}{I_3 + C_1} - \frac{C_1 \dot{\psi}_1}{I_3 + C_1} - \frac{H \gamma \theta \cos \phi_1}{I_3 + C_1}$$

$$+ \rho_z \left(\frac{I_1 + A_1}{I_3 + C_1}\right) \left(- \dot{\phi} \theta \cos \psi + \dot{\theta} \sin \psi - \dot{\alpha} \gamma \right) \quad (3)$$

If the relationship $\frac{H}{I_1 + A_1} \gamma = (\rho_z + \gamma) \bar{\dot{\alpha}}$ is imposed, where $\bar{\dot{\alpha}}$ is the

average of $\dot{\alpha}$, and if it is noted that $\dot{\phi} + \dot{\psi} = \dot{\alpha}$, the following equations can be found,

$$\dot{\theta} = \frac{-H}{I_1 + A_1} (\mu\, \theta \sin 2\psi + \rho_y\, \theta \cos 2\psi) - \left(\frac{H - C_1 \dot{\psi}_1}{I_3 + C_1}\right)(\mu\, \gamma \sin \psi + \rho_y\, \gamma \cos \psi) \tag{4}$$

$$\dot{\phi} = \frac{H}{I_1 + A_1} - \frac{H - C_1 \dot{\psi}_1}{I_3 + C_1} - \rho_y \frac{H}{I_1 + A_1} \sin 2\psi - \rho_y \left(\frac{H - C_1 \dot{\psi}_1}{I_3 + C_1}\right) \frac{\gamma}{\theta} \sin \psi + \mu \left(\frac{H - C_1 \dot{\psi}_1}{I_3 + C_1}\right) \frac{\gamma}{\theta} \cos \psi + \mu \frac{H}{I_1 + A_1} \cos 2\psi \tag{5}$$

$$\bar{\dot{\alpha}} = \frac{H - C_1 \dot{\psi}_1}{I_3 + C_1} \tag{6}$$

$$\ddot{\dot{\alpha}} = - \frac{H\, \theta(\gamma + \rho_z) \cos \psi}{I_3 + C_1} \quad , \text{where } \alpha = \bar{\alpha} + \ddot{\alpha} \tag{7}$$

Approximate solutions of these euqations can be found by using the method of averaging. This results in,

$$\theta = \theta_o - \frac{H\,\theta_o}{2R(I_1 + A_1)}\left[\mu\cos(2\tau + 2\psi_o) + \rho_y \sin(2\tau + 2\psi_o)\right]$$

$$- \frac{\nu_s\,\gamma}{R}\left[\mu\cos(\tau - \psi_o) + \rho_y \sin(2\tau + 2\psi_o)\right] \qquad (8)$$

$$\alpha = \nu_s t + \alpha_o - \frac{H\,\theta_o(\gamma + \rho_z)}{R[I_3 + C_1]}\sin(\tau + \psi_o) \qquad (9)$$

$$\phi = -\psi = \tau + \psi_o - \frac{\rho_y H}{2R(I_1 + A_1)}\cos(2\tau + 2\psi_o)$$

$$- \frac{\rho_y\,\nu_s\,\gamma/\theta_o}{R}\cos(\tau + \psi_o)$$

$$+ \mu\nu_s\,\gamma/\theta_o\,\sin(\tau + \psi_o)$$

$$+ \frac{\mu H}{2R(I_1 + A_1)}\sin(2\tau + 2\psi_o) \qquad (10)$$

$$\gamma = \frac{\rho_z\,\bar{\dot{\alpha}}}{\frac{H}{I_1+A_1} - \bar{\dot{\alpha}}} = \frac{\rho_z\,\nu_s}{\frac{H}{I_1+A_1} - \nu_s} \approx \frac{I_{xz}\,\nu_s}{C_1\,\dot{\psi}_1} \qquad (11)$$

where

$$R = \frac{H}{I_1 + A_1} - \frac{H - C_1\,\dot{\psi}_1}{I_3 + C_1}$$

$$\tau = t/R$$

$$\nu_s = \bar{\dot{\alpha}} = \frac{H - C_1\,\dot{\psi}_1}{I_3 + C_1}$$

Equations 8, 9, 10, and 11 describe the motion. The motion is shown in Figure 3. The motion is made up of: (1) a slow conical motion described by the angles γ and α, i.e., the $\hat{k}_4$ axis of the body moves along the cone at the scan rate ν_s; (2) a conical motion described by θ and ϕ (this corresponds to the precession in the rigid body problem); (3) a fast oscillatory motion with a small amplitude. The amplitude is dependent on the difference in the moments of inertia and the product of inertia (this oscillation corresponds to the nutation in the rigid body problem).

Up to this point the value of θ_o has not been established. θ_o will be dependent on the angular momentum $\bar{H}$ and the initial angular rate of the body perpendicular to the spin axis, i.e.,

$$\tan \theta_o = \frac{\bar{H} \cdot \hat{P}}{H \cdot \hat{k}_4} \quad , \hat{P} = \text{unit vector in the } \hat{i}_4, \hat{j}_4 \text{ plane}$$

For large values of $\dot{\psi}$, which is expected in this application, θ_o can be approximated by,

$$\theta_o = \frac{(I_1 + A_1)\, \omega_o}{C_1\, \dot{\psi}_1} \quad ,$$

where ω_o is the initial angular rate perpendicular to the spin axis.

Figures II-17, II-18, II-19 show relationships in γ, θ_o, and θ (nutation) in regard to the parameters. Simplified equations which recognize the large value of $\dot{\psi}_1 / \nu_s$ in this application are used.

These equations are:

$$\theta = \frac{(I_1 + A_1)\,\omega_b}{C_1\,\dot{\psi}_1} - \frac{\omega_b}{\dot{\psi}_1}\left(\frac{I_1+A_1}{2C_1}\right)\sqrt{I_{xy}^{\,2} + \tfrac{1}{4}(I_2-I_1)^2}\,\cos(2\tau + \delta)$$

$$\gamma = \frac{I_{xz}\,\nu_s}{C_1\,\dot{\psi}_1}$$

In these, R is considered to be of order 1; R could be chosen zero depending on the parameters H, $\dot{\psi}_1$ I_1 I_3 C_1 and A_1, but the case when R is near zero is not considered.